Environmental Determinants of Malaria Risk in Europe: Past, Present and Future

A thesis submitted for the degree of Doctor of Philosophy (PhD)
of the University of London

Disease Control and Vector Biology Unit
Department of Infectious and Tropical Diseases
London School of Hygiene and Tropical Medicine
Keppel Street
London WC1E 7HT
United Kingdom

By

Katrin Gaardbo Kuhn

Numerous Originals in Colour

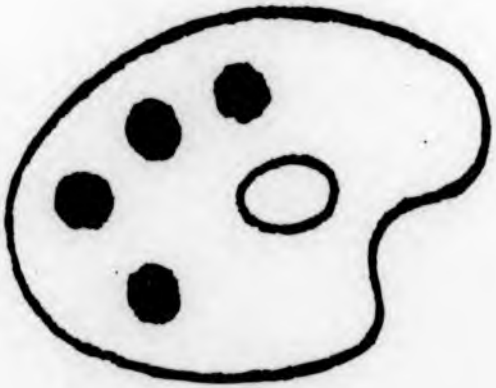

Abstract

Malaria is today the most important vector-borne disease in the world. Like all vector-borne diseases, its distribution depends on a complex array of environmental factors, including climate. The historical global distribution of malaria was considerably greater than today's, and there has been much recent speculation addressing whether the predicted climate changes could lead to the re-emergence of malaria in previously endemic areas, such as Europe. This thesis quantifies the role of climate and other environmental factors in the temporal and spatial pattern of malaria risk within England and across Europe using historical and current data and uses the findings to simulate the likely changes in malaria risk in Europe as the result of global warming.

The inter-annual variability and spatial variation in ague (malaria) mortality rates in English and Welsh counties during the 19th century were significantly related to changes in marsh wetlands, cattle density, average temperature and rainfall. Model simulations indicated that increasing cattle densities and decreasing marshlands accounted for at least 19% of the drop-off in English malaria. Further simulations showed that the changes in climate predicted for 2050 may increase malaria risk by 8-14%, clearly insufficient to lead to the re-emergence of the disease in England.

Temporal and spatial patterns of malaria incidence throughout Europe during the 20th century were significantly related to changes in woodlands, rice cultivation, cattle densities and average temperature. According to model simulations, at least 12-15% of the decrease in European malaria was due to increased woodland coverage and cattle densities. Simulations of global warming predicted for the 2050s showed that malaria transmission is likely to increase by 10-24% with more pronounced effects in northern areas. In comparison to current levels of indigenous transmission, these increases are insignificant and will not lead to the re-emergence of local transmission in Europe.

Current malaria risk across Europe was quantified using environmentally-based risk maps of the present distribution of five mosquito vectors. For each anopheline, spatially defined measurements of relative vectorial capacity (RVC) were calculated from published temperature-dependent and independent measurements of relevant parameters and then converted into an absolute measure of malaria risk, R_0, using country-specific ratios predicted from GDP and life expectancy. The relationship between these national indicators and the ratios of RVC: R_0 was empirically derived from the ratio of recent

indigenous: imported malaria cases in 5 European countries with available data. Simulations indicated that projected climate changes may expand the geographical distribution and/or increase the abundance of both southern and northern vectors. Calculations of RVC showed that there are only few locations in Europe where the five mosquitoes can currently act as efficient vectors of *P. vivax* malaria. With projected climate changes, these areas expand so that by the 2080s, three of the five mosquitoes may have more important roles in malaria transmission across Europe. R_0 was currently predicted to be above 1 (i.e. conditions suitable for malaria transmission) in areas of Moldova and Romania and projected climate changes could considerably increase the risk of transmission in these areas by the 2080s while the risk of disease in the rest of Europe remains very low.

"Fever, represented as a frenzied beast, stands racked in the centre of a room,
while a blue monster, representing ague, ensnares its victim by the fireside;
a doctor writes prescriptions to the right.
And feel by turns the bitter change of extremes by change more fierce."

Coloured etching by T. Rowlandsson after J. Dunthorne 1788.
(British Museum, 1938).

This work is dedicated to my grandparents –

particularly Dolle whose memory has inspired me

for many years

Acknowledgements

My sincerest thanks go to Clive Davies for his excellent guidance, supervision and support during the past years and to Diarmid Campell-Lendrum for his great sense of humour and for spending so much time discussing this work over numerous cups of coffee and tea.

This work was financially supported by Kuhn Spedition KG, Roblon Fonden, Novo Nordisk Fonden, Løvens Kemiske Fabrik, Christian den Tiendes Fond and Det Obelske Familiefond whom I acknowledge with thanks.

So many people have helped with all aspects of this thesis in a very different number of ways. I am much indebted to the kindness shown by Menno Bouma, David Bradley, Paul Coleman, Jon Cox, Chris Curtis, Philippe Grandjean, Rob Hutchinson, Sari Kovats, Pim Martens, Tony McMichael and Clem Ramsdale.
I am especially thankful to Annemarie ter Veen for taking time to comment on the finished manuscript.

For advice on statistics I am grateful to Neal Alexander and Ben Armstrong and for excellent information on GIS and general mapping I thank Chris Grundy. Climate data and guidance on their use were provided by Mike Hulme, David Lister, Matt Livermore and Phil Rogers to whom I am grateful.

Many thanks to Bo Drasar and Vanessa Harding for advising me on historical aspects of disease patterns in England. Considerable thanks are also due to Carlos Aranda, Christine Dahl, Gabriella Gibson, Leonard Munstermann, Natalia Nikolaeva and Willem Takken who provided invaluable information on European *Anopheles*.

My warmest thanks also go to friends and colleagues at the School to whom I will always be grateful for making my studies here so memorable. Sincere thanks to Cheryl Cooper, Patricia Aiyenuro, Lyda Osorio, Jan Kolaczinski, Mary Marimootoo, Julia Mortimer, James Patterson and Orin Courtenay. Special thanks to Anne Carstensen, Henrik Folden, Dominique Brookes, Khadija Kamaly and Mary Garner for their outstanding friendship which I value greatly.

My deepest thanks to Lars; for introducing me to the kindest people possible and for the future!

Lastly, for the support given by my family I am truly grateful. Mor, Viggo, Onkel, Far, Maria, Sebastian and Thomas have been unfailing in their encouragement and I thank them with all my heart.

Contents

Figure Legends

Table Legends

General Introduction and Study Rationale

Analysing and predicting malaria patterns in Europe: Study rationale and aims

Published literature which goes back as far as the early 1980s has demonstrated the wide use of environmental variables in statistical and biological models in order to describe the spatial and temporal distribution of a range of vector-borne diseases. By looking critically at these studies we have learned the importance of using suitable entomological, epidemiological and environmental data at appropriate spatial resolutions.

This thesis will use a combination of historical and current data on malaria and mosquitoes in Europe to investigate the past, present and future patterns of vector and disease distributions in relation to climatic, agricultural and land cover features. Considering the many speculations about the role of climatic and other environmental changes in the possible re-emergence of malaria in the European region, this is an analysis which is long overdue. At present we are unable to make qualified assumptions about the future of European malaria because we do not fully understand the factors which influenced historical patterns of this disease.

The thesis is divided into four main studies which have the following main objectives:

- To identify and quantify the roles of climate and agricultural factors in the spatial and temporal variation of English malaria (ague) during the 19th century.
- To identify and quantify the impact of climate and agricultural factors on the temporal and spatial variation of malaria throughout Europe during the 20th century.
- To identify and quantify the association between climate and land cover variables on the current distribution of the five former European malaria vectors, *Anopheles atroparvus*, *An. labranchiae*, *An. messeae*, *An. sacharovi* and *An. superpictus*, their relative vectorial capacity and the current risk of malaria (R_0) in Europe.
- To quantify the risk of malaria re-emergence across Europe on the basis of the models developed for the above three studies.

The main thesis thus consists of 4 chapters which will address each of the above objectives. Specific aims and objectives are described separately in each chapter which is divided into an introduction and literature review of the subject, followed by methods, results and discussion. A discussion section, drawing information from each of the separate studies is presented in the final chapter.

This chapter will provide an overview of the data and methods which have previously been used to quantify the association between environmental factors and the distribution and intensity of vector-borne disease transmission across the world. Specific examples related to malaria will be discussed at length in following chapters and have therefore not been included here.

General Literature Review: vector-borne diseases and the environment

Life cycle and epidemiology of malaria

Malaria is today recognised as the most important vector-borne disease, causing an estimated 300 million acute illnesses and at least 1 million deaths annually (Roll Back Malaria 2002). Ninety percent of these deaths occur in Sub-Saharan Africa where it is the main cause of death in children under 5 years of age. (Greenwood and Mutabingwa 2002). Approximately 40% of the world's population currently live in areas at risk of malaria (Mendis *et al.* 2001). There are four parasite species which cause disease in humans; *Plasmodium falciparum, P. malariae, P. ovale* and *P. vivax* all of which are transmitted by mosquitoes of the genus *Anopheles*. There are around 420 anopheline species distributed throughout the world but only about 70 of these are considered natural malaria vectors (Service 1993). Malaria parasites develop in a sexual cycle in the mosquito and an asexual cycle in the human host (Figure 1.1). Humans become infected when sporozoites are injected into the blood stream by an infected female mosquito taking a blood meal. The parasite undergoes a series of changes, allowing it to invade the liver, red blood cells and immune system before it develops into a gametocyte which can be ingested by a mosquito vector feeding on an infected host. The sexual cycle in the mosquito starts in the midgut and ends in the salivary glands from where parasites again – some 10 to 14 days later – can be injected into a new human host.

Published
Papers
Not filmed
for Copyright
reasons

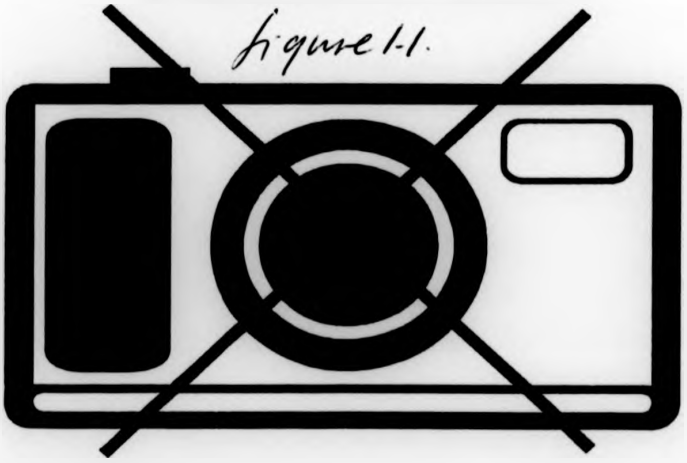

Figure 1.1 Life cycle of *Plasmodium* parasites
(copyright: TDR/Wellcome Trust, 2002).

The transmission of malaria is directly linked to temperature which primarily determines the duration of the extrinsic incubation period (the number of days it takes for the parasite to develop in the mosquito) with development ceasing below and above certain temperature thresholds (e.g. below 15-16°C and above 40°C for *P. vivax*, McDonald 1957, Jetten and Takken 1994). Ambient temperature also has a significant effect on the rate of vector development and the frequency of blood feeding (due to effects on egg development and adult survival, Jetten and Takken 1994). Because all anophelines breed in or near water, rainfall is significantly related to both the distribution and abundance of vectors (Smith *et al.* 1995) which is also highly associated with the presence of man-made water areas such as lakes and river beds (Service 1993). Gill (1921) described the positive relationship between disease distribution and marshes and additionally showed that higher ambient humidities increased vector survival and blood feeding. In this context, it is important to note that all environmental associations are species-specific – i.e. different mosquitoes have different breeding and feeding preferences, development thresholds and so on. In addition to the climatic factors, there are also observed associations between the distribution and transmission of malaria and agricultural factors

such as live stock densities (Bouma and Rowland 1995) and crop features (Bruce-Chwatt and de Zulueta 1980). These will be discussed in detail in the following chapters.

Environmental factors and malaria in Europe

From evidence presented in historical literature it has become clear that malaria was once an important health problem in Europe. At its maximum point the disease covered most of the continent limited only by the 15°C July isotherm which extends as far as Scandinavia and northern Russia where severe epidemics were being reported (Hackett 1937, Bruce-Chwatt and de Zulueta 1980). Transmission at this time has since been linked to several members of the *Anopheles maculipennis* complex, all of which are associated with the distribution of inland fresh and brackish water (see Chapter 4). During the mid-nineteenth century malaria began to spontaneously disappear from the northernmost areas – a decline which has frequently been attributed to changes in agricultural practices (such as increasing cattle densities and draining wetlands) as well as socio-economic improvements (e.g. Whitley 1863, Wesenberg-Lund 1921, James 1929 and Reiter 2000) but never formally analysed in terms of quantifying the relative importance of the different factors. In the countries bordering the Mediterranean, malaria continued to cause extensive morbidity until the European-wide eradication programme consisting of extensive DDT residual spraying was initiated by the WHO and the disease formally eradicated from Europe in 1975, some 20 years later. The persistence of the disease in southern and eastern Europe has often been attributed to a combination of climatic, agricultural and socio-economic factors with continued rice cultivation in these areas being considered as one of the most important (Hackett and Missiroli 1931). From these accounts it is evident that both the distribution, prevalence and later disappearance of malaria in Europe was intricately linked to the environment. With the resurgence of malaria transmission in the former Soviet Union and European Turkey already in the late 1970s and early 1980s also came concern that the disease could yet again spread to the rest of Europe. Since then, there have been numerous speculations about whether the projected anthropogenic climate changes will cause the re-emergence of European malaria (e.g. Kovats *et al.* 1999, IPCC 2001, Reiter 2001). Indeed, the Chief Medical Officer for England recently stated that "by 2050 the climate of the UK may be such that indigenous malaria could become re-established" (Department of Health 2002). However, predictions based on biological and statistical modelling are contradictive with

Martens *et al.* (1995) predicting that future transmission of malaria in Europe is likely while Rogers and Randolph (2000) suggest that this is an unlikely scenario.

It is our view that, before we can make such future predictions with any confidence, we first need to fully understand the history of the disease. In the case of European malaria, this means to quantify the factors which influenced the past distribution of the disease and its decline as well as determining how the distribution of the former malaria vectors is currently related to the environment. This thesis will present a novel approach to predicting malaria in a previously endemic country by examining firstly how environmental factors impacted on the historical risk of disease and then using entomological and socio-economic information to predict malaria risk across Europe both for current and future scenarios.

Environmental factors and global distribution of vector-borne diseases

In the 4th century BC Hippocrates said " *Whoever would study medicine aright must learn of the following subjects. First, he must consider the effect of the seasons of the year and the differences between them. Second, he must study the warm and cold winds, both those which are common to every country and those peculiar to a particular locality*".

As highlighted for malaria, the risk of all vector-borne diseases is a function of the spatial and temporal patterns of disease transmission (vector breeding habitats, host distribution, human activities etc.) all of which are related to environmental factors in complex ways. Temperature and humidity have the most important direct and indirect effects on vector biology and ecology through influences on insect development and survival, blood feeding and geographical distribution (Sellers 1980). Additionally, the development and hence transmission of the pathogen is also highly sensitive to temperature (Bradley 1993). Because of the large public health burden of vector-borne diseases (Curtis and Davies 2001), there has been growing interest in the mapping and predictive modelling of their geographical limits and transmission dynamics using environmental variables as driving factors (Hay *et al* 2000a). In light of the increasing concern about the impacts of man-made climate changes (see Chapter 5), a considerable proportion of this work has focused on producing risk maps which predict future patterns in disease distribution and transmission as a result of the projected changes in climate. Thus, combinations of environmental, entomological and disease data have been used to identify associations between temperature, rainfall and vegetation (land cover) and the

distribution of various diseases and/or their arthropod vectors (Tab. 1.1). The published works presented in Table 1.1 do not cover all vector-borne diseases for which environmental associations have been identified but show a representative selection of the numerous studies undertaken. Most of these analyses have utilised the recent advent of Geographic Information Systems (GIS) and climate and habitat databases from satellites and ground-based meteorological stations which have created an unprecedented amount of available information. The combination of remotely sensed data and GIS is a potentially powerful tool in disease control, including monitoring and management of mosquito control as well as chemotherapy distribution.

Table 1.1. Environmental factors associated with the distribution of some vector-borne diseases (derived from spatial correlation analyses).

Disease/vector	Location (s)	Factors associated with disease and/or vector distribution	Selected references
Leishmaniasis/ sandflies	Sudan and Southwest Asia	Temperature Soil type Land cover Altitude Dewpoint	Cross and Hyams 1996, Kuhn 1997, Thomson *et al.* 1999a.
Malaria/ anopheline mosquitoes	Europe, Africa, South America and India	Land cover Temperature Precipitation Cloud cover El Niño patterns Altitude	Sharma *et al.* 1996, Beck *et al.* 1997, Hay *et al.* 1998, Poveda *et al.* 2001, Kleinschmidt *et al.* 2001a.
Schistosomiasis/ aquatic snails	Egypt	Temperature Land cover	Malone *et al.* 1994, Brooker 2002.
Lyme disease/ ticks	North America	Land cover Temperature Precipitation	Dister *et al.* 1997, Estrada-Peña 1998.
Dengue/ culicine mosquitoes	Thailand and North America	Temperature Precipitation El Niño patterns	Morrison *et al.* 1998, Hay *et al.* 2000b.
African trypanosomiasis/ tsetse flies	Africa	Temperature Land cover Saturation deficit Altitude Agriculture	Rogers and Williams 1994, Rogers *et al.* 1996, Robinson *et al.* 1997, Hendrickx *et al.* 1999.
Livestock diseases/ ticks, *Culicoides*	South America and Africa	Land cover Temperature Precipitation Altitude	Rogers and Randolph 1993, Randolph 1997, Baylis *et al.* 1998.

Geographical Information Systems (GIS)

GIS are computerised systems designed for the mapping, display and, to some degree, spatial analysis of large quantities of georeferenced data. Data are stored in raster or vector format. Raster data are geographic or graphic images in a matrix of gridded cells

while vector data are simply co-ordinates; usually points, lines or polygons (areas). A GIS database consists of several map layers where the basic layer (or "theme) is often the administrative boundaries of an area. Other layers (e.g. information on vector distributions, climate and major geographic features) can be superimposed onto the boundary theme and displayed simultaneously. Within these layers, a GIS can select areas which meet certain selection criteria that are important, for instance, in planning vector control strategies. Due to the limited statistical capacity of GIS, most data are statistically modelled in other programmes and later input into a GIS for display.

The growth rate of industrial GIS applications reached approximately 25-35% during the 1990s (Boelaert *et al.* 1998) and to date they have been used in the surveillance of numerous tropical diseases, respiratory diseases, cancer, sexually transmitted diseases and various contamination monitoring programmes (Mott *et al.* 1995, Croner *et al.* 1997, Vine *et al.* 1997). From such studies we have gained knowledge on the focality and clustering of tropical diseases and their vectors, disease risk in different geographical areas, the geographical and climatic features related to disease transmission and how the transmission pattern may change with geographical and climate changes.

More importantly, GIS have been shown to be useful tools in the designing and planning of control and monitoring programmes for vector-borne diseases such as African trypanosomiasis in the tsetse fly belt in Sub-Saharan Africa (e.g. Robinson 1998), imported malaria in Israel (Kitron *et al.* 1994), onchocerciasis in Guatemala (Richards 1993) and dracunculiasis in Africa (Clarke *et al.* 1991).

Remote sensing

Remotely sensed data have been used to study and map the abiotic and biotic components of our earth since 1972. This information is today used in a variety of practises such as agriculture, forestry, geology and environmental planning but has proven especially useful for human health application because it shows the extent of environmental factors related to disease transmission dynamics in space and time.

Most satellites which produce images for the use in human health are polar-orbiting , i.e. they circle the globe repeatedly, producing images of areas (pixels) of varying size depending on the orbit and the sensors of the satellite. Pixels may vary in size from around 10 x 10 m for high spatial resolution satellites to an entire hemisphere with low resolution satellites. Generally, the higher resolution satellites operate with a lower temporal frequency, creating a trade-off between time and space.

The most commonly used low resolution satellites (typically a pixel size of 1.1 by 1.1 km) are operated by the National Oceanic and Atmospheric Administration of the USA (NOAA satellites). Each of the NOAA series of advanced very-high-resolution radiometers (AVHRR) satellites provides one global covering image every 12 hours which is processed by NOAA and made freely available for users (Hay *et al.* 1996). Typical environmental proxies derived from these satellites include estimates of rainfall, sea surface temperature, land surface temperature and vegetation indices (especially the Normalized Difference Vegetation Index, NDVI). The low spatial, high temporal resolution NOAA images have been used to study Rift Valley fever outbreaks in Kenya (Linthicum *et al.* 1990), to predict the abundance of *Aedes albifasciatus* in Argentina (Gleiser *et al.* 1997) and to predict malaria infection rates in the Gambia (Thomson *et al.* 1999b).

High resolution satellite images are, among others, provided by the Landsat Thematic Mapper which has a spatial resolution of 30 m and a temporal resolution of 16 days (Thomson and Connor 2000). These images have been extensively used for highly localised studies of vector breeding and resting sites where all environmental information can be contained within a single image. Land cover images from the Landsat series was used for investigating the distribution and abundance of malaria vectors in Mexican villages (Beck *et al.* 1997, Rodriguez *et al.* 1996) with the aim of predicting the abundance of anophelines in nearby villages. The Satellite pour l'Observation de la Terre (SPOT) is another high resolution satellite which has been used for studying local relationships between environment, vectors and disease. Roberts *et al.* (1996) predicted the distribution of *An. pseudopunctipennis* with SPOT images of waterways in Belize and Thomas and Lindsay (1999) used remotely sensed data on larval habitats to correlate with entomological inoculation rate which was then predicted across a wider area.

Ground measured environmental variables

With the rapid advent and increasing availability of remotely sensed environmental variables, the use of ground-based observations of climate and land cover has decreased. Usually derived from meteorological station recordings, ground-measured climate data include atmospheric temperatures (primarily monthly or daily mean, minimum and maximum), humidity, atmospheric pressure and precipitation (daily or monthly total). Other information which has been obtained at the ground-level includes altitude, water

characteristics (e.g. salinity and pH), soil profiles as well as observations on land cover (including vegetation and water bodies).

The draw-back with such data is that they do not provide accurate measurements of the climate in the actual study sites unless the climate station(s) are located or deliberately set up there (e.g. Baylis *et al.* 1998) or appropriate extrapolation methods are applied to the data (Bouma *et al.* 1996, Lindsay *et al.* 1998). As will be demonstrated in this study, meteorological station climate data are particularly useful when studying spatial and temporal disease patterns during historical periods for which no remotely sensed images of climate and land cover are available. Another potentially valuable use of ground-observed climate data is the measurement of micro-climatic conditions. It has often been argued that micro- and not macro-climate is the real determinant of vector biology and ecology in a particular area (Cheng *et al.* 1998) but at present the relationship between micro- and macro-climate has not been well studied. A possible correlation between ground-measured micro-climate and remotely sensed data could therefore improve currently existing climate-disease models.

Modelling the relationship between environmental factors and vector-borne diseases

As described above, a range of environmental variables has been used to analyse and later predict the distribution and abundance of arthropod vectors as well as the distribution and intensity of disease. All of these examples have followed various approaches of linking disease or vector distributions (the outcome variables) to the environmental explanatory variables.

There are two main recognised methods of doing this; the statistical and the biological approach. The statistical (empirical approach) determines the association between environmental factors and the spatial or temporal distribution of vectors and disease by the use of statistical procedures (such as regression or discriminant analysis). This can only be accurately applied where there are extensive records on vector/parasite distribution through time and/or space. The aim of statistical methods is usually to quantify the relative importance of different factors in determining vector and parasite distributions and generate testable hypotheses and guidelines for future studies. In the past methods such as uni- and multivariate logistic regression and stepwise discriminant analysis have most commonly been used. On some occasions, models have included the use of spatial statistics such as kriging and co-kriging (e.g. Kitron and Kazmierczak 1997) which account for the clustering of disease in space (a term known as spatial

autocorrelation). However, these methods require extensive statistical skills and data manipulation and have therefore not been included in the majority of models for simple predictions. The statistical models far outweigh the biological in numbers and if used correctly they are probably just as accurate in predicting and analysing vector and disease distributions as the more complex biological models (Randolph and Rogers 1993).

The biological (experimental) approach requires information on the relationship between individual climatic variables and different aspects of vector and pathogen population dynamics observed either in nature or artificial conditions (laboratory settings). These associations are incorporated into a mathematical model, more often than not centred around the basic case reproduction R_0 which is defined as the number of secondary cases arising from a primary one in a fully susceptible host population (see Chapter 4). The biological approach requires detailed understanding of vector and parasite population dynamics but, once developed, models are flexible and can provide insight into specific mechanisms such as how parasite or vector development rates and densities change with temperature or humidity. Biological models have so far only been developed for diseases and vectors for which the various parameters of the life cycles are relatively well known. As such detailed information is restricted for most diseases, there are only a limited number of these models for vector-borne diseases. Existing biological models generally belong in one of two categories:

(1) General models based on temperature-dependent estimations of parameter values combined to generate a measure of vectorial capacity and, hence, R_0. R These models vary greatly in their use of parameters; for instance Martens *et al.* 1995 used arbitrarily defined values while Randolph (1997) collected original observations on temperature-related population dynamics for her model.

(2) Models based on the selection of arbitrary stressors to define, for instance, temperature thresholds for transmission and geographic distribution of disease and/or vectors (e.g. Martin and Lefebvre 1995).

Model variables

A wide range of explanatory and outcome variables have been incorporated into numerous statistical and biological models to study the determinants of the spatial and temporal distribution of vector-borne diseases.

As discussed above, climate and land cover data used in models have been either remotely sensed or ground measured/observed.

Hand held Global positioning systems (GPS) certify the latitude and longitude of a specific location and have been especially valuable at the very high resolution for detecting the location of houses and human or animal disease cases for later incorporation into a GIS. This has been used for mapping the location of dengue cases (Morrison *et al.* 1998), LaCrosse encephalitis (Kitron *et al.* 1997) and malaria (Schellenberg *et al.* 1998, Beck *et al.* 1997).

Data on disease prevalence have been collected from literature surveys or National Health Records (Cross and Hyams 1996, Bouma *et al.* 1997), field studies (e.g. Hightower *et al.* 1998) and hospital records (e.g. Hay *et al.* 1998). The quality of these data depend on the collection method; literature surveys are somewhat reliable but the source (active or passive case detection) should be considered and, whenever possible, population screening (selecting appropriate age, gender and occupation groups) is preferable.

Entomological data which have been used for studying the relationships between vector-borne diseases and climate have commonly been collected in one of two ways: sampling the relevant site(s) (Beck *et al.* 1997, Dister *et al.* 1997, Elnaeim *et al.* 1998) or literature surveys (Cross and Hyams 1996, Lindsay *et al.* 1998, Estrada-Peña 1998). Field sampling is preferable as it often provides density measures (assuming results are standardised to account for variation in trapping effort and method) but difficult and costly to carry out on a large scale. Published literature is easily accessible and can often supply extensive presence/absence data but do normally not provide useful abundance measures. Construction of large, standardised databases containing entomological and disease information has been proposed and initiated by, for instance, the MARA/ARMA project which aims to construct a widely available Pan-African malaria dataset, including data on parasite rates, vectors and epidemic highland malaria (MARA/ARMA 1998). The DAVID (disease and vector integrated database) for African trypanosomiasis and tsetse flies is another example of a large and freely accessible database, developed by Oxford University (Robinson 1997). There is great potential in constructing similar databases under international collaboration for other vector-borne diseases such as dengue and leishmaniasis.

The following sections provide disease-by-disease examples of how these variables have been incorporated into models in order to determine the correlation

between environment and disease with the aim of constructing present and future risk maps of disease and/or vector distributions. Specific examples for mosquitoes and malaria are not included here as they will be discussed in later chapters.

Biological Models: tick-borne diseases and dengue

Because of its world-wide impact, the majority of biological models have focused on malaria. The remaining approaches are limited to tick-borne diseases and dengue virus, most likely because the population dynamics of both parasites and vectors are relatively well-understood.

Randolph and Craine (1995) presented a first step towards a biological model for European Lyme (i.e. tick-borne) disease by determining the effects of squirrel density and transovarial parasite transmission on R_0. Ultimately this model can also incorporate temperature-dependent effects on disease transmission and provide us with a more sophisticated way of predicting the risk of Lyme disease in temperate regions.

The biological approach has been taken further in the study of the African tick, *R. appendiculatus*. Perry *et al.* (1990) used the CLIMEX model to predict the distribution of this tick across Africa as a function of climate and vegetation. CLIMEX determines the climatic suitability of particular areas for insects using a temperature- and moisture-limited growth index (Sutherst *et al.* 1995, Sutherst 1998). The outcome of the model is the Ecoclimatic Index (EI) which indicates the overall suitability of a location. The EI was predicted across Africa at a resolution of 25 km and compared visually (not statistically) to recorded distributions of *R. appendiculatus*. The model predicts false positive areas in parts of western Africa but seems to be accurate in predicting presence in southern areas. CLIMEX is limited in its crude definition of the climatic requirements from the observed geographical distribution of a vector species and (if available) knowledge of its development thresholds. For species where no data on geographical distribution are available, the estimation of the growth index relies purely on approximation and can thus be subject to large errors. An added limitation of the model used by Perry *et al.* (1990) is the very low resolution at which it operates. Again this fails to identify local environmental risk factors and as such is not much use for reliable predictions.

A significantly more sophisticated approach was adopted by Randolph and Rogers (1997) with the construction of RaPOP, a full biological model for *R. appendiculatus* which incorporates extensive background information on the factors determining the

mortality in each stage of the tick's development. Each of these temperature- or density dependent relationships were derived from quantitative analyses of field data from a number of locations in Africa (Randolph 1993, Randolph 1994, Randolph 1997). The model is run by fixing site-specific climate variables and the output is the number of ticks per host per month. For all four locations tested, the model explained between 42 and 71% of the monthly variation in tick numbers. The relatively good fit is not surprising due to the small number of validation sites – ideally, model fits should have been tested in more locations. This model represents the ultimate ideal goal for biological limits of the distribution of insect vectors. Because of the extensive background studies on *R. appendiculatus*, it was constructed with relative ease and predictions can be made at the highest resolution possible (e.g. a village). However, this is only the first step towards the ultimate prediction of disease transmission as the link between disease transmission and vector dynamics still needs to be quantified. The feasibility of constructing similar models for other vectors is at present relatively low but, given time and resources, should be considered for the future.

The entomological and disease dynamics of dengue transmission have been described using two biological models. CIMSiM (the container-inhabiting mosquito simulation model) is a life-table model which produces local estimates of *Aedes* population density parameters, using calculations of temperature-dependent development rates and fecundity (Focks *et al.* 1993a,b). Heterogeneity of larval habitat is taken into account, allowing modelling of cohorts in up to 9 different container types. CIMSiM can be used to run simulations in specific locations with reference to local hosts abundance, larval habitat and climate (temperature and humidity).

The DENSiM (dengue simulation model) is a corresponding model to CIMSiM which simulates the prevalence and incidence of dengue in humans (Focks *et al.* 1995). The model first creates a human population to which it assigns immune status using defined viraemic parameters such as incubation time and prevalence of dengue antibodies. To describe the human-mosquito contact and the probability of virus passage to humans, DENSiM uses four CIMSiM outputs: daily emergence, weight and survival of female mosquitoes and the proportion of gonotrophic cycle completed daily. These models are comprehensive biological approaches to site-specific analysis of dengue and *Aedes* dynamics, including relationships between temperature and development of mosquitoes, virus incubation in humans and mosquitoes and the transmission of virus from humans to mosquitoes and back again. They can provide information on how climate variations

influence dengue transmission, how transmission patterns can change over time and how the abundance of larval habitats may limit transmission. Interestingly, CIMSiM provides the first documented attempt to relate measure air temperature (macroclimate) to container temperature (microclimate); an approach which was later improved, taking into account water depth (Cheng *et al.* 1998). However in spite of this, the two models have some limitations in their use of data. These limitations include: assuming adult microclimate is identical to weather station observations, no estimate of the proportion of containers infested, no-density dependent population regulation at the egg stage, assuming that mortality rate is independent of age. Additionally, there are problems with the data used such as a suspected low number of weather stations supplying weather data and extreme variability in the quality of the biological data for the various life stages of *Aedes aegypti*.

The impacts of global warming on dengue have been predicted using the epidemic potential or critical density model developed by Martens *et al.* (1995, see Chapter 5) with specific adaptations for *Aedes* mosquitoes (Jetten and Focks 1997, Patz *et al.* 1998). Relationships between temperature and various parameters such as extrinsic incubation cycle, gonotrophic cycle, human virus titre generated by CIMSiM and DENSiM were used as explanatory variables in the model. It predicts that climate changes (represented here as temperature increases) will have the largest effect on dengue transmission in temperate regions, increasing both the latitudinal and altitudinal range of dengue as well as the duration of seasonal transmission. Because dengue transmission involves only one (or occasionally two) mosquito species, the dengue epidemic predictions can be better generalised than those for malaria. In addition, the DENSiM can be parameterised to incorporate more localised data, allowing risk assessment more applicable to the local level.

Statistical Models: Tsetse flies and African Trypanosomiasis

Because of a relatively large amount of data readily available from both historical and recent field surveys, a number of analytical models of African trypanosomiasis have been developed. The earliest models include descriptive models for the periodicity of epidemics (Rogers 1988) and the effects of vector seasonality on disease transmission dynamics (Milligan and Baker 1988). More recently developed approaches have all used statistical models (mainly discriminant analysis and multiple stepwise regression) to analyse the distribution of tsetse flies in various African locations. Entomological data

used in these models were obtained in two ways: by insect collections in a number of pre-selected areas along transects (e.g. Brightwell *et al.* 1992, Hendrickx *et al.* 1999) or from historical maps showing the presence and absence of tsetse (e.g. Rogers and Williams 1994, Robinson *et al.* 1997). Data from field surveys is potentially the most useful as this can provide abundance measures (assuming that trapping methods are standardised for all collection areas) while the use of historical maps is less advantageous because of a number of caveats including uncertainty about the original source(s) of entomological data as well as potential problems with determining the resolution of the map. The tsetse models have used either remotely sensed climate and vegetation data (Hendrickx *et al.* 1999, Rogers and Randolph 1993) or a combination of remote sensed and ground-observed data such as temperature and precipitation from meteorological stations (Brightwell *et al.* 1992, Robinson *et al.* 1997). The advantage of remotely sensed data is its availability across larger areas – i.e. unlike meteorological station data there is no need to interpolate between points when producing risk maps. However remotely sensed images are limited to recent times making the combination of historical tsetse distributions with recent satellite data (e.g. Robinson *et al.* 1997) somewhat inaccurate. Using their discriminant analysis model based on tsetse abundance (separated into low, high and medium), remotely sensed and ground measured climate data and remotely sensed vegetation, Hendrickx *et al.* (1999) predicted the abundance of *Glossina* spp. in Togo at a relatively high resolution of 0.125° (approximately 13.6 km) with between 63-75% correct predictions. Rogers and Randolph (1993) predicted the probability of presence for *Glossina morsitans* in Zimbabwe, Kenya and Tanzania with 79-84% correct predictions at a comparatively low resolution of 5-minute degrees (around 12 by 12 km) . By arbitrarily increasing the temperature in the models by 1 - 3°C, they predicted that the tsetse would extend into highland regions. The limitations of these predictions are the discrepancies between the use of historical (1890 and 1977) tsetse data and relatively recent satellite data as well as the rather crude simulations of global warming.

Statistical Models: Ticks and tick-borne diseases

The published studies on associations between environmental factors and ticks/tick-borne diseases have focused on both temperate (e.g. Lyme disease transmitted by *Ixodes scapularis*) and tropical regions (e.g. *Rhipicephalus appendiculatus* transmitting East Coast fever to cattle).

Using published records of *I. scapularis* presence and absence (point data) in combination with 8 km resolution NOAA AVHRR climate in a discriminant analysis model (including spatial autocorrelation), Estrada-Peña (1998) analysed the correlation between tick distribution and environmental factors throughout North America and Canada. A predictive map was constructed at 8 km resolution, showing the habitat suitability for ticks (probability of presence) at the continental level. The model predicted tick habitats with a 97% sensitivity and 89% specificity. On a more localised scale, Kitron and Kazmierczak (1997) analysed the spatial correlation between ticks, Lyme disease (at the county level) and remotely sensed vegetation data (NDVI) at a 1 km resolution in the counties of Wisconsin using correlation statistics (again corrected for spatial autocorrelation). Entomological data were again based on point data but these were converted to tick presence/absence and relative abundance for each county as a whole. Using the generated model, Lyme disease endemicity was predicted for all counties with no tick data. There was no attempt to validate the model with existing data. In Rhode Island, Nicholson and Mather (1996) used measures of tick density in 80 sample sites in combination with ground-observed vegetation, land use and hydrography (10 km resolution) to estimate tick densities across the whole of the state at a 10 km resolution. Again, no attempt was made to validate the predictions. For all of the above approaches, the main caveats are caused by the discrepancies between the resolution of entomological (typically points) and environmental data (grid cells of 1-10 km in size). By focusing the analysis and predictions on whole counties or large grid cells (pixels), rather than individual points or smaller pixels, much of the variation in the association between ticks and environment has been lost (i.e. geographical patchiness is not identified). Although the environmental factors related to ticks and tick-borne diseases have been identified at the coarse scale, there is still much work needed in order to produce more reliable and useful predictions at the localised level.

A single statistical model for the distribution of *R. appendiculatus* in Zimbabwe, Kenya and Tanzania was developed by Rogers and Randolph (1993). Using discriminant analysis, they identified relationships between tick observations (point data from historical maps) and remotely sensed vegetation and temperature and predicted the present and future distribution of ticks throughout the three countries at 5-minute resolution (approximately 12 km). The present distribution of *R. appendiculatus* was predicted with an accuracy of 72-73% and 1-3°C temperature increases (simulated arbitrarily in the model) were predicted to decrease the geographical distribution of this

tick in Zimbabwe. This study is heavily limited by statistical restrictions, hence the relatively low accuracy of predictions. As highlighted by the authors, discriminant analysis assumes that unsampled areas between points where ticks have been collected are unsuitable for ticks. This clearly reduces the ability of the model to predict correctly. Other approaches such as logistic regression could be more successfully applied to this kind of data.

Statistical models: Leishmaniasis

To date only a few attempts have been made to analyse the association between environmental factors and the distribution of sandflies or leishmaniasis. Cross *et al.* (1996) used published records on the presence and absence of *Phlebotomus papatasi* and leishmaniasis (to indicate vector presence or absence) at village/town level across Southwest Asia to determine the effect of ground observed climate (114 weather stations) and remotely sensed vegetation data on sandfly distributions. A discriminant analysis model containing only climate data was used to predict the monthly probability of vector occurrence for around 1,700 locations (0.5 being the cut-off for presence). The model predicted absence with a 74% accuracy and presence with a 67% accuracy. To simulate global warming, temperatures were increased by 1-5° and the probability of presence again calculated for each location (Cross and Hyams 1996). The simulated global warming was predicted to increase the geographic distribution and to extend the seasonality of disease transmission. This model is primarily limited by the original data (i.e. assuming that the presence and absence of leishmaniasis indicated presence and absence of sandflies) which may have created bias in the analysis. An additional problem is the use of only 114 weather stations in 9 countries in comparison to more than 800 locations with sandfly data. There are no indications to how climate data were derived from the extra 900 locations for which predictions of sandfly presence were made. In this instance, the use of 1 km resolution NOAA AVHRR climate data would have been ideal. Simulations of global warming are also somewhat crude as they do not account for changes in precipitation and are not immediately linked to any formal predictions (e.g. outputs from the Hadley Centre's climate change models).

Using data on the presence and absence of *P. orientalis* in 44 study sites in central Sudan, Thomson *et al.* (1999a) developed a logistic regression model to determine the relationship between sandfly distribution (point data) and ground observed soil type, vegetation and elevation data at 0.05° resolution (Elnaiem *et al.* 1998, Thomson *et al.*

1999a) as well as remotely sensed climate and vegetation data (5km resolution). From this model, a risk map of visceral leishmaniasis (i.e. the probability of *P. orientalis presence*) was created for Sudan. The model fit was quoted as good (residual deviance of 10.7 with 8 degrees of freedom). From the spatial perspective, this model uses more compatible environmental and entomological data. However, to equate the risk of leishmaniasis with *P. orientalis* presence is inaccurate. A number of other factors must be taken into consideration before any such approximations can be attempted. For instance, the use of sandfly density in the model (assuming that trapping methods were standardised) would have been more useful as a first step towards producing disease risk maps (vector abundance is an important variable in the calculation of R_0).

Statistical Models: Arboviruses

Because of its comparatively high impact, dengue has been the focus of most attempts to correlate disease-or vector distributions with environmental factors. The two biological models described above provided significant insight into population dynamics but did not attempt to produce any spatial risk maps. Using a statistical approach, Hay *et al.* (2000b) analysed the correlation between reported dengue cases collected from Bangkok hospitals during 1966 to 1998, ground observed climate (from one meteorological station) and El Niño Southern Oscillation parameters (e.g. sea level pressure and temperature) but found no significant association between climatic factors and disease patterns. They concluded that the fluctuations in dengue cases are therefore most likely caused by intrinsic parasite and vector factors. This study highlights how long-term disease data can successfully be used in combination with ground-observed environmental variables to study temporal fluctuations in infections.

Rift Valley fever (RVF) is the second most studied arbovirus with respect to environmental determinants of disease transmission. Linthicum *et al.* (1987) found that ground observed rainfall and remotely sensed vegetation (NDVI at 15 km resolution) were correlated with mosquito densities and RVF virus activity at village level in Kenya during 1982-85. In a study examining temporal disease fluctuations, remotely sensed vegetation and sea surface temperatures were found to be the best predictors of RVF activity during 1950-1998 (Linthicum *et al.* 1990). These examples show how both the temporal and spatial patterns in RVF activity can be predicted using ground measured and remotely sensed environmental variables. However, particularly the spatial study is

limited by the differences in the resolution at which disease data (village level) and environmental data (15 km) were collected.

Statistical Models: Indirectly transmitted helminth infections

Because most of the vector-transmitted parasitic worms have a comparatively low disease burden (WHO 2002b), there have only been few attempts to determine the environmental variables related to their distribution.

Lindsay and Thomas (2000) used published information on the presence and absence of lymphatic filariasis in 129 sites across Africa in a logistic regression model to determine the relationship between filariasis presence and climate factors derived from interpolation of 621 station measurements. The analysis was performed for the whole of Africa and on a subset of data from within Egypt only. Results indicated that the presence of lymphatic filariasis is positively asssociated with rainfall and minimum temperatures. The final model was used to map the population at risk of microfilaraemic sites at a resolution of 21.5 km^2 and was validated on a subset of the original data, excluded from the analysis. Predictions for the whole of Africa showed that 36-62 % (303-548 million) of the African population may be at risk of filariasis (depending on the cut-off for prediction of presence). The model predicted filariasis sites with an accuracy of 76%. The African risk map failed to identify risk areas in Egypt, most likely because of local differences in vector biology. This problem is the main limitation with the model; using explanatory data at a higher resolution would have enabled the authors to make more accurate predictions at a local scale.

Using microfilariae (mf) prevalence data collected in 201 villages in the Nile Delta during two years, Hassan *et al.* (1998a) analysed how the spatial distribution of mf infection was related to ground observed humidity and temperature (from two stations nearest to the 25mm and 50 mm rainfall isohyets). Thus, the climate data assigned to a particular study location depended on its proximity to either of the isohyets. Villages with high mf prevalence were shown to have higher temperatures and lower humidities than those with low mf prevalence. Although this study provides a preliminary indication of how climate determines the spatial distribution of lymphatic filariasis, it is limited by the crude climate data used. By assigning climate data from only 2 meteorological stations to over 200 villages spread across 5 districts (the furthest more than 100 km apart), any fluctuations in local disease patterns caused by climate patchiness are ignored. In another study of Nile Delta filariasis, Hassan *et al.* (1998b)

used similar mf data from 130 villages in combination with Landsat vegetation and moisture measures (28.5 m resolution) to predict the mf prevalence category (high or low) of the study villages. The resulting discriminant analysis model predicted high mf prevalence with an 80% accuracy and low mf prevalence with a 74% accuracy. The spatial resolutions of the explanatory and outcome data correlate well but predictions may have benefited from the inclusion of temperature data as the authors previously showed that mf prevalence is positively related to temperature (Hassan *et al.* 1998a).

Thomson *et al.* (2000) produced the only published example which describes the relationship between *Loa loa* prevalence and environmental factors. Data on the presence and absence of *Loa loa* from 100 locations in west and central Africa were collected from published papers (1953 to 1997) and combined with remotely sensed climate data (1km resolution) and soil profiles in a logistic regression model. The model was then used to produce a risk map of *Loa loa* in Cameroon, Gabon, Democratic Republic of Congo, Congo Brazzaville and Equatorial Guinea which was used to determine the extent of overlap between *Loa loa*-endemic regions and the use of ivermectin in the Oncocerciasis Control Programme. Because the model was not designed specifically to map only *Loa loa* risk (but rather examine if the future planning of ivermectin use may impact on *Loa loa* transmission) there was no attempt to validate the predictions. The main limitations with this approach is the use of long-term disease data in comparison with relatively recent satellite data as well as the small sample size (100 locations in 6 countries).

The geographical distribution of *Schistosoma mansoni* in the Nile Delta was described by Malone *et al.* (1994) using NOAA AVHRR vegetation and temperature data (5.5 km resolution). Parasite prevalence data were obtained from surveys in 41 villages and were correlated with diurnal temperature differences and NDVI using correlation statistics. Areas with high prevalence of *S. mansoni* were found to have lower temperature differences, suggesting that remotely sensed data may be used to construct disease risk maps. Like others, this study could also be improved by using higher resolution environmental data. The results presented by Malone *et al.* (1994) were confirmed by Abdel-Rahman *et al.* (1997) who found that densities of *Biomphalaria* snails in Egypt were positively associated with low diurnal temperature ranges. They used well correlated outcome and explanatory data; snails were collected in waterways at the village level while temperature differences were derived from NOAA AVHRR images at a 1.1 km resolution. Also in Egypt, *Yousif et al.* (1998) correlated the seasonal

abundance of snails collected from 3785 sites with locally measured temperature and showed that fluctuations in snail densities correlated well with temperature oscillations. The spatial distribution of snails was show to be highly clustered in canals and drains. A similar, recent study using GPS defined locations of local geographical features showed that high prevalences of *Schistosoma haematobium* infections in Tanzania occurred near Lake Victoria which provides a suitable habitat for the aquatic snail intermediate hosts (Lwambo *et al.* 1999). Both of these examples did not attempt to quantify the relationship between spatial or temporal environmental factors and disease risk, instead using visual interpretation of GIS maps.

Conclusion

From the studies discussed above it has become clear that the use of environmental variables to predict present and future disease and vector distributions has great potential. By looking at the published literature we can learn how best to approach the problem of gathering relevant data; how to obtain accurate disease and vector data and which environmental factors may be readily available at suitable resolutions in currently endemic countries. Although vector-borne diseases are of most importance in tropical areas we should not neglect the historical impact that, for instance, malaria had in temperate regions such as North America and Europe. As a general rule, we must learn about history before we can understand the past. Thus, it is necessary to investigate how our current methods of describing disease patterns using climate and land cover data can be adapted to studying past trends in vector-borne diseases. This thesis will examine how a combination of biological and statistical, remotely sensed and ground-observed environmental data can be applied to predictions of malaria risk in a non-endemic region, namely Europe. The ultimate goal of the thesis is to contribute to the avert debate on the risk of malaria re-emergence in England and throughout Europe.

Ague in 19th Century England and Wales

Abstract

From historical records we know that a malarious illness referred to as 'the ague' caused high levels of mortality in the English and Welsh marshlands and fens from the 15th to the 19th century. From the early 1800s, physicians throughout the country reported a decline in ague cases which has mainly been attributed to marsh drainage, increased livestock densities as well as improved health care. Although this theory is widely accepted the relative importance of the different factors has only rarely been discussed and never quantified.

This study uses ague data collected from 43 English and Welsh counties during 1840 to 1910 to analyse the role of climate, agricultural factors and land cover in the inter-annual variation of ague death rates. Multivariate logistic regression modelling showed that temporal ague patterns were positively related to marsh wetland coverage, average temperatures and precipitation and negatively associated with cattle densities. Above average temperatures and precipitation patterns were most likely responsible for the ague epidemics in 1848 and 1859 but there was no evidence for any climatic impact on the long-term malaria trend which was surprisingly consistent during the study period. A model developed to examine the spatial pattern (i.e. inter-county variation) in ague deaths contained the same explanatory variables with effects in the same direction as those of the temporal model, indicating that the impact of these environmental factors were the same on both spatial and temporal levels. In contrast, the four explanatory variables for ague death rates had opposite or no effect on temporal variation in all-cause mortality which suggests that the variation in ague was not merely reflecting factors which affected general mortality. Using the derived coefficients, it was simulated how ague deaths in any year may have changes if cattle densities and marsh wetland coverage had remained at 1840-levels. These results indicated that at least 19% of the drop-off in ague was attributed to the increasing cattle population and draining of marshes (of which approximately 60% was due to marsh draining alone). Thus, using quantitative models containing extensive historical datasets, it has been confirmed that the consistent temporal decline of English and Welsh malaria was driven mainly by agricultural factors.

Introduction

As referred to in Chapter 1, a number of previous studies have demonstrated how environmental data can be used to define spatial variation in malaria throughout currently endemic areas with the ultimate goal of predicting future transmission patterns. In regions where the disease has disappeared as a result of natural causes or eradication programmes, the most informative approach is to analyse how climatic and other factors of interest impacted on the historic inter-annual variation. Using such an approach, this study will examine the relative roles of climate, agricultural and other environmental factors in the disappearance of English and Welsh malaria (or 'ague') during the 19th and 20th centuries. Quantitative estimates of how these factors impacted on the temporal ague patterns will enable us to make more qualified assumptions about the potential re-emergence of malaria in England as a result of future climatic – or other environmental - changes.

The geography of ague

Evidence of the presence of a malarious illness in England go back as far as the 11th and 12th century when the Anglo-Saxons described the continued fever 'lencten ádl' (spring ill). References to 'ague' or 'intermittent fevers' became more common during the following centuries and are evident in the works of William Shakespeare and Daniel Defoe. Oliver Cromwell reportedly died from the ague and when Sir Walter Raleigh awaited execution in the Tower of London, recurrent fevers troubled him. He prayed 'that he might not be seized with an ague-fit on the scaffold, lest his enemies should proclaim that he had met his death, shivering with fear' (MacArthur, 1951). Descriptions of severe epidemics during the sixteenth and seventeenth centuries indicate that the disease, although not one of the great killers, was responsible for many deaths. According to Ewart (1897), the mortality from agues in London in 1558 'was such that the living could hardly bury the dead'.

The English marshlands and fens in particular were singled out for their unhealthiness due to the 'noxious vapours arising which subject the inhabitants to continued intermittents and shorten their lives at a very early period' (Dobson 1997, Nicholls 1997). The most 'agueish' areas of London (Pimlico, Battersea, Chelsea, Plaistow and along the River Lea) were all very swampy with unhealthy inhabitants (Ewart 1897). In the rural areas, marshland burial rates were 2-3 times higher than in neighbouring

parishes and the life expectancy at birth in the marshes was less than 30 years (Dobson 1980, Dobson 1997). More than 50% of all recorded deaths from parish records were in the under 10 year olds. This would be consistent with the hypothesis that these deaths were due to malaria as most malaria deaths today are reported in children (Greenwood and Mutabingwa 2002). From descriptions of ague throughout history, it has become clear that the disease was distributed throughout the fens (Cambridgeshire, Huntingdonshire, Lincolnshire, Norfolk and Suffolk), along the Thames Estuary in London, Kent and Essex, by the south-east coast of England, in the Somerset Levels and in Lancashire and Yorkshire.

When Defoe visited the Essex marshes in 1722, he was told that:

> the men always go into the uplands for a wife, and when these young lasses come out of their wholesome native air where they were healthy, fresh and clear, into the marshes, among the fogs and damps, they get the ague and seldom last above half a year or a year at most. Then the men go to the uplands again and fetch another, so that it is very frequent to meet with men that have had from five or six to fourteen or fifteen wives, "nay, and some more!"

In the seventeenth century Thomas Sydenham, perhaps the most influential physician in historical England, wrote that 'if one spends two or three days in a locality of marshes and lakes, the blood is in the first instance impressed with a certain spirituous miasma, which produces quartan ague' (Creighton 1891).

According to Dobson (1997), vicars in the 18th century rarely lived in their marshland parishes because of the 'badness of the situation and unhealthiness of the air'. The vicar of Northfleet commented that 'the Thames having a very foul shore in this parish which is inclosed within land by many salt marshes I soon found myself attacked by so many repeated agues'. As late as 1870, the garrison at Tilbury fort in Essex was still changed every six months due to the prevalence of ague in the soldiers (MacArthur 1951). Inhabitants of the marshes were generally described as ignorant, apathetic, dull and sluggish and, in some cases, likened to the beast of the land (Dobson 1997). This pattern of notorious fevers and ill-hued inhabitants was the same throughout the marshes and fens of England and even across the European continent.

The miasma theory

Because of the close association with wetlands, the ague was directly attributed to the vapours and stagnant waters of marshes and fens, a term now known as 'marsh miasmata'. This miasma theory led to the use of the word 'mal'aria' meaning 'bad air'. The word was introduced to England in 1740 by Horace Walpole who, after travelling in Rome, came across the disease and wrote' there is a horrid thing called mal'aria, that comes to Rome every summer and kills one...'. However, ague remained a household word well into the early 20th century where most lay people and even many physicians continued to use the term (Bruce-Chwatt 1976).

During the 1860s, the search for the airborne agents of malaria had begun both in the USA and in England. After the publication of Koch's Germ Theory in 1876, Klebs and Tommasi-Crudeli argued that ague was really caused by a bacillus (*Bacillus malariae*) which had been seen in the blood of several patients (Worboys 1994 and Bristowe 1880). In spite of this, there was no shift in the theory of ague transmission and the vast majority of physicians still strongly believed in the miasma hypothesis. Consequently, Laveran's discovery of the *Plasmodium* parasite in 1880 was poorly received and even refuted by many practitioners (Nicholls 1997). When the elucidation of the parasite and, later, the role of the *Anopheles* mosquito, came about in the early 20th century, ague fevers were largely a thing of the past and little attention was therefore paid to determine whether the few remaining cases were really of malarious origin. Today our best means of resolving the puzzle of ague therefore lie in careful examination of historical literature.

Distinguishing ague from other fevers

There is no convincing evidence that the epidemics of various agues ('ague', 'burning ague', 'strange ague' and 'quartan ague') during the 15th and 16th century were of malarious origin and it has been hypothesised that many of the intermittent fevers described by Sydenham and his contemporaries later on in the 17th century were also not malaria (Bruce-Chwatt and de Zulueta 1980). An exception was Talbor (1672) who described ague symptoms and pathology which strongly indicated malaria (see below) while most other accounts of ague were less likely to have been malaria (e.g. Willis 1685). These problems relate mainly to medical terminology. 'Ague' literally means 'acute' and thus any sudden onset of fever (influenza, typhoid and remittent fever and malaria) may often have been classified together under the term ague.

The trial of cinchona bark (Peruvian bark) or quinine on a large scale during 1780-86 was of great importance in the differentiation of true malaria and it gradually emerged that the only types of ague which were susceptible to cinchona bark were mainly limited to the marshes and fens. This was the first point at which (malarious) ague started to be separated from the other acute fevers. Following this, the first half of the 19th century was a period of even greater advance in fever differentiation. Creighton (1891) states that from 1830-40, the 'three grand types of fever' (i.e. remittent fever, typhoid fever and relapsing fever) had become so clearly distinguished from each other and from ague that 'no one remained in doubt or confusion' (Table 2.1). Evidence suggests that, by the 1840s, the majority of reported ague cases were most likely due to malaria. At this time, the pattern of ague symptoms was so striking and characteristic that most physicians would diagnose correctly (Ewart 1897) and could even give an accurate account of the distribution of the disease in the whole country (Whitley 1863).

Signs, symptoms and treatment

By piecing together evidence based on descriptions and observations from 19th century standard medical textbooks and manuals and historical scientific accounts, a picture emerges of a disease which bears a striking resemblance to malaria and can probably not be ascribed to any other category of diseases (Tanner 1854, Barlow 1861, Aitken 1866, Tanner 1865, Bristowe 1880, Hartshorne 1881, Taylor 1891, Aitchison 1893, Taylor 1893, Taylor 1894). According to such medical textbooks, the ague that we now believe to be malaria was characterised by a tertian fever (tertian indicating that the patient had a paroxysm or ague fit every two days). The fit consisted of three stages: the cold, the hot and the sweating stage. The cold stage lasted for 3-4 hours while the hot stage could last from 3-12 hours and the sweating stage 2-4 hours. After the blood circulation had returned to normal, the patient would be free from an attack until the 'morbific matter' again gathered in the spleen, causing another attack several days, weeks or months after the primary episode (Talbor 1672). Unlike typhoid fever, ague was not considered contagious and there were no recommendations for physicians to avoid infection. Throughout the endemic regions, the most prevalent ague (i.e. majority of cases) was observed in the spring or early summer (infections acquired the previous year) and in the autumn (infections acquired the present year). "Have you had your ague this spring" was a common greeting among the marshland

inhabitants in the nineteenth century. It was also common knowledge that, unlike all other fevers which gradually disappeared, ague would reappear again and again throughout the season (Worboys 1994). These observations closely resemble current diagnostic evidence based on knowledge of the *Plasmodium* parasite life cycle (Manson 1987). The pathology of ague is one of the most convincing links to malaria: invariably the patient would be anaemic, suffer from splenomegaly and 'morbid liver changes'. The enlargement of the spleen was such a characteristic feature of ague that it was referred to in medical reference books as 'ague cake'(Talbor 1672). Aitken (1864) reported that the spleen of some patients with ague cake could weigh as much as 10-30 pounds compared to 5-7 ounces in a healthy adult.

Until the 18th century there were many traditional treatments of ague. Opium pills which provided temporary relief (or escape) from symptoms were sold in local shops (MacArthur 1951) and other more puzzling antidotes included consumption of burned rods (Dobson 1997) and small quantities of arsenic (Tanner 1854) and displaying notes with the inscription 'Ague farewell, till we meet in Hell' on the patient. However, the only effective remedy was quinine, the use of which became widespread in the 18th century and significantly sped up the separation of ague from remittent, relapsing and typhoid fever.

In summary, the characteristic signs of ague which differed from those of the other three grand fevers and demonstrate that this disease was most likely malaria were: (1) non-contagious transmission (2) distinctive cold, hot and sweating stages, (3) periodic (tertian) onset of symptoms, (4) relapses following the primary attack, (5) anaemia, (6) splenomegaly or 'ague cake and (7) yield to quinine (Table 2.1).

Table 2.1. Relationship between ague and the three other grand fevers of the 19th century (based on information from 16th – 20th century medical textbooks).

Disease	Transmission	Stages	Symptoms and Pathology	Treatment	Timing
Ague (Intermittent fever, marsh fever)	Non-contagious	Cold, hot and sweating stages. Fever not continuous.	Sudden onset. Anaemia, jaundice, enlargement of liver and spleen (ague cake). No abdominal pains and diarrhoea. No immunity.	Quinine, opium. Quinine breaks chills but does not prevent relapse.	- Highly regular relapses every 24 (quotidian),48 (tertian) or 72 hours (quartan). - Relapses occur again and again until cure is effected. - Disease can persist for months or years. - Cases peak in early spring and autumn.
Remittent Fever (Lake fever, pernicious fever, malarious yellow fever)	Non-contagious	Cold (frequently absent), hot and sweating stages. Continued fever.	Sudden onset. Enlargement of spleen and liver, cerebral affections (severe headache), diarrhoea, abdominal pain and black vomiting. No anaemia. No immunity.	Blood letting, opium, quinine (used as a tonic).	- Irregular relapses every 12-36 hours. - Five or less relapses. - Disease lasts for 7-21 days. - Cases peak in autumn.
Typhoid Fever (Enteric fever, bilious fever, common continued fever)	Contagious	No well-defined stages. Continued fever.	Gradual onset. Swelling of abdomen, rose coloured spots, convulsions and watery diarrhoea. No jaundice. Immunity to second infection.	Wine, calomel, castor oil, opium, mustard poultices, bismuth. Prevention: ventilate rooms, dispose of stools in chloride of zinc, disinfect bedclothes and water closet.	- No relapses. - Disease lasts for 20-23 days. - No seasonal pattern.
Relapsing Fever (Five-day fever, seven-day fever, bilious relapsing fever)	Contagious	No well-defined stages. Continued fever.	Sudden onset. Rigors, headache, jaundice, enlarged liver and spleen, constipation and vomiting. No immunity.	Castor oil, opium, calomel.	- Symptoms terminate 5-8 days after onset. - Relapse on the 14th day. - Two to five relapses. - No seasonal pattern.

Transmission

As described above, the signs and symptoms of ague were relatively well understood but the mode of transmission remained a mystery. Centuries ahead of his time, but not necessarily referring to mosquitoes, Sydenham wrote in 1666 ' When insects do swarm extraordinarily and when...agues appear early as about midsummer, then autumn proves very sickly'. Because of the distinctive association between wetlands and the ague, the main vector at the time was most likely *Anopheles atroparvus* which is known to breed in the brackish waters of marshes and fens. A less important vector, near forests and in cities, is the tree-hole mosquito *An. plumbeus* which is thought to have been responsible for the last two indigenous cases of *P. vivax* in south London (Marchant *et al.* 1998). *An. atroparvus* which rests indoors in animal stables or human dwellings feeds mainly on cattle and pigs but also on humans. The adults undergo incomplete diapause; i.e. they overwinter in warm buildings whilst continuing to feed, thereby making it possible for malaria transmission to occur during the winter as it was famously observed in Holland (Bruce-Chwatt and de Zulueta 1980). Service (1968) collected data on the seasonal abundance of *An. plumbeus* on Brownsea island in Devon by three weekly human bait catches during 1964-1966 which indicate that the mosquito starts emerging in May and finishes the outdoor season in October (Fig. 2.1). This correlates with the general assumption that the outdoor mosquito season in England starts in April-May and finishes in September or October (Jetten and Takken 1994).

Figure 2.1. Monthly total *An. plumbeus* caught in bait catches at Brownsea island (Dorset) during 1964 (from Service 1968).

The parasite responsible for ague is thought to have been *Plasmodium vivax* which can persist as a dormant hypnozoite in the liver during colder seasons, enabling it to cope with the English climate. As shown by Daskova and Rascinyn (1982) South American, African and Asian strains of this parasite are able to develop to the sporozoite stage in European *An. atroparvus* (see Table 4.4 page 150) suggesting that the mosquito is able to support development and possibly transmit tropical *P. vivax* strains. On the other hand, Shute (1940) and Ramsdale and Coluzzi (1975) demonstrated complete refractoriness by *An. atroparvus* to African *P. falciparum* while Marchant *et al.* (1998) were able to infect one (out of 5 fed) *An. plumbeus* with African *P. falciparum* to the oocyst stage. Additionally, James *et al.* (1932) showed that Italian *P. falciparum* were able to develop to the sporozoite stage in English *An. atroparvus*. These results show a strong possibility that ague was caused by *P. vivax* but also that there may have been some transmission of a *P. falciparum* strain which was possibly different to tropical strains.

However, if the parasite was indeed *P. vivax*, then the high ague death rates observed in this study and commented on by previous authors (Dobson 1997, Reiter 2000) are surprising. The present form of tropical *P. vivax* is relatively benign and very rarely fatal and could not have been responsible for such mortality rates. However, it has been hypothesised that the historical English (and North European) *P. vivax* may have been a different, more lethal

strain of the parasite we know today. Another possible explanation is that the observed deaths were due to co-infections with *P. vivax* and a non-vector borne disease such as gastric enteritis (Willem Takken and David Bradley, personal communication). Infection with *P. vivax* would have weakened the patient who was then more susceptible to - and less likely to survive - a secondary infection. As suggested above, an alternative explanation suggests that the high death rates in England were due to transmission of the European strain of *P. falciparum* which is now extinct. Microscopic evidence suggests that this parasite caused major epidemics with high death rates in Russia and Poland in the early 20th century (Reiter 2000) and in Italy before that time (Bruce-Chwatt and de Zulueta 1980) but it is uncertain whether it could have been transmitted by *An. atroparvus* at higher latitudes. Because the parasite strains involved are now extinct the question of which parasite caused the high ague death rates in England will most likely never be resolved.

The disappearance of ague

A natural decline in the incidence of ague began in the early 19th century and Willan was among the first to comment on this in 1800. He wrote that ague epidemics had not been seen in London for the past twenty years due to the 'practice of draining, and the improved models of cultivating land in Essex, Kent and other counties...' (from Creighton 1891). In 1863, George Whitley in his extensive report on ague in England quotes comments from medical practitioners who had observed the demise of ague on a first hand basis: 'there has been a decided decrease in the amount and severity of intermittent diseases since 1860' (Isle of Sheppey), 'ague is greatly on the decrease' (Milton), ague was formerly extremely common and very severe, but [has been] gradually on the decrease' (Gravesend), ' ...30 years ago there was a good deal of ague which decreased gradually...' (St. Ives), ' much ague from 1827... until 1831 (Christchurch). This report highlights what is known to be the last epidemic of ague in 1857-59 which caused high levels of mortality throughout the endemic regions. In 1897, Dr William Ogle from St. George's hospital stated that '... in the fifties, cases of ague were by no means rarities. They came to us from Kent and the lower Thames valley. I was surprised when in the seventies...I was unable for many months to find a case either at St. George's or at other hospitals..'.

Indigenous transmission at epidemic levels occurred after the First World War in the Isle of Grain (Kent) where *An. atroparvus* spread imported *P. vivax* to more than 50% of the population. To prevent a similar outbreak after World War II, infected soldiers were deliberately, and with remarkable success, kept out of areas where malaria was most likely

to spread. During 1940-1947, only 43 indigenous cases were reported compared to almost 500 cases in 1917-1920 (Shute and Maryon 1974, Bruce-Chwatt and de Zulueta 1980).

Accompanying the decline in ague was also an apparent decrease in the severity of symptoms. Mild 'chills' were reported from locals in Kent who had never been abroad and found to be caused by infection with malaria parasites.

Many unsubstantiated but commonly accepted hypotheses have been put forward to explain the slow disappearance of ague from England. The main factors identified are (1) drainage of marshes (land reclamation) (2) Increased livestock densities (3) Improved housing (4) Better access to healthcare and medication and (5) Improved nutrition, sanitation and hygiene.

According to almost all physicians interviewed by Whitley in 1863, the decrease in ague could be explained by the land drainage (i.e. the removal of mal'aria) throughout the marshlands. It was believed that marsh drainage would have reduced the number of *An. atroparvus* breeding sites and hence adult densities. However, James (1929) reported that, in spite of the wetlands disappearing, mosquitoes were still prevalent throughout most rural districts in greater abundance than 'in many exceedingly malarious places in the tropics'. Indeed, *An. atroparvus* is still present in English marshlands today in a so-called 'anophelism without malaria' situation and therefore the partial removal of breeding sites alone does not necessarily fully explain the decline of ague throughout England.

Vast agricultural changes (such as crossing and rotating crops) in the 19th century led to the availability of more and better livestock foods (crops) which increased the size, health and density of cattle, pigs and horses. Consequently, increasing numbers of animal stables were constructed - usually at larger distances from human houses to reduce the disruption from animal noise and waste. This may be one of the first examples demonstrating that decreasing human proximity to cattle also decreases the chance of disease transmission - a theory that has stimulated investigations of the efficacy of zooprophylaxis in areas currently endemic for malaria (Hewitt *et al.* 1994, Bouma and Rowland 1995). The stables additionally provided more favourable resting habitats (i.e. dark and moist) than human dwellings which had become better lighted, ventilated and less crowded due to socio-economic developments. Thus, feeding by the zoophilic *An. atroparvus* gradually diverged towards the livestock, reducing the human-mosquito contact necessary for malaria transmission.

Another strong influence on malaria prevalence at that time was the increasing availability and decreasing price of quinine. As its effects became more evident, people would make

more frequent trips to the chemist to purchase quinine, encouraged by the falling prices. In 1840, a drachm (approximately 4 grammes) of quinine cost £1 while the cost fell to 8 shilling 6d per ounce in 1875 and 10d per ounce in 1892 (James 1929, Dobson 1980). Partial immunity from decades of exposure to ague, improved nutritional status due to better diets and better overall health because of decreases in other infectious diseases such as typhoid, cholera and smallpox are all thought to have had an influence on the severity of ague symptoms. General sanitation and hygiene (including health systems) also underwent extensive improvements during the 19th century. For instance in London, after the Great Stink of 1858 when the consequences of pumping sewage into the Thames became apparent, a sewage system was constructed in a major effort to clean up the Victorian city.

Studying historical patterns in malaria using climatic and agricultural data

Though the many theories about the disappearance of ague from England are widely accepted, the relative importance of the different factors has only rarely been extensively studied and never quantified. In 1920, Angus MacDonald noted the strong correlation between high summer temperatures and increased ague cases. He observed that, in 1859, there were 49 consecutive days with temperatures above 15.5°C or 60°C (often assumed to be the developmental threshold for *P. vivax* although development has also been observed at 15°C, George McDonald 1957) and 371 cases of ague in Kent. Indeed, as described elsewhere, the ague epidemic of 1857-59 had been ascribed to the unusually hot summers by most observers. Gill (1920-21) showed that the endemic malaria cases of the early 20th century were all distributed within a zone where the mean monthly temperature during July and August was between 15.5-16.7°C (Fig. 2.2). Dobson's analysis of crude burial rates (i.e. deaths from all causes) showed uncommonly high levels of mortality in the marshlands which had 3-4 times higher burial rates (especially evident in 0-5 year old children) than non-marsh parishes (Dobson 1980). Burial rates peaked in the autumn and early spring which correlated with the pattern exhibited by malaria cases in other areas of Europe where *P. vivax* was transmitted (relapses in the spring and new infections in the autumn). However, because this study focused on deaths from all causes, it does not enable us to make any real conclusions about malaria. The pattern observed by Dobson (1980) may also have been caused by the strong seasonality of some food-and water-borne diseases. For instance, Elliott *et al.* (1983) showed that the incidence of gastro-enteritis in Nottingham during the 1980s was highest during the summer months. This positive association between diarrhoeal diseases and temperature has also been well documented in the tropics using 20-

year data on diarrhoeal notifications in Fiji and Peru (Checkley *et al.* 2000, Singh *et al.* 2001). Duncan (1993) graphically presented the correlation between years of malaria outbreaks ('malaria years') in Scotland and England, summer precipitation and temperatures during the 16th to the 19th century and concluded that malaria outbreaks coincided with hot, wet summers. There was no attempt to quantify the roles of climate in these outbreaks and no measures of disease prevalence or mortality were used. The term 'malaria year' referred to malaria outbreaks but it is not clear how many cases or deaths defined an outbreak. Temperatures were derived from the central England temperature dataset which provides average temperature measurements for central England only and thus does not identify spatial variation in climate (especially in the marsh areas in south-east England).

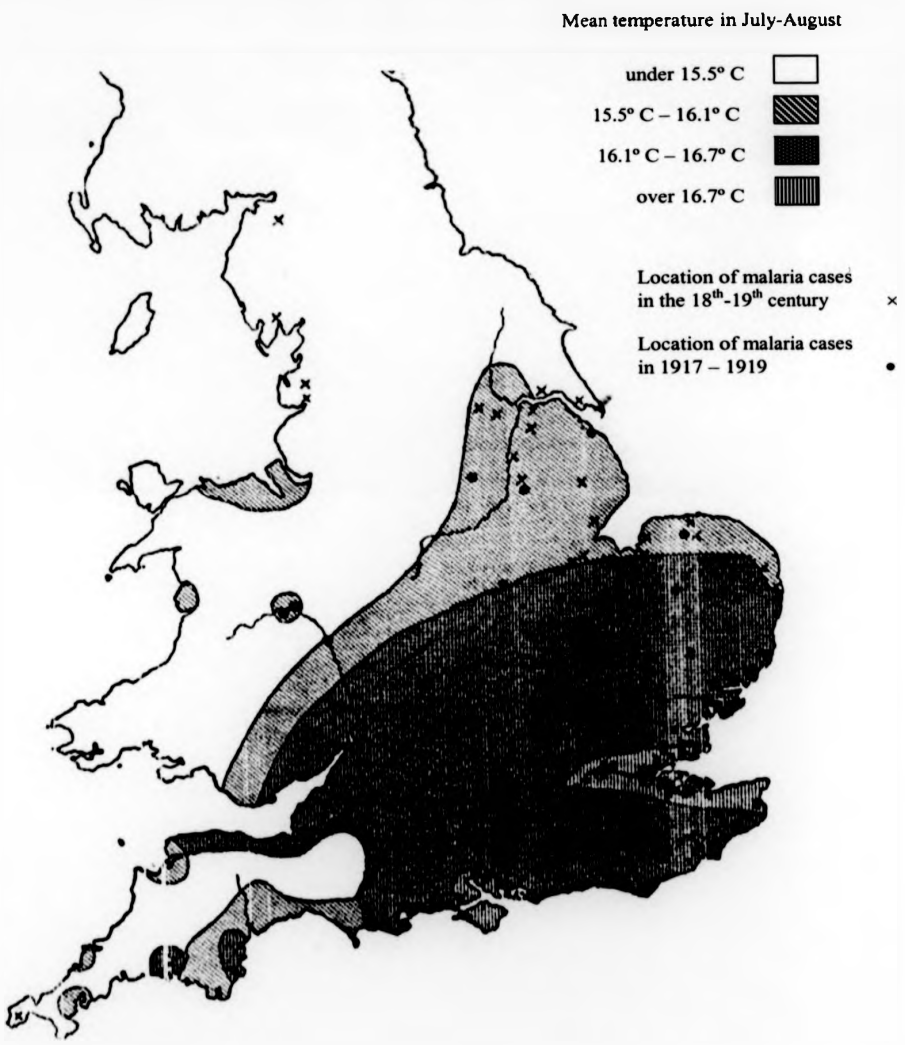

Figure 2.2. Distribution of malaria in different temperature zones during the 18th - 20th century (From Gill 1920-21).

Considering the potentially large amount of data available in the tropics, studies of inter-annual variability in malaria in these areas may provide useful information applicable to understanding present distributions both in the tropics and temperate regions. However, there have been remarkably few of these. Using long term (1867 to 1943) data on fever deaths during October to July from both the Punjab and Sri Lanka Bouma *et al.* (1996) and Bouma and van der Kaay (1996) showed that temporal peaks in fever deaths (assumed to be malaria epidemics) were positively correlated to sea surface temperatures (SST) which are directly linked to the El Niño Southern Oscillation. The quality of the disease data in these studies is debatable. Fever deaths will incorporate deaths from a variety of diseases which are not necessarily malaria but may also show seasonal trends (e.g. gastro-enteritis as discussed above). Rainfall data were derived from 20-121 meteorological station measurements (depending on year) while temperature data were from the eastern equatorial Pacific SST dataset at an unknown resolution. In a similar study, Bouma and Dye (1997) analysed malaria mortality data from 1910-1935 in 21 Venezuelan states and found strong positive correlations between malaria outbreaks and drought in the preceding year. Again rainfall data were ground observed measurements (from 29 stations) which had been converted to averages for the entire state. In Colombia, Bouma *et al.* (1997) showed that the deviation in the trend of reported malaria cases (passive case detection) during 1960-1992 was positively correlated with El Niño years and sea surface temperature anomalies (from the eastern equatorial dataset). The main limitation with this study is the use of data at country level only (i.e. only one region is analysed) while, in comparison, the study presented here uses data from 43 counties to analyse the inter-annual variation in malaria death rates. Recently, Hay *et al.* (2000b) analysed monthly hospital admissions for malaria in Kericho, Kenya during 1966-1998 in relation to mean monthly temperature and total precipitation from one meteorological station as well as parameters of the El Niño Southern Oscillation. As there was no evidence of an increasing trend in temperatures, Hay *et al.* concluded that the observed recent increases in malaria admissions, cases fatality and patients originating from highland areas (Shanks *et al.* 2000) were most likely due to intrinsic population factors, including drug resistance.

Although an association between agricultural practices and malaria distribution and prevalence both in tropical and temperate regions has been suggested and discussed numerous times (e.g. de Zulueta 1994, Coluzzi 1994, Mouchet *et al.* 1998, Ijumba and Lindsay 2001), there have only been few attempts to quantify the role(s) played by relevant factors. In a notable example, Lindblade *et al.* (2000) showed that houses

situated alongside swamps in Uganda had higher mosquito densities, sporozoite rates and entomological inoculation rates - i.e. a higher risk of malaria. The presence of any animals outside the house additionally increased the density of indoor resting mosquitoes by 60%.

As shown above, past studies have demonstrated the feasibility of linking historical malaria outbreaks to temporal fluctuations in climate. The quality of the malaria data used on previous occasions varies: from 'year of malaria outbreaks' (with no definition of outbreak) to using all deaths from fever and, in the most reliable assessment, using malaria morbidity. This study will attempt to use disease data which are as accurate as possible, namely by analysing reported mortality from English 'ague' - an affliction which is strongly suggestive of malaria. In concordance with previous work, historical climate data will consist of measurements from meteorological stations throughout English and Welsh counties and - later in the study period - from a gridded climate database. Explanatory variables will consist of agricultural factors such as cattle and pig densities as well as land use, all of which have been associated with the distribution and later decline of malaria in this country.

Aims and Objectives

The aim of this study is to quantify the role of environmental, climatic and agricultural factors in the temporal variation of ague (or malaria) deaths in English and Welsh counties during 1840-1910. The starting period of 1840 was selected because at this time ague had been very well distinguished from other acute fevers with which it had been previously classified (see Introduction) and we can be confident that the majority of ague deaths used in the database were really due to malaria. The study terminates in 1910 as this was the last year that deaths from ague were reported at county level. Agricultural data were collected at the county level while climate data were derived from low resolution gridded databases or meteorological station measurements.

The specific objectives of the study are:

1. To map the geographical distribution of ague deaths at county and statistical district level and compare this to various historical records of ague (or malaria)
2. To test whether inter-annual variability in ague death rates within English and Welsh counties was significantly affected by inter-annual changes in cattle and pig density, crop acreage, wetland acreage, temperature and precipitation.
3. To quantify the impact of changes in these parameters on the inter-annual variability of ague (by model simulations).

This study will be the first to quantitatively investigate the link between climate, agriculture and the decrease of English malaria. By doing this, we will be able to test the common theories about why malaria disappeared from this country and show in a 'virtual experiment', using predictive modelling, how the extinction of the disease may have been delayed or advanced if one or several of the explanatory factors had remained unchanged or been altered in a different way.

Methods

System of recording deaths

During the study period from 1840 to 1910, any death was recorded first at the parish level by the local physician and noted in the bills of mortality which stated the cause of death as well as the patient's name, age and address. All parish deaths would then be reported to the corresponding statistical district. A statistical district was a large parish (or town) which accumulated and reported mortality and population data from the surrounding smaller parishes. The data from the statistical districts would ultimately be assembled at county and country level by the Registrar General who was responsible for producing an annual report of mortality statistics at statistical district, county and country level.

Malaria ("ague") and other deaths

Measures of ague deaths and deaths from all causes (excluding accidental and violent deaths, suicides and stillbirths) at county and statistical district level from 1840 to 1910 were collected primarily from the Annual Report of the Registrar General published by His Majesty's stationery offices. On 5 occasions, ague deaths were not recorded for London and were instead collected from the Weekly Notifications of Infectious Diseases.

Data from 43 counties (as defined geographically in 1840) and 316 statistical districts were available for the whole period. Over the 70 year period, 2 counties were separated into smaller regions (North and South Wales both separated into 6 new counties in 1903) and all ague or total deaths for these were pooled to comply with the original (1840) county borders. At different times deaths were reported either for the whole of Yorkshire or separately from the three counties North, East and West Riding. For continuity, all data from Yorkshire were collected only for the whole county and not separately for North, East and West Riding.

As shown in Appendix 2.1, deaths in the Annual Report of the Registrar General were classified under headings and sub-headings. No deaths were shown as '-'. In 1840, there were 102 causes of death registered (excluding accidental, violent deaths, suicides and stillbirths), in 1880 there were 141 and in 1900 there were 157 causes of death (Appendix 2.2).

During 1840 to 1870, ague was classified as a subcategory under the heading 'zymotic diseases' together with 15 other diseases (Appendix 2.1, 2.3 and 2.4). In 1871 'zymotic

diseases' was split into four sub-headings: enthetic, dietic, parasitic and miasmatic. Ague and 15 other diseases were classified as 'miasmatic diseases'. In 1881, ague and remittent fever were still classified as 'zymotic diseases' but were now listed under their own sub-heading 'malarial diseases' which contained only the two. In 1901, ague was renamed malaria and listed as a separate disease. The database used in this study contains measures of deaths from ague only as these are the most likely to represent true malaria deaths. During the 70-year period, deaths from 11 other fevers were reported in all three sources (Table 2.2).

After 1910, malaria deaths or cases were no longer reported at county level in the Annual Report of the Registrar General. From 1919 to 1997, the number of indigenous and imported malaria cases and deaths due to malaria were recorded in the Ministry of Health report by the Chief Medical Officer on the state of the public health. There was no distinction of deaths due to indigenous and imported cases. From 1998 onwards, the same data were provided by the Malaria Reference Laboratory at the London School of Hygiene & Tropical Medicine.

Table 2.2. List of all fever deaths reported in mortality statistic sources during 1840 to 1910.

Ague
Cerebro-spinal fever
Influenza
Puerperal fever
Relapsing fever
Remittent fever
Rheumatic fever
Scarlet fever
Simple-and ill defined fever
Splenic fever
Typhoid fever
Typhus fever

Demographic, environmental and agricultural data

Annual population figures for each county up to 1910, interpolated from 10-year population census data - were taken from the Annual Report of the Registrar General.

Total county land cover (i.e. size) and water acreage (inland water, including marshes,

rivers, lakes and brackish water areas) for each county in each year were collected from the Annual Report of the Registrar General.

Crop acreage (all crops, bare fallow and grasses) and the number of pigs and cattle at county level were available at 5 year intervals. These were provided by the Ministry of Agriculture, Fisheries and Food (MAFF), now known as the Department of Environment, Food and Rural Affairs (DEFRA).

Water and crop acreage were converted to percentages of total county size and pig and cattle numbers to animal density per 100 acres of land. Annual crop acreage and pig and cattle densities were calculated by smoothing two 5-year values into 10 annual values.

Climate data

Climate data for each year during the 70 year period were extrapolated from two databases: (1) from the 0.5° Gridded 1901- 1995 CRU climate dataset and (2) from historical meteorological station data, kindly provided by D. Lister at the University of East Anglia Climatic Research Unit. Although meteorological station data do extend beyond 1901, it was decided to use the CRU gridded dataset for simplicity and better coverage. Climate data from the two sources did not differ significantly - e.g. in 1905, the mean average annual temperature measured from London meteorological stations was 9.18°C compared to 9.14°C calculated from the gridded data.

The CRU 0.5° Gridded 1901- 1995 climate dataset from the University of East Anglia consists of monthly measures of mean temperature, precipitation, cloud cover, diurnal temperature range, vapour pressure, ground frost frequency and wet day frequency. This climate surface has been constructed by New *et al.* (2000) by direct interpolation from station observations and estimation of synthetic data from predictive relationships between variables. The database was validated by cross-validation and intercomparison.

The historical meteorological station data comprises measurements from 104 stations throughout the UK, some of which supply recorded data from the mid 17th century. Climate variables for 1840 to 1900 obtained from this dataset consisted of mean monthly temperatures derived from daily series where: mean daily temperature = (maximum daily temperature + minimum daily temperature)/2 and mean monthly temperature = sum of mean daily temperatures/ number of days in the month. The station data also provided measures of total monthly precipitation.

All meteorological stations were georeferenced and plotted on the 1843 map of England (Appendix 2.5) which had been scanned into the Geographical Information System

ArcView 3.1. For all counties, climate data up to 1900 were then derived by calculating the average of all meteorological stations within the county borders. Between 1901 and 1910, climate data for each county was calculated as the average of all 0.5° grid cells lying inside the 1840 county boundaries. In order to do this, the 0.5° grid map from the climate dataset was overlaid on the 1843 map and all grid cells (with their ID number) with the majority of the cell lying inside the county boundaries were identified visually. In a separate spreadsheet, all 43 counties were then linked to a specific number of cells each with a unique ID number which were used to calculate temperature and precipitation values for the county.

For each year, the 12 monthly averages were converted into annual maximum, minimum and mean average values and precipitation to annual total (Table 2.3.). For instance, the annual mean average temperature was calculated as the average of 12 monthly mean temperatures.

A full database listing ague deaths, all cause mortality and explanatory variables for each county in each year during 1840-1910 was assembled in Excel '97. This database was exported into STATA 7.0 for analysis. A summary of all explanatory variables, their availability and conversion is presented in Table 2.3 below.

Table 2.3. Explanatory variables and their availability and final conversion for use in the models.

Variable	Availability	Conversion
Population	Annual	N/A
County size (area)	Annual	N/A
Inland water acreage	Annual	Annual percentage of county area
Crop acreage	5-year	Annual percentage of county area
Cattle	5-year	Annual density per 100 acres
Pigs	5-year	Annual density per 100 acres
Minimum temperature	Monthly	Annual minimum average
Mean temperature	Monthly	Annual mean average
Maximum temperature	Monthly	Annual maximum average
Total precipitation	Monthly	Annual total

Geographical Information System maps

The centre (i.e. name) of all statistical districts was georeferenced using historical atlases or, alternatively (when required), the Worldwide Directory of Cities and Towns (2002).

The map of English county boundaries which forms the baseline of all maps shown in this paper was originally a 1983 boundary map kindly provided by C. Grundy (copyright County Boundaries Crown and ED LINE). This was edited within the Geographical Information System (GIS) ArcView 3.1. to correspond with the 1843 county boundaries. Manipulation and display of geographical data was performed in ArcView 3.1.

Descriptive and univariate analyses

The temporal pattern in ague deaths and death rates, all-cause mortality and all explanatory variables during the 70 years was plotted in Excel '97. Descriptive statistics (mean, minimum and maximum) and frequency distribution of all explanatory variables were generated using the statistical package in Excel '97.

Univariate analyses (binomial regression) were performed in STATA 7.0 to (1) determine the relationship between ague death rates and each potential explanatory variable in turn and (2) test for non-linearity in the effect of explanatory variables on ague death rates. All univariate analyses were undertaken by adding the explanatory variable of interest to the null model described below.

Multivariate models

In order to investigate the causes of the temporal variation in ague deaths, multivariate models were generated using the General Linear Model (GLM) command in STATA 7.0. The outcome was defined as a binomial variable, with ague deaths in each county in each year as the numerator, and the corresponding population size as the denominator. All explanatory variables as described above were included in the analysis.

Because the model was designed to test if explanatory variables affected the inter-annual - not inter-county - variation in ague deaths, county was added as a categorical explanatory variable. This is a conservative approach for testing the significance of the factors of interest, as a certain proportion of the inter-county variation which is being removed is also likely to be due to variation in climate, crops and livestock. The variables which affected the inter-county variation were tested later using a 'spatial' approach (see below).

For data with a strong temporal trend (as that observed for ague deaths) it is impossible to distinguish actual causal correlations from coincidental correlations which show a similar trend during the study period. Coincidental correlations are factors which, logically, are unrelated to ague (e.g. the number of cars or telephones in England) but, due to a strong temporal trend, may have been significant if added to the model. Any interaction role for

these 'coincidental' associations was excluded by taking out the overall (average) temporal trend from the data - i.e. by including a 'calendar year' variable in the model. The variable was tested for linearity and, because it showed a quadratic relationship with ague deaths, was included in the model both as a linear and a quadratic term.

To test for possible temporal autocorrelation, the residuals from previous years (the difference between observed number of deaths and the number predicted by the model including only the temporal trend and the categorical county variable, in a particular year) were also included as explanatory variables (Brumback *et al.* 2000). The residuals were added to the model in a forward step-wise manner starting with the residual from one year previously, then the residual from two years previously and so on until the addition of a residual was no longer significant. If for instance only the residuals from 1 and 2 years previously are significant in the model ($p < 0.05$), it is concluded that ague death rate in a specific year will depend on the death rates from the two previous years.

The null model was defined as the model containing only the categorical county variable, the temporal trend and the temporal autocorrelation and no explanatory variables.

A minimal adequate model was constructed by adding all explanatory variables and then using a backwards stepwise logistic regression in which the least significant variables were removed one at a time until all remaining variables were significant ($p < 0.05$).

The fit of the minimal adequate model was assessed by (1) inspecting the scatter plot of residuals and (2) comparing the deviance of the minimal adequate model to that of the null model. By investigating individual variables in comparison to the minimal adequate model it was possible to determine the importance of each explanatory variable. Because of the specially defined null model, the fit of the model refers to percentage residual variation explained instead of percentage variation explained.

For comparison, a temporal model for all-cause mortality (excluding ague, accidental and violent deaths, suicide and stillbirths) was constructed containing the same explanatory variables which were significant in the temporal ague model.

For ague deaths, spatial model was also created to explain the inter-county variation in ague mortality. As before, ague death rates were used as the binomial outcome but this time year instead of county was added as a categorical variable to determine the factors which influenced the difference in ague between counties. Spatial autocorrelation was not accounted for in this model. In an ideal situation, this problem should be addressed,

however including spatial autocorrelation in models like these requires sophisticated techniques which are beyond the scope of this study. Excluding spatial correlation may have led to under-estimation of confidence intervals and p-values rather than bias in the estimates of effects and thus the results may have been somewhat different if this had been accounted for. The minimal adequate model was constructed in the backwards stepwise manner and the model fit and importance of explanatory variables all assessed as outlined previously.

All models were scaled for overdispersion using the Pearson chi-squared statistics divided by the degrees of freedom as the scale parameter.

Prediction scenarios

Using the temporal minimal adequate model developed for ague deaths, the number of ague deaths during 1840-1910 was predicted for four different scenarios: (1) Observed historical conditions (2) No change in wetlands *and* cattle densities (3) No change in wetlands and (4) No change in cattle densities. The 'no change' scenarios for cattle and wetlands use the initial (i.e. 1840) values for cattle densities or inland water acreage throughout the 70 years, thereby keeping either (or both) variable constant. For all prediction scenarios, the residuals were not revised (which would have generated a positive feedback in the absence of any dampening regulatory factor in the model). These regulatory factors (e.g. herd immunity) were not available for inclusion in the model and thus all predictions represent the expected increase or decrease in ague deaths for any county due to a change in the particular parameter value in a single year.

The number of deaths (n) for each county in each year was predicted using the following back-transformation:

$$p = \frac{1}{1 + \left(1 / \exp(A) \right)}$$

(Equation 2.1)

where A is the logit number of malaria cases - i.e. the result from the multivariate logistic regression model:

logit number of cases = $c + t_1x_1 + t_2x_2 + t_3x_3 + ...t_nx_n$

c, t_1, t_2, t_3 and t_n are constants, c is a county-specific constant (i.e. there was a different model for each country). For the spatial predictions, c was a year-specific constant.
x_1, x_2, x_3 and x_n are explanatory variables

Results

The frequency distributions of all explanatory variables are shown in Appendix 2.6. All variables were normally distributed. Their mean, maximum and minimum values were identified and are shown below.

Table 2.4. Mean, minimum and maximum for explanatory variables

Explanatory variable	Arithmetic Mean	Minimum (County, year)	Maximum (County, year)
Inland water acreage (% of county size)	2.04	0.02 (Rutlandshire, 1845)	10.4 (Essex, 1880)
Crop acreage (% of county size)	11.8	8.22 (Rutlandshire, 1845)	94.7 (Derbyshire, 1910)
Pig density (per 100 acres)	7.38	0.26 (Rutlandshire, 1865)	72.3 (Derbyshire, 1905)
Cattle density (per 100 acres)	11.8	1.02 (Cumberland, 1845)	31.2 (Cheshire, 1910)
Mean average temperature (° C)	9.01	5.18 (South Wales, 1840)	11.8 (Cornwall, 1859)
Minimum average temperature (° C)	2.69	-3.21 (Devonshire, 1880)	7.48 (Cornwall, 1859)
Maximum average temperature (° C)	16.2	9.59 (South Wales, 1840)	20.1 (Cornwall, 1859)
Total precipitation (mm)	802	379 (Devonshire, 1855)	1661 (North Wales, 1850)

(mean, min and max for each variable selected from 3053 data points; i.e. 71 year recordings in 43 counties).

Temporal trends - deaths and demography

A total of 8209 ague deaths were observed during the study period.

The number of ague deaths and the ague death rate decreased gradually over the 70 years (Figs. 2.3 and 2.4). There were distinctive 'epidemics' in 1848 and 1859 where the total number of deaths reached 228 and 367 respectively. As the only war during the study period, the Crimean War, finished in 1856, none of these epidemics is likely to have been caused by an influx of infected soldiers from the tropics.

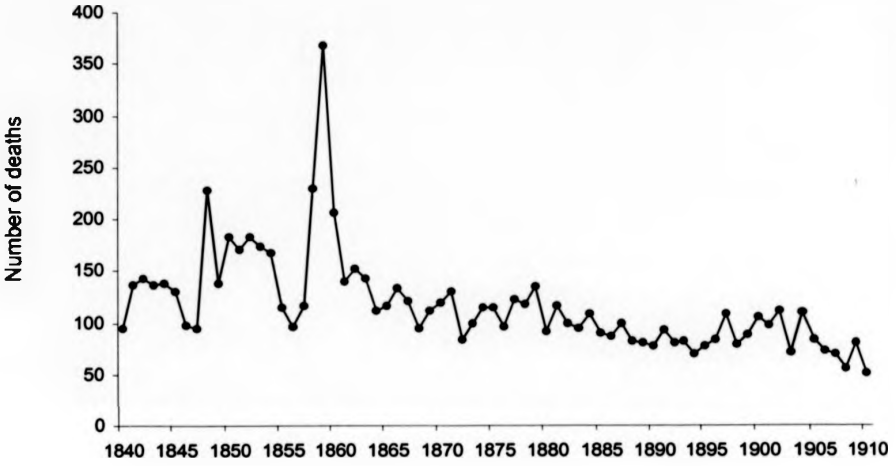

Figure 2.3. Annual deaths from ague in England and Wales during 1840-1910.

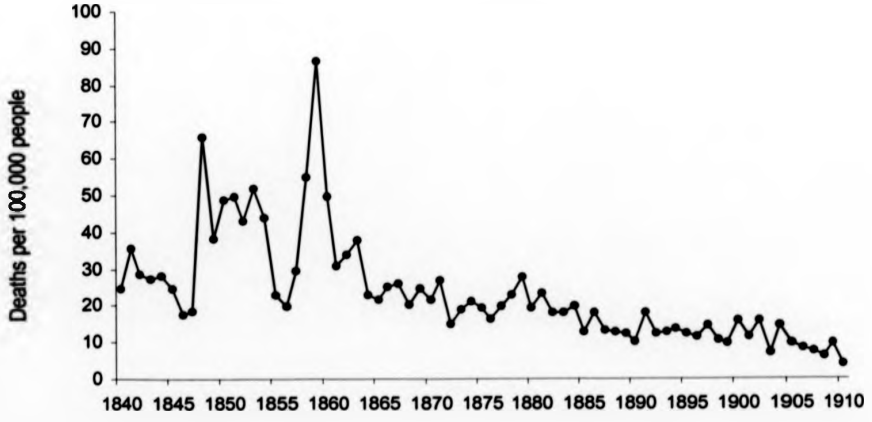

Figure 2.4. Annual ague death rates in England and Wales during 1840-1910.

A grand total of 34.6 million deaths from all causes (excluding ague, accidental and violent deaths, suicide and stillbirths) were observed throughout the 70 years. The total mortality rate from all causes decreased during 1840 to 1910 (Fig. 2.5). There were no apparent years of remarkably high mortality and nothing unusual during the epidemic ague years in 1848 and 1859.

The total population of England and Wales increased by 127% during the 70 years, from 15.9 million in 1840 to 36.1 million in 1910.

Figure 2.5. Annual all-cause mortality rate in England and Wales during 1840-1910.

Temporal trends - explanatory variables

Fig. 2.6 demonstrates the well-known decrease in wetlands (inland water) in the UK. The combined total size (area) of England and Wales during 1840 to 1910 was 37 million acres. In 1840, there were 942,268 acres (1 km^2 = 247 acres) of wetland and in 1910, there were 866939 - a decrease of 75,329 acres (8%).

As forests, heathland and wetlands were gradually replaced by agricultural land, the

acreage of crops, bare fallow or grasses increased by 1.4 million acres or 5% during 1840 to 1910 (Appendix 2.7). In this same period, the density of pigs and cattle per 100 acres increased by 14% and 115% respectively (Fig. 2.7). In 1840 there were 2.2 million pigs and 2.8 million cattle in England and Wales and by 1910 this had increased to 2.4 million pigs and 6.1 million cattle.

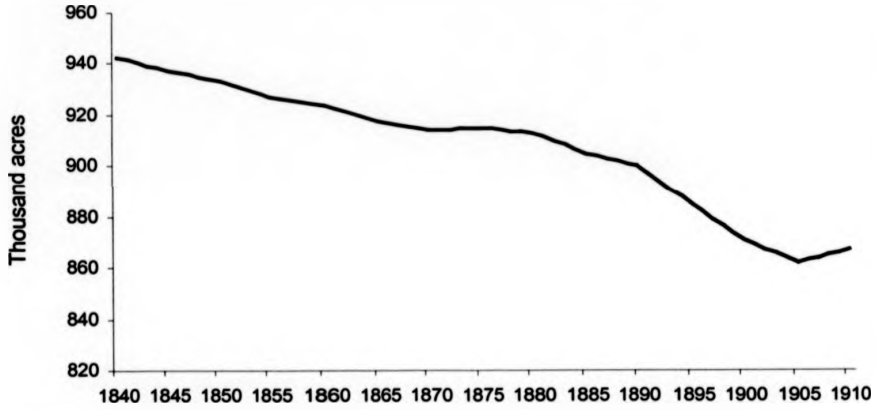

Figure 2.6. Total inland water (wetland) acreage in England and Wales during 1840-1910.

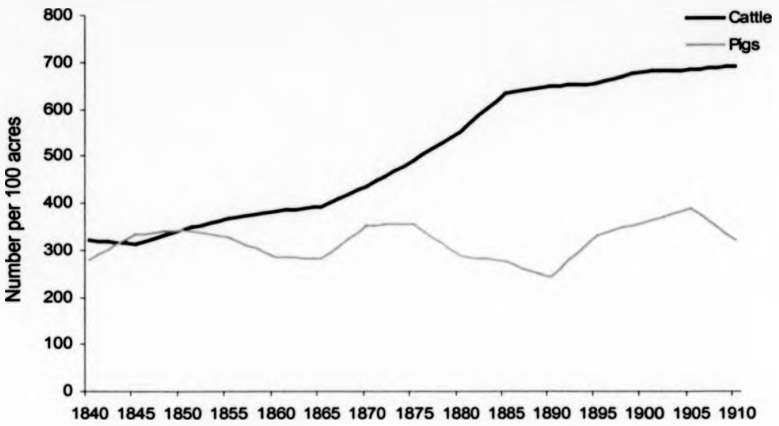

Figure 2.7. Total annual density of pigs and cattle in England and Wales during 1840-1910.

There were no distinctive trends in temperature or precipitation during the study period (Fig. 2.8 and Appendix 2.7). The period from 1880 to 1884 saw a succession of cold winters which was reflected in both the minimum average and mean average temperatures (Fig. 2.8, Appendix 2.7). In 1848, 1859 and in the latter part of the 19th century, there were periods of high summer temperatures (Fig. 2.8. Appendix 2.7). Precipitation fluctuated annually with periods of high rainfall during the late 1840s and 1850s which corresponded with the observed peaks in ague deaths (Fig. 2.8).

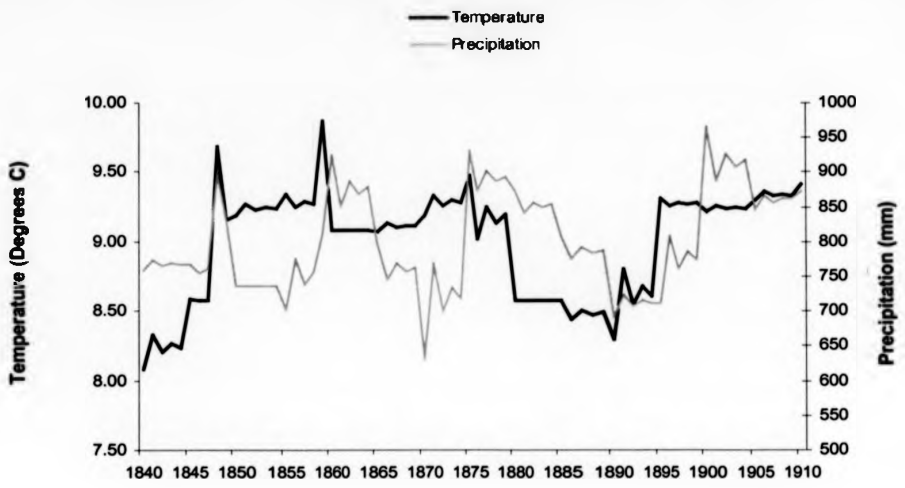

Figure 2.8. Annual mean average temperatures and total precipitation in England and Wales during 1840-1910.

Spatial trends - deaths

The total ague death rate during 1840-1910 at statistical district level is shown in Fig. 2.9. During this time, there were 121 statistical districts (38%) with no ague deaths (e.g. Canterbury in Kent and Exeter and Plymouth in Devon). The highest death rates per 70 years (2833 per 100000 people) were recorded from Romney Marsh (Kent), Hoo in Kent (2205), City of London (1574), Ely in Cambridgeshire (819) and Isle of Sheppey in Kent (711). This figure corresponds well with the observations of Nuttall *et al.* in 1901 who showed that ague was concentrated along the East coast and in Lancashire and Somersetshire during the 19th century and by Duncan (1993) who reported ague along the English-Scottish border.

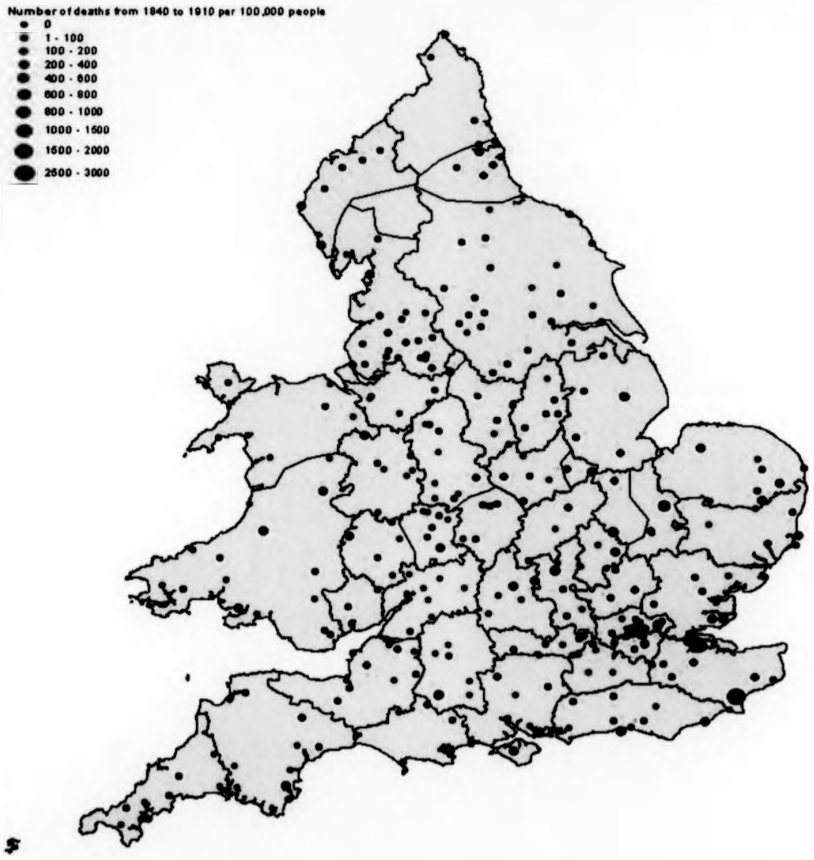

Figure 2.9. Total ague death rate in English and Welsh statistical districts during 1840 to 1910. (All statistical districts existing at the time have been included in this figure. Population denominator was the average population size from 1840 to 1910).

Table 2.5 shows the total number of ague deaths and total ague death rates during 1840-1910 in the 43 counties. The most populous counties (London and Lancashire) had the highest number of deaths whereas smaller counties such as Huntingdonshire and Cambridgeshire had higher death rates. There were no counties with zero ague deaths during the study period. As shown in Fig. 2.10, high ague death rates were mostly concentrated along the coastline. .

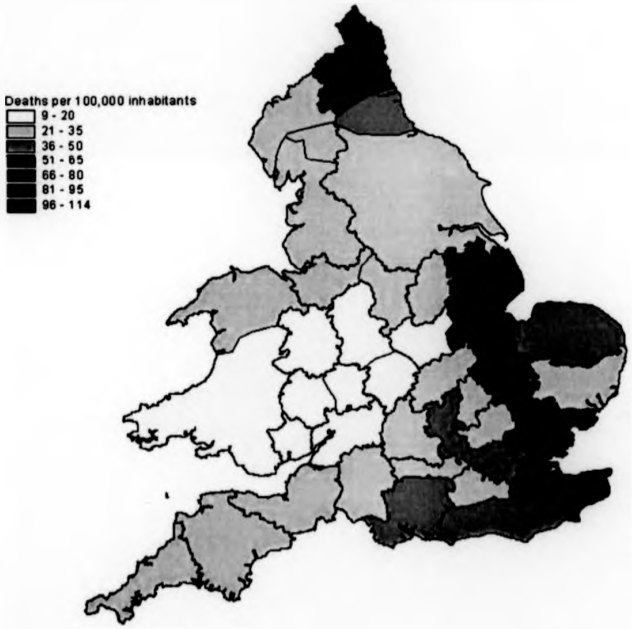

Figure 2.10. Total ague death rate in English and Welsh counties during 1840 to 1910.

For all-cause mortality, London and Lancashire recorded the highest total death rate over the 70 years with 2457 and 2176 deaths per 100,000 people, respectively. The smallest total death rates from all causes were recorded from Herefordshire (1710 deaths per 100,000 people) and Surrey (1687 deaths).

Spatial trends - explanatory variables

Essex, Lincolnshire and Kent had the highest acreage of inland water while Rutlandshire, Wiltshire and Leicestershire had the least (Table 2.6 and Fig. 2.11). The largest decreases in wetland acreage were observed in Cheshire, Essex and Kent (Fig. 2.12) while Yorkshire and Northumberland both had an increase in wetlands during the study period.

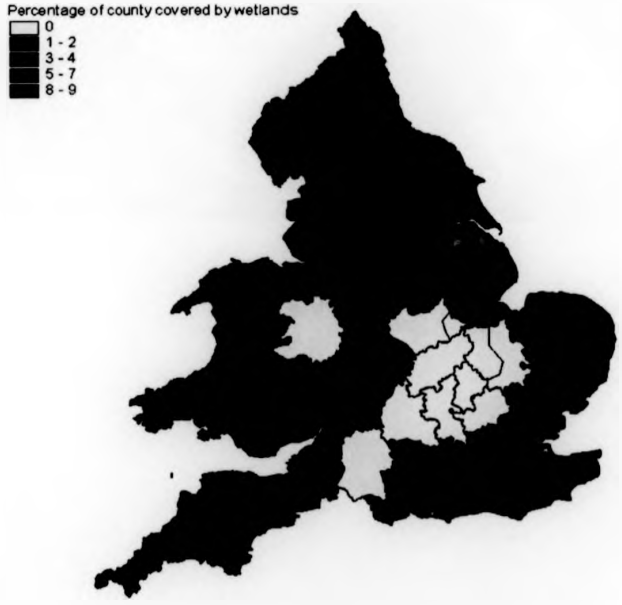

Figure 2.11. Average wetland (marsh) coverage in English and Welsh counties during 1840 to 1910.

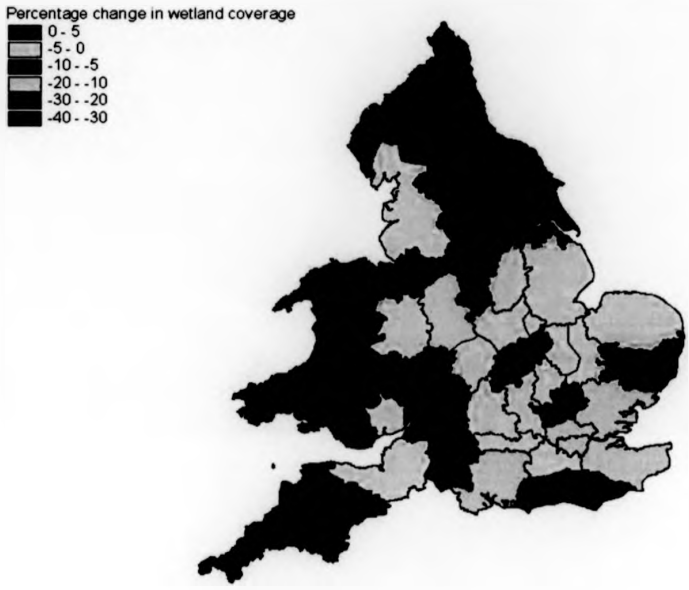

Figure 2.12. Percentage change in wetland (marsh) coverage in English and Welsh counties from 1840 to 1910.

Leicestershire, Essex and Cheshire had high average cattle densities over the 70 years (Table 2.6 and Fig. 2.13) and the lowest number of cattle per 100 acres were observed in Northumberland, Rutlandshire and Derbyshire. The largest increases in cattle densities were observed in Berkshire, Hampshire and Oxfordshire (all above 300% increase in the number of cattle per 100 acres) while London and Lancashire had the lowest increases of 7.1 and 17.3% respectively (Fig. 2.14). Average pig densities were highest in Leicestershire, Suffolk and Bedfordshire and lowest in Westmoreland, Cumberland and Durham (Table 6 and Appendix 2.8). On average, Wiltshire, Derbyshire and Essex had the largest acreage of crops, bare fallow and grasses throughout the 70 years while London, North Wales and Durham had the smallest (Appendix 2.8).

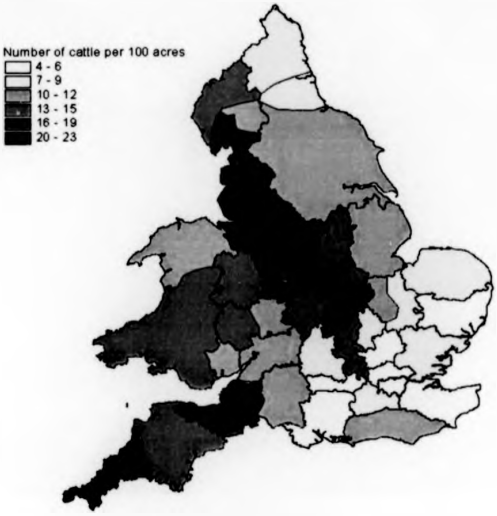

Figure 2.13. Average cattle densities in English and Welsh counties during 1840 to 1910.

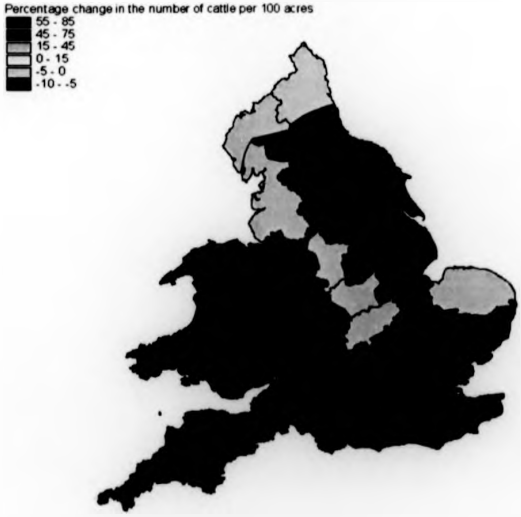

Figure 2.14. Percentage change in cattle densities in English and Welsh counties from 1840 to 1910.

Monthly mean temperatures were on average highest in Cornwall (10.2°C), Devon (10.1°C) and London (10.1°C) and lowest in Northumberland (8.2°C), Monmouthshire (8.1°C) and Yorkshire (8.1°C), Fig. 2.15. During the study period North Wales, Dorset, South Wales, Westmoreland and Somerset received the highest amount of rainfall while Cambridgeshire, Huntingdonshire, Bedfordshire, Hampshire and Middlesex received the smallest (Fig. 2.16).

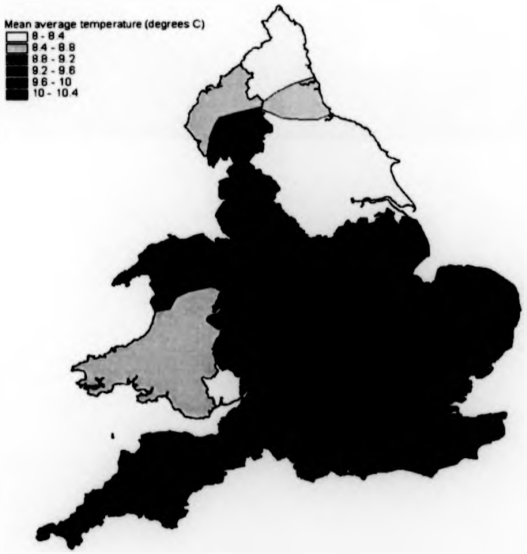

Figure 2.15. Mean average temperature in English and Welsh counties during 1840 to1910.

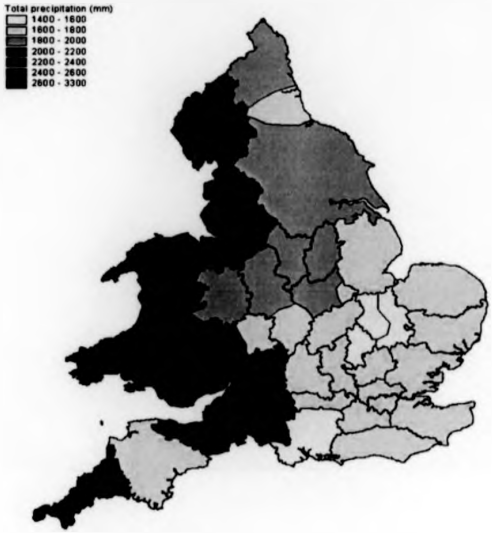

Figure 2.16. Average total precipitation in English and Welsh counties during 1840 to 1910.

Table 2.5. Total ague deaths and death rates in English counties during 1840 to 1910.

TOTAL AGUE DEATHS		TOTAL AGUE DEATH RATES	
County	**Deaths**	**County**	**Deaths per 100000 inhabitants**
London	1296	Kent	124.4
Lancashire	1124	Huntingdonshire	107.5
Kent	736	Cambridgeshire	103.5
Yorkshire	648	Essex	83.8
Essex	366	Lincolnshire	76.4
Durham	336	Northumberland	70.1
Lincolnshire	286	Durham	65.1
Hampshire	262	Rutlandshire	56.2
Northumberland	251	Sussex	49.5
Sussex	209	Hampshire	44.6
Cambridgeshire	193	London	44.0
Norfolk	180	Middlesex	42.6
South Wales	176	Lancashire	41.5
Cheshire	158	Norfolk	41.2
Devonshire	145	Buckinghamshire	38.6
Somersetshire	128	Suffolk	34.4
North Wales	121	Bedfordshire	34.1
Middlesex	117	Northamptonshire	33.1
Suffolk	116	Cumberland	32.1
Surrey	116	Surrey	31.1
Nottinghamshire	108	Derbyshire	30.9
Staffordshire	102	Cheshire	30.1
Derbyshire	94	Yorkshire	30.0
Cornwall	90	Nottinghamshire	29.7
Warwickshire	84	Somersetshire	28.5
Gloucestershire	81	North Wales	28.2
Northamptonshire	79	Cornwall	26.8
Worcestershire	71	Wiltshire	25.2
Cumberland	68	Devonshire	23.6
Huntingdonshire	62	Berkshire	23.6
Wiltshire	62	Dorsetshire	23.5
Buckinghamshire	58	Hertfordshire	23.2
Berkshire	53	Monmouthshire	22.0
Bedfordshire	51	Oxfordshire	21.7
Monmouthshire	49	South Wales	21.3
Dorsetshire	44	Worcestershire	21.2
Hertfordshire	44	Westmoreland	21.1
Oxfordshire	38	Gloucestershire	15.6
Shropshire	35	Warwickshire	13.5
Leicestershire	29	Shropshire	13.4
Rutlandshire	13	Staffordshire	12.1
Westmoreland	13	Herefordshire	10.1
Herefordshire	12	Leicestershire	9.3

Table 2.6. Counties with the five highest and five lowest average inland water coverage, pig density and cattle density during 1840-1910.

INLAND WATER		PIG DENSITY		CATTLE DENSITY	
County	% Coverage	County	Number/ 100 acres	County	Number/ 100 acres
Essex	9.31	Leicestershire	35.6	Leicestershire	23.9
Lincolnshire	6.79	Suffolk	15.5	Derbyshire	22.6
Lancashire	5.67	Middlesex	11.9	Cheshire	21.5
Kent	5.55	Bedfordshire	10.6	Cornwall	19.2
London	4.94	Somerset	10.4	Somerset	18.8
Shropshire	0.37	Rutlandshire	2.6	Hertfordshire	5.9
Northamptonshire	0.37	London	2.4	Berkshire	5.8
Leicestershire	0.36	Durham	2.1	Hampshire	5.7
Wiltshire	0.33	Cumberland	1.0	Suffolk	5.4
Rutlandshire	0.17	Westmoreland	0.9	London	3.9

(values for all 43 counties are given in Appendix 2.9)

"Univariate" analyses

As discussed previously, the univariate analyses were performed by adding each explanatory variable to the null model containing the categorical county variable, the temporal trend and the temporal autocorrelation. The use of the term univariate does not indicate that only one variable was used in the model but instead that only one explanatory variable - together with the time trend, county indicator variable and temporal autocorrelation - was analysed at a time.

All variables except for crop acreage were significantly ($p < 0.05$) associated with ague death rates in the univariate analyses (Table 2.7). Each explanatory variable showed a linear relationship with ague death rates, i.e. there were no non-linear (e.g. quadratic) trends. Inland water coverage (wetlands), temperature and precipitation were positively associated with increases in ague death rates while pig and cattle densities were negatively associated with the outcome.

Table 2.7. Results of univariate analyses

Variable	Relationship with ague death rates	Coefficient*	Significance
Inland water coverage (% of county size)	Linear	0.3646 *	$p < 0.001$
Crop acreage (% of county size)	Linear	-0.0069	$p > 0.05$
Cattle density (per 100 acres)	Linear	-0.0126	$p < 0.001$
Pig density (per 100 acres)	Linear	-0.1172	$p < 0.001$
Minimum average temperature (°C)	Linear	0.0785	$p < 0.001$
Mean average temperature (°C)	Linear	0.0202	$p < 0.001$
Maximum average temperature (°C)	Linear	0.0750	$p < 0.001$
Total precipitation (mm)	Linear	0.0052	$p < 0.001$

* log odds of an ague death in one year increases by 0.36 for each 1% increase in inland water coverage (where odds = p/(1-p) and p is the proportion of ague deaths per population)

Multivariate binomial models: inter-annual variation in ague

Inland water coverage, cattle density, mean average temperature and total precipitation were significantly associated with ague death rate (Box 2.1). The ague death rate in a particular year is positively associated with that of the previous year (Box 2.1: rate -1) i.e. there is a temporal autocorrelation of one year. Thus, a high number of ague deaths in one year will significantly increase the number of ague deaths the following year. The trend test for 'year' as described above showed a significant quadratic decrease with time.

Wetlands, average temperature and total precipitation were positively associated with ague deaths while cattle density had a negative effect on the outcome (Box 2.1). Wetlands had the greatest effect on ague deaths (i.e. this variable explains the largest amount of variation), followed by cattle density. This corresponds well with the commonly accepted theory that the drainage of wetlands and increases in cattle densities contributed significantly to the decline of malaria in England. The minimal adequate model explained 38.2% of the temporal variation in ague deaths, compared to the defined null (Table 2.8). This good fit is illustrated by the confusion matrix in Fig. 2.17 where the values of all cells surrounding the highlighted numbers are reassuringly low, indicating that the model does not often predict wrongly (for 100% correct predictions, the value of all cells surrounding the highlighted cells should be zero). A plot of residuals (observed - predicted ague deaths) against predicted ague deaths (Fig. 2.18) with the residuals evenly scattered throughout the graph also illustrates the validity of the model. The strength of the model is also demonstrated in Fig. 2.19 which shows a strong linear relationship between observed and

predicted ague deaths as well as by the normal distribution and even scattering of residuals when plotted against explanatory variables (Appendix 2.10). Separate models were constructed in which the least malarious counties were omitted from the analysis (i.e. only counties with malaria death rates greater than 60, 40 or 30 per 100,000 inhabitants during the 70 years were included). The coefficient values of the four explanatory variables were the same as those in the model shown below (Appendix 2.11) which indicates that the full analysis did not underestimate the effect of the explanatory variables by including possibly non-malarious counties (i.e. where reported sporadic malaria cases may have been infections acquired outside their own county).

Box 2.1. Minimal adequate temporal ague model; amended output from STATA 7.0.

STATA command

```
xi: glm ague water% cattle tave ptotal year yearsq rate-1 i.county,
f(b population) scale(x2)
```

Statistics

```
Generalized linear models                 No. of obs        =       3010
Optimization     : ML: Newton-Raphson     Residual df       =       2960
                                          Scale param       =          1
Deviance         =  3712.038553           (1/df) Deviance   =   1.254067
Pearson          =  3748.265286           (1/df) Pearson    =   1.278468
```

Explanatory variables

(43 county coefficients and statistics not shown)

ague	Coef.	Std. Err.	z	P>|z|	[95% Conf.	Interval]
water%	.413779	.0826741	5.00	0.000	.2517172	.5747408
cattle	-.0302873	.0090819	-3.33	0.001	-.045771	-.012485
tave	.0301441	.0186787	3.16	0.018	.0235655	.0396537
ptotal	.0043111	.0013245	3.26	0.001	.0017168	.0069065
year	-.018058	.0030166	-5.99	0.000	-.0239703	-.0121456
yearsq	-.0001742	.0000418	-4.16	0.000	-.0002562	-.0000922
rate-1	.0284019	.0025546	11.12	0.000	.0233954	.0334088

(Standard errors scaled using square root of Pearson X2-based dispersion)

Table 2.8. Inter-annual variation in ague death rates: significance and fit of the minimal adequate model and its explanatory variables.

Model	Deviance	Variance explained by model or variable (%)
Complete null *	9078	N/A
Temporal trend	6325	30.3†
Spatial autocorrelation	6882	24.2†
County categorical variable	6692	26.3†
Null model (defined)	6005	33.9†
Minimal adequate model	3712	38.2‡
Wetlands	4632	22.9‡
Cattle	4666	22.3‡
Wetlands and cattle	4617	23.1‡
Mean average temperature	4668	22.3‡
Total precipitation	4651	22.6‡
Temperature and precipitation	4634	22.8‡

* the most basic model - without the year trend, categorical county variable and temporal autocorrelation

† indicates that the model deviance is compared to the residual deviance of the complete null model.

‡ indicates that the model deviance is compared to the residual deviance of the defined null model (i.e. this column is the percentage residual variation explained by the model).

		Predicted ague deaths				
		0-2	3-6	7-10	11-20	21+
Observed ague deaths	0-2	2178	19	0	0	0
	3-6	19	482	14	0	0
	7-10	8	12	121	0	0
	11-20	2	0	15	139	1
	21+	6	0	0	5	32

Figure 2.17. Confusion matrix of observed and predicted ague deaths.

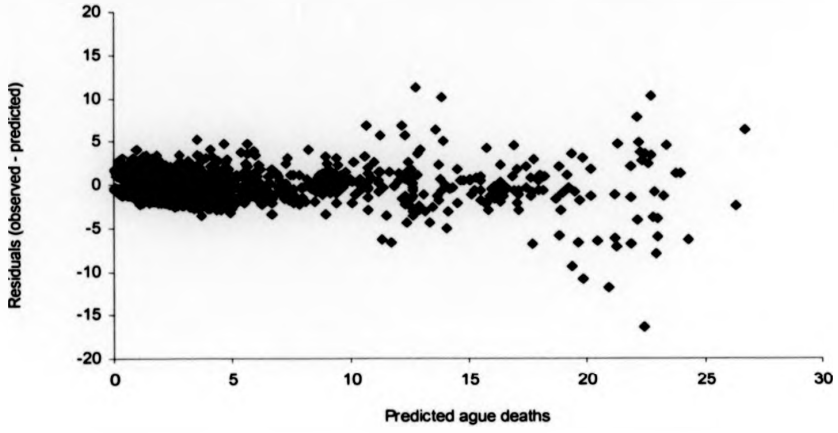

Figure 2.18. Inter-annual variability in ague: residuals versus predicted ague deaths.

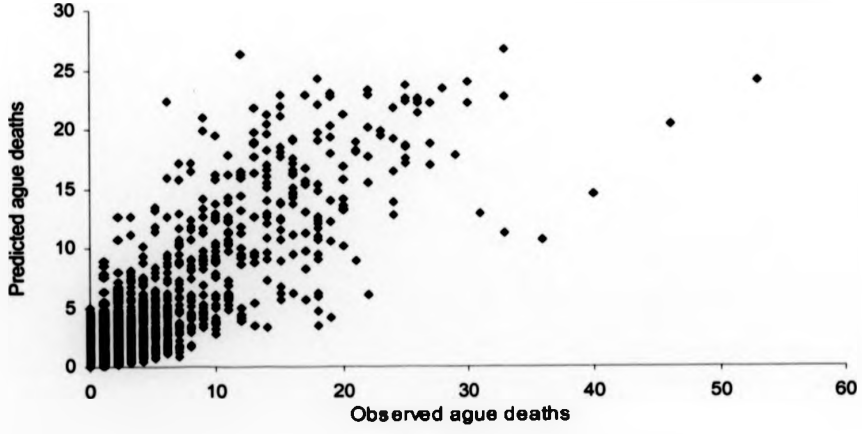

Figure 2.19. Inter-annual variability in ague: predicted versus observed ague deaths.

Multivariate binomial model: inter-annual variation in all-cause mortality

The all-cause mortality model was firstly created using the variables identified as significant by the stepwise process for ague death rates. This model output (Box 2.2) shows that the four variables (wetland coverage, cattle density, average temperature and total precipitation) had significantly different (inland water, cattle and precipitation) or no effects (average temperature) on all-cause mortality. No temporal autocorrelation was identified and is therefore not included in the model. This result indicates that modelled and observed variation in ague deaths was not merely reflecting factors which affected general mortality.

The minimal adequate model for all-cause mortality (not shown) demonstrated significant positive relationships with minimum and maximum temperatures (as well as cattle density) and negative relationships with crop acreage (as well as inland water). This explained 18.1% of the temporal variation in mortality (Table 2.9). The appropriateness of the minimal adequate model is illustrated by the normal distribution of the residuals (Appendix 2.10).

Box 2.2. All-cause mortality model (including only variables from minimal adequate temporal ague model); amended output from STATA 7.0.

```
STATA command

xi: glm deaths water% cattle tave ptotal year yearsq i.county, f(b
population) scale(x2)

Statistics
Generalized linear models                 No. of obs      =       3010
Optimization     : ML: Newton-Raphson     Residual df     =       2961
                                          Scale param     =          1
Deviance         =  5002.6338915          (1/df) Deviance =   2.427285
Pearson          =  4903.3715851          (1/df) Pearson  =   1.655985

Explanatory variables
(43 county coefficients and statistics not shown)
------------------------------------------------------------------------------
deaths |   Coef.   Std. Err.      z    P>|z|     [95% Conf. Interval]
-------+----------------------------------------------------------------------
water% |  -.0400213   .0093923    -5.37   0.000    -.0586127   -.0214299
cattle |   .0037574   .0008732     4.30   0.000     .0020461    .0064688
  tave |   .0007216   .0002039     0.36   0.721    -.0012576    .0067106
ptotal |  -.0013344   .0005264    -10.01   0.000    -.0015954   -.0010734
 year  |  -.0158686   .0025413    -16.25   0.000    -.0748569   -.0084586
yearsq |  -.0064666   .0001483    -43.61   0.000    -.0067572    -.006176
------------------------------------------------------------------------------
(Standard errors scaled using square root of Pearson X2-based
dispersion)
```

Table 2.9. All-cause mortality: significance and fit of the minimal adequate model and its explanatory variables.

Model	Deviance	Variance explained by model or variable (%)†
Complete null *	1245125	N/A
Year trend (linear only)	398421	68†
County categorical variable	412276	66.9†
Null model (defined)	283191	77.3†
Minimal adequate model	252824	10.9‡
Wetlands	274112	3.2‡
Cattle	270000	4.7‡
Crop acreage	273848	3.3‡
Minimum average temperature	263891	6.8‡
Maximum average temperature	266990	5.7‡
Total precipitation	278651	1.6‡

* the most basic model - without the year trend or the categorical county variable.

† indicates that the model deviance is compared to the residual deviance of the complete null model.

‡ indicates that the model deviance is compared to the residual deviance of the defined null model (i.e. this column is the percentage residual variation explained by the model).

Multivariate binomial models: inter-county variation in ague

The spatial ague model is different from the temporal in that the null model is defined as containing only the categorical year variable.

The spatial variation in ague death rate between counties was significantly associated with inland water, cattle density, average temperature and total precipitation (Box 2.3). Cattle density had a negative effect on the outcome while inland water, average temperature and total precipitation were positively associated with ague death rates. The minimal adequate model explained 40.4% of the inter-county variation (Table 2.10). Wetlands and mean average temperature explained the highest variation in the model while cattle density and precipitation explained the least. A critical rule when generating linear models is that the residuals (observed - predicted) should be normally distributed which in this case is confirmed by the frequency histogram in Appendix 2.10. The robustness of the model is further affirmed in Figs. 2.20 and 2.21 where residuals are evenly scattered throughout the graph and there is a strong linear relationship between observed and predicted ague deaths. The explanatory variables in this model and the direction of the effects are the same as those of the temporal model. Only the inland water coefficient is significantly different (i.e.

the confidence intervals do not overlap) in the two models, indicating that inland water coverage is more important in time than space. It can therefore be confirmed that both the spatial and temporal patterns of ague during 1840-1910 were influenced by the same factors in approximately the same order of magnitude.

Box 2.3. Minimal adequate spatial ague model; amended output from STATA 7.0.

```
STATA command
xi: glm  ague water% cattle tave ptotal i.year, f(b population) scale(x2)

Statistics
Generalized linear models                       No. of obs      =       3053
Optimization     : ML: Newton-Raphson           Residual df     =       2978
                                                Scale param     =          1
Deviance         =  3882.642808                 (1/df) Deviance =   1.303775
Pearson          =  3931.183359                 (1/df) Pearson  =   1.320075


Explanatory variables
(70 year coefficients and statistics not shown)
------------------------------------------------------------------------------
-
   ague |      Coef.   Std. Err.      z    P>|z|     [95% Conf. Interval]
------------------------------------------------------------------------------
 water% |   .1075917   .0072132    14.92   0.000      .093454     .1217294
 cattle |  -.0236435   .0036547    -6.47   0.000     -.0308065    -.0164805
   tave |   .0563458   .0200901     2.80   0.005      .0157216     .091697
 ptotal |   .0052155   .0010784     4.84   0.000      .0033277     .0071031
------------------------------------------------------------------------------
(Standard errors scaled using square root of Pearson X2-based dispersion)
```

Table 2.10. Inter-county variation in ague death rates: significance and fit of the minimal adequate model and its explanatory variables.

Model	Deviance	Variance explained by model or variable (%)
Complete null *	9077	N/A
Year categorical variable	7510	17.3†
Null model (defined)	6515	28.2†
Minimal adequate model	3882	40.4‡
Wetlands	4003	38.6‡
Cattle	4168	36.0‡
Mean average temperature	4114	36.8‡
Total precipitation	4353	33.2‡

* the most basic model - without the year variable.

† indicates that the model is compared to the residual deviance of the complete null model.

‡ indicates that the model deviance is compared to the residual deviance of the defined null model (i.e. this column is the percentage residual variation explained by the model).

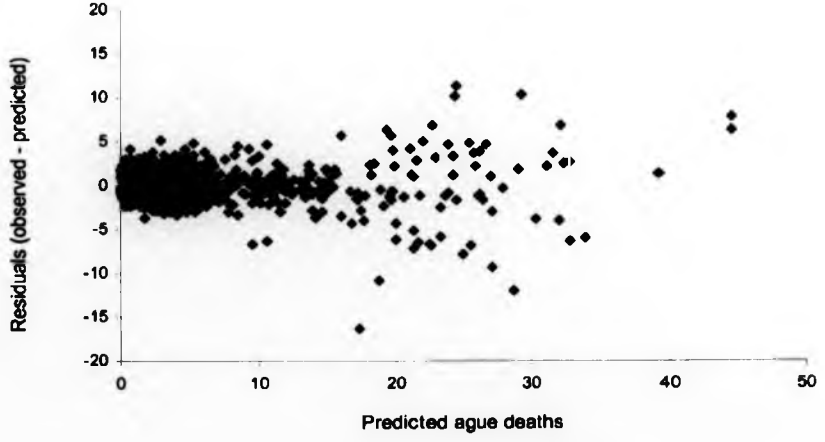

Figure 2.20. Inter-county variation in ague: residuals versus predicted ague deaths.

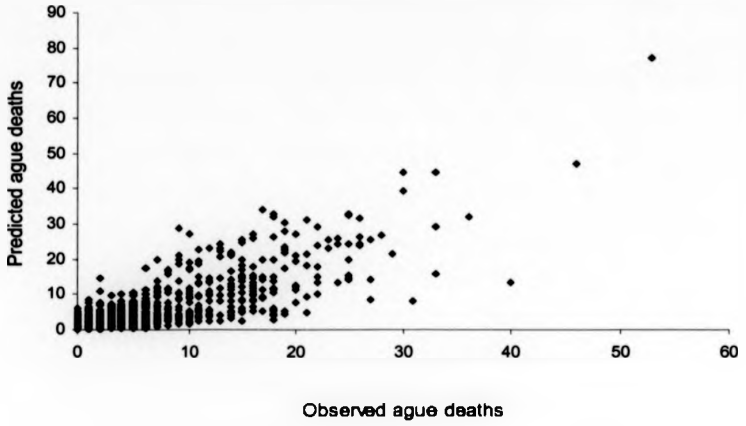

Figure 2.21. Inter-county variation in ague: predicted versus observed ague deaths.

Prediction scenarios

Using the minimal adequate model for temporal variation in ague, the number of ague deaths during 1840-1910 was predicted for the following scenarios: (1) Observed historical conditions (2) No change in wetlands *and* cattle densities since 1840 (3) No change in wetlands since 1840 and (4) No change in cattle densities since 1840. These predictions provide a useful indicator for predicting the future impact of environmental change (probably the best available) but still need to be interpreted with caution because of a number of problems:

- The ratio of imported : indigenous ague deaths probably changed between 1840 and 1910 (see Discussion) but the number of imported cases are not considered in the model, causing overestimation of indigenous malaria deaths.
- The trend in ague (malaria) deaths is greatly affected by the rapid advances in chemotherapy during the late 19th century.
- The use of non-revised residuals in the predictions (as described in the Methods section) does not account for the cumulative effect of any consistent simulated change in risk over time. However, this caveat may be relatively unimportant because spatial and temporal ague models had similar explanatory variables with similar coefficient (i.e. spatial but not temporal differences reflect the cumulative impact of a consistent

difference in risk).

- The proportional impact of agricultural changes may not have been the same throughout the study period as well as in the future (due to the vast agricultural alterations during the 20th and 21st centuries).
- The environmental data used were averaged over large areas (i.e. counties) and thus did not accurately represent the situation in local areas where malaria was transmitted (i.e. local patchiness was not identified).

Predicted and observed ague deaths during 1840-1910 are shown in Fig. 2.22 and the predicted number of deaths for scenario 2 in Fig. 2.23. The null model predictions in Fig. 2.22 show a decreasing trend with no marked peaks. The difference between the null model and the minimal adequate model plots is due to the inclusion of the agricultural and environmental explanatory variables which seem to explain the ague epidemics in 1848 and 1859 as well as the overall temporal variation in ague deaths.

If cattle densities or wetland coverage had remained at 1840 levels, the predicted number of deaths attributable to ague in any county in any year would have increased by 8.7% and 10.8%, respectively (Table 2.11, Fig. 2.23). If there had been no changes wetlands and cattle, ague deaths would have increased by 19.5%. These results provide strong evidence in support of the theory that changes in cattle densities and wetland coverage were major factors responsible for the disappearance of ague from England and Wales.

Table 2.11. Observed and predicted ague deaths 1840-1910

Scenario	Total deaths (95% CI)	% Difference (95% CI)*
Observed	8209	N/A
No change in cattle and wetlands	9809 (9653-9949)	19.5 (17.6-21.2)
No change in wetlands	9095 (8964-9202)	10.8 (9.2-12.1)
No change in cattle	8923 (8833-9021)	8.7 (7.9-9.9)

* compared to the observed. The differences shown reflect increases in ague deaths for any county in any given year.

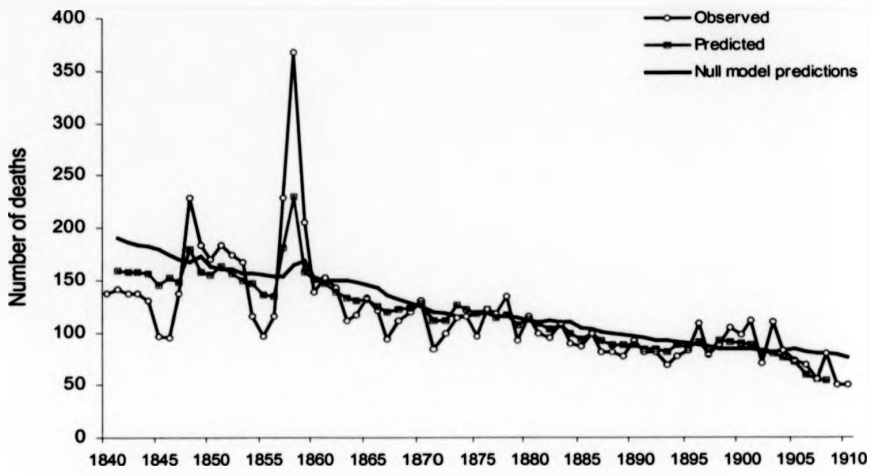

Figure 2.22. Observed and predicted ague deaths in England and Wales during 1840-1910.

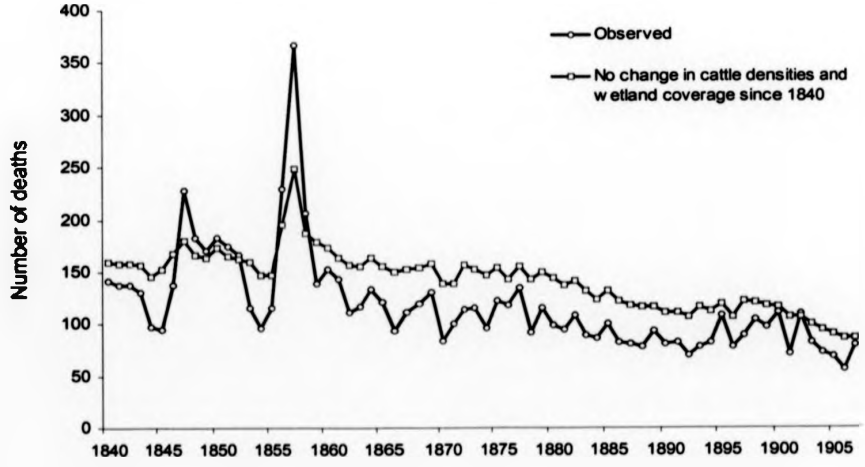

Figure 2.23. Predicted ague deaths in England and Wales during 1840-1910

Imported and indigenous malaria in the UK during the 20th century

The imported number of malaria cases to the UK showed a rapid drop after 1919 which was probably due to the fact that most soldiers with malaria had returned to the UK before 1920. From 1920, there was a constant low trend until the 1960s when the number of imported cases started increasing again (Fig. 2.24). On the other hand, the number of indigenous cases remained very low throughout the period, peaking at 103 in 1919 after which it decreased dramatically (Fig. 2.25). The number of deaths (from both imported and indigenous cases) and death rates (i.e. number or deaths/number of cases) also showed a generally decreasing trend until the end of the 1980s when a very slight increase was observed (Fig 2.25 and 2.26). This pattern is probably due to the continued improvement of malaria chemotherapy the benefits of which, however, have now been somewhat reduced due to the increase in parasite drug resistance and the increased number of total imported cases.

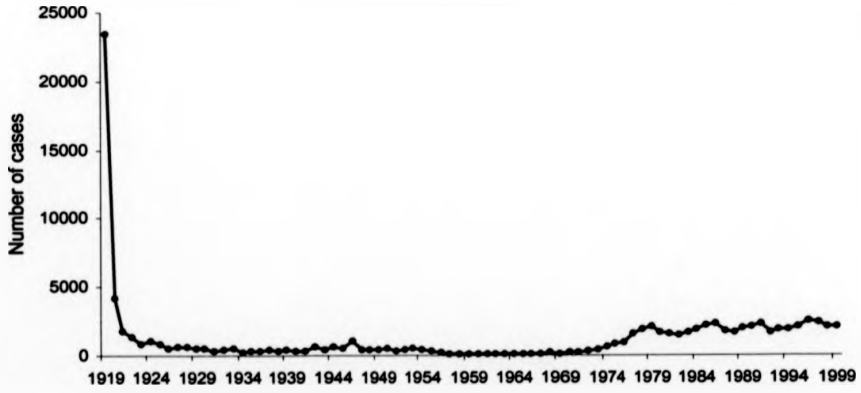

Figure 2.24. Imported malaria cases in the UK during 1919 to 2000.

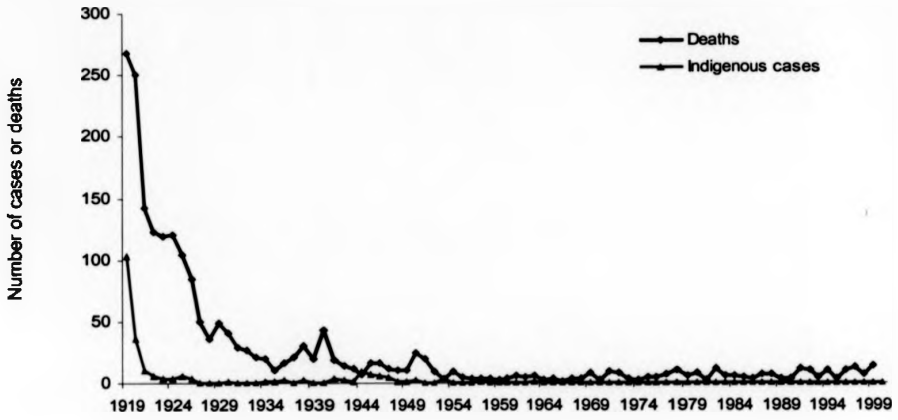

Figure 2.25. Indigenous malaria cases and deaths (both indigenous and imported) in the UK during 1919 to 2000.

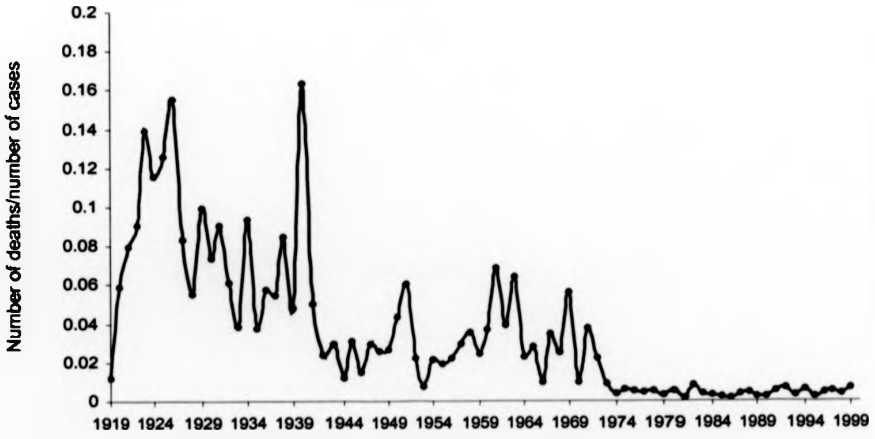

Figure 2.26. Malaria death rate in the UK during 1919 to 2000.

Discussion

The decline of English ague (or malaria) has been successfully analysed using quantitative explanatory variables. The results confirm the theory that the disappearance of ague from the UK was greatly influenced by marsh drainage (decreases in wetlands) and the introduction of more livestock. Speculations about links between the decrease in ague and the drainage of wetlands and increasing cattle densities go back as far as the 1860s (Whitley 1863, Ewart 1897, MacArthur 1951) and these models authenticate such century old views.

Of course these were only two of many factors which contributed to the demise of the disease; others include changes in socio-economic conditions such as better ventilated and lighted houses and improved sanitation and medical care. In spite of this, wetlands and cattle density in the model presented here explains at least as 23% of the temporal variation in ague deaths. This is a highly conservative estimate of the variation explained due to three main reasons. Firstly, much of the variation in ague was already removed by the year trend. Secondly, local environmental factors do not explain variation due to imported cases (see below) and, thirdly, the virtual scenarios did not use revised residuals which would have caused a positive feed-back in ague deaths. As observed from the model outputs, the disappearance of wetlands and the increasing cattle densities played almost equally important roles in the decline of ague. This is not surprising due to the interactions between (1) increasing cattle densities and *Anopheles* feeding habits and (2) wetlands and mosquito breeding sites as discussed in detail in the Introduction. Pig density was not significantly associated with the decline of ague, most likely because - in comparison to cattle density - this variable only increased by a relatively small amount (14% compared to 115%) during the study period. The exact feeding preferences of English *An. atroparvus* have not been investigated, but we have found them to be very abundant in both pig sties, cattle sheds and horse stables. The general consensus is that *An. atroparvus* will feed on the most abundant warm-blooded animals in the area - which is more likely to be cattle than pigs due to the difference in their abundance.

Crop acreage did also not appear in the minimal adequate ague models. The increase in crop acreage over time reflects the loss of wetlands, forests, heathland and other ecotypes which were converted to fields. None of these land cover types (except for wetlands) or crops are logically related to the distribution of ague (or *An. atroparvus*) which explains why the crop variable was not significant in the analyses.

The results show a significant effect of both temperature and precipitation, explaining the malaria epidemics of 1848 and 1859 which were observed both in the UK and across the whole of Europe (Hirsch 1883) and corresponded with 'unusually hot summers' (Whitley 1863, MacDonald 1920, Smith 1956). None of these epidemics seem to be related to wars (the Crimean ranged from 1853-56) and thus the most likely explanation for these peaks is, according to the models presented, fluctuations in climate. In recent times, throughout the tropics, similar patterns have been observed where increases in malaria incidence have been linked to warmer years, brought about by the El-Niño Southern Oscillation (Bouma *et al.* 1997).

Interestingly, maximum or minimum temperatures were not significantly related to the spatial or temporal pattern of ague deaths in this study. There is no apparent reason why average - and not minimum - temperatures should limit the development and transmission of *P. vivax* in England. It has previously been stated that high minimum temperatures can be associated with increased malaria prevalence in highland areas (Bouma *et al.* 1994) and Snow *et al.* (1998) showed that minimum and maximum monthly temperatures are significantly related to *P. falciparum* prevalence in Kenya. The most likely explanation for the findings in this work is the use of monthly data converted to mean annual averages instead of simple monthly averages or daily temperature measurements which would have shown more variation in extremes and possibly have made the minima and maxima better correlated with ague epidemics.

The effects of the significant explanatory variables from the ague model were quite different in the all-cause mortality model. Additionally, the years of epidemic ague do not correspond with years of high general mortality (1845-47, 1853 and 1863-65). These observations suggest that the ague death pattern was unique in comparison to other diseases and driven by factors which had a different effect on other types of mortality. While this does not strictly confirm that ague really *was* malaria (see below), it is an important indication that ague as a disease was not comparable to the other common fevers.

The minimal adequate model for inter-annual variability in ague death rates predicts both the epidemics of 1848 and 1859 (the peaks of the predicted values are dampened due to the inclusion of the previous year's residuals in the model). By arbitrarily keeping cattle density and wetland coverage constant at 1840 levels, a 19.5% increase in ague deaths was simulated. This indicates that the overall decreasing trend in English malaria was highly influenced by the observed changes in live stock densities and marsh wetland coverage.

An important caveat of the models is the lack information on imported malaria

cases (and deaths thereof) during the study period. The original 1840-1910 data do not distinguish between deaths from indigenous and imported ague. Even at this time, there would have been a small number of deaths from imported cases of malaria; from returning soldiers or more wealthy tourists travelling to south Europe or North Africa which were relatively accessible by sea or land. Imported cases increase immediately after overseas wars in malarious zones, but, as already mentioned, this study period was relatively peaceful. The 51 malaria deaths in 1910 are unlikely all to be due to indigenous malaria because this would mean a drastic reduction to zero indigenous deaths in 1925. What are thought to be the last cases of indigenous malaria in England were observed in 1953 (Crockett and Simpson 1953) in two neighbours, both living in Stockwell, South London. The last death from indigenous malaria is more difficult to determine. In 1921, Blacklock reported a death from indigenous *P. falciparum* in an 18 year old female from Liverpool. Ross (1921) suggested that it was contracted from blood-to-blood transmission by a dentist while Blacklock (1921) argued that it was mosquito transmitted. Therefore, the model predictions are not exclusively indigenous English malaria. Because international travel was not unheard of at this time it is hypothesised that an unknown proportion of the observed ague deaths was due to imported infections. While indigenous malaria slowly disappeared, the number of imported cases of malaria has increased dramatically - especially during the past 40-50 years - primarily due to increased travel (English people acquiring infection abroad) and migration (infected refugees or immigrants arriving in England). The shift from predominantly indigenous deaths (and cases) towards imported occurred gradually throughout the late 19th and early 20th centuries but is impossible to pin-point or quantify. The mean annual number of imported cases reported from 1925 to 1935 was 464. Therefore, the predictions of ague deaths from the original model reflect two processes (1) the reduction in local deaths and (2) the increase in imported deaths.

In spite of these problems, the model predictions are still remarkably accurate in predicting the deviations from the observed general trend in ague deaths during the study period. The spatial pattern of ague deaths as shown in Figures 2.9 and 2.10 and Table 2.5 also corresponds accurately with the observation made by George Whitley in 1863 in what is probably the most reliable survey of ague in 17 English counties. He confirms the presence of ague in the marshy areas of Kent and Essex, the Fen districts of Cambridgeshire and Lincolnshire, along the Thames estuary (e.g. London), in Somerset and Lancashire and near the Scottish borders. Hirsch (1883) reported endemic ague transmission in Lincolnshire, Huntingdonshire, Cambridgeshire, London and Somerset; and

Davidson (1892) quoted the highest death rates from ague in Kent, Huntingdonshire and Cambridgeshire during 1883-1887 which is confirmed by the data collected for this study. As discussed previously, there is very limited evidence that the ague of the 15th - 17th century was malaria. However, by the beginning of the 19th century, great fevers had been differentiated and ague symptoms very well described. By collecting ague data from 1840 onwards, the period during which the disease was clearly understood and distinguished from other fevers has been selected. From published sources it has therefore become clear that the database used for this study is a reliable representation of deaths from English malaria.

To provide further evidence of the accuracy of these historical diagnoses, it is confirmed that factors associated with spatial and temporal variability in ague death rates were similar and factors associated with temporal variability in other causes of death were different.

In conclusion, the quantitative analysis of role played by environmental factors in the inter-annual variation in English malaria (ague) patterns has produced results in support of theories dating back to the 19th century. These show that at least 20% of the drop-off in malaria deaths was attributed to the increasing cattle population and decreasing acreage of marsh wetlands. Although both rainfall and temperatures were associated with the inter-annual variability in death rates there is no evidence for any association with the long-term malaria trend. The strength of the ague models is supported by three main observations: (1) All significant explanatory variables go in the direction expected on the basis of transmission cycle knowledge (e.g. decreases in wetlands decreases the number of ague deaths), (2) Variables which were significantly associated with the temporal pattern of ague were also significantly associated with the spatial pattern of the disease and (3) The significant explanatory variables identified in the temporal ague model had a significantly different effect on temporal patterns in all-cause mortality.

The presence and characteristics of malaria in the UK during historical times was not unique. Similar patterns of high death rates in marshy areas followed by a natural decline during the late 19th century were observed in many other high-latitude European countries while malaria persisted in southern Europe until the initiation of eradication programmes in the late 1940s. The following chapter will determine to what extent some of the environmental variables examined in relation to English malaria impacted on the inter-annual variability of malaria in 17 European countries. Such results will enable us to make generalised conclusions about the historical patterns of malaria in a previously endemic continent and should be potentially useful for making future predictions of disease patterns.

Spatial and Temporal Patterns of Malaria in 20th Century Europe

Abstract

Although the disappearance of European malaria has been well-documented and discussed, there have been no previous attempts to quantify the roles of the various environmental factors involved. This study uses historical (1900-1975) malaria data from 17 European countries in combination with country-level agricultural variables and low resolution climate parameters to model the inter-annual variability in indigenous malaria cases at the country resolution. The model explicitly controls for the long-term European trend in malaria case incidence and investigates instead the impact of a series of explanatory variables on the year-to-year variation from this trend in each country. On a priori scientific grounds, and from inspection of the data, two distinct underlying trends were permitted depending on whether malaria disappeared from a country 'naturally' or following DDT spraying campaigns during and/or after the 1940s. The model also takes into account the extreme deviations from these long-term trends during the World War years due to the unusually high rates of imported cases. Finally, the model also considers spatial heterogeneity in risk by controlling for inter-county differences in average incidence rate during the 75 year study period.

A multivariate statistical model assuming Poisson errors was set up to test the effect of a series of explanatory variables on the inter-annual variation in malaria. A minimal adequate model was constructed using the backwards stepwise approach in which the least significant variables were deleted until only significant variables ($p < 0.05$) remained. Results indicated that cattle densities and woodland coverage were negatively associated with temporal malaria patterns while rice cultivation and average temperatures were positively related to the disease. The minimal adequate model explained 15.4% of the observed residual variance in malaria cases (i.e. the residuals from the null model incorporating general temporal trend and inter-country variability in average incidence).. A spatial model developed to examine the overall inter-country variation in malaria cases contained the same explanatory variables with effects in the same direction as those of the temporal model, indicating that both temporal and spatial patterns of malaria in 20th century Europe were influenced by the same factors in the same order of magnitude and that the temporal model did not significantly underestimate the cumulative effect of a difference in parameter values.

Model simulations showed that if cattle densities and woodland coverage had reverted to 1900 levels in any year across the whole of Europe during the study period, malaria

cases within Europe would have increased by 12.4 and 15.3%, respectively with the most pronounced effects in northern countries such as Finland and Sweden where 27-92% increases were predicted. If rice cultivation was kept constant, the overall number of malaria cases in Europe would have decreased by 13.2% in any year. This effect varied between countries according to the national temporal pattern in rice cultivation; for example an 8.1% decrease was predicted for Italy where rice cultivation increased in the 20th century but an increase of 20)% predicted for Spain where rice cultivation decreased during the 20th century.

The results obtained using relatively crude datasets correlate well with published hypotheses about the past distribution and later disappearance of European malaria. They also show the relative ease with which historical disease and environmental data can be combined to produce meaningful predictions of temporal and spatial malaria patterns in a previously endemic continent. In the absence of current transmission such retrospective analyses provide us with a useful handle for making predictions of how environmental changes could impact on the future risk of malaria transmission.

Introduction

To date there have been few published attempts to quantify the relationship between environmental factors and historical malaria patterns at local levels and none at the continental scale. Previous studies have focused on currently endemic countries and there has not been any progress in quantifying the environmental determinants of disease distribution in previously endemic regions such as Europe, North America and Australia. By focusing on 20th century malaria in Europe, this study will present an initial attempt to provide such an analysis for a region where malaria is now extinct and will enable us to test common hypotheses about the disappearance of malaria from Europe as well as predict how changes in relevant environmental factors may have affected the historical risk of transmission as well as present and future patterns of disease. Rogers *et al.* (2002) recently stated that "attempts to relate climate to past trends in malaria prevalence are the critical tests of the real role of climate in the recent history of malaria and therefore its likely impact in the future". However, because trends in likely explanatory variables also show temporal trends a more reliable approach is to examine the effect of climate – and other factors - on inter-annual variation in malaria (e.g. Bouma *et al.* 1997). Thus, as with the study presented for the UK, this work will examine the inter-annual variability in malaria cases at country level rather than attempt to explain long-term temporal trends.

The introduction section presented below will focus on the parasitological and epidemiological aspects of malaria transmission in Europe. Entomological details such as the distribution and competence of European mosquitoes as malaria vectors will be discussed in detail in Chapter 4.

The history of malaria in Europe until the 19th century

While human malaria may have existed in the tropics for more than two million years, it is unlikely to have become properly established in Europe until much more recently because of climatic restraints during the last Ice Age 18,000 years ago. At this time summer temperatures were, on average, 9°C lower than today (i.e. the average summer temperature in the UK would have been 6-7°C), making malaria transmission virtually impossible (de Zulueta 1994). Although there are no fossil records of mosquitoes from this time, it is likely that the current northern representatives of the *An. maculipennis* group were found in southern areas of Europe during and after the Ice Age (Marshall

1938 in Bruce Chwatt and de Zulueta 1980). By the beginning of the Neolithic (8000 to 5000 BC), the climate was such that these mosquitoes could have started spreading northwards (Dansgaard and Tauber 1969). It was also during this time that malaria parasites (*Plasmodium vivax* and *P. malariae*) may have been imported to the Mediterranean from tropical Africa (Bruce-Chwatt and de Zulueta 1980) and disease transmission properly established. These assumptions are based on calculations of ancient temperatures (from snowline depressions) and the introduction of agriculture which created favourable conditions for disease transmission (Brothwell and Sandison 1967 in Bruce-Chwatt and de Zulueta 1980). At the time, the refractoriness of European *Anopheles* to *P. falciparum* (see below) is thought to have acted as a barrier to the introduction of this parasite (Bruce-Chwatt and de Zulueta 1980). Despite the presence of *Plasmodium vivax* and *P. malariae*, the effects of the disease at this time were presumably not major. Judging by references in ancient literature, however, prevalences increased during the early Hellenistic days (around 400 BC, Jones 1907). This is thought to be because two highly efficient vectors (see Chapter 4), *Anopheles labranchiae* and *An. sacharovi* (both members of the *An. maculipennis* complex) were apparently introduced into southern Europe from North Africa and West Asia due to increased navigation and trading (de Zulueta 1974). The present coastal distribution of these two vectors suggests a nautical dispersal which correlates well with this theory (Bates *et al.* 1949). Additionally, local vector populations may have slowly become adapted to *P. falciparum* which was also introduced at an increasingly greater rate by population movements and army invasions. The breakdown of the *P. falciparum* refractoriness barrier is thought to have been slow and not widely spread until centuries later (Bruce-Chwatt and de Zulueta 1980). Following the colonisation of the two important anophelines and, possibly, the establishment of *P. falciparum* transmission, malaria became a gradually more serious endemic disease in the Mediterranean as indicated by descriptions in Roman medical and philosophical literature. Historical literature indicates that, from the thirteenth century onwards, malaria was endemic in nearly all Mediterranean cities. The disease was generally widespread in maritime areas, along river valleys and in areas of rice cultivation which were ideal mosquito breeding sites. It was from these strongholds that the disease could have spread throughout the continent, until – by at least the 13th century – it had become established across Europe, limited only by the 15°C July isotherm (in the case of *P. vivax*) which includes Denmark, Finland, Sweden and large parts of northern Russia (Hackett 1937). The distribution of *P.*

falciparum was less extensive, restricted mainly to the Mediterranean with the northernmost areas of transmission being reported from southern France (Bruce-Chwatt and de Zulueta 1980).

Indigenous malaria in Europe during the 19th and 20th centuries

In the early nineteenth century, malaria spontaneously started disappearing from most northern European countries. Wesenberg-Lund (1921) famously suggested that the decline of malaria in Denmark was due to the construction of pigsties and stables which created more attractive resting sites for local *An. atroparvus* than human houses. Before this time, malaria was considered an important health problem with high prevalences in even the Scandinavian countries – a fact which has been mainly attributed to the wide-spread presence of *An. atroparvus* and *An. messeae* in coastal areas (Hackett and Missiroli 1931, Ekblom 1945, Jaenson *et al.* 1986). Throughout this region, *P. vivax* is thought to have been the only parasite transmitted mainly due to unfavourable climatic conditions for *P. falciparum* (Bruce-Chwatt and de Zulueta 1980). In Germany, the northern marshes and areas along the Rhine were notoriously malarious (Hirsch 1883), but in spite of the adverse circumstances and localised outbreaks during the two World Wars, the disease disappeared soon after the Second World War. This was the case in the majority of central Europe, however, the Netherlands were an interesting exception. In 1955, there were still 22 indigenous cases due to the very high abundance of *An. atroparvus* in the low-lying marshlands (Takken *et al.* 2002) . When DDT spraying was introduced in 1946, the mosquito populations declined rapidly, effectively reducing transmission which was officially zero by 1962. Like other countries at this latitude, the gradual decline of English malaria was also linked to agricultural and social changes which eventually eradicated a disease that had previously been responsible for high mortality in the marsh parishes (see Chapter 2). The decreasing trend in the UK and other countries in North-west Europe was briefly interrupted by the First and Second World Wars which led to outbreaks of local transmission as a result of infected soldiers returning home (e.g. 500 indigenous cases in the UK in 1920 compared to 231 in 1915). It was also after the First World War that malaria for the first time appeared within the Arctic circle as transmission was reported from Archangel (Hackett 1937). In spite of this, we can now safely conclude that even these outbreaks did not halt the natural disappearance of malaria from the northern part of the continent.

The scenario was different in the Mediterranean and eastern Europe where prevalences remained high. In Eastern Europe, the vast marshes of Poland created many endemic foci and serious epidemics in the late 1800s (Bruce-Chwatt and de Zulueta 1980). Already in 1925, malaria control regulations consisting of early diagnosis, compulsory case notification and increasing quinine distribution had been applied, but these were halted during the Second World War which created a large wave of malaria epidemics, mainly due to *P. vivax*. This pattern was also observed in the former Soviet Union (FSU) where occupied areas were especially vulnerable.

All southern countries along the Mediterranean were among the most malarious in Europe due to the very favourable temperatures and the presence of the two highly competent vectors, *An. labranchiae* and *An. sacharovi*. When given a choice these mosquitoes prefer human blood meals, they are highly endophilic and have on several occasions been found infected in nature (e.g. Hackett and Missiroli 1935, Hackett 1937, Jetten and Takken 1994). Parasitological evidence (see below) has confirmed that both *P. vivax* and *P. falciparum* were transmitted in the Mediterranean which explains the peak of malaria mortality due to *P. falciparum* observed particularly in Greece and Italy during September and October (Hackett 1937, Bruce-Chwatt and de Zulueta 1980). At the end of the nineteenth century, the annual total number of cases in Italy may have been as high as 2 million in a population of only 30 million (Bruce-Chwatt and de Zulueta 1980). The disease was particularly severe in Sardinia, a fact which prompted the numerous entomological and parasitological investigations that now form the basis of much of our knowledge of European malaria.

Before the Second World War the Balkans were highly malarious, especially around the shores of the Black Sea where mosquito breeding conditions are ideal. At this time, most reported cases were due to *P. vivax*, however infections with *P. falciparum* resulted in high mortality rates. Like in most of Europe, the years immediately following the Second World War were especially serious with epidemic infection rates reaching as high as 70% (Bruce-Chwatt and de Zulueta 1980). Greece was considered to be one of the most malarious countries in Europe with 1-2 million people infected annually during 1931-35 and a death rate of 74 per 100, 000 inhabitants (Bruce-Chwatt and de Zulueta 1980).

The continued transmission of malaria in eastern and southern Europe during the time when incidences were decreasing in the rest of the continent prompted the initiation of vector control programmes using DDT residual spraying in the early 1940s. Most

programmes soon broke down due to the Second World War but were resumed in the late 1940s or early 1950s and caused incidences to decline dramatically in Italy, Portugal, Cyprus, Spain and Corsica (e.g. there were 133,820 indigenous cases in Italy in 1944 compared to only 150 in 1950, a reduction of 99.9%). In 1959, The WHO Regional Committee for Europe urged all currently endemic countries to reach the consolidation phase of the eradication programme established in 1955. This was followed by a string of country-wide eradications ranging from Spain in 1964 to the Netherlands and Italy in 1970 until the last focus of malaria in the Greek republic of Macedonia was officially eradicated and Europe declared malaria free in 1975.

Table 3.1. Summary of malaria extinction and eradication in Europe (from Bruce-Chwatt and de Zulueta 1980.

Country	Last indigenous case	Extinction process
Switzerland	1900	Natural
Denmark	1901	Natural
Finland	1920	Natural
Belgium	1932	Natural
Sweden	1939	Natural
France	1940	Natural
Germany	1941	Natural
Austria	1950	Natural
United Kingdom	1953	Natural
Poland	1956	Eradication programme
Portugal	1958	Eradication programme
Bulgaria	1960	Eradication programme
Netherlands	1961	Eradication programme
Hungary	1962	Eradication programme
Italy	1962	Eradication programme
Romania	1962	Eradication programme
Spain	1962	Eradication programme
Yugoslavia	1964	Eradication programme
Albania	1966	Eradication programme
Greece	1975	Eradication programme

European malaria parasites

The role of European anophelines in the transmission of malaria will be discussed in detail in Chapter 4. Here, it is therefore sufficient to mention that most vectors of malaria in Europe belong to the *An. maculipennis* complex and that the most important of these were *An. atroparvus*, *An. labranchiae*, *An. messeae* and *An. sacharovi* (Jetten and Takken 1994).

The description of tertian and quartan fevers in the Hippocratic writings of the 4th century BC (Jones 1907) suggests that *P. vivax* and *P. malariae* were probably the parasites responsible. As mentioned, the history of *P. falciparum* in Europe remains unclear. However, the presence of the glucose-6-phosphate deficiency (G6PD) and thalassaemia (both of which are associated with *P. falciparum*) in Mediterranean populations strongly points to its presence here in historical times (e.g. Monteiro *et al.* 1989, Astolfi *et al.* 1999). According to Tishkoff *et al.* (2001), the Mediterranean G6PD could have arisen within the past 1600 to 6400 years which correlates with the theory that *P. falciparum* transmission was established relatively late in Europe.

More direct evidence about the strains of parasites transmitted in Europe did not emerge until the beginning of the 20th century. From the 1920s onwards, European *P. vivax* was identified in local patients from Denmark, Germany, France, Romania, the Netherlands, the UK, Spain, Italy and Greece by microscopic analysis of infected blood (Hackett 1937, Bruce-Chwatt and de Zulueta 1980). Giovannola (in Hackett 1937), De Buck (1936) and Hackett (1937) all observed significant differences when comparing these indigenous strains of *P. vivax* to a strain from Madagascar. The European strains were a different size (generally smaller) and produced higher fevers than the tropical parasites. This difference can also to some extent be inferred from the fact that European *P. vivax* was often fatal (e.g. Bruce-Chwatt and de Zulueta 1980, Dobson 1997, Reiter 2000) while the current tropical strains very rarely result in any deaths (Mendis *et al.* 2000). The possible reasons for this apparently high fatality of European *P. vivax* has been discussed in detail in Chapter 2.

The more virulent *P. falciparum* has only been isolated from Italy (Rome and Sardinia), Greece and Albania (Hackett 1937). There are no identifications of *P. falciparum* in northern Europe and the northernmost transmission area was thought to be in southern France (the evidence based on average summer temperatures and not parasite identifications, Bruce-Chwatt and de Zulueta 1980). This suggests that *P. falciparum* transmission was restricted to the Mediterranean while *P. vivax* was more wide spread.

Because it was far less common and less easy to work with than *P. vivax*, there have been no studies to examine how this parasite differs from the tropical strains. It has been suggested that the European strain of *P. falciparum* originated from a tropical strain but then became adapted to temperate conditions and vectors and, like the European *P. vivax*, finally became a different parasite (de Zulueta 1974, Bruce-Chwatt and de Zulueta 1980). The only evidence currently available to support this theory is the well-documented refractoriness of European malaria vectors to tropical *P. falciparum* which will be discussed in detail in Chapter 4.

Records of indigenous *P. malariae* infections have been reported from a wider range of countries than *P. falciparum* (France, Germany, Greece, Italy, the Netherlands, Spain), but due to difficulties establishing laboratory colonies, the relationship between the European and tropical strains of this parasite also remains unknown.

These accounts of parasite identifications are most likely far from complete but, as they are the only published evidence, we can only assume that they represent a relatively accurate picture of European malaria parasites.

The relative importance of each parasite in areas where all three or only two species were transmitted cannot be fully documented due to lack of data. There are only a few published accounts which describe the parasite rates in specific locations and all of these are limited to Greece and Italy. Examinations of school children in Greek villages during 1930-1933 (Balfour 1935) showed a large geographical variation in the prevalence of the three parasites. One particular village had 100% *P. falciparum* infection rates while another had 40% *P. vivax* and 60% *P. falciparum* and a third 68% *P. vivax*, 23% *P. falciparum* and 9% *P. malariae*. In all 7 villages studied, *P. falciparum* rates were highest accounting for an average of 64% of infections followed by *P. vivax* with 29% and *P. malariae* with 15%. In a similar survey during 1934, the pattern showed almost similar rates between the parasites with 34% *P. vivax*, 33% *P. falciparum* and 31% *P. malariae* (Balfour 1936). In a study in an Italian village in 1924 (quoted in Hackett 1937), the prevalence of *P. vivax* and *P. malariae* (reported together) was found to be 71% compared to 29% *P. falciparum*. Thus evidence indicates geographical variation in the prevalence of *P. vivax*, *P. falciparum* and *P. malariae*, the pattern of which was most likely determined by a combination of entomological and environmental factors such as temperature (i.e. the development threshold of *P. vivax* versus *P. falciparum*).

Like the distribution and prevalence of parasites, the seasonality of transmission was also geographically determined. In the northern countries (e.g. Denmark and Finland), there was a single peak of *P. vivax* cases in May and a less noticeable (sometimes not present) one in September or October (Ekblom 1945). Generally, throughout central and western Europe, there were two clear peaks of *P. vivax* cases; one in early spring (from the previous year's infections) and in late summer (from infections acquired in the same year, e.g. Whitley 1863, Dobson 1997). In countries where both *P. vivax* and *P. falciparum* were transmitted, *P. vivax* cases peaked early in the spring or summer (e.g. May in Italy) and *P. falciparum* in the autumn (e.g. October in Italy, Hackett 1937, Bruce-Chwatt and de Zulueta 1980).

Current malaria transmission in the WHO European Region: Turkey and the Former Soviet Union

There are fifty-one countries in the WHO European Region of which Azerbaijan, Tajikistan and Turkey are currently endemic for malaria (Fig. 3.1, Table 3.2). There have also been small recent outbreaks in Armenia, Kazakhstan, Kyrgyzstan, Turkmenistan, Georgia, and Uzbekistan and sporadic transmission of autochthonous malaria in Bulgaria, Belarus, Germany, Greece, Italy, the Republic of Moldova, and Russia some of which are discussed below. In 1990, a total of 8884 cases of indigenous malaria were reported in the WHO European region. By 1995 this had increased to 90,712 but in 2000 the reported number was 32,456 of which 59% were from Tajikistan (WHO 2002a). Today all countries within the WHO European region are asked to provide information on the annual number of laboratory-confirmed cases. Considering that this may pose difficulties in some countries, many of the numbers quoted in this section are likely to be underestimating the true prevalence of indigenous malaria.

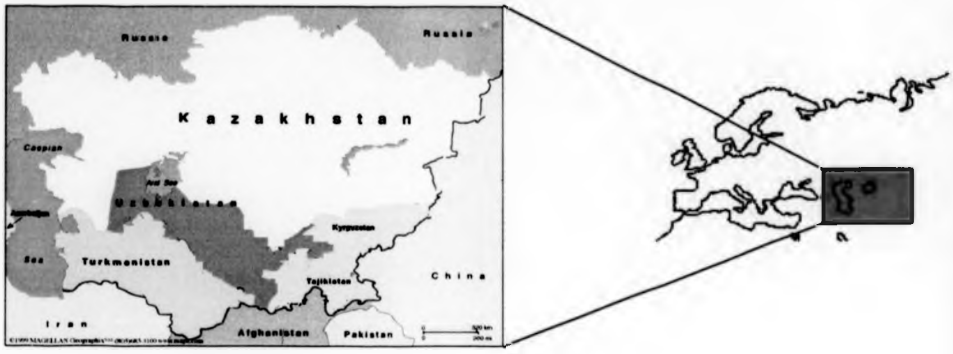

Figure 3.1. Map showing the location of some of the currently malaria endemic countries in the WHO European region.

Table 3.2 . Indigenous malaria (annual cases) in the three most endemic countries of the WHO European region since 1990.

Country	Indigenous malaria 1990	Indigenous malaria 1995	Indigenous malaria 2000
Azerbaijan	24	2,840	1,526
Tajikistan	175	6,103	19,064
Turkey	8,675	81,754	11,381

Turkey is today one of the most malarious countries in the region with 15 million people (or 23% of the population) at risk from malaria in the whole country (i.e. including both the European and the Asian parts). Although *P. falciparum* transmission ceased and *P. vivax* incidence decreased drastically after the introduction of a malaria eradication programme in 1960, ten years later transmission levels had started increasing again and reached endemic proportions by 1980 with more than 34,000 reported cases almost all due to *P. vivax* (Ramsdale and Haas 1978, WHO 2002a). The gradual decrease observed in the late 1990s has been mainly due to the WHO Roll Back Malaria programme which has commissioned local and international governmental and non-governmental organisations to improve case detection and treatment, residual insecticide spraying as well as monitor vector populations and their sensitivity to insecticides (Gockchinar and Kalipsi 2001).

A similar pattern with steadily increasing indigenous malaria cases has been observed in countries of the former Soviet Union (Fig. 3.1) since malaria eradication was confirmed in 1961. This situation has occurred particularly as a result of several wars, leading to a steady movement of infected people across borders and a lack of governmental funding for appropriate vector control programmes and health system improvements. Tajikistan is the worst affected with 19,064 reported cases in 2000 followed by Azerbaijan with a total of 1,526 cases in the same year. As in Turkey, over 90% of all reported cases in these countries are caused by *P. vivax* (Sabatinelli *et al.* 2001). Since 1997, the WHO Roll Back Malaria programme has supported non-governmental institutions to initiate malaria control activities especially in Tajikistan including the distribution of treated and untreated bed nets, mass treatment with primaquine and indoor residual insecticide spraying (Aliev and Saparova 2001).

Current malaria transmission in the WHO European Region: European Union countries

Reports of local malaria transmission in the more temperate regions of Europe (i.e. EU countries) can broadly be divided into two categories: indigenous and airport malaria.

An indigenous case is defined as transmission of malaria by a local vector. Since 1975, true indigenous cases have been reported from Italy, Germany and Greece (Baldari *et al.* 1998, Kruger *et al.* 2001, Kampen *et al.* 2002). The most recent cases in Greece were observed in 2001 when two German tourists became infected with *P. vivax* in Halkidiki. Before that, in 1994-1995 four cases (2 *P. vivax*, 1 *P. falciparum* and 1 *P. malariae*) were microscopically diagnosed in local Greek residents who had never travelled, had blood transfusions or visited an international airport (Kampen *et al.* 2002). The Italian case was observed in a woman living in rural Maremma (west Italy) with no travel or blood transfusion history. Her *P. vivax* infection had most likely been transmitted by *An. labranchiae*, the previous vector of Italian malaria, which had acquired the parasite from a neighbour infected with *P. vivax* during a trip to India. Maremma lies near the Po Valley which was historically a very malarious area, providing ideal breeding sites for *An. labranchiae*. In 1997, two German children – again with no travel or blood transfusion history – were infected with *P. falciparum* in a hospital in Duisburg by the Rhine valley. In the absence of imported tropical vectors (see below), the authors concluded that local *An. plumbeus* (a suspected possible vector of tropical *P. falciparum*) had picked up the infection from an Angolan *P. falciparum* patient in the

hospital and transmitted it to the German patients. While the German route of infection needs further confirmation, it is interesting to note that both cases occurred during the 1997 heat wave and in locations which had previously been highly malarious.

The definition of airport malaria is an infection from the bite of an imported tropical mosquito in people who work in or live near airports. It is important to note that airport malaria cannot correctly be classified as local, indigenous or autochthonous malaria which is an infection transmitted by a local (i.e. indigenous) mosquito (Holvoet *et al.* 1983). Some tropical vectors can survive in the low temperatures of a luggage compartment and are therefore ideal for overseas transportation (e.g. *An. arabiensis* from Madagascar overwinters in altitudes above 1500 m., Castelli *et al.* 1994). All infective anophelines identified in or near airports have originated from sub Saharan Africa (Guillet *et al.* 1998). From 1969 to 1997, 63 cases of airport malaria were reported in Western Europe, the majority of them due to *P. falciparum* infection (Guillet *et al.* 1998). During the very hot summer of 1994, six new cases of airport malaria were described in and around Charles de Gaulle airport, Paris, and consequently aircraft spraying using residual pyrethroids is now regularly carried out at this airport (Giacomini *et al.* 1995).

Imported malaria in Europe

With the advance of commercial travel as well as increasing levels of immigration, Europe has experienced a steady rise in the number of imported cases of malaria (i.e. infections acquired in the tropics). Over the past thirty years, there has been an eight-fold increase in the reported number of imported cases (from 1,500 in 1972 to 13,000 in 1999) and since 1989, there have been 680 deaths from imported *P. falciparum* infections in Europe (WHO 2002a). The largest numbers of imported cases are reported from France, The UK, Germany and Italy (Table 3.3) where considerable numbers of people are originally from abroad and return regularly to visit family. It has been demonstrated that such overseas visits by immigrants settled in Europe account for as much as 22-37% of the total number of imported cases (Bradley 1989, WHO 1997). The second largest group responsible for imported malaria cases are European tourists travelling abroad and foreign visitors who fall ill while in one of the European countries (Bradley 1989).

Table 3.3. Imported malaria cases in 4 European countries in 1995 and 2000.

Country	Total cases in 1995 (% *P. falciparum*)	Total cases in 2000 (% *P. falciparum*)
France	3675 (82)	8056 (81)
Germany	941 (64)	732 (78)
Italy	743 (71)	986 (81)
UK	2055 (54)	2069 (76)

Although imported malaria is rising throughout Europe, the detection and treatment of cases is so rapid and efficient in all central and western countries that the risk of these infections being transmitted by local vectors is clearly very low. However, many physicians are not aware that malaria is a notifiable disease, and consequently under-reporting of cases is far too common in Europe. It has been estimated that 56% and 59% of malaria cases brought into the UK and France, respectively, are not reported (Eurosurveillance 1998). This lack of notification may especially become a problem in countries bordering the current endemic regions. For instance, the number of cases being imported into Bulgaria and Romania from the Former Soviet Union is now increasing and this causes concern of local transmission potential in areas which are already vulnerable due to slow development of health systems (Vutchev 2001, Nicolaiciuc *et al.* 1999). The significance of imported cases, their detection and treatment will be discussed in detail in Chapter 5 with reference to the potential re-emergence of malaria transmission in Europe as a result of climate changes.

Malaria and the environment

To my knowledge, the interaction between malaria patterns and the environment has never been studied for historical malaria across the European continent. However, the strong association between recent spatial patterns in malaria and environmental factors (such as temperature, rainfall and vegetation) has been quantified numerous times with the aim of predicting malaria risk in the tropics.

At the continental level, a major advance in the study of African malaria was the development of the Mapping Malaria Risk in Africa/ Atlas du Risque de la Malaria en Afrique (MARA/ARMA) project which has established a database on all available malaria data in Africa (MARA/ARMA 1998). One of the first objectives of the MARA/ARMA was to identify the geographical limits of stable malaria

transmission. This was done by Craig *et al.* (1999) who completed a malaria distribution model based on the assumption that malaria transmission in the Sub-Saharan African continent is limited mainly by temperature and rainfall. Weather station data of mean monthly temperature and precipitation during 1920-80 were interpolated to a grid of 5 km (0.03°) resolution. A fuzzy logic model which expresses degrees of climate suitability ranging from 0 (non-suitable) to 1 (suitable) was used to convert the climate grids to malaria suitability maps. Suitable conditions for malaria had been defined using empirical data on mosquito and parasite development; the cut-off between epidemic and non-malarious zones (identified using MARA/ARMA and other data) being 18°C and at least 80 mm rainfall per month for 5 months. The predictive risk map based on these thresholds correlated well with previously published (1930-1997) maps of malaria transmission. The model was next used to estimate the number of people at risk of malaria by reclassifying model outputs so that a value of 0.5 and above indicated malarious areas and overlaying the risk map with a 4.5 km resolution population grid (Snow *et al.* 1999). The map estimated that 360 million people currently live in predicted malaria-endemic areas. The main draw-back with the original approach (Craig *et al.* 1999) is the relatively crude definition of malaria presence or absence which neglects small-scale variations in land cover and climate. Such assumptions can easily lead to predictions that mosquito-free areas should be malarious - and vice versa. Another limitation is the use of 1920-80 climate averages to predict present scenarios. Ideally, more recent climate data should have been used.

Also at a relatively low resolution, Kleinschmidt *et al.* (2001a) used annual parasite prevalence from the MARA/ARMA database to map the distribution of malaria in West Africa. Point data from 250,000 children in 450 locations in West Africa from 1970 onwards were used in combination with 5 km resolution monthly rainfall, temperature and NDVI. Data were divided into four agro-ecological zones depending on the amount of time when water is available for vegetative production. A logistic regression model (including spatial autocorrelation) was developed to predict parasite prevalence as a function of environmental variables in each zone. A 5 km resolution map of predicted malaria risk was overlaid on a population density grid to estimate the population at risk in West Africa. Predictions were made with 78% accuracy and it was estimated that 153 million people live in areas with 30-70% malaria parasite prevalence. The analysis presented here uses 5 km

environmental data which, in correlation with point disease data, is a relatively low resolution. Use of the NOAA-AVHRR 1 km resolution data may have provided more accurate predictions. The disease data collected from 1980 onwards do not correlate with the climate data which represent monthly averages from 1920-80 only. The authors correctly conclude that, in order to improve predictions further, information on socio-economic factors should also be included.

On a more local scale, Hay *et al.* (1998) used linear regression to identify the relationship between monthly malaria hospitalisations in three regions of Kenya and monthly Fourier processed (smoothed) remotely sensed vegetation, land surface temperature and cold cloud duration at 8 km resolution. The results showed that an NDVI threshold of 0.35-0.4 was required for more than 5% of malaria cases to present in a given month. This threshold was then used to define the number of months with conditions suitable for malaria and to produce a malaria risk map for Kenya. The map corresponded well with expert opinion of malaria seasonality. As with the previous studies, the environmental data used were relatively low resolution, disallowing the identification of small areas suitable for malaria transmission.

Also in Kenya, the parasite prevalence in children from 124 surveys at village level after 1965 was collated from literature surveys (Omumbo *et al.* 1998) and classified into high (70%), intermediate (20-69%) and low (< 20%) transmission areas. These results were analysed against rainfall and temperature data (interpolated from station measures to a 5 km resolution grid) as well NDVI measures (5 km resolution) using a stepwise discriminant analysis approach which allocated all locations into one of the transmission categories (Snow *et al.* 1998). Ninety-six locations (77%) were correctly allocated. A risk map was then constructed and overlaid on a 4.5 km resolution population density map to show the population at risk of different levels of malaria transmission. The main problem with this study is the interpolation of climate data from station measurements. The number of stations is not given but in order to obtain relatively accurate results this should have been considerable.

In Mali, at the country level, Kleinschmidt *et al.* (2000) used annual parasite prevalence (collected from active surveys in children) data from 101 sites throughout the country since 1960. Environmental data consisted of monthly NDVI, temperature and rainfall at a 5 km resolution. Temperature and rainfall were averaged over 3 month periods while NDVI was aggregated over two 6-month

periods to correspond with the wet and dry seasons. A predictive model was constructed using logistic regression (including spatial autocorrelation) the outcome of which was used to construct a risk of map of malaria prevalence in children throughout Mali. The observed disease data were clustered in malarious areas, creating a bias in the outcome. Predictions will be less correct in areas with lower malaria prevalence but, as the authors conclude, if malaria is not a problem then predictions of transmission will be less valuable.

In South Africa, Kleinschmidt *et al.* (2001b) analysed small-scale variation in annual malaria cases (obtained by both active and passive case detection) in 220 divisions (size range 1.1-263 km^2) during 1994-95 in combination with 5 km resolution monthly rainfall and temperature as well as the distance to water from the centroid of each section. Malaria data were converted into annual incidences and climate variables to 6-month averages. The relationship between malaria incidence and climate was analysed using generalised linear models (including spatial correlation analysis by a variogram) and the final model used to generate a map of predicted malaria incidence rates at the section level. The climate data used were long-term averages for 1920-1980 which does not correlate well with the malaria data used (1994-95).

Work from the Gambia has demonstrated that malaria infection rates can be related to NDVI seasonality (Thomson *et al.* 1999b). Cross-sectional malaria prevalence data were collected from 2276 children in 65 villages and correlated with monthly NDVI (1 km resolution) using a logistic regression model adjusted for the effects of treated and untreated bed nets. The number of *P. falciparum* infected children was predicted for all villages for different net scenarios showing that if all children slept under treated nets, parasite prevalence would decrease from 36 to 30%. This study uses well correlated disease and environmental data (relatively high resolution) and is also one of the first to account for behavioural risk factors which are of vast importance when considering malaria patterns.

In comparison to these examples of how environmental factors have been used to investigate spatial patterns of malaria, inter-annual variations in malaria have only rarely been examined. The lack of long time historical analyses of malaria in relation to climate and other environmental factors is unfortunate considering the large amount of data available in many countries. Studies by Bouma *et al.* (1996) and Bouma and van der Kaay (1996) in the Punjab and Sri Lanka using possibly the longest duration of time-

series of disease data (76 years) have been discussed in detail in Chapter 2. A few other examples relating to the use of historical climate and disease data have also been discussed previously. All of these studies have examined temporal patterns at one location (i.e. one site or country) while the analysis presented here, as in Chapter 2, will attempt to explain inter-annual variability in several countries using a single environmentally-driven model.

The studies summarised above have confirmed the usefulness of both remotely sensed and ground-observed environmental data for investigating the spatial and temporal patterns of malaria. From these we have learnt the importance of selecting appropriate climatic, land cover, agricultural and possibly socio-economic variables at an adequate resolution to correspond with disease data. On numerous occasions it has been concluded that the use of high resolution environmental data is particularly desirable as this will allow us to identify small-scale variations in risk factors and produce more accurate predictive maps. The idea of using long-term historical disease and environmental data is, however, relatively understudied. For this analysis of malaria in Europe, country-wide measures of climate (interpolated from 0.5° resolution gridded data) and land cover (ground-observed) as well as other agricultural variables will be used to investigate the inter-annual variability in malaria as reported by European countries (at the national level) during the early to the late 20th century. Though at lower resolution this study is designed in a similar way to that described in Chapter 2 (with similar caveats) and the results will allow identification of the determinants of malaria risk in historical Europe, providing a prime handle to predict future risk as the result of environmental changes.

Aims and Objectives

The aim of this study is to quantify the roles(s) of environmental, climatic and agricultural factors in the inter-annual variability in indigenous malaria case rates in European countries during 1900-1975. The starting period of 1900 was selected because this was the first year the malaria data were available for the majority of the 17 countries and the study terminates in 1975 because this is the latest year when any indigenous malaria cases were reported in the countries included in the study. Disease data and agricultural variables were all collected at the country level as this was the only resolution available. Climate data at 0.5° resolution (derived from meteorological station data) were obtained for all years with available malaria data in order to obtain the best possible temporal correlation between outcome and explanatory data.

The specific objectives of the study are:

1. To investigate the factors determining the inter-country variability in average indigenous malaria case incidence rates within Europe during the 20th century.
2. To test whether inter-annual variability in the incidence rate of indigenous malaria cases within European countries in the 20th century was significantly affected by inter-annual changes in cattle density, woodland coverage, rice cultivation, temperature and/or rainfall.
3. To quantify the impact of changes in these parameters on the inter-annual variability in malaria (by model simulations).

Methods

Collection of indigenous malaria data

Cases of indigenous malaria at country level from 1900 up to 1970 were supplied by national statistics offices in the relevant countries and also collected from tables presented by Bruce-Chwatt and de Zulueta (1980). For those countries in which indigenous and imported malaria cases were not distinguished throughout parts of or the whole study period, the number of indigenous malaria cases were estimated using information from the first ten years with definite data on imported malaria (i.e. the first 10 years following national eradication). For those years, an average number of imported cases was calculated which was then subtracted from the data reported in these years without the imported-indigenous distinction, in order to obtain an estimated number of indigenous cases. For instance, the last indigenous case was reported from Portugal in 1958 (when there were 11 imported cases). In order to estimate the number of indigenous cases per year before 1958, the average number of imported cases during 1958-1967 was calculated (70.2) and subtracted from the total number of cases reported each year before 1958.

Malaria data after 1970 were collected from the World Health Organisation Regional Office for Europe malaria database (WHO 2002a) which supplies data on both imported and indigenous cases at country level for the whole of the WHO European region. In total, data from 17 countries were collected (see Table 1). During the whole period, both Yugoslavia and Germany were considered as one country (i.e. data reported separately for East and West Germany were pooled and, similarly, all data from the former Yugoslav republics were combined to give one value for Yugoslavia). Because of inconsistencies in data availability from country to country, malaria data were not available for every year in every country. However, malaria data for all 17 countries were available for the years: 1900, 1905, 1910, 1915, 1920, 1925, 1930, 1935, 1940, 1945, 1950, 1955, 1960, 1965, 1970 and 1975. The data point at each of these years represents the number of malaria cases in the specific year only (i.e. not an average or total for the preceding years). For the years in between, the availability of the data varied from country to country (Table 3.4). A total of 677 country-year data points were collected for the 17 countries during the 76 years.

Table 3.4. European countries included in the malaria database.

Country	Additional data available*	Total data points
Albania	-	17
Austria	-	17
Bulgaria	1946-1959	28
Denmark	-	17
Finland	1901-1939	48
Germany	-	17
Greece	1954-1974	33
Hungary	1946-1974	40
Italy	1902-1974	75
Netherlands	1946-1974	40
Poland	1919-1939, 1946-1974	56
Portugal	1938-1974	46
Romania	1948-1974	38
Spain	1936-1974	48
Sweden	1901-1939	48
United Kingdom	1917-1974	63
Yugoslavia	1929-1939, 1947-1974	46

* The additional data available refer to annual malaria data collected for the years not listed in the text above (- indicates that no additional data were available).

Collection of demographic and agricultural data

Annual population figures (projected by the EC from 10-year census data) for each country were supplied by the European Commission Statistical Database, Eurostat (2002). These were downloaded for all years with malaria data (see above).

This data shop also provided a measure of total country land cover (i.e. size) as well as data on woodland coverage, rice cultivation and the number of cattle in each country for the years and countries of interest.

Collection of climate data

Measures of temperature and precipitation for 1900 only were derived from the historical meteorological station data described in Chapter 2. The full European dataset consisted of measurements from approximately 1200 stations which were georeferenced and overlaid onto a map of Europe which outlines all country borders. Climate data for each country

was then calculated as the average of all stations lying within each country. For the years 1901-1975, climate data for each year in each country with available malaria data were extrapolated from the 0.5° Gridded 1901-1995 CRU climate dataset. This database has been described in detail in Chapter 2. The 0.5° climate grid map was overlaid on an ArcView map of Europe and all climate grid cells lying within each country border identified as described in Chapter 2. For all countries, climate data were then calculated as the average of all the 0.5° climate grid cells within each country. As described previously, all temperature data were converted into annual maximum, minimum and mean average values and precipitation into annual total for the relevant years listed earlier.

A full database listing indigenous malaria cases, population measures and all explanatory variables for each country in each year was assembled in Excel '97.
This database was exported into STATA 7.0 for analysis. A summary of all explanatory variables, their availability and conversion is presented in Table 3.5 below.

Table 3.5. Explanatory variables; their availability and final conversion for use in the models.

Variable	Availability (units)	Conversion
Population	Annual	N/A
Country size (area)	1 value to cover the whole period	N/A
Woodland area	Annual (km^2)	Percentage of country area
Rice cultivation	Annual (km^2)	Percentage of country area
Cattle	Annual	Density per 1 km^2
Minimum temperature	Monthly	Annual minimum average
Mean temperature	Monthly	Annual mean average
Maximum temperature	Monthly	Annual maximum average
Precipitation	Monthly	Annual total

Geographical Information System maps

The ArcView 3.2 World Map which is supplied with the GIS package ArcView 3.2 forms the baseline of all maps shown in this paper. Manipulation and display of geographical data was performed in the GIS ArcView 3.1.

Descriptive and univariate analyses

Descriptive statistics (mean, minimum and maximum) and frequency distribution of all explanatory variables were generated using the statistical package in Excel '97.

Univariate analyses (Poisson regression, see below) were performed in STATA 7.0 to (1) determine the relationship between indigenous malaria and each potential explanatory variable in turn and (2) test for non-linearity in the effect of explanatory variables on indigenous malaria. All univariate analyses were undertaken by adding the explanatory variable of interest to the null model described below.

Multivariate models

To investigate the causes of temporal variation in indigenous malaria, multivariate models were generated using the GLM command in STATA 7.0. Poisson models were then used in GLM to investigate the spatial and temporal patterns in disease with the explanatory variables as described above. Because the malaria data were highly overdispersed, the model was scaled for overdispersion using the Pearson chi squared-based dispersion. Poisson GLM models again take a linear form where:

$$\ln(\text{malaria case}) = c + t_1x_1 + t_2x_2 + t_3x_3 + \ldots.t_nx_n$$

c, t_1, t_2, t_3 and t_n are constants, c is a country specific constant (i.e. there was a different categorical variable for each country). For the spatial predictions, c was a year-specific constant.

x_1, x_2, x_3 and x_n are explanatory variables

In order to predict the number of malaria cases from the final model output, the following back-transformation is used:

$$\text{malaria cases} = \exp(A) \qquad \text{(Equation 3.1)}$$

where A is the fitted value calculated from the model output using all significant explanatory variables.

For the temporal model, following the same rationale as described for the UK ague analysis, a categorical 'country' variable and a temporal trend were included. The temporal trend was tested for non-linearity and found to have a significant quadratic

relationship with malaria rates. On a priori grounds and by inspection of the data, two different categories of countries were defined; eradication by DDT or natural decline (Table 3.1); hence DDT was added as a categorical variable in an interaction with the temporal trend (see Box 3.1 below). The value of this variable was set to 1 for countries which had ever used DDT and 0 for countries which had not used DDT to eradicate malaria. The interaction between the DDT variable and the year variables is to account for the fact that the temporal trend in malaria was different in DDT versus non-DDT countries (Fig. 3.3-3.5). To include the effect of the two World Wars, war was also included as a categorical variable. The variable was set to 1 for war years (1915-1920 and 1940-1946) and 0 for years with no World War. The year 1915 was chosen as the start year of World War I as, for most countries, there were no data available for 1914 while 1920 was chosen as the end point after inspection of the data which generally showed a return to pre war levels after 1920. The Second World War was represented by the years 1940-1946 for the same reason (i.e numbers of cases during these years were above pre-war levels). There was no significant temporal autocorrelation, most likely because a significant proportion of the 'previous year's' residuals were missing data points.

The temporal null model was defined as the model containing (1) the county categorical variable, (2) the war/peace categorical variable and (3) the interaction between DDT and both the linear plus the quadratic temporal trend. Because no temporal autocorrelation was detected this was not included in either the null or the minimal adequate models. The minimal adequate model was constructed in a backwards stepwise manner and its fit assessed as described in Chapter 2. The variance explained by a significant explanatory variable was derived by running the minimal adequate model with the particular variable and comparing the resulting deviance to that of the null model.

A spatial model to explain the inter-country variation in indigenous malaria was also created following the same steps as outlined in Chapter 2. This time the null model was defined as a model containing only a categorical 'year' variable in interaction with the DDT variable. There was no attempt to correct for spatial autocorrelation as the computer software and techniques this requires are beyond the scope of this study.

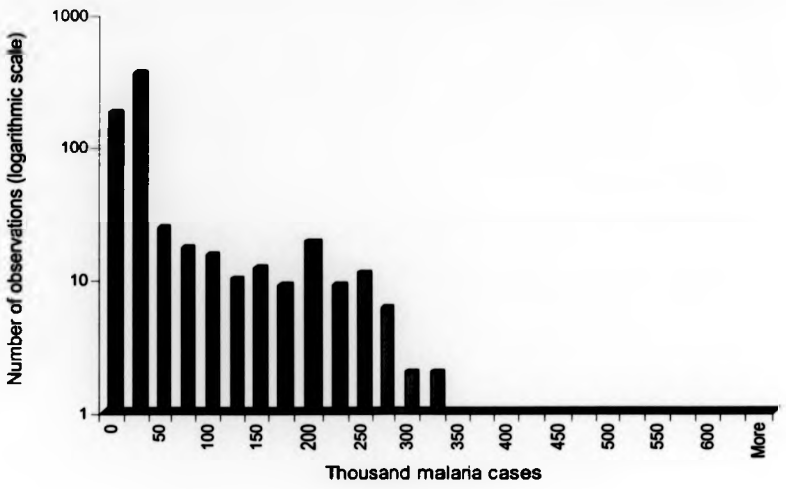

Figure 3.2. Frequency distribution of malaria cases in Europe during 1900-1975.

Prediction scenarios

Using the temporal minimal adequate model developed for indigenous malaria, the number of malaria cases were predicted for five different scenarios: (1) Observed historical conditions (2) No change in woodland coverage (3) No change in rice cultivation (4) No change in cattle densities and (5) No change in woodlands, rice *and* cattle.

The number of cases for each country in each year was then predicted from the minimal adequate model with the back-transformation equation given on page 106 (Equation 3.1).

As in Chapter 2, the 'no change' scenarios use the initial (i.e. 1900) values, keeping the relevant variable(s) constant. As was also described in Chapter 2, these predictions do not show the cumulative effect of the simulated changes as this would require modelling of herd immunity to dampen out the predicted positive feedback effect. Instead the results demonstrate the predicted effect of changes in a given parameter for a single year. In practice, this model does not include temporal autocorrelation and thus there was no evidence for a cumulative effect within Europe, unlike the inter-annual

variability model developed for English malaria which incorporated a significant temporal autocorrelation of one year.

Results

The frequency distribution of explanatory variables are shown in Appendix 3.1 All variables were normally distributed. Their mean, maximum and minimum values are shown below.

Table 3.6. Mean, minimum and maximum for explanatory variables.

Explanatory variable	Arithmetic Mean	Minimum (country, year)	Maximum (country, year)
Cattle density (per $1km^2$)	28.3	4.2 (Finland, 1975)	131 (Netherlands, 1975)
Woodland acreage (% of country size)	30.5	5.7 (UK, 1920)	68.5 (Finland, 1975)
Rice cultivation (% of country size)	0.1	0 (*)	0.7 (Italy, 1975)
Mean average temperature (°C)	10.7	0.6 (Finland, 1975)	17.3 (Spain, 1970)
Minimum average temperature (°C)	0.6	-19.9 (Finland, 1975)	10.5 (Spain, 1970)
Maximum average temperature (°C)	20.4	15.2 (Finland, 1970)	28.1 (Spain, 1970)
Total precipitation (mm)	690.5	315 (Spain, 1975)	1287 (Albania, 1915)

* There were eight countries with no rice cultivation during the whole study period (see Table 3.9).

Temporal trends – malaria and demography

A total of 20,974,539 reported malaria cases were included in the analysis. This decreased from 1,086,475 in 1900 to zero in 1975. There were 6 and 2 cases in 1973 and 1974, respectively. Because of the variation in the number of available data points for each year, for illustrative purposes the annual trend of total cases was plotted at country level for the four countries with the most data available (namely Finland, Italy, Spain and Sweden). The UK is not included as the full data has already been described and discussed in Chapter 2. Malaria cases in Finland and Sweden show a general decrease with marked peaks during and after the First and Second World Wars (i.e. 1914-1918 and 1940-1945, Fig. 3.3 and 3.4). In both countries there are no distinctive epidemics apart from the ones related to the wars. In Italy and Spain, where DDT was used to

eradicate malaria, the trend is significantly different (Fig. 3.5 and 3.6). There are still peaks which correlate with the two World Wars but there is no significant overall decreasing trend and the effect of DDT is clearly visible after the Second World War when control effort was initiated in these countries (see Introduction). The temporal trend in Italy shows a number of peaks in cases not related to any wars (i.e. 1905, 1910, 1925, 1928 and 1934) while there are no such apparent years of malaria epidemics in Spain, probably because many data points are missing (Fig 3.6).

The total population of the 17 countries increased by 60% from 238 million in 1900 to 381 million in 1975. The most populous countries in the dataset were Germany and the UK with average populations of 68 and 47 million, respectively, during the study period.

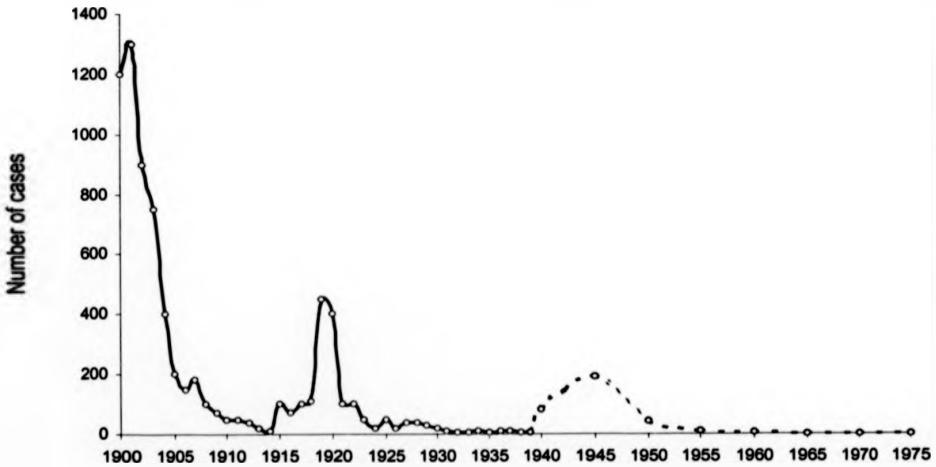

Figure 3.3. Annual indigenous malaria cases in Finland during 1900-1975. Dotted lines indicate that annual data were only available at 5-year intervals.

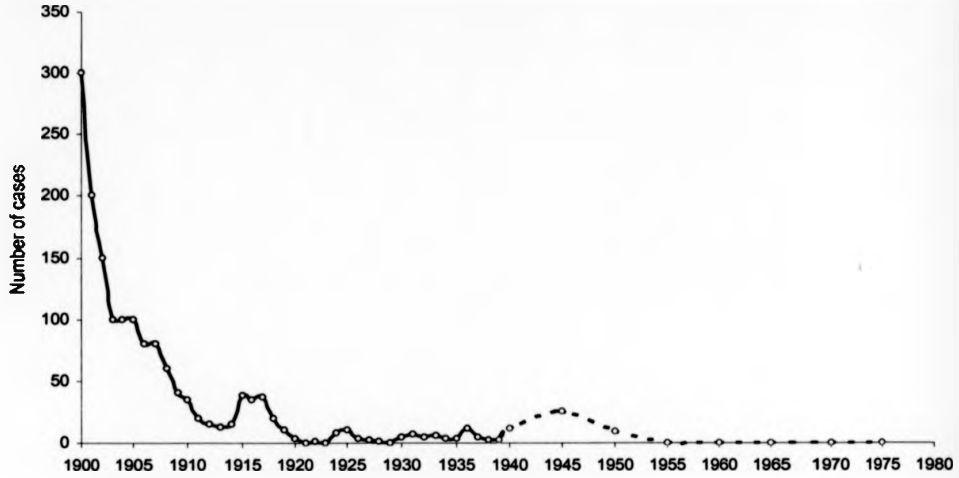

Figure 3.4. Annual indigenous malaria cases in Sweden during 1900-1975.
Dotted lines indicate that annual data were only available at 5-year intervals.

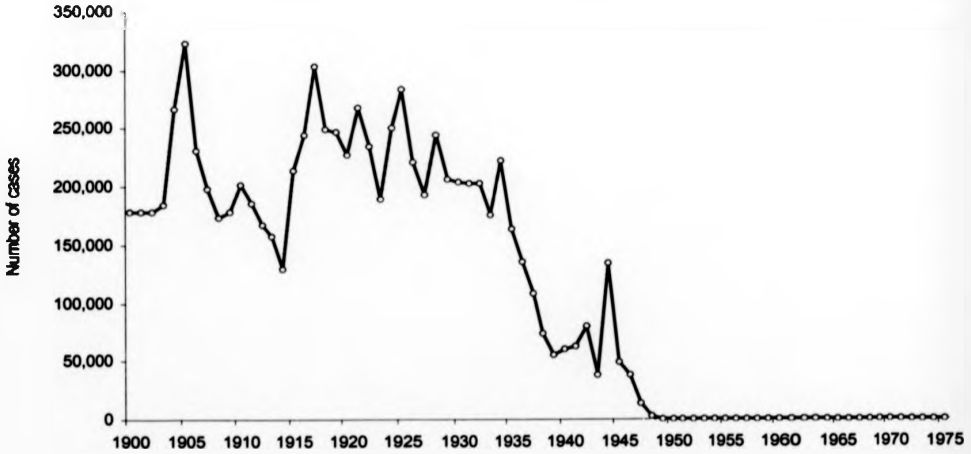

Figure 3.5. Annual indigenous malaria cases in Italy during 1900-1975.

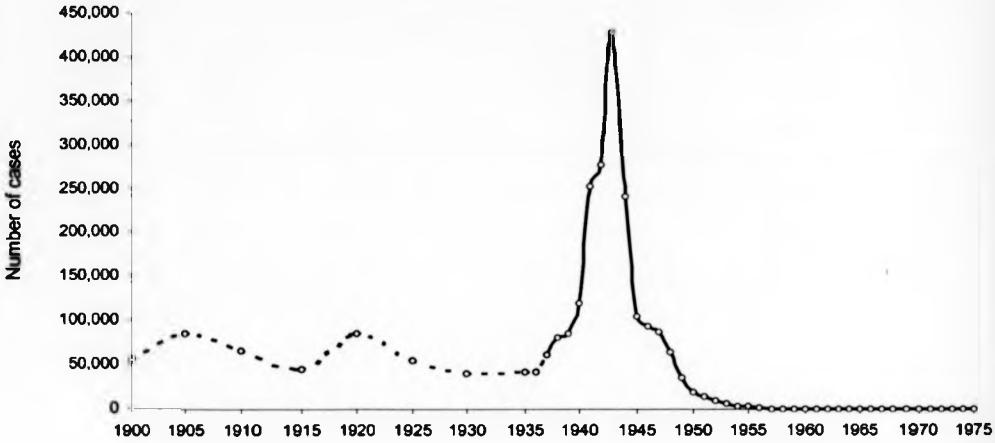

Figure 3.6. Annual indigenous malaria cases in Spain during 1900-1975.
Dotted lines indicate that annual data were only available at 5-year intervals.

Temporal trends – explanatory variables

Woodland coverage in all 17 countries increased by 15% from 1.1 to 1.2 million km^2 from 1900 to 1975. During this time, the total rice cultivation (km^2) increased by 19.1% from 3056 to 3642 km^2 and the density of cattle per $1km^2$ increased by 49.3 %. In 1900 there were 62 million cattle in the 17 countries and by 1995, this had increased to 92 million.

The annual temporal trend in climatic variables cannot be easily examined due to the variation in the number of data points in each year. Instead, temperatures and precipitation for each 5-year point with data from all 17 countries were investigated and the ranges for the whole study period calculated (Table 3.7).

Table 3.7. Average climate in Europe during 1900-1975.

Variable	Range during 1900-1975
Mean average temperature (°C)	10.1 – 12.9
Minimum average temperature (°C)	-0.2 – 1.2
Maximum average temperature (°C)	19.9 – 22.3
Total precipitation (mm)	632 – 797

Values are based on the average of climate measurements for 17 countries during 1900-1975.

Spatial trends – malaria

The average annual number of reported indigenous malaria cases and rates during 1900-1975 at country level are shown in Fig 3.7 and 3.8. During the study period, only Denmark reported an average of less than 10 cases (Table 3.8). The highest average number of malaria cases was reported from Italy followed by Romania and Yugoslavia while the highest rates were found in Albania, Greece and Romania. The lowest malaria rates and number of cases were observed in Sweden, the UK and Denmark. This pattern corresponds with historical observations which suggest that malaria prevalence was highest in the Balkans and countries around the Mediterranean while Scandinavian countries reported lower case numbers (Bruce-Chwatt and de Zulueta 1980). Extinction (i.e. zero reported cases) of locally transmitted malaria was also observed first in the UK (1953), Sweden (1939) and Denmark (1901) whereas the more prevalent countries reported indigenous malaria transmission up to 1975 (Romania and Greece). This mirrors the fact that malaria disappeared without control effort from most of northern Europe and Scandinavia while eradication was only achieved in southern Europe after the initiation of DDT spraying campaigns.

Figure 3.7. Average annual malaria cases in 17 European countries during 1900-1975.

Figure 3.8. Average annual malaria rates in 17 European countries during 1900-1975.

Spatial trends – explanatory variables

Netherlands, Germany and Denmark had the highest average cattle density per 1km^2 during the study period while Spain, Finland and Sweden reported the lowest (Table 5, Fig. 3.9).

The largest increases in cattle density were observed in the Netherlands and Albania (both above 100% increase in the number of cattle per km^2) while Greece, Bulgaria and Hungary reported as much as 50% decreases in cattle density over the study period.

Average woodland coverage was highest in Finland, Sweden and Poland and lowest in Denmark, the Netherlands and the UK (Fig. 3.10). The largest increases in woodland coverage were observed in Italy (72%), the UK (60%) and Portugal (57%) and the largest decreases in Bulgaria (10%), Germany (16%) and Albania (21%). Rice cultivation was most common in Italy, Portugal and Hungary and was not practised in 8 of the 17 countries (Fig. 3.11, Table 3.9). During the study period, Greece and Italy reported 135% and 126% increases in rice cultivation, respectively, while rice cultivation in both Bulgaria and Hungary declined by 81% (Fig. 3.12).

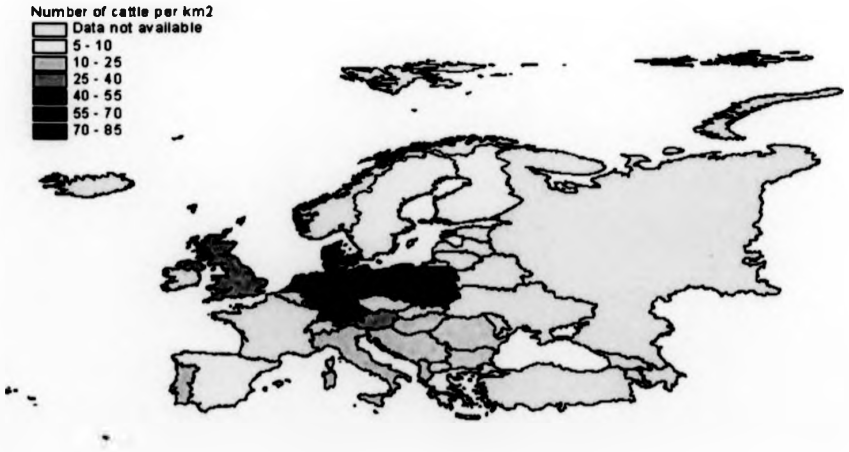

Figure 3.9. Average cattle density per km^2 in 17 European countries during 1900-1975.

Figure 3.10. Average woodland coverage in 17 European countries during 1900-1975.

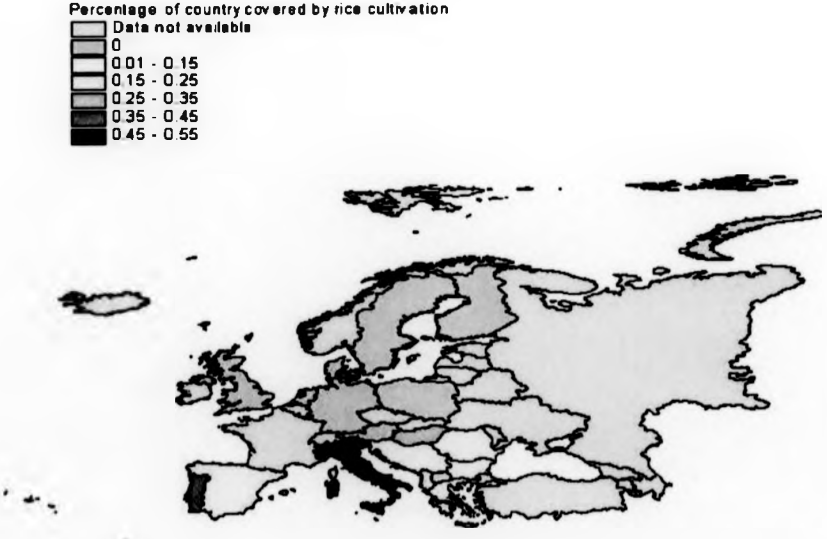

Figure 3.11. Average rice cultivation coverage in 17 European countries during 1900-1975.

Figure 3.12. Percentage change in rice cultivation in 17 European countries from 1900 to 1975.

Annual mean temperatures were on average highest in Portugal, Italy (15.6°C) and Spain (14.8°C) and lowest in Austria (7°C), Sweden (6.2°C) and Finland (4°C) as demonstrated in Fig. 3.13. During the study period, Albania, Austria and the Netherlands received the highest average amount of rainfall while Romania, Spain and Finland were the driest countries (Fig. 3.14).

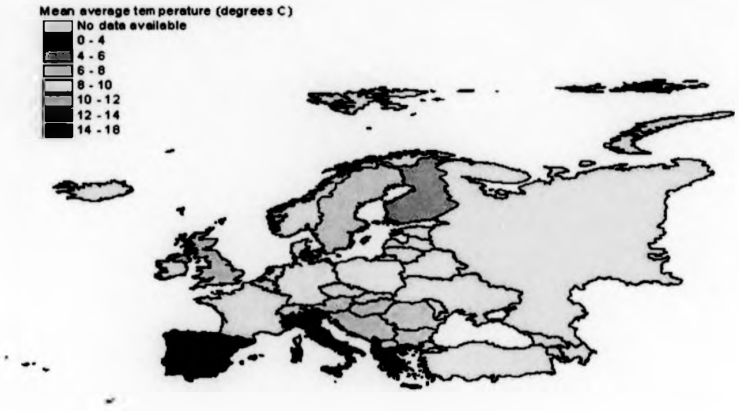

Figure 3.13. Mean average temperatures in 17 European countries during 1900-1975.

Figure 3.14. Average total precipitation in 17 European countries during 1900-1975.

Table 3.8. Indigenous malaria cases and rates in European countries during 1900-1975.

AVERAGE ANNUAL MALARIA CASES		AVERAGE ANNUAL MALARIA RATE	
Country	**Cases**	**Country**	**Rate per 10,000**
Italy	111,315	Albania	80.4
Romania	78,729	Greece	72.3
Yugoslavia	60,422	Romania	46.1
Greece	56,871	Bulgaria	42
Spain	52,223	Yugoslavia	34.2
Bulgaria	29,278	Italy	25.1
Portugal	20,635	Portugal	24.2
Albania	9,919	Spain	18.4
Netherlands	5,084	Netherlands	4.9
Poland	2,201	Austria	1.6
Germany	1,178	Poland	0.9
Austria	1,077	Hungary	0.9
Hungary	833	Finland	0.6
Finland	211	Germany	0.2
UK	48	Sweden	0.02
Sweden	32	UK	0.01
Denmark	2	Denmark	0.001

Table 3.9. Average annual cattle density, woodland coverage and rice cultivation in European countries during 1900-1975.

CATTLE DENSITY		WOODLAND COVERAGE		RICE CULTIVATION	
Country	**Number/ km²**	**Country**	**% coverage**	**Country**	**% coverage**
Netherlands	73.7	Finland	64.4	Italy	0.47
Germany	69.6	Sweden	56.3	Portugal	0.39
Denmark	66.2	Poland	54.1	Hungary	0.26
Poland	55.5	Germany	46.6	Spain	0.15
UK	36.8	Albania	44.9	Albania	0.12
Austria	27.3	Austria	37.5	Greece	0.08
Italy	23.6	Yugoslavia	34.3	Romania	0.08
Yugoslavia	23.2	Bulgaria	32.4	Bulgaria	0.07
Hungary	21.1	Romania	27.7	Yugoslavia	0.04
Romania	18.6	Spain	23.6	Austria	0
Albania	13.7	Portugal	22.4	Denmark	0
Bulgaria	12.3	Greece	18.8	Finland	0
Portugal	11.8	Italy	16.7	Germany	0
Greece	9.4	Hungary	14.1	Netherlands	0
Spain	6.5	Denmark	11.1	Poland	0
Finland	5.9	Netherlands	7.2	Sweden	0
Sweden	5.3	UK	6.5	UK	0

"Univariate" analyses

The univariate analyses were performed by adding each explanatory variable in turn to the temporal null model containing the categorical country and war variables as well as the interaction between DDT and the quadratic year trend. All variables except for minimum temperature and total precipitation were significantly ($p < 0.05$) associated with malaria rates (Table 3.10). Only maximum average temperature showed a quadratic relationship with the malaria rates.

Cattle density and woodland coverage were negatively associated with malaria rates while rice cultivation and average temperatures were positively associated with the outcome.

Table 3.10. Results of univariate analyses.

Variable	Relationship with malaria cases	Coefficient	Significance
Cattle density (per km^2)	Linear	-0.059	$p < 0.001$
Woodland coverage (% of country size)	Linear	-0.074	$p < 0.01$
Rice cultivation (% of country size)	Linear	0.167	$p < 0.001$
Minimum average temperature (°C)	Linear	0.046	$p > 0.05$
Mean average temperature (°C)	Linear	0.189	$p < 0.001$
Maximum average temperature (°C)	Quadratic	3.55† -0.075‡	$p < 0.01$
Total precipitation	Linear	-0.001	$p > 0.05$

† shows the linear coefficient ‡ indicates the quadratic coefficient

Multivariate Poisson models: inter-annual variation in indigenous malaria

Cattle density, woodland coverage, rice cultivation and mean average temperature were significantly associated with malaria rates (Box 3.1). Rice cultivation and average temperature were positively associated with malaria rates while cattle density and woodland coverage had a negative effect (Box 3.1). Rice cultivation had the greatest effect on malaria rates (i.e. this variable explains the largest amount of residual variation), followed by cattle densities, average temperature and woodland coverage. This corresponds well with the theory that rice cultivation played an important role in the epidemiology of European malaria due to the fact that the anopheline vectors may breed in rice fields. There are also very strong similarities with the results from the temporal analysis of English malaria; in both cases, malaria was significantly associated with cattle densities and mean average temperature (cattle density had a negative effect while temperature had a positive effect).

The strong effect of the DDT, temporal and county categorical variables are evident (Box 3.1 and Table 3.11). The low p-value of the DDT-year interaction indicates that there was indeed a significant difference between the temporal trend of malaria cases in

countries with and without DDT application. The effect of war years is also clear from the p-value (< 0.001) presented in Box 3.1.

The minimal adequate model explained 17% of the temporal variation in malaria, above the general temporal trend and inter-country difference in average incidence. As demonstrated in Table 3.11., the effects of cattle densities, woodland coverage and rice cultivation are not independent (i.e. the variance explained by these three factors together in the model are far from additive). In contrast, the effects of cattle and wetlands on English malaria were roughly independent (Chapter 2). This may be because of a possible strong relationship between cattle, woodlands and rice in European countries (e.g. a country with much woodland has less cattle) while cattle and wetlands in England are not apparently inter-connected.

The model fit is illustrated in the confusion matrix below (Fig. 3.7) where the values of all cells surrounding the highlighted numbers are relatively low (for 100% correct predictions, the value of all cells surrounding the highlighted cells should be zero). A plot of residuals (observed – predicted malaria cases) against predicted malaria cases (Fig. 3.8), shows more or less evenly scattered points and there is a reasonably linear relationship between observed and predicted malaria cases (Fig. 3.9) which supports the validity of the model. The even scatter of the residuals when plotted against each significant explanatory variable again indicates that the model is strong (Appendix 3.2).

Box 3.1. Minimal adequate temporal malaria model: amended output from STATA 7.0

```
STATA command
xi: glm malaria cattle woodlands rice tave year i.ddt*year i.ddt*yearsq
i.country i.war,f(p)

Statistics
Generalized linear models                    No. of obs      =        677
Optimization     : ML: Newton-Raphson        Residual df     =        651
                                             Scale param     =          1
Deviance         =  10042420.31              (1/df) Deviance =   15426.14
Pearson          =  14215788.90              (1/df) Pearson  =   21836.85

Explanatory variables
(17 country variables not included)
------------------------------------------------------------------------------
malaria    |  Coef.      Std. Err.     z      P>|z|     [95% Conf. Interval]
------------------------------------------------------------------------------
   cattle  | -.661575    .023537    -2.83    0.005    -.9127079    -.2204421
woodlands  | -.127345    .060387    -2.11    0.005    -.1457021    -.0089887
     rice  |  1.04256    .662815     1.97    0.003     .9565311     1.841659
     tave  |  .304439    .174894     1.74    0.012     .1383474     .6472263
     year  | -.024026    .116997    -0.21    0.837    -.2533361     .2052828
 ddt*year  |  .113515    .117277     1.97    0.003     .0916342     .3433738
ddt 1      | 3.488431    1.69473     2.32    0.005     2.832281     6.809141
   yearsq  |-.0003193    .002038    -2.86    0.006    -.0043142    -.0000155
ddt*yearsq|-.0016351    .002041    -3.80    0.003    -.0563591    -.0002365
      war  |  .3575049   .087398     4.09    0.000     .1862081     .52880183
------------------------------------------------------------------------------
```

Predicted malaria cases

Observed malaria cases	0-100	101-1000	1001-10000	10001-100000	100001-300000	300001+
0-100	423	52	23	18	2	0
100-1000	5	18	6	1	4	0
1001-1000	0	0	17	16	2	0
10001-100000	0	0	10	38	9	1
100001-300000	0	0	0	18	12	1
300001+	0	0	0	0	1	0

Figure 3.15. Confusion matrix of observed and predicted malaria cases.

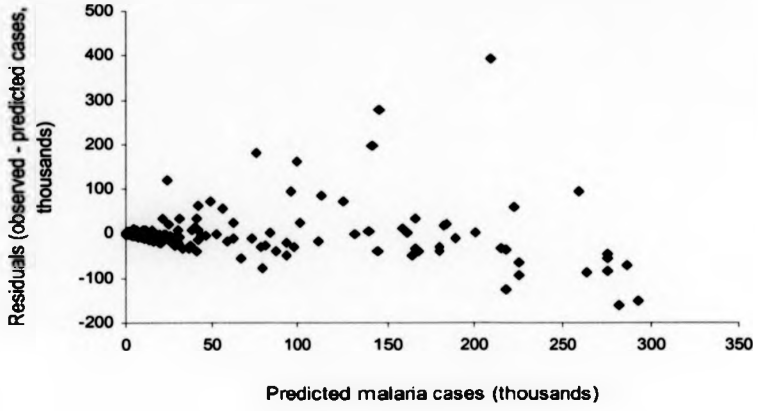

Figure 3.16. Inter-annual variation in malaria: residuals versus predicted malaria cases.

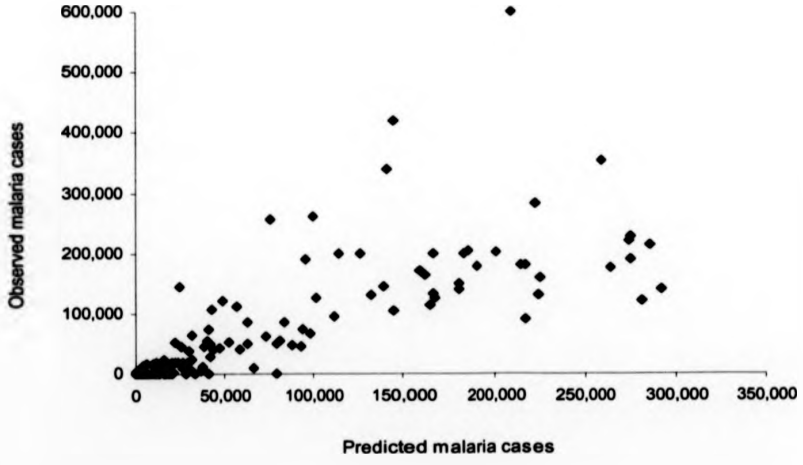

Figure 3.17. Inter-annual variation in malaria: Observed versus predicted cases.

Table 3.11. Inter-annual variation in malaria: significance and fit of the minimal adequate model and its explanatory variables.

Model	Deviance	Variance explained by model or variable (%)
Complete null *	67898289	N/A
DDT*year interaction	35715004	47.4†
Country categorical variable	35479567	47.7†
War categorical variable	36373901	46.4†
Null model (defined)	12105246	82.2†
Minimal adequate model	10042420	17.0‡
Rice cultivation	10229877	15.5‡
Woodland coverage	10918809	9.8‡
Cattle density	10465818	13.5‡
Rice, woodland and cattle	10200151	15.7‡
Mean average temperature	10800656	10.8‡

* the most basic model – without the year trend or categorical country variable.

† indicates that the model deviance is compared to the residual deviance of the complete null model

‡ indicates that the model deviance is compared tot he residual deviance of the defined null model (i.e. this column is the percentage residual variation explained by the model or variable)

Multivariate Poisson models: inter-country variation in indigenous malaria

The spatial malaria model is different from the temporal model in that the null model is defined as containing only the interaction between DDT and a categorical year variable (i.e. the model assesses how the explanatory variables impacted on inter-country variation in average malaria rates between 1900-1975).

The spatial variation in malaria in the 17 European countries was significantly associated with cattle density, woodland coverage, rice cultivation and mean average temperature (Box 3.2). Cattle density and woodland coverage had a negative effect on the outcome while rice cultivation and average temperature were positively associated with malaria rates. The minimal adequate model explained 29.9% of the inter-country variation in malaria rates (Table 3.12). The suitability of the model is confirmed in Fig. 3.10 which shows the evenly scattered points in a plot of residuals versus predicted malaria cases as well as the close linear relationship between the observed and predicted values in Fig. 3.11. Residuals are normally distributed and their scatter against each of the significant explanatory variables is even, indicating that the model is appropriate (Appendix 3.2).

When compared to the temporal malaria model, it is evident that the explanatory variables and the direction of their effects from this analysis are similar. All variables analysed are equally important in both analyses (i.e. the confidence intervals from the temporal model all overlap with the ones shown below). It can therefore be concluded that spatial and temporal patterns of European malaria were influenced by the same factors, and that the cumulative impact of a permanent change in a parameter value was not much greater than a one year change in the same value. This spatial model also shows encouraging similarities to that developed for English malaria in Chapter 2; both cattle density and average temperature were significant (and had the same effect as in the temporal model).

Box 3.2. Minimal adequate spatial malaria model: amended output from STATA 7.0

```
STATA command
xi: glm malaria cattle woodlands rice tave i.ddt*i.year, f(p)

Statistics
Generalized linear models                       No. of obs      =        677
Optimization     : ML: Newton-Raphson           Residual df     =        522
                                                Scale param     =          1
Deviance         =   13779055.09                (1/df) Deviance =   26396.66
Pearson          =   16486754.75                (1/df) Pearson  =   31583.82

Explanatory variables
(75 year variables and 75 year*ddt interaction variables not included)
------------------------------------------------------------------------------
malaria |      Coef.   Std. Err.      z    P>|z|     [95% Conf. Interval]
------------------------------------------------------------------------------
    cattle |  -.1891756   .0057111    -6.11   0.000    -.2203691   -.1579821
 woodlands |  -.0228372   .0047802    -4.78   0.000    -.0322063   -.0134681
      rice |   1.420863   .2554496     3.50   0.000     .5813771    1.820349
      tave |   .8899091   .2544968     2.56   0.000     .3911043    1.388714
------------------------------------------------------------------------------
```

Table 3.12. Inter-county variation in malaria: significance and fit of the minimal adequate model and its explanatory variables.

Model	Deviance	Variance explained by model or variable (%)
Complete null *	67898289	N/A
Null model (defined)	19650599	71.1†
Minimal adequate model	13779055	29.9‡
Rice cultivation	11819314	14.2‡
Woodland coverage	12844157	6.8‡
Cattle density	12513082	9.2‡
Rice, cattle and woodland	11300151	17.9‡
Mean average temperature	12187185	11.6‡

* the most basic model – without the year trend or categorical country variable.

† indicates that the model deviance is compared to the residual deviance of the complete null model.

‡ indicates that the model deviance is compared to the residual deviance of the defined null model (i.e. this column is the percentage residual variation explained by the model).

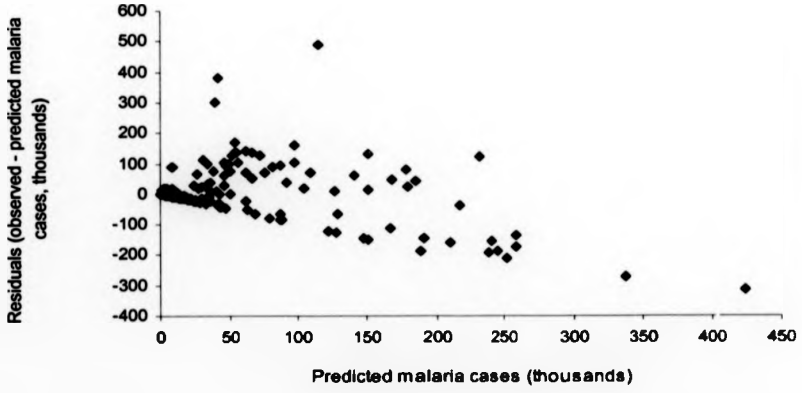

Figure 3.18. Inter-county variation in malaria: residuals versus predicted malaria cases.

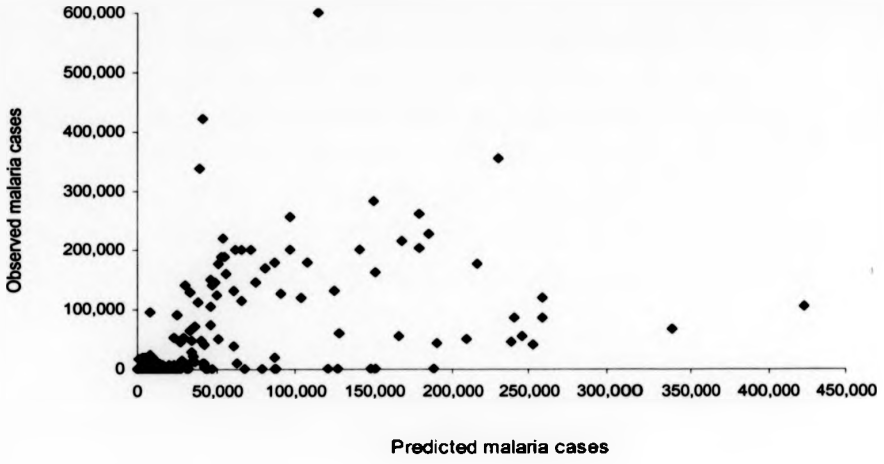

Figure 3.19. Inter-county variation in malaria: observed versus predicted malaria cases.

Predictions

Using the minimal adequate model for temporal variation in malaria rates, the number of malaria cases during 1900-1975 was predicted for the following scenarios: (1) observed historical conditions, (2) No change in woodland coverage since 1900, (3) No change in rice cultivation since 1900, (4) No change in cattle densities since 1900 and (5) No change in woodland coverage, rice cultivation *and* cattle densities since 1900.

A total of 20,974,542 malaria cases was predicted during 1900-1995 which, as expected, differed by 0.00001% from the observed . The model outcomes were used to illustrate the predicted temporal pattern of malaria cases separately for Finland, Italy, Spain and Sweden (Figs 3.12-3.15)

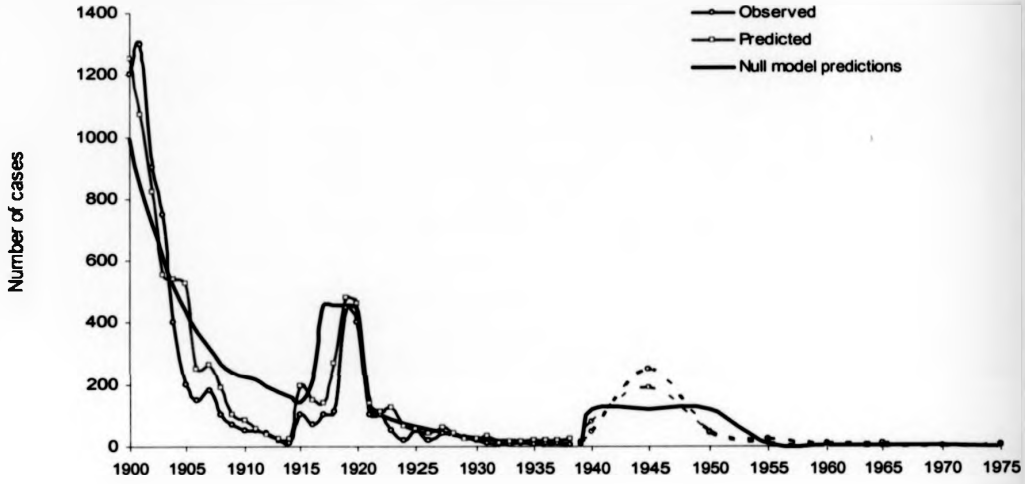

Figure 3.20. Observed and predicted malaria cases in Finland during 1900-1975. Dotted lines indicate that annual data were only available at 5-year intervals.

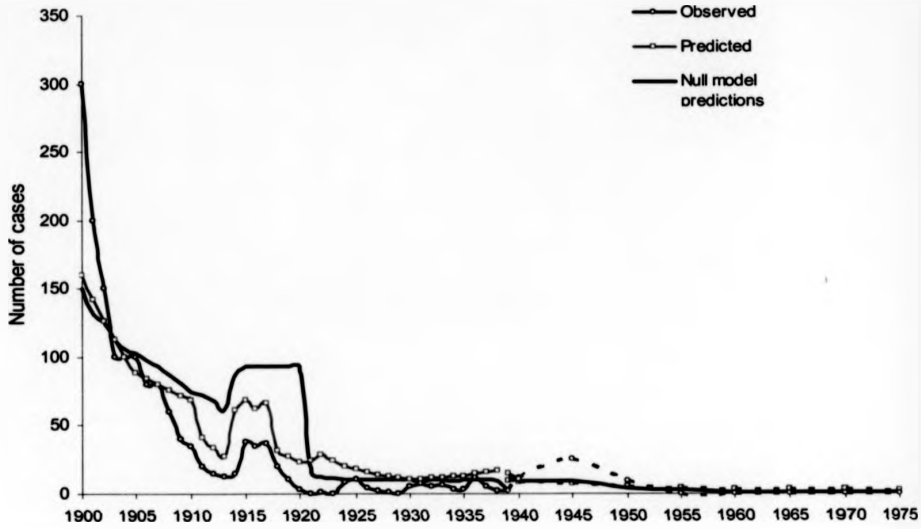

Figure 3.21. Observed and predicted malaria cases in Sweden during 1900-1975. Dotted lines indicate that annual data were only available at 5-year intervals.

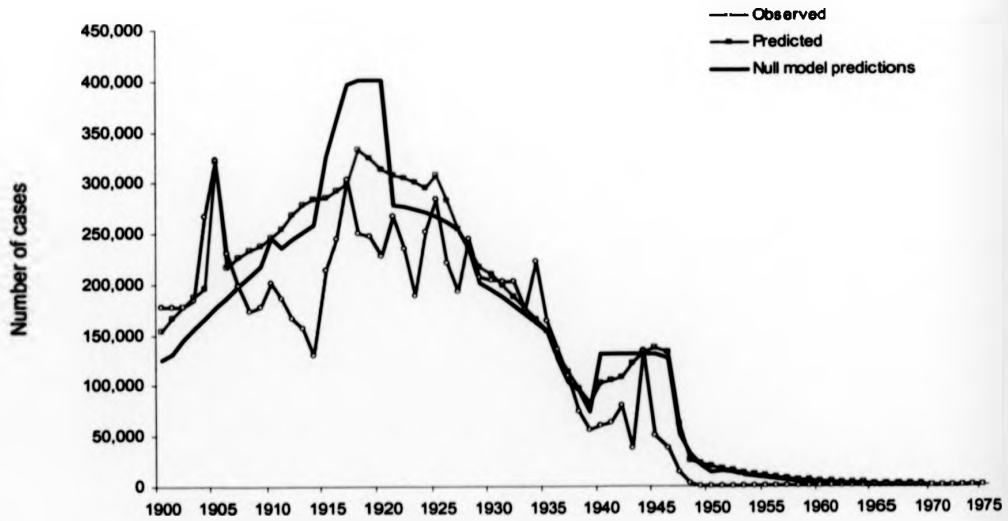

Figure 3.22. Observed and predicted malaria cases in Italy during 1900-1975.

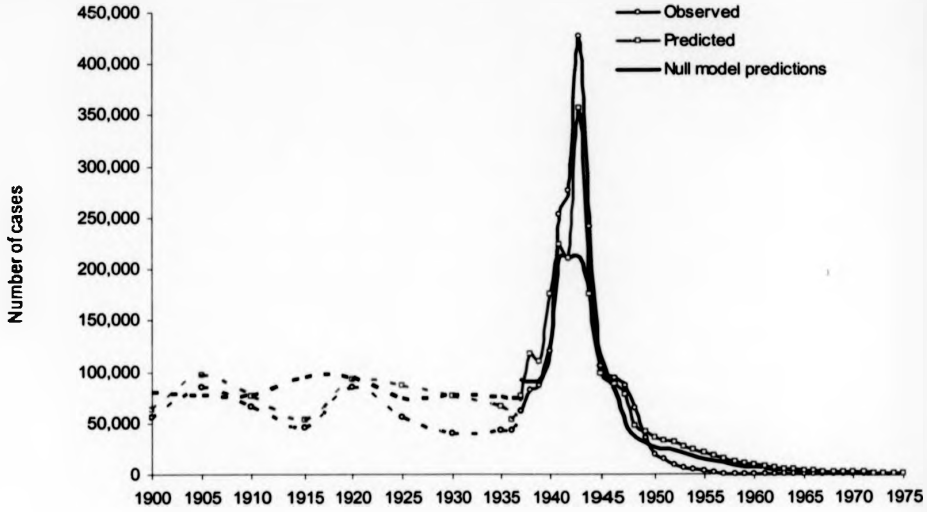

Figure 3.23. Observed and predicted malaria cases in Spain during 1900-1975. Dotted lines indicate that annual data were only available at 5-year intervals.

Table 3.13. Observed and predicted malaria cases in Europe during 1900-1975.

Scenario	Total cases (95% CI)	% Difference (95% CI)†
Observed	20,974,539	N/A
No change in woodland coverage	24,351,440 (23,869,025 –24,980,676)	15.3 (13.8,19.1)
No change in rice cultivation	18,059,078 (17,199,122 – 19,002,932)	13.9 (-18.0,-9.4)
No change in cattle densities	23,701,229 (23,197,840 – 24,309,491)	13.0 (10.6,15.9)
No change in all variables	26,469,868 (25,609,912 – 27,245,926)	26.2 (22.1,29.9)

† compared to the observed

If woodland coverage or cattle densities had remained at 1900 levels, the predicted number of malaria cases in Europe would have increased on average by 15.3% and 13%, respectively. Had rice cultivation remained unchanged since 1900, the predicted number of malaria cases would have decreased by 13.9%. If all three agricultural variables had remained unchanged since 1900, the number of malaria cases would have increased by 26.2%. The four countries selected previously (Finland, Italy, Spain, Sweden) were examined in detail and predictions calculated separately for each country (Table 3.14). The effects of constant cattle densities and woodland coverage were more pronounced in Finland and Sweden which confirms the theory that agricultural changes in northern countries played a more important role in the decline of malaria than in the southern countries (Appendix 3.3, Fig. 3.16-3.19). The effect of constant rice cultivation varies significantly between Spain and Italy (an increase of 211% versus a decrease of 9.5%, respectively) due to the different patterns in rice cultivation in the two countries. During the study period, rice cultivation increased by 65% in Italy but decreased by 30% in Spain, explaining why keeping this variable constant would increase cases in Spain but decrease cases in Italy (increases in rice cultivation is positively related to increases in malaria, see Box 3.1).

Table 3.14. Observed and predicted malaria cases in four European countries during 1900-1975.

Country	Observed	No change in cattle densities (% difference)	No change in woodland coverage (% difference)	No change in rice cultivation (% difference)
Finland	7,512	9,555 (27.2)	13,980 (86.1)	N/A
Italy	8,348,636	9,509,096 (13.9)	10,535,979 (26.2)	7,555,516 (-9.5)
Spain	2,506,691	2,529,251 (0.9)	2,975,442 (18.7)	7,795,809 (211)
Sweden	1,545	2,966 (92.2)	2,843 (84)	N/A

Values refer to the number malaria cases and the difference from the number of observed cases. The effects of rice cultivation changes were not predicted for Finland and Sweden as there was no rice cultivation in these countries during the study period.

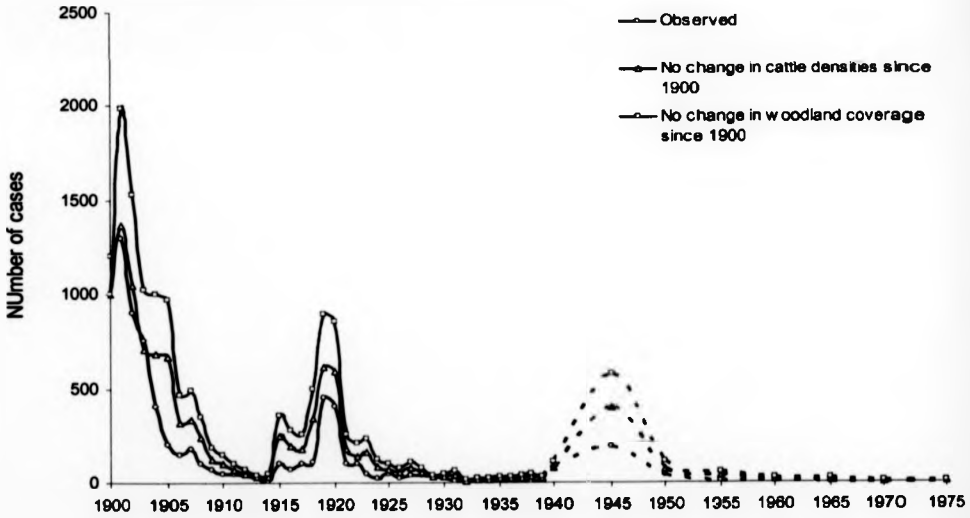

Figure 3.24. Observed and predicted malaria cases for virtual scenarios in Finland during 1900-1975. Dotted lines indicate that annual data were only available at 5-year intervals.

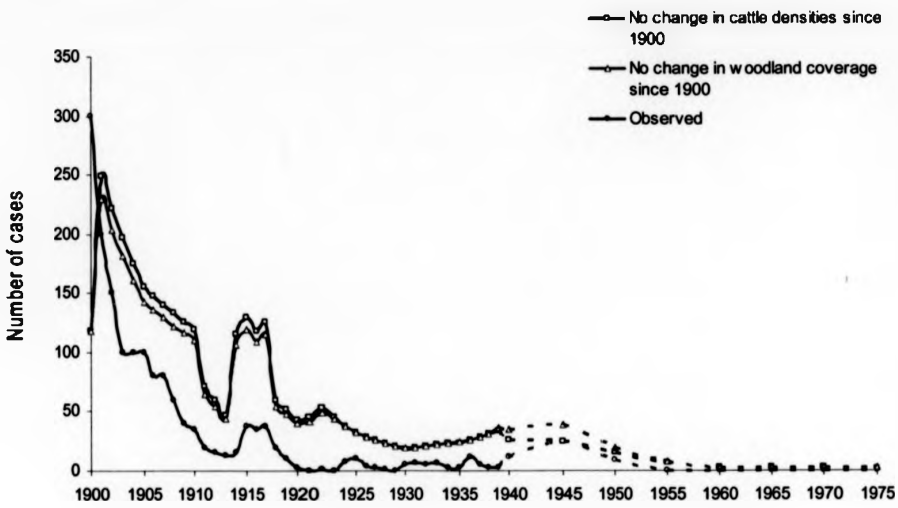

Figure 3.25. Observed and predicted malaria cases for virtual scenarios in Sweden during 1900-1975. Dotted lines indicate that annual data were only available at 5-year intervals.

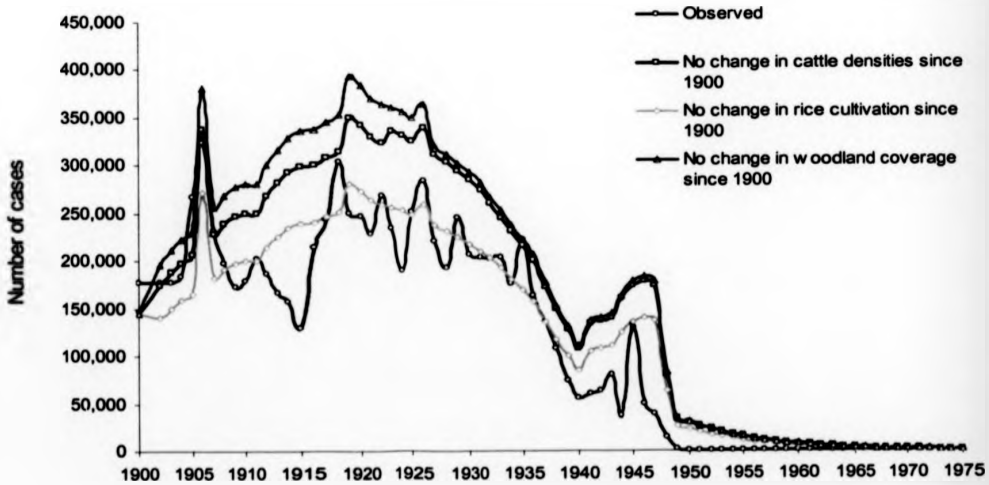

Figure 3.26. Observed and predicted malaria cases for virtual scenarios in Italy during 1900-1975.

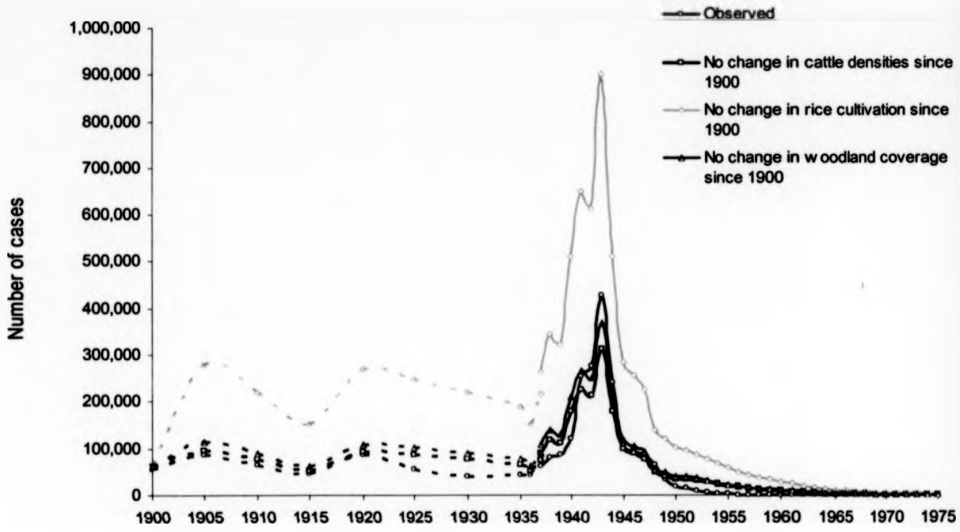

Figure 3.27. Observed and predicted malaria cases for virtual scenarios in Spain during 1900-1975. Dotted lines indicate that annual data were only available at 5-year intervals.

As explained in Chapter 2, the predictions need to be interpreted with caution because of a range of problems (e.g. history is not constant) all of which have been discussed previously. However, these results provide strong evidence in support of the theory that agricultural changes such as increasing cattle densities had a major impact on the spontaneous disappearance of European malaria.

Discussion

This is the first study which attempts to quantify the importance of climate and agriculture in the disappearance of malaria from an entire continent. These results confirm that extensive changes in agricultural practices, namely increasing cattle densities and woodland coverage, were likely to have had an effect on the trend in European malaria. Other major important factors, which were not included in this analysis, were socio-economic changes (e.g. improvement of general living conditions), health system improvements (such as better access to medication) and, most crucially, the inter-annual variability in residual insecticide spraying (i.e. the malaria eradication programmes). Due to difficulties in standardising variables (especially socio-economy) and obtaining data (e.g. amount of insecticide sprayed in each country per year) these important factors remain unanalysed, however their general effect has been taken into account by the use of the 'year' trend in the temporal model. Another special feature of the model was the inclusion of an interaction between DDT spraying and year to account for the facts that (1) the temporal trend in malaria cases was significantly different between countries which used DDT to eradicate malaria and those which did not (as shown by the significance of the DDT-year interaction in Box 3.1) and (2) after the discovery and wide-spread use of DDT in the 1940s, the pattern of malaria in DDT countries changed dramatically. Thus, the differences between northern and southern countries in their approach to malaria control has been included in the analysis.

The effect of rice cultivation on malaria patterns in southern and eastern Europe has been extensively discussed (e.g. Bruce-Chwatt 1977, Riera Palmero 1994) and this study confirms the well-known positive association between rice and malaria transmission. This relationship is presumably caused by the tendencies of *An. labranchiae* to breed in rice fields (Romi *et al.* 1997a). Indeed, it seems that the 19% increase in rice cultivation in Europe to some extent may have delayed the extinction of malaria from areas where this crop was grown such as for instance Italy where the model predicts an 8 % decrease in malaria cases if rice cultivation had not changed since 1900. The models presented here predict that if rice cultivation had remained at 1900 levels throughout Europe, the number of malaria cases would have decreased by 13% which supports the observations that rice growing areas were more malarious and that malaria probably persisted longer in these places.

The explanation for the negative association between woodlands and malaria is not immediately obvious. There are two possible hypotheses for this, both of which are entomologically related. Firstly, most of the efficient vectors were not associated with woodlands (the only exception being *An. plumbeus* which breeds in treeholes, Jetten and Takken 1994) – as is indeed demonstrated in Chapter 4 where the presence of *An. labranchiae*, *An. sacharovi* and *An. superpictus* is shown to be negatively associated with deciduous and conifer forests. Secondly, the increase in woodlands most likely reflects a decrease in inland water (i.e. marshes) which, in most instances, provided highly suitable breeding habitats for the vectors.

As was also observed in the analysis of English malaria, minimum or maximum temperatures were not significantly related to spatial or temporal patterns in disease. Again, this is most likely due to the conversion of monthly data into annual averages which show less variation. In order to show such a relationship, previously observed in Africa (e.g. Snow *et al.* 1998), raw monthly data should ideally have been used. Alternatively, if daily temperature data had been available, these could have been reduced by Fourier processing to identify temporal trends (e.g. Rogers 2000). The positive association between malaria and average temperature observed in this study indicates that above average temperatures may have been responsible for Europe-wide epidemics in malaria. A possible association between European malaria epidemics and above average temperatures has previously been discussed with reference to the 1848 and 1859 epidemics (see Chapter 2). Because of the inconsistencies in the number of data points per year, the temporal trend in total malaria cases for all 17 countries could not be plotted in order to compare any malaria epidemics with temperature. However, the observed 'epidemic' years in Italy (1905 and 1925) were both in years with above average temperatures (16.3 and 16.8°C compared to an average of 15.8°C) and were predicted by the model generated here. Unlike in England, there was no apparent association between rainfall and malaria throughout Europe. This may be due to the very different requirements of the various *An. maculipennis* species. As will be shown in the following chapter the probability of presence for some of these vectors is not significantly associated with rainfall.

The minimal adequate spatial and temporal models explain 29.9 and 17% of the inter-annual variation in malaria patterns in 17 European countries using only four explanatory variables. The spatial and temporal patterns in malaria in Europe are associated with the same environmental factors which confirms that the data used are a

reliable source of malaria transmission in Europe. By simulating different virtual scenarios, it has been demonstrated that if cattle densities and woodland coverage had not changed during the 75 years, the natural disappearance of malaria in some parts of Europe could have been delayed considerably. According to the predictions presented here, if no major changes had occurred in agriculture during the first half of the 20th century, there would have been some 15,160 cases in 1975 whereas the last two cases of indigenous malaria in Europe were reported in 1974. As described in the Methods section, data on indigenous malaria were not available for some countries in some years and were thus estimated using the available information on total (i.e. imported and indigenous) cases. This is obviously not an ideal approach which may have caused some errors, especially during the early part of the study period where the proportion of imported cases was smaller. In the estimation used here, it is assumed that the number of imported cases was constant throughout the 76 years. However, as with the English data, there remains some confusion about the proportion of imported cases during the early part of the 20th century. Some of the earliest information on this were reported from the Netherlands in 1946 where approximately 98% of all cases were indigenous; by 1950 this had decreased to 50% (Bruce-Chwatt and de Zulueta 1980). It is very likely that this pattern was repeated throughout most of Europe.

The spatial pattern of malaria rates based on the data collected corresponds with general observations which report that the most malarious areas in Europe were the southern and eastern areas (Bruce-Chwatt and de Zulueta 1980). It is also primarily from these areas that there have been reports of isolated indigenous cases since eradication in 1975 (apart from the former Soviet Union and Turkey). Because this study uses data from 1900 onwards, the reliability of the malaria data used is probably even higher than that used in the England national study (Chapter 2). Hackett (1937) discusses results of extensive malaria surveys which were undertaken in Italy and Greece in the late 1920s and early 1930s, demonstrating that already at this time the understanding of malaria as a parasitic disease was good. While it is possible that the earliest reports in the European dataset include some cases of related fevers (as discussed in Chapter 2), this number is probably negligible. This is also reflected by the fact that the geographical pattern of the observed malaria cases corresponds so well with previous observations.

Previous authors have commented on the decline of European malaria and the possible causes thereof without any formal quantitative analysis (Reiter 2000 and de Zulueta 1994). Additionally, the potential effects of future climate changes on malaria

transmission in Europe have been modelled using relative measures of vectorial capacity but without incorporating any direct information about the relationship between the incidence of disease (and distribution of vectors) and environmental factors (Jetten *et al.* 1996, Rogers and Randolph 2000). In the tropics, the use of historical data to explain the correlation between malaria transmission, climate and land use has also been very limited; the only published example being Bouma and van der Kaay (1996) which correlated fever deaths with climate variables over a 76 year period. However, this analysis focuses on two points (namely the Punjab and Sri Lanka) so it is unclear how general the results are, whereas the study presented in this thesis analyses the patterns in 17 different countries. Most published spatial analyses of malaria, which form the basis of predictive risk mapping, are based on disease data collected entirely within the last 15-20 years. While this is sensible for currently endemic countries, these procedures cannot be applied to regions where the disease has disappeared due to eradication programmes or natural decline. Given the large amount of potential historical data available at national levels, the potential of repeating the approach presented here in previously malarious areas other than Europe (e.g. Australia and North America) is encouraging. Following such studies, we will be able to make more qualified assumptions about any future changes in malaria transmission (i.e. possible re-emergence in currently non-endemic areas) as a result of environmental changes.

Despite the relatively crude data used in this analysis, the model developed shows a surprisingly good fit in Finland and Spain which demonstrates the feasibility of using historical disease and environmental data to explain inter-annual variability in malaria cases. The robustness of the results is further supported by the observations that: (1) all significant explanatory variables go in the *a priori* expected direction (e.g. increases in rice cultivation increases the number of malaria cases) and (2) variables which were significantly associated with the temporal pattern of malaria were also significantly associated with the spatial pattern of the disease.

Explaining past inter-annual variability in malaria risk is one approach for generating predictions of the potential impact on malaria risk of future environmental change. However, as conditions change it is feasible that the proportional impact on risk due to a given change in one environmental factor may not stay the same. Hence, in order to provide independent support to the conclusions drawn from the inter-annual variability 'historical' models of Chapter 2 and 3, the following chapter will focus on the environmental factors determining spatial heterogeneity in the *current* risk of malaria

across Europe. As there are currently so few indigenous cases in Europe, the next chapter instead focuses on measurements of risk which can be derived from investigating the current distribution of European malaria vectors.

Current Risk of Malaria in Europe

Abstract

Though malaria was officially declared eradicated from Europe in 1975, its former vectors, mainly members of the *Anopheles maculipennis* (Meigen) complex, are still distributed throughout the continent. The present situation of Anophelism without malaria indicates that current socio-economic and environmental conditions maintain the basic case reproduction number, R_0, below 1. As a preliminary step towards predicting future scenarios, models were constructed to test whether the current distribution of the five former European malaria vectors *An. Atroparvus*, *An. labranchiae*, *An. messeae*, *An. sacharovi* and *An. superpictus* can be explained by environmental parameters, including climate. Multivariate logistic regression models using climate surfaces derived from interpolation of meteorological station data (resolution 0.5 x 0.5 degrees) and remotely sensed land cover (resolution 1 x 1 km) were fitted to 1833 reported observations of the presence and absence of each species across Europe. These relatively crude statistical models predicted presence and absence with an accuracy of 74 - 85.7% and 73.4 - 98.1% (kappa ranged from 0.35-0.68), with climate a significantly better predictor than land cover type. A geographically independent validation of the models gave a sensitivity of 72.9 - 88.5 % and a specificity of 72.7 - 99.6 % (kappa: 0.45-0.85). Using predicted probability of presence as a proxy measure of mosquito abundance, the relative vectorial capacity was calculated for each of the five species. These measures were then combined with information on current indigenous malaria transmission in Europe (in relation to the number of imported cases) as well as socio-economic variables to predict the present risk (R_0) of malaria throughout the continent. Risk maps of mosquito distributions, relative vectorial capacity and malaria risk were then constructed at a 0.25° resolution. These indicated that *An. atroparvus*, *An. labranchiae* and *An. superpictus* are potentially the most efficient vectors in Europe. Estimations of current malaria risk indicated that R_0 is currently above 1 in areas of eastern Europe (concentrated in Moldova and Romania), while there is no or little risk of malaria transmission in the rest of Europe. These techniques would be equally useful for estimating the risk of re-emergence in other non-endemic, but previously malarious, areas such as the United States and Australia, as well as changes to risk within endemic areas.

Introduction

A number of previous studies have demonstrated the great potential in using climate and land cover data for studying the distribution and abundance of malaria vectors in the tropics. Although the former European malaria vectors are widely distributed across the continent, the relationship between their geographic range and environmental factors has not yet been properly quantified. This is an important first step towards assessing the potential of malaria re-emergence in Europe, particularly as a result of man-made climate changes. The current study will identify the association between the present distribution of European *Anopheles* species and various environmental factors. These results will then be used to calculate relative vectorial capacity for the mosquitoes and, ultimately, to predict the current risk of malaria throughout Europe.

The Anopheles maculipennis complex

Even though malaria has been eradicated from Europe, the former vectors are still present throughout the continent. The majority of these belong to the *Anopheles maculipennis* complex which was first described by Van Thiel in 1927. The discovery of different breeding habits and morphological characters (long- versus short-winged) among adult *An. maculipennis* during the late 1920s provided the first evidence that this was in fact a complex of species. Among others, Hackett and Missiroli (1935) supplied further observations (e.g. differences in breeding habitats) in support of this theory, and by the early 1940s most of the current members of the complex had been named and described (Bates 1940). Proof that members of the complex are separate biological species has since been presented for the majority of the species using chromosome inversion studies (Frizzi 1951 in Buonomini and Mariani 1953), crossing experiments (Buonomini and Mariani 1953) and recently using cuticular hydrocarbon profiles (Phillips *et al.* 1990) and polymerase chain reaction assays (Proft *et al.* 1999).

White (1978) described 13 members of the *An. maculipennis* complex, including 9 palaearctic[†] species and 4 nearctic[†] (Table 4.1). The nearctic species *An. aztecus*, *An. earlei*, *An. freeborni* and *An. occidentalis* and the recently identified *An. hendersoni* (Barr 1988) will not be discussed here as they are not of interest to this study.

[†] The Palaearctic is the zoogeographic region comprising Europe, North Africa, western Asia, Siberia, northern China and Japan. The Nearctic region is North America and Greenland.

Mosquitoes which are not members of the *An. maculipennis* complex have also been associated with the transmission of malaria in Europe. These are *Anopheles superpictus*, *An. plumbeus*, *An. hispaniola*, *An. claviger* and *An. sergenti* of which the most important are *An. superpictus* and *An. plumbeus* (Jetten and Takken 1994).

Table 4.1. Palaearctic members of the *Anopheles maculipennis* complex (based on White 1978 and Jetten and Takken 1994).

Species	Described	Approximate distribution
An. atroparvus	Van Thiel, 1927	North and west Europe, Balkans, Spain, Portugal, Italy, western Russia and Black Sea.
An. beklemishevi	Stegnii & Kabanova, 1976	Russia and northern Scandinavia.
An. labranchiae	Falleroni, 1926	Mediterranean and east Europe.
An. maculipennis s.s	Meigen, 1818	North and west Europe, Balkans, Greece and Russia.
An. martinius	Shingarev, 1926	Asia
An. melanoon	Hackett, 1934	Mediterranean and Turkey.
An. messeae	Swellengrebel & De Buck, 1933	Scandinavia, north Europe (reported from Russia and Balkans but may be *An. beklemishevi*)
An. sacharovi	Favr, 1903	Italy, Balkans and Turkey.
An. sicaulti	Roubaud, 1935	Morocco, Algeria.

European mosquitoes as malaria vectors

Although the role played by the *An. maculipennis* complex in the transmission of malaria is universally accepted, only a few studies have reported the finding in nature of mosquitoes infected with malaria parasites (Table 4.2). Most of the evidence which 'incriminates' these mosquitoes as vectors is instead based on the geographical distribution and abundance of the vectors in malarious areas and, to a smaller extent, their tendencies to feed on humans.

Local surveys of mosquito faunas to identify infected anophelines were especially concentrated in the more malarious areas of Europe, i.e. in Mediterranean and eastern European countries. Lőrincz (1937) found malaria parasites in five out of 462 (1.1%) *An. messeae* in north-east Hungary while Barber and Rice (1935) reported infection rates of 1.29 and 1.57 % in *An. sacharovi* and *An. superpictus*, respectively, in

eastern Greek Macedonia. In laboratory settings, the same authors demonstrated that local *P. falciparum* and *P. vivax* developed equally well in *An. sacharovi* and *An. superpictus* but that only *P. vivax* was able to infect *An. maculipennis*. In Cyprus, Barber (1936) detected natural infection rates of 1.8 and 7.8% in *An. sacharovi* and *An. superpictus*, respectively. The only evidence of natural infection in northern European mosquitoes is the finding of *P. vivax* in 14.8% of *An. atroparvus* collected in northern Holland (Hackett 1937). Apart from this, naturally infected *Anopheles* have never been reported from North and West Europe. Thus, James (1920) examined mosquitoes (reported as *An. maculipennis* but most likely *An. atroparvus*) in Sheerness, England, but found no infections. In all the literature examined, there have been no reports of naturally infected mosquitoes found in England. The situation is similar in Scandinavia where the roles of *An. atroparvus* and *An. messeae* in malaria transmission have been inferred simply on the basis of their distribution and abundance in malarious areas (Ekblom 1945, Jaenson *et al.* 1986). Thus, from the finding of naturally infected mosquitoes, it seems that *An. atroparvus* and *An. superpictus* may be the most competent vectors. However, these reports are inconsistent (e.g. 17.4% of *An. superpictus* in Cyprus were infected while only 1.3% of the same mosquito in Greece were found to be infected with malaria parasites). Additionally, there were no indications of whether mosquitoes were found with sporozoites and/or oocysts.

The roles of *An. labranchiae, An. sacharovi* and *An. superpictus* in the transmission of historical malaria can to some extent be inferred from their current status as vectors. *An. superpictus* is presently a vector of malaria in Uzbekistan, Kazakhstan, Kyrghyzstan and Tajikistan and possibly Turkey (Ramsdale and Haas 1978, Mingaleva and Artem'ev 1993, Abdikarimov 2001, Bismil'din *et al.* 2001, Razakov and Shakhgunova 2001). *An. sacharovi* is currently considered to be the main mosquito responsible for *P. vivax* transmission in Turkey – this role has mainly been inferred from observations of seasonal densities in malarious areas (Kasap 1990) and, to my knowledge, is not based on the recent finding of naturally infected specimens. Finally, *An. labranchiae* is thought to have transmitted *P. vivax* in Italy during the 1990s (see below), but again this is not based on the finding of naturally infected mosquitoes but rather on observations that *An. labranchiae* were abundant in the area (Baldari *et al.* 1998).

The feeding preferences of European *Anopheles* has been another major subject of interest when considering their roles in malaria transmission. Generally, the

availability of humans and animals is the most important factor which determines the degree of anthropophily (i.e. tendency to bite humans) in European mosquitoes (Hackett 1934, Garrett-Jones *et al.* 1980) and this will clearly vary with location. However, a number of studies of *Anopheles* in various sites in Europe (mostly where both humans and livestock were nearby) have demonstrated that there are differences between the *An. maculipennis s.l* species (Table 4.3). These and numerous other observations have formed the basis of anecdotal suggestions that *An. sacharovi* is the most anthropophilic mosquito followed by *An. atroparvus*, *An. labranchiae* and *An. superpictus* while the other species are more reluctant to bite humans, preferring instead larger livestock (Jetten and Takken 1994). This contrasts with the Human Blood Index (HBI) values presented in Table 4.7 which indicate that *An. messeae* is the most anthropophilic of the five mosquitoes. However, as will be discussed later, the measures of HBI used in this chapter may not be wholly representative of the true vector competence of the five mosquitoes as this value is geographically dependent and thus may be subject to bias if measured only in selected areas.

Table 4.2. Natural infection in European malaria vectors

Location	Mosquito	No. examined	No. infected (%)	Parasite	Reference
Hungary	*An. messeae*	462	5 (1.1)	not indicated	Lörincz (1937)
Greek Macedonia	*An. sacharovi*	22,200	286 (1.29)	not indicated	Barber and Rice (1935)
Greek Macedonia	*An. superpictus*	12,023	189 (1.57)	not indicated	Barber and Rice (1935)
Cyprus	*An. sacharovi*	428	8 (1.8)	not indicated	Barber (1936)
Cyprus	*An. superpictus*	1613	281 (17.4)	not indicated	Barber (1936)
Holland	*An. atroparvus*	742	110 (14.8)	*P. vivax*	Hackett (1937)
United Kingdom	*An. atroparvus* (?)	42	0	-	James (1920)

Table 4.3. Feeding preferences of five European malaria vectors (based on Hackett 1937 and Jetten and Takken 1994).

Species	Degree of anthropophily	Preferred hosts
An. atroparvus	+ +	Cattle, pigs, humans
An. beklemishevi	-	Cattle, horses, pigs
An. labranchiae	+ +	Cattle, pigs, humans
An. maculipennis s.s.	+	Cattle, horses, pigs
An. messeae	+	Cattle, horses, pigs
An. martinius	-	Cattle, horses, pigs
An. melanoon	-	Cattle, horses, pigs
An. plumbeus	+ (?)	Cattle (?) , humans
An. sacharovi	+ + +	Humans, cattle
An. sicaulti	-	Cattle, horses, pigs
An. superpictus	++	Cattle, pigs, humans

+++ indicates that the species is highly anthropophilic, ++: moderate degree of anthropophily, + slightly anthropophilic, - indicates that the mosquito is predominantly zoophilic but will feed on humans when encountered. The exact feeding preferences of *An. plumbeus* are unknown, however, the populations present in the UK readily bite humans (C. Curtis, personal communication).

Parasite transmission

As discussed in Chapter 3, *Plasmodium vivax* was probably the most common malaria parasite transmitted in Europe and it is still prevalent in large parts of the Former Soviet Union and Turkey. As early as 1920, Blacklock and Carter demonstrated that English *An. plumbeus* were susceptible to *P. vivax* (presumably from a European patient although details are not given). Later, Daskova and Rasnicyn (1982) showed that Russian *An. atroparvus*, *An. sacharovi* and *An. messeae* were susceptible to *P. vivax* from Africa, Asia and South America (Table 4.4). As mentioned above, *An. superpictus* is currently a vector of *P. vivax* in large parts of Uzbekistan, Kazakhstan, Kyrghyzstan and Tajikistan and *An. sacharovi* is probably responsible for *P. vivax* transmission in Turkey which demonstrates the vector competence of these mosquitoes. Though transmission here is predominantly of *P. vivax*, the presence of *An. superpictus* in some *P. falciparum* foci across the Middle East and south-east Asia indicate a possible role of falciparum malaria transmission for this mosquito (de Zulueta *et al.* 1975, Bashwari *et al.* 2001). It has

also been suspected that *An. messeae* played a potential role in the transmission of indigenous *P. vivax* cases in Ekaterinburg in the Middle Urals during the 1990s (Natalia Nikolaeva, personal communication). However, since these cases have not been officially confirmed and no infected *An. messeae* have been found in Russia, this still needs to be investigated further.

There has been much speculation about the possible role of European *Anopheles* in the transmission of tropical *P. falciparum* parasites. James *et al.* (1932) observed that English *An. atroparvus* could not be infected with tropical (Indian) strains of *P. falciparum* (Table 4.4) but that Italian *P. falciparum* developed to the sporozoite stage in the same mosquito. This was further confirmed by Shute in 1940 who showed refractoriness in *An. atroparvus* to Indian and African *P. falciparum* but susceptibility to strains of Italian origin. These results provide more evidence that the European strain of *P. falciparum* was different from the Indian and African ones. More recent similar experiments have since shown that European *An. atroparvus*, *An. messeae*, *An. sacharovi* and *An. labranchiae* are refractory to strains of *P. falciparum* from Africa and India (Ramsdale and Coluzzi 1975; de Zulueta *et al.* 1975; Marchant *et al.* 1998). However, the development of *P. falciparum* to the oocyst stage in *An. atroparvus* (Ramsdale and Coluzzi 1975, Marchant *et al.* 1998) and *An. plumbeus* (Marchant *et al.* 1998) as well as the suspected role of *An. plumbeus* in the recent transmission of *P. falciparum* in Germany certainly indicate that further studies are needed to clarify the exact interaction between European anophelines and tropical *P. falciparum*. The inconsistencies in the data presented in Table 4.4. indicates that there is no clear evidence for any difference in the vector competence of the different *An. maculipennis* members (i.e. when calculating relative vectorial capacity later in this Chapter, we can assume that ***b*** is constant, see page 164).

In light of the evidence presented above, five European Anopheles species have been selected for analysis in this study; *An. atroparvus*, *An. messeae*, *An. labranchiae*, *An. sacharovi* and *An. superpictus*. These mosquitoes have been chosen as they all fit the majority of five key criteria (see Table 4.5): (1) a wide spread historical and present distribution in what was known to be highly malarious areas in Europe, (2) the finding in nature of the species infected with European malaria parasites, (3) a tendency to feed on humans, (4) the ability to become infected with

tropical strains of *P. vivax* and (5) existing evidence that the species is currently involved in malaria transmission.

Table 4.4. Experimental infectivity studies of European *Anopheles* with different malaria parasites.

Mosquito (origin)	Parasite (strains)	No. dissected	No. infected * (with sporozoites)	Reference
An. plumbeus (UK)	*P. vivax* (not given)	17	7 (4)	Blacklock and Carter (1920).
An. atroparvus (UK)	*P. falciparum* (1 Italian)	56	13 (10)	James *et al.* (1932).
An. atroparvus (UK)	*P. falciparum* (1 Indian)	283	0 (0)	James *et al.* (1932)
An. atroparvus (UK)	*P. falciparum* (1 Indian and 2 African)	399	0(0)	Shute (1940).
An. atroparvus (Italy)	*P. falciparum* (1 African)	20	0 (0)	Ramsdale and Coluzzi (1975).
An. atroparvus (Italy)	*P. falciparum* (1 African)	117	3 (0)	Ramsdale and Coluzzi (1975).
An. labranchiae (Italy)	*P. falciparum* (1 African)	17	0 (0)	Ramsdale and Coluzzi (1975).
An. atroparvus (Russia)	*P. vivax* (3 Asian, 1 South American and 2 African)	1067	228 (74)	Daskova and Rascinyn (1982).
An. atroparvus (Russia)	*P. falciparum* (8 African and 2 Asian)	1950	0 (0)	Daskova and Rascinyn (1982).
An. messeae (Russia)	*P. vivax* (1 Asian)	95	25 (2)	Daskova and Rascinyn (1982).
An. messeae (Russia)	*P. falciparum* (8 African and 2 Asian)	568	0 (0)	Daskova and Rascinyn (1982).
An. sacharovi (Russia)	*P. vivax* (1 Asian)	64	16 (4)	Daskova and Rascinyn (1982).
An. sacharovi (Russia)	*P. falciparum* (8 African and 2 Asian)	354	0 (0)	Daskova and Rascinyn (1982).
An. superpictus (Turkey)	*P. vivax* (1 Turkish)	513	453 (269)	Kasap (1987).
An. sacharovi (Turkey)	*P. vivax* (1 Turkish)	553	410 (231)	Kasap (1990).
An. superpictus (Turkey)	*P. vivax* (1 Turkish)	508	310 (190)	Kasap (1990).
An. atroparvus (The Netherlands)	*P. falciparum* (1 African)	54	1 (0)	Marchant *et al.* (1998).
An. plumbeus (United Kingdom)	*P. falciparum* (1 African)	5	3 (0)	Marchant *et al.* (1998).

* The number of infected mosquitoes refers to the number of mosquitoes which developed oocysts and/or sporozoites (i.e. if there were no sporozoites, this refers to numbers with oocysts only).

Table 4.5. Selection of five major European malaria vectors.

Species	Infection in nature	Degree of anthropophily *	Susceptible to infection with tropical *P. vivax*	Currently involved in malaria transmission	Vector efficiency index
An. atroparvus	++	medium	+	no	+ + +
An. labranchiae	?	medium	?	yes	+ +
An. messeae	+	low	+	possibly	+
An. sacharovi	+	high	++	yes	+ + +
An. superpictus	++	medium	++	yes	++

+++ indicates that the species has a high infection rate in nature/susceptibility to *P. vivax* or vector efficiency index, ++: medium infection in nature, susceptibility tropical *P. vivax* or vector efficiency index, + indicates that the species had a low natural infection rate, susceptibility to P. vivax or vector efficiency index and ? no information available.

* this has been based on anecdotal evidence as well as the upper limit of the human blood index ranges given in Table 4.7. The means from Table 4.7 are not taken into consideration and thus do not correlate with these observations.

In conclusion, there is very limited evidence to support or reject the anecdotal theories about the efficiency of the various *An. maculipennis* members. The evidence that does exist is clearly inconsistent and does not allow us to make any reliable conclusions about the vector status of any mosquito. However, the five mosquitoes chosen as the focus for this study have - without exception – been considered as the most important malaria vectors by historical entomologists and malariologists working in European endemic areas.

The history and biology of European Anopheles

Because temperatures in Europe during the last ice age (18,000 BC) were considerably lower than today, it is unlikely that any mosquito populations existed in northern Europe at this time (de Zulueta 1973). Instead, the northern species *An. atroparvus* and *An. messeae* were probably present only in the southernmost areas and the current southern species *An. labranchiae* and *An. sacharovi* were most likely absent, confined instead to north Africa and western Asia (Bruce-Chwatt and de Zulueta 1980). The climatic, agricultural and social changes during the Holocene period (ca 8000 BC) are thought to have facilitated the spread of *An. atroparvus* and *An. messeae* towards the north of Europe and, with the increase in trading during the Hellenistic (around 400 BC), *An.*

labranchiae and *An. sacharovi* are thought to have invaded southern Europe via the nautical route from Africa and Asia. Although there are no fossil records to support these hypotheses, the present restricted distribution of *An. labranchiae* and *An. sacharovi* along the Mediterranean coastline indicates a nautical dispersal (Hackett 1949, Bruce-Chwatt and de Zulueta 1980). During the Hellenistic and following centuries, historical descriptions of malarious illnesses (see Chapter 3) indicate that the disease – and presumably vectors – slowly spread throughout Europe to reach its stronghold in the 13th to late 18th centuries during which it covered most of the continent.

Today members of the *An. maculipennis* are still distributed throughout Europe. These mosquitoes breed in clear standing or slow-flowing water. *An. atroparvus* is highly associated with the brackish water of European marshes and river deltas while *An. messeae* prefers the less saline environments in lakes, rivers and ditches (e.g. Hackett 1934, Pires *et al.* 1982). Further south, *An. labranchiae* and *An. sacharovi* are also brackish water breeders and are particularly common in rice fields, irrigation canals, marshes and lagoons (e.g. Bruce-Chwatt and de Zulueta 1980, Bruce-Chwatt 1985). *An. superpictus* is known to breed in saline swamps, irrigation channels and rice fields (Bates 1939, Postiglione *et al.* 1973).

Members of the *An. maculipennis* are all morphologically similar and thus indistinguishable at the adult, pupal and larval stages. However, egg shell patterns are highly characteristic and allow relatively easy separation into species. Recently developed methods such as PCR and gas chromatography (cuticular hydrocarbon profile identification) have allowed more reliable identification of adult mosquitoes (Phillips *et al.* 1990, Proft *et al.* 1999).

During the winter months, all European anophelines go into complete or incomplete diapause (induced by shorter day lengths rather than decreased temperatures). Incomplete diapause where insects seek shelter in warm buildings and continue taking blood meals (but do not lay eggs) is seen in *An. atroparvus, An. labranchiae, An. sacharovi* and *An. superpictus*. As was famously observed in the Netherlands, incomplete diapause can ensure that malaria transmission continues during the colder months of the year (Verhave 1987). The other members of the complex undergo complete diapause in which females form a fat body and remain inactive until spring (Jetten and Takken 1994). In northern Europe, diapause generally starts in September and ends in March-April (Martini *et al.*. 1932; Ramsdale and Wilkes 1985). In the south, diapause starts in October-November and may end as early as February,

depending on latitude (e.g. Hackett and Missiroli 1935). The end of diapause is thought to be determined by increasing temperatures as well as increasing amount of daylight (Jetten and Takken 1994).

Control of European Anopheles: past and present

The spraying of DDT to kill endophilic *Anopheles* was initiated during the 1940s in Frosinone, Italy, with remarkable success (Bruce-Chwatt and de Zulueta 1980). This was followed by programmes in Sardinia and Greece where it was realised that the eradication of vectors was not necessary to halt malaria transmission. Although agricultural and socio-economic changes are usually proposed as the main factors in the disappearance of European malaria, the role of DDT – especially in the Mediterranean and eastern Europe – was surely of major importance (de Zulueta 1994). Apart from *An. sacharovi* in Cyprus and *An. labranchiae* in Sardinia, the spraying campaigns failed to eradicate malaria vectors, but nevertheless decreased mosquito densities enough to break the transmission cycle and ultimately eradicate malaria.

However, since individual Mediterranean countries achieved malaria eradication and DDT spraying consequently stopped, the *Anopheles* situation in Europe has reportedly undergone important changes. In Sardinia, *An. labranchiae* is now the most frequently collected species of its genus (Marchi and Munstermann 1987) in contrast to soon after the eradication campaign where it had been replaced by *An. hispaniola* which is now only rarely encountered. In Maremma and Grossetto provinces in Italy, *An. labranchiae* almost disappeared following DDT spraying but has now reappeared again, probably due to large scale rice cultivation (Romi *et al.* 1997a). *An. sacharovi* accounted for 96-98% of anophelines found in Greece during 1969-1970 (Hadjinicolaou and Betzios 1973) and was present at densities similar to before the DDT campaign. A similar pattern has been reported in Ekaterinburg in the Middle Urals where increases in overgrown lakes and ponds as well as relatively high spring temperatures are thought to have caused the density of *An. messeae* to recently increase by 900 % in 10 years to 7,392 female mosquitoes per km^2 (Nikolaeva 1996, Natalia Nikolaeva personal communication).

In the WHO European region, only the currently endemic countries (i.e. Azerbaijan, Kazakhstan, Tajikistan and Turkey) control mosquito populations with the aim of reducing malaria transmission (Aliev and Saparova 2001, Bismil'din *et al.* 2001, Gockchinar and Kalipsi 2001). Efforts in these countries are not centrally managed but

have instead been initiated by the Roll Back Malaria programme (Roll Back Malaria 2002) or various non-governmental organisations undertaking programmes in the areas. In the rest of Europe, there are currently control efforts aimed at the larval stages of nuisance mosquitoes (mainly *Aedes* and *Culex* spp.) in France, Germany, Italy and the UK (Becker and Ludwig 1989, Karch *et al.* 1990, Becker and Ludwig 1993, Ramsdale and Snow 1995, Romi *et al.* 1999). In all cases the biological insecticide *Bacillus thuringiensis israelensis* (Bti) has been most commonly used and with the most success. For instance in Germany, along the Rhine Valley, *Aedes vexans* has been successfully controlled since the early 1980s (Becker and Ludwig 1983, Becker and Rettich 1994). Control efforts using Bti are also undertaken today in southern France near Montpellier, in 9 regions of Italy and as well as in Hampshire, Kent, Essex and London in the UK (Ramsdale and Snow 1995). The effects on *Anopheles* populations in most of these areas are unlikely to be as successful as on the culicine mosquitoes as the culicines generally do not breed in brackish water but instead prefer fresh water near forests (Schafer *et al.* 1997, Zamburlini and Cargnus 1998). However, in areas where anophelines and culicines breed in the same locations, the effect on potential malaria vectors may be beneficial.

Predicting mosquito distributions using environmental variables

One of the key factors in the eradication of European malaria was probably the reduction of human exposure to mosquito bites, which among other things helped to maintain the basic reproduction rate R_0 below 1. Recently, an increasing number of studies have examined the relationship between environmental variables (such as climate and land cover) and the distribution and abundance of malaria vectors in order to predict possible effects of man-made or natural environmental changes on mosquito abundance and, ultimately, disease risk.

In endemic countries, it is feasible to investigate the impact of environmental variables on malaria risk directly from entomological data which are directly linked to disease transmission, e.g., by comparing measurements of the entomological inoculation rate (Hay *et al.* 2000c). However, this method cannot be applied in non-endemic regions such as Europe. Theoretically, in the absence of transmission, risk can be estimated by measurements of vectorial capacity (Jetten *et al.* 1996). Though this approach may not be fully reliable due to the many uncertainties in the parameter values required for the calculation (Dye 1992) it is the only method available which permits the measurement of

absolute malaria risk in the absence of transmission. A cruder approach, which is the first step in this study, is to focus on vector abundance as a rough marker of risk. This has the advantage of simplicity, but again the results need to be interpreted with caution, as vector abundance is only one of many variables contributing to risk.

In order to predict changes in vector abundance and distribution as the result of environmental change, it is first necessary to determine the degree to which current distributions can be explained by environmental variables. Environmental factors are directly and indirectly linked to the development, behaviour, distribution, and competence of all disease vectors (Mellor and Leake 2000). It has been well established that temperature affects mosquito development and survival rates, while rainfall and land use patterns influence the availability of larval breeding sites (Molyneux 1997). Depending on the resolution and coverage of the explanatory variables, it is feasible to quantify such environmental associations and extrapolate them to different locations and scales. For example, predictions using highly localised parameters such as the location of houses, larval breeding sites and animal hosts (e.g. Hightower *et al.*. 1998) are impossible to project to other locations where information on these variables is unavailable. Predictive maps of unsurveyed areas can only be generated using environmental parameters which have been measured at a suitable spatial resolution over a wide geographic range. In practice, this means using information either derived from remote (satellite-mounted) sensors, or from interpolation of ground measured variables.

Previous attempts to use applications of remotely sensed images to predict mosquito distributions have tended to use high spatial resolution imagery from SPOT, Landsat, or IRS satellites with 20-30m resolution to measure spectral properties on the ground such as for instance the NDVI (see Chapter 1). These properties are used to characterise land cover classes, which are then identified by aerial photos or ground truthing (e.g., Rejmankova *et al.* 1995; Roberts *et al.* 1996; and Beck *et al.* 1997). Such high-resolution studies have necessarily focused on small areas, and the predictions have rarely been tested far from the original mosquito surveys which were used to formulate the statistical models. For instance, Sharma *et al.* (1996) predicted mosquito abundance in villages which were 50 away from the original sampling location. High resolution climate data are not readily available unless they have been specifically collected in the required locations and climate is unlikely to vary much within the small regions investigated in these studies. Therefore, none of the above investigations have addressed the role of climate on mosquito distributions.

In order to make predictions over a much wider areas, and to investigate the effects of environmental changes over time, it is preferable to use low-spatial resolution (i.e., 1 km or greater) satellite images, such as those from the National Oceanic and Atmospheric Administration Advanced Very High Resolution Radiometer (NOAA-AVHRR) or Meteosat sensors (Thomson *et al.* 1996). In addition to information on land cover, these low resolution images can also provide proxy measurements of climate, such as Land Surface Temperature (LST), and Cold Cloud Duration (CCD) (Hay and Lennon 1999). Alternatively, low spatial resolution maps of climate (e.g. atmospheric temperatures, humidity, dewpoint, and precipitation) can be generated by interpolation from ground-based meteorological stations (e.g., Bryan *et al.* 1996; Lindsay *et al.* 1998).

When generating predictions of mosquito distributions over wide areas, it is rarely practical to carry out new mosquito surveys, as these would have to cover the whole region described by the required risk map. Instead, this type of study tends to rely on the collation of published and unpublished records of past surveys, which may vary significantly in both sampling methodology and effort, making quantitative predictions of mosquito abundance hazardous (Coetzee *et al.* 2000).

Vectorial capacity and disease risk

This study will provide the first risk maps of relative vectorial capacity for European mosquitoes (using probability of presence as a measure of abundance) and from this the risk of malaria (R_0) throughout Europe The vectorial capacity of Italian *An. labranchiae* populations has previously been calculated using observed mosquito densities, human biting rate, parous rate and vector survival in different regions (Romi *et al.* 1997a and Romi *et al.* 2001). In both cases, vectorial capacity was calculated for mean summer temperatures of 25° and no attempts were made to assess how varying temperatures could affect the efficiency of *An. labranchiae* as a vector. The other members of the *An. maculipennis* complex have been studied with respect to human biting preferences, density in selected areas and longevity (Jetten and Takken 1994). To date these measures have only been combined to calculate vectorial capacity for *An. labranchiae*. There have been no previous calculations of malaria risk (R_0) in Europe based on information on indigenous malaria cases and vectorial capacity of the most important vectors. The analysis by Martens *et al.* 1999 used information related to vectorial capacity (such as human blood index, survival rate and gonotrophic cycle duration – see below) for *An. atroparvus* and *An. messeae* in Europe. However, instead of R_0, their estimate of risk

was the critical mosquito density threshold – i.e. the number of mosquitoes per human which result in $R_0 > 1$. In a seminal study Lindsay and Thomas (2001) calculated R_0 for *Plasmodium vivax* in England using measures of vectorial capacity for *An. atroparvus* at varying temperatures which showed similar characteristics to this study. Although they did include the human recovery rate (i.e. duration of infectiousness) – a parameter which is not considered here – they did not attempt to model the effect of temperatures on vector abundance which is a crucial component of vectorial capacity.

The value of appropriately chosen climate and land cover data when studying the distribution and abundance of malaria mosquito vectors has been demonstrated on numerous occasions. Using relatively low resolution land cover and climate data in combination with recorded mosquito surveys, this study is designed to examine how climate and land cover affects the current distribution of five former – and possibly future – malaria vectors across Europe. As most of the recorded mosquito surveys in Europe were carried out before satellite images were available, the climate measurements are from interpolated ground data from, or close to, the year when each mosquito collection was made. In contrast, the land cover was obtained from satellite images, since historical land cover data at the resolution required here were not easily accessible. The information on the quantitative relationship between climatic factors (i.e. temperature) and mosquito presence was then used to derive measures of relative vectorial capacity and disease risk throughout Europe taking into account current socio-economic circumstances.

Aims and Objectives

The aim of this study is to examine how well the observed distribution of five European malaria vectors can be explained by spatial variation in climate and land cover, using multivariate statistical models. The outcome measurement of the models is the probability of mosquito presence. The study makes the working assumption that this is a reasonable proxy for mosquito abundance, i.e. it is expected that in regions of high mosquito abundance, the probability of a positive field collection should also be high. Using the initial predictions of vector presence/absence (or relative abundance) spatial relative measures of vectorial capacity for all five European mosquitoes were then generated. Based on the assumption that probability of presence is a marker of mosquito abundance, relative vectorial capacity is calculated following the approaches described by Jetten *et al.* (1996) and Lindsay and Thomas (2001), i.e. empirically derived average measurements of human blood index, adult survival and transmission efficiency taken from published sources and temperature-driven measurements of gonotrophic cycle and extrinsic incubation period and climate- and land cover- driven estimates of relative vector abundance are used. Although vectorial capacity is an important factor when considering vector control, the real outcome of interest is disease risk, namely R_0. Using up-to-date knowledge about recent indigenous malaria transmission in Europe (in relation to the number of imported cases), measures of R_0 are derived from the relative vectorial capacity calculations in combination with local socio-economic indicators. The specific objectives are:

1. to map the observed distribution of *Anopheles atroparvus*, *An. labranchiae*. *An. messeae*, *An. sacharovi* and *An. superpictus* throughout Europe.
2. to identify which climate and land cover variables correlate with the observed distribution of each of the five *Anopheles* vector species.
3. to generate a spatial map of the relative vectorial capacity of each of the five species throughout Europe as predicted by local climate and land cover characteristics.
4. to generate a spatial map of malaria risk by combining these relative vectorial capacity measures with socio-economic predictors which impact on the frequency of secondary local malaria cases for each imported case (i.e. R_0).

Methods

The mosquito database

Information on the distribution (presence and absence) of *Anopheles atroparvus*, *An. labranchiae*, *An. messeae*, *An. sacharovi* and *An. superpictus* in Europe was collected from 163 published papers (including abstracts, short reports and reviews) and various unpublished materials kindly provided by collaborators in Finland, Holland, Italy, Norway, Romania, Russia, Sweden and the UK. All published or unpublished records of mosquito surveys date from 1927 to 2001 (83% between 1970 and 2001). The search found 1833 survey points in 34 European countries (Appendix 4.1)

Data were collected as point data and each data point consists of:

- Country.
- Sampling village or location.
- Latitude and longitude in decimal degrees (East of Greenwich) of sampling village or location.
- Presence and absence of mosquito species (0=absence, 1=presence).
- Date of capture or survey (if available).
- Name of investigator and date of publication (if available).
- Full reference of published data.

Sampling or capture methods were seldom given and were not included in the database. The majority of collections were of adult mosquitoes. Mosquito absence is defined as either: (a) the absence of the particular species from surveys which explicitly contained a list of all species caught; or (b) specific mention by the author(s) that the species was not caught.

Latitudes and longitudes of study sites were obtained from the Worldwide Directory of Cities and Towns (2002) or, if not listed in this directory, identified using world or regional atlases.

Generation of explanatory variables

Climate variables at 0.5 by 0.5 degrees (approximately 17 by 17 km) were extrapolated from the University of East Anglia, CRU 0.5 Degree 1901-1995 Monthly Climate Time-Series (CRU 2002) comprising mean temperature, precipitation, cloud cover, diurnal temperature range, vapour pressure, ground frost frequency and wet day frequency. This

climate surface has been constructed by New *et al.* (2000) using direct interpolation from station observations and estimation of synthetic data from predictive relationships between variables (see detailed description in Chapter 2). For each study location, climate variables from the year of survey or publication were downloaded. The annual monthly minimum, maximum and average was calculated for each variable, i.e., TMIN is the average temperature of the coldest month of that year (Table 4.6).

Table 4.6. Environmental variables and their range throughout the study area.

Code	Description	Range
TMIN	Minimum of the average temperature (° C)	-25.5 - 23.9
TMAX	Maximum of the average temperature (° C)	4 – 39.6
TAVE	Average of the average temperature (° C)	-5.3 – 28.6
PTOT	Total annual precipitation (mm)	9.4 - 377
CCMIN	Minimum of the average cloud cover (%)	5 - 67
CCMAX	Maximum of the average cloud cover (%)	43 - 80
CCAVE	Average of the average cloud cover (%)	30.8 - 70
TRMIN	Minimum of the average diurnal temperature range (° C)	0 - 21
TRMAX	Maximum of the average diurnal temperature range (° C)	5.7 - 23.4
TRAVE	Average of the average diurnal temperature range (° C)	3.7 - 22
WDFMIN	Minimum of the average wet day frequency (days)	0 - 19
WDFMAX	Maximum of the average wet day frequency (days)	3 - 31
WDFAVE	Average of the average wet day frequency (days)	3.5 - 19.2

Land cover values were extracted from the 1 by 1 km resolution 1992 Eurasia Land Cover Characteristics Data Base, distributed by USGS EROS (USGS 2002) encompassing 94 land cover classifications (Global Ecosystems). These data are derived from 1 km NOAA-AVHRR 10 day NDVI composites for April 1992 to March 1993, classified into land cover types according to their spectral characteristics throughout the year. The resulting land cover map was validated by comparison of sample point pixels with cover type identified from Landsat or SPOT images, giving an over-all accuracy of 66.9%. The land cover image and observed mosquito data points were overlaid in ERDAS IMAGINE 8.4 and the land cover type at each point identified using a vector zonal attribute model. This model assigns a land cover type from the land cover raster image to each sampling point in the mosquito vector image (converted from a simple point map into a vector image using ARCINFO). Of 94 land cover classes, 36 (38%)

were represented in the observed dataset. Five of these were highly infrequent (0.05-0.003%) and were subsequently merged with others of similar description to allow for greater flexibility in the final models. The five most common land cover types sampled were: Crops (15.2%), mixed forest (10.4%), cool crops (9.9%), deciduous forests (6.4%) and Mediterranean shrubs (6.2%).

Data analysis and generation of formulae

Data were analysed in STATA 7.0 first by univariate and then multivariate analyses.

The purpose of the univariate analyses was to explore linear and non-linear (i.e. quadratic) associations between explanatory variables and mosquito presence and absence. Any quadratic relationships between climate variables and mosquito distribution were used to calculate climatic optima (e.g. temperature optima) by differentiating the quadratic equation:

$y = a + bx + cx^2$

(where x is the climatic variable and b and c are the linear and quadratic constants, respectively)

When differentiated and rearranged, this gives:

$x = -b/(2c)$

which is the equation used for calculating climatic optima.

The multivariate logistic regression models were constructed in STATA 7.0 using the GLM feature. The models take the logit form:

$$\text{logit } p = c + t_1x_1 + t_2x_2 + t_3x_3 + \ldots.t_nx_n$$

where p is the probability of mosquito presence

c, t_1, t_2, t_3 and t_n are constants

x_1, x_2, x_3 and x_n are explanatory variables (see also Box 4.1).

From this equation, the probability of mosquito presence is then calculated as:

$$p = \frac{1}{1 + \left(1 / \exp(A)\right)}$$

(Equation 4.1)

where A equals logit p (i.e. the results from the multivariate logistic regression model). Because the Pearson deviance (Box 4.1) was much lower than 1 for all minimal adequate models (range 0.03-0.25), the models were not scaled for overdispersion like the previous models developed in Chapters 2 and 3. The models were constructed by the backwards stepwise approach in which all non-significant ($p > 0.05$) climate variables were removed until only significant variables remained in the model. Land cover was maintained as a categorical variable in models for all mosquito species. The probability cut-off for a prediction of presence was set to 0.5 as this value maximises the overall proportion of correct predictions. The null model was defined as the model containing no explanatory variables.

The fit of the final model predictions was tested against the observed data using percentage correct, sensitivity (correct prediction of presence) and specificity (correct prediction of absence) as well as the percentage deviance explained by the final model compared to the null. For all predictions the kappa measure of agreement was calculated (Armitage *et al* 2001) This takes into account the proportion of correct predictions as well as the true positives and true negatives in the original dataset:

$$k = \left(\frac{\left(\frac{a+d}{n} \right) - (a+c)*(a+b)+(b+d)*(c+d)/n^2}{1-\left((a+c)*(a+b)+(b+d)*(c+d)/n^2 \right)} \right) \qquad \text{(Equation 4.2)}$$

where

a = number of observed points of presence predicted to be presence

b = number of observed points of absence predicted to be absence

c = number of observed points of presence predicted to be absence

d = number of observed points of absence predicted to be presence

n = total number of observed points

In practice, values of kappa range between 0 to 1 (mathematically, a negative value is possible but this rarely occurs), with a value of one representing perfect agreement. Kappa takes a value of zero if there is only chance agreement.

A validation of the methods and models was performed using logistic regression on a subset of the original dataset lying outside 3 to 18 degrees longitude (a total of 939 data points or 51%). The resulting models were tested against independent data from the

omitted central region (within 3 to 18 degrees longitude, e.g. approximately from Lille in France to Budapest in Hungary, Fig. 4.2) and the relevant goodness-of-fit measures calculated. The data between these two longitudes were selected after inspection of the geographical spread of all study locations. By selecting in this way, it is ensured that the largest possible range of climate, land cover, and mosquito presence/absence (i.e. from North to South) was included in the validation dataset.

Predictive maps of mosquito distributions

Predictions of the distribution of all five mosquitoes were made for the whole of Europe, covering –13.6 to 37 degrees longitude (e.g. from the Atlantic ocean near Ireland to Ukraine) and 31 to 73 degrees latitude (from central Morocco to the northernmost point of Scandinavia). Predictions were made at a 0.25 by 0.25 degrees (approximately 8.5 km) resolution to increase the resolution of the predictions and make optimal use of the land cover dataset. Using the formula presented above, a probability of mosquito presence was calculated for each 0.25 degree grid cell. The CRU 0.5 Degree (17km) 1961-1990 Mean Monthly Climatology dataset was used as the baseline climate for the prediction maps (see above for details). The 0.5 degree climate grid was extrapolated to a 0.25 degree grid by adding new cells to the grid and calculating the climate value of each new 0.25 degree cell as the mean of all surrounding 0.5 degree cells. For each 0.25 degree cell, an ERDAS IMAGINE vector zonal attribute was used to calculate the most common land cover type. Maps of the predicted distributions of *Anopheles* in Europe were made in the Geographical Information System (GIS) ArcView 3.1. Predictions were only made within the climate and land cover ranges represented in the observed dataset (Table 4.5). All cells outside these ranges were labelled 'no prediction'. The frequencies of the different land cover types throughout the whole of Europe were similar to those of the observed dataset as described above. Seven European land cover types were not represented in the observed dataset and thus classified as 'no prediction' areas in the predictive maps. Additionally, for each *Anopheles* species, any grid cells containing land cover types which did not appear in the final model, were also labelled 'no prediction'.

Relative vectorial capacity

A measure of relative vectorial capacity was calculated for all five mosquito species throughout Europe. Vectorial capacity is defined as the mean number of potentially

infective contacts made by a mosquito population per infectious person per time unit (Jetten *et al.* 1996) and expresses the potential for a malaria epidemic following 1 infectious case.

Vectorial capacity can be calculated as:

$$VC = mbca^2\left(\frac{p^n}{-\ln p}\right) \qquad \text{(Equation 4.3)}$$

where:

a = number of bites on a human per mosquito (human biting rate) *

b = the probability that an infected mosquito transmits malaria when biting

c = the probability that a mosquito acquires infection when biting a malaria infected human

m = number of mosquitoes per person

n = duration of extrinsic incubation cycle *

p = daily survival rate *

* indicates that the variable is temperature-dependent

All variables which are not temperature-dependent have been set using previous examples from the literature. The value of b is given as 0.19 (James 1931, Lindsay and Thomas 2001) and c is arbitrarily set to 1 (Jetten *et al.* 1996). As mentioned, this study assumes that the probability of mosquito presence is a proxy relative measure of abundance (i.e. abundance is a function of probability of presence), hence m is the probability of presence predicted by the minimal adequate models described above.

The human biting rate, a, is directly related to the human blood index HBI (the proportion of blood meals taken on man) and the time between two blood meals u (i.e. the time between feeding, digesting and oviposition – also known as the gonotrophic cycle):

$$a = \frac{HBI}{u}$$

The human blood index has been calculated for all five species and is based on data quoted in Jetten and Takken (1994). Values of HBI (Table 4.7) have previously been

obtained by examining wild caught engorged *Anopheles* species in various locations throughout Holland, Italy, Greece, eastern Europe and North Africa.

Table 4.7. Human blood index for five European mosquitoes.

Species	Human blood index	Range (no. observations)	Sources
An. atroparvus	0.299	0.03 – 0.84 (8)	Olivaria and Hill (1935); Swellengrebel and De Buck (1938); Garrett-Jones *et al.* (1980).
An. labranchiae	0.175	0.04 – 0.65 (8)	Cefalu *et al.* (1961); Garrett-Jones *et al.* (1980).
An. messeae	0.343	0.005 - 0.63 (6)	Barber and Rice (1935); Swellengrebel and De Buck (1938).
An. sacharovi	0.252	0.007 – 0.87 (17)	Barber (1936); Barber and Rice (1935); Hadjinicolaou and Betzios (1972); Garrett-Jones *et al.* (1980); Kligler and Mer (1932).
An. superpictus	0.231	0.016 – 0.30 (3)	Barber and Rice (1935).

The average HBI for each mosquito does not correspond to the anthropophily measures described in the Introduction. Instead, the upper limit of the range seems to be more similar to the anecdotal evidence about the man-biting habits of the vectors. As discussed previously, this is most likely due to the geographic variation in the HBI. The average HBI in Table 4.7 is probably low because most of the experiments were performed in rural settings with live stock nearby. We chose to use average HBI in the calculations as we are predicting relative vectorial capacity across a range of habitats (i.e. both rural and urban). Ideally, HBI should be included as a location-specific variable but there is clearly insufficient data to do this.

According to Shlenova (1938), the gonotrophic cycle can be described as follows:

$$u = \frac{TSv}{T - Nv}$$

where TSv is the accumulation of temperature units over time to complete the mosquito cycle (36.5 degree days for *An. maculipennis;* Detinova *et al.* 1963), T is ambient temperature and Nv is the threshold below which mosquito development ceases (9.9°C;

Detinova *et al.* 1963). Maximum temperature (TMAX) is used as ambient temperature because this variable represents temperatures during the summer – i.e. the season where malaria transmission is more likely to take place.

The duration of the extrinsic incubation cycle of the parasite (n) is highly dependent on temperature but may only vary slightly between different species of mosquitoes. Moshkovsky and Rashina (in Jetten and Takken, 1994) used the equation described by Shlenova (1938) to describe the effect of temperature on the extrinsic incubation cycle:

$$n = \frac{TSp}{T - Np}$$

where TSp is the accumulation of temperature units over time to complete the parasite cycle (105 degree days for *P. vivax*), T is maximum temperature and Np is the threshold below which parasite development ceases (15°C; McDonald 1957). For this exercise, the critical values for *P. vivax* have been used as this is the parasite most likely to be transmitted in Europe.

Mosquito daily survival rate (p) was calculated separately for each of the five species (Table 4.8) using data based on laboratory tests. Although survival rate is temperature-dependent it was decided to keep this parameter fixed. Daily survival has previously been calculated at varying temperatures using the following equation:

$$p = x^{1/u}$$

where x is the proportion of mosquitoes surviving the gonotrophic cycle (assumed to be 50%)
and u is the length of the gonotrophic cycle (Lindsay and Birley 1996, Martens *et al.* 1999). The rationale for this formula is that survival rate per gonotrophic cycle (i.e. x) is temperature-independent. However, this assumption has not been empirically validated and in the present study mosquito daily survival rate is consequently assumed to be temperature-independent.

Table 4.8. Daily survival rate of five European mosquitoes.

Species	Daily survival rate	Range* (no. measurements of p)	Sources
An. atroparvus	0.971	0.706 – 1 (24)	Shute and Ungurenau (1939); Rosa (1936); Leeson (1939); Meller (1962).
An. labranchiae	0.979	0.968 – 0.989 (2)	Shute and Ungurenau (1939).
An. messeae	0.851	0.739 – 0.947 (13)	Shute and Ungurenau (1939); Rosa (1936).
An. sacharovi	0.811	0.567 – 0.955 (7)	Rosa (1936); Kasap (1990).
An. superpictus	0.943	0.940 – 0.945 (2)	Kasap (1990).

* The value of p was calculated as the average of all given measurements from various references (range of all measurements shown).

Consequently, the final equation used for calculation of the relative vectorial capacity of e.g. *An. atroparvus* is as follows:

$$RVC = \textit{probability of presence} * 0.19 * \left(\frac{0.299}{36/t\max - 9.9}\right)^2 * \left(\frac{0.971^{(105/t\max - 15)}}{-\ln 0.971}\right)$$

(Equation 4.4)

Daily survival rate (***p***) and human blood index (***h***) were used as species-specific variables and maximum temperature (tmax) as a location (latitude – longitude) specific variable. The outcome, RVC, is distinct from an absolute measure of vectorial capacity because (1) it is assumed that the probability of mosquito presence is linearly related to ***m*** and (2) the value of ***c*** is not entered as the data are too few and inconsistent (Table 4.1). It is acknowledged that if ***c*** varies significantly between the species, this has introduced a bias in the calculations.

Predictive maps of relative vectorial capacity

The vectorial capacity predictions were made using the same baseline climate maps as for the mosquito distributions. For each 0.25 degree grid cell, a measure of RVC was calculated using Equation 4.4 (or the equivalent for each species). Because the duration of the extrinsic incubation and gonotrophic cycles cannot be negative, areas with

maximum temperatures below 15°C (see equation) were labelled 'no prediction' in the final map (i.e. this indicates areas where no transmission can take place).

Disease risk, R_0

R_0 - the basic case reproduction number - is defined as the number of secondary cases arising from a primary one in a fully susceptible host population. It is related to vectorial capacity by:

$$R_0 = VC * 1/p \qquad \text{(Equation 4.5)}$$

where 1/p is the number of days a case remains infectious (an unknown constant which is geographically independent). For any European country, average R_0 can be estimated in theory as the ratio of indigenous : imported cases if the population is wholly susceptible. When this ratio is known, it can be used to calculate the combined value of the unknown constants from the vectorial capacity and R_0 equations (Table 4.8). These unknown constants are: 1/p (as above); c (the probability that a mosquito acquires infection when biting a malaria infected human)and α (a constant which links mosquito abundance to probability of presence).

Data on indigenous and imported malaria in Europe during 1990-2000 were collected from the WHO European Regional Office for Denmark website (WHO 2002a). An indigenous case is defined as transmission of malaria by a local (not imported) *Anopheles*. During the ten years, five countries had reported indigenous malaria transmission (Table 4.9). All indigenous cases, apart from the 2 cases reported in Germany, were *P. vivax*. For consistency with the vectorial capacity calculations where *P. vivax* data were used, only imported *P. vivax* cases were used for calculations of R_0. The use of imported *P. vivax* cases in Germany instead of *P. falciparum* is justified as the two were almost equal during the 10 year period (5992 imported *P. falciparum* cases compared to 5922 *P. vivax* cases, WHO 2002a).

Table 4.9. Indigenous and imported malaria in Europe during 1990-2000.

Country	Total indigenous cases	Total imported *P. vivax* cases	R_o	Population-weighted relative vectorial capacity (RVC)	"Constant" (R_o/RVC)
Belarus	5	35	0.1429	0.0064	20.756
Bulgaria	18	260	0.0692	0.0102	10.031
Germany	2	5922	0.0003	0.0053	0.079
Greece	4*	105	0.0381	0.0677	0.563
Italy	5	5920	0.0008	0.117	0.008

* indigenous cases from Greece do not include the two cases reported in 2001 (see Chapter 3).

Using the previously generated 0.25° resolution map of RVC, a measure of total RVC was calculated for each grid cell (i.e the sum of the RVC of all vectors present in the cell). Next, a population-weighted measure of RVC was determined for each 0.25° grid cell in the European mosquito map. This was done by firstly determining the population density using the Gridded Population of the World dataset at a 1km resolution (CIESIN 2002). The population density in each 0.25° grid cell was calculated in ERDAS IMAGINE using the vector zonal attribute model (see above). A total population density for each of the countries represented in the map was calculated by taking the sum of all cells where the majority of the cell lay within the country boundaries. For each 0.25°cell, a population-weighted total RVC was then calculated by multiplying the total RVC for the cell by the population density ratio in the same cell (i.e. population density in that cell as a ratio of the total population density in the country). A country total was produced by adding up all cells within the country borders.

The number of secondary (i.e. indigenous) malaria cases in a country is determined by a combination of the number of primary (i.e. imported) cases as well as socio-economic factors which impact on health system quality, availability of chemotherapy etc. In order to best predict secondary cases in any European country, the relationship between socio-economic factors and indigenous malaria first needs to be described for the five countries with available data. Using these countries (Table 4.9) as datapoints, a series of linear regressions was performed containing socio-economic factors (GDP, number of doctors per population, number of nurses per population, literacy rates and life expectancy at birth) as explanatory variables and "constant" as the outcome. Socio-economic variables were obtained from the World Bank Report (1993).

The best prediction of the "constant" (R^2 = 0.90) was obtained using GDP and life expectancy as explanatory variables (Fig. 4.1) in the equation below. These variables were then collected for the remaining 36 countries in Europe (Appendix 4.2) and the equation used to calculate constants for the countries with no reported indigenous cases of malaria in the 1990s:

"constant" = exp (-27.59 + 3022.6*1/life expectancy –1.548*ln GDP) (Equation 4.6)

Because GDP and life expectancy measures from North African and Middle Eastern countries (i.e. Algeria, Egypt, Israel, Libya, Morocco and Tunisia) were vastly outside the ranges observed in the rest of Europe (e.g. GDP was only $610 in Egypt compared to 1390 in Romania, the lowest in Europe) no predictions of disease risk were made for these countries. GDP and life expectancy measures for European Turkey were set equal to those for Bulgaria as the values quoted in the World Bank Report represent the whole of Turkey (i.e. European and Asian part) while only the European part of Turkey is of interest to this study. Bulgaria was selected both because of its geographical proximity to the European part of Turkey but also because of similarities in socio-economy (i.e. neither of the two countries are EU members). All former Yugoslavian countries were given the values reported for Yugoslavia as, in 1993, these republics were still part of Yugoslavia.

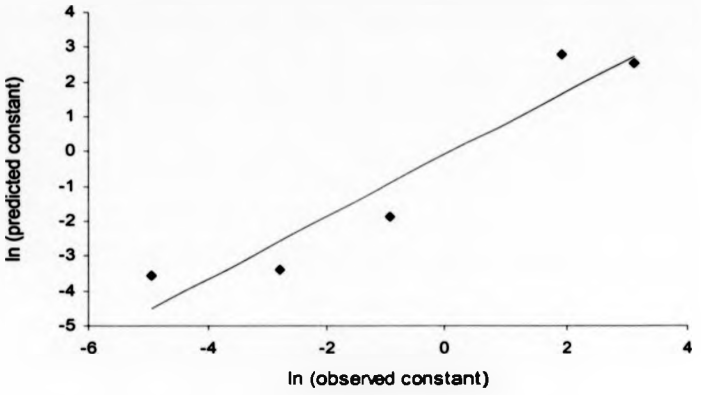

Figure 4.1. Predicted versus observed constants (i.e. R_0/relative vectorial capacity) for five European countries.

The impact of errors (i.e. uncertainty) on the predictions of R_0 was assessed by varying the daily survival rate (***p***). Thus, malaria risk was calculated using the lowest and the highest values of ***p*** quoted for each mosquito species (Table 4.8). This resulted in two 'error maps' – one for a low ***p***-value and one for a high survival rate.

Predictive maps of malaria risk

A measure of R_0 for each 0.25° grid cell in the European map was calculated by multiplying the total RVC in a cell by the relevant country-specific constant for that cell. The constant for a particular cell was identified by relating the cell to a country (i.e. overlaying the 0.25° map on a map showing the European country borders). Disease risk was then mapped throughout Europe at the 0.25° level. No predictions were made for the whole of North Africa, parts of the Middle East and the Asian part of Turkey due to factors described above and thus these regions are labelled 'no prediction' in the maps.

Results

Observed mosquito distributions

The 1833 study locations are scattered throughout Europe with particular areas clearly less represented than others; for instance, 16.3% of all data points are from Portugal whereas only 0.1% are from Norway (Appendix 4.1, Figure 4.2). Poor coverage in these areas is probably more due to the inability to obtain neither published nor unpublished material from the countries in question rather than a real absence of surveys.

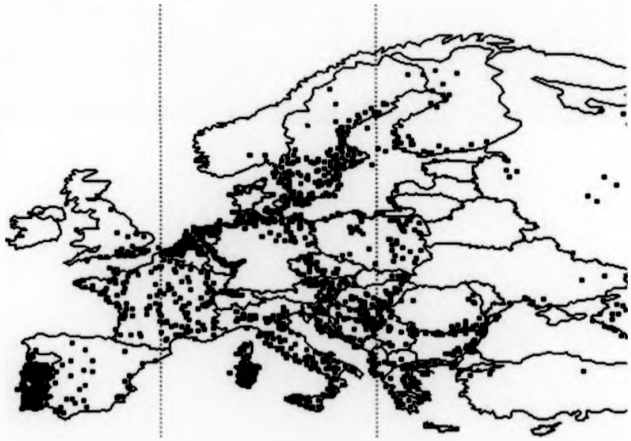

Figure 4.2. The distribution of study locations across Europe. The two inserted lines represent the longitude lines within which data points were selected for the model validation.

Anopheles atroparvus was the most common and widely distributed mosquito in the observed dataset being present in 974 (53%) of locations. Points of presence were found in areas with comparatively low temperatures, high amount of rainfall and where the predominant land cover types were crops, forests and fields and marsh wetlands (Table 4.9).

Anopheles messeae was the second most common mosquito in the dataset being present at 868 points (47.4%). Like *An. atroparvus* this mosquito was present mainly in

areas with lower temperatures and high precipitation with crops and forests being the main land cover types (Table 4.9).

An. labranchiae was present in 239 (13.1%) of sampled locations which had higher temperatures and less rainfall than locations where the two northernmost species were found. It was mainly observed to be present in areas with Mediterranean shrub, irrigated cropland and marsh wetlands (Table 4.9).

Anopheles sacharovi was present in 200 (10.9%) locations sampled and therefore the least commonly reported of the five mosquitoes. It was present in areas with comparatively low rainfall and high temperatures where grass crops, irrigated croplands and forests and fields were the main land cover types (Table 4.9).

An. superpictus (the only vector of European malaria which is not a member of the *An. maculipennis* complex) was present in 412 (22.5%) locations in the original dataset. Like the two other southern species, it was observed mainly in areas of high temperatures and low rainfall with grass crops, irrigated cropland and marsh wetland being the most dominant land covers (Table 4.10).

Table 4.10. Observed distribution of *Anopheles* in Europe in relation to temperature, precipitation and land cover.

Species	Observed number of presence points (%)	Mean average temperature *	Total precipitation *	Land cover (%) †
An. atroparvus	974 (53)	-3 – 17	202 – 1730	Cool crops (10%) Forests and fields (9%) Marsh wetland (9%)
An. messeae	868 (47.4)	-4 – 16	253 – 1756	Grass crops (9%) Cool crops (8%) Cool conifer forest (8%)
An. labranchiae	239 (13.1)	3 – 18	94 – 1436	Mediterranean shrub (17%) Semi desert shrub (15%) Irrigated cropland (12%)
An. sacharovi	200 (10.9)	-1 – 18	94 – 1528	Grassland (16%) Irrigated cropland (15%) Forests and fields (10%)
An. superpictus	412 (22.5)	-1 – 18	94 – 1539	Grassland (16%) Irrigated cropland (12%) Marsh wetland (11%)

* Shows the range of mean average temperature and total precipitation in which all observed presence points lie.

† Shows the percentage of observed presence points which are distributed in the specific land cover type.

Mosquito distributions: univariate analyses

Univariate analyses were performed by adding each explanatory variable (except land cover) in turn to the 'null model' described above (Table 4.11).

Table 4.11. Results of univariate analyses.

Variable	*An. atroparvus*	*An. messeae*	*An. labranchiae*	*An. sacharovi*	*An. superpictus*
TMIN	n.s	s (l)	s (l)	n.s	s (q)
TMAX	s (q)	s (q)	s (q)	s (q)	s (q)
TAVE	s (q)	s (q)	s (q)	s (q)	s (q)
PTOT	s (q)	s (q)	s (l)	s (l)	n.s
CCMIN	n.s	n.s	n.s	n.s	n.s
CCMAX	s (q)	n.s	n.s	n.s	n.s
CCAVE	s (q)	s (q)	s (q)	s (q)	s (q)
TRMIN	s (l)	n.s	n.s	n.s	n.s
TRMAX	n.s	s (q)	s (l)	n.s	n.s
TRAVE	s (q)	s (l)	s (q)	s (q)	s (q)
WDFMIN	n.s	n.s	n.s	n.s	n.s
WDFMAX	n.s	n.s	n.s	n.s	n.s
WDFAVE	s (q)	s (q)	s (q)	s (q)	s (q)

where n.s indicates that the variable was not significant (i.e. $p > 0.05$), s (l) that the variable was significant ($p < 0.05$) and linear and s (q) that the variable was significant and showed a quadratic relationship with mosquito presence. See Table 4.6 for explanation of variable abbreviation.

Mosquito distributions: minimal adequate models

The minimal adequate model for *An. atroparvus* showed that the presence of this mosquito was positively associated with precipitation, maximum cloud cover, average wet day frequency and negatively related to minimum diurnal temperature range (Table 4.12). The *An. atroparvus* model output from STATA is shown in Box 4.1 as an example. Outputs from the four other mosquitoes are not presented. The model provides a preliminary indication that this mosquito is probably more associated with higher latitudes where there is more rainfall and cloud cover and a lower diurnal temperature range. The minimal adequate model predicts 74.1% correct with a sensitivity of 74.6% and specificity of 73.4% and it explains 39.7% of the variation in the observed data. The kappa measure of agreement for the *An. atroparvus* model was 0.35. Quadratic associations between minimum and average temperature and average diurnal temperature range and mosquito distribution were observed (Table 4.12). The optimum minimum temperature for *An. atroparvus* is 8.5°C, the optimum average temperature 17.9°C and the optimum average temperature range 15.8°C. This is consistent with the relationship between these variables and the proportion of sampling locations positive for *An. atroparvus* (Fig. 4.3). The presence of *An. atroparvus* was not significantly

associated with particular land cover classes (Table 4.13) due to its wide distribution across Europe and, hence, across a wide variety of land cover types.

Box 4.1. Minimal adequate model for *An. atroparvus*.

```
STATA command
xi: glm  atroparvus tmin tminsq tave tavesq ccmax ptotal trmin trave
travesq wdfave i.ecosyst_land, l(l)

Statistics
Generalized linear models                    No. of obs      =       1833
Optimization     : ML: Newton-Raphson        Residual df     =       1786
                                             Scale param     =    .179681
Deviance         =  320.9102346              (1/df) Deviance =    .179681
Pearson          =  320.9102346              (1/df) Pearson  =    .179681

Explanatory variables
(37 land cover variables not included)
------------------------------------------------------------------------------
atroparvus |      Coef.   Std. Err.      z    P>|z|     [95% Conf. Interval]
------------------------------------------------------------------------------
      tmin |  -.3807435   .1011903    -3.76   0.000    -.579073    -.1824141
     tminsq |    .005589    .001978     2.83   0.005    .0017122     .0094658
      tave |   4.502956   .5286773     8.52   0.000    3.466767     5.539144
     tavesq |  -.053219   .0067693    -7.86   0.000   -.0664866    -.0399515
     ccmax |   .0205804   .0082768     2.49   0.013    .0043581     .0368028
     ptotal |  -.017478   .0028474    -6.14   0.000   -.0230589    -.0118971
      trmin |  -.0723114   .0318899    -2.27   0.023   -.1348145    -.0098083
      trave |  -.7437242    .270984    -2.74   0.006   -1.274843    -.2126053
     travesq|   .0397845   .0149254     2.67   0.008    .0105313     .0690377
     wdfave |    .423689    .039436    10.74   0.000    .3463958     .5009821
------------------------------------------------------------------------------
```

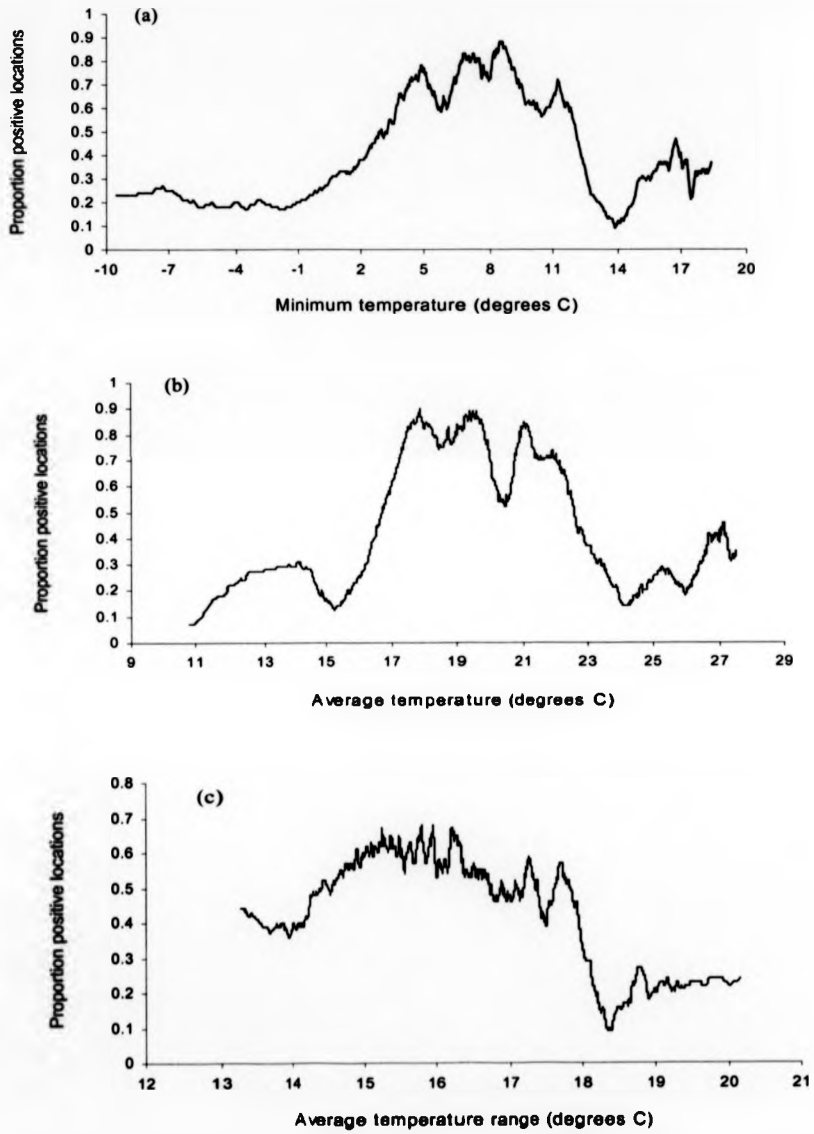

Figure 4.3. Relationship between the proportion of sampling locations positive for *An. atroparvus* in different temperature intervals and (*a*) minimum temperature, (*b*) average temperature and (c) average diurnal temperature range. (Derived using shifting intervals with an average of 1°C).

The minimal adequate model for *An. messeae* showed a significant positive relationship between mosquito presence and precipitation and negative associations with average temperature and minimum diurnal temperature range (Table 4.12) again indicating a possible higher latitude distribution. The model predicts 79.4% correct with a sensitivity of 85.7% and specificity of 73.7% and explains 47.8% of the variation in the observed data with a kappa of 0.41. The optimum conditions for *An. messeae* include a minimum temperature of 6.2°C, average cloud cover 64.7%, average diurnal temperature range 16.8°C and average wet day frequency of 16 days. Due to its relatively wide-spread distribution, *An. messeae* – like *An. atroparvus* – was not significantly associated with any particular land cover type (Table 4.13).

The presence of *An. labranchiae* is positively correlated with maximum and average temperatures and negatively correlated with minimum cloud cover (Table 4.12). This suggests that *An. labranchiae* prefers habitats with higher temperatures and less cloud cover. The minimal model predicts 96.3% correct with a sensitivity of 84.5% and a specificity of 98.1% and explains 74.8% of the variance. Kappa was calculated to 0.68 indicating that this model has the best fit of all the models developed. The optimal conditions for *An. labranchiae* were calculated and are: minimum temperature 14.3° C, average cloud cover 45.9%, and average diurnal temperature range 12.7° C. The distribution of this mosquito was positively associated with Mediterranean and semi-desert shrubs, marsh wetlands and irrigated croplands and negatively associated with cool conifer forests (Table 4.13). This corresponds with its presence in the Mediterranean (see below) where it breeds in marshes and rice fields and its absence in the north of Europe where conifer forests are more common.

The distribution of *An. sacharovi* is positively correlated with precipitation and minimum wet day frequency and negatively correlated with maximum and average wet day frequency and average cloud cover (Table 4.12). These relationships indicate a distribution mainly in areas which receive some rainfall but are not too cloudy. The minimal adequate model explains 44.9% of the variance and correctly predicts 92.3% of the points with a sensitivity of 74% and a specificity of 97.8%. Kappa is 0.39 indicating that there is agreement between the observed and predicted data. Optimum minimum temperature and optimum average diurnal temperature range are 15.2° C and 13.4° C, respectively. The land cover types which were positively associated with this mosquito were Mediterranean shrub, marsh wetlands and irrigated croplands while deciduous and mixed forests had a negative effect on the distribution of *An. sacharovi* (Table 4.13).

Again this correlates well with its presence in marshes and rice fields of the Mediterranean and eastern Europe and absence in the northern parts which are more covered by forests (see below).

The presence of *An. superpictus* is positively associated with average temperature and negatively associated with average diurnal temperature range and maximum and average wet day frequency (Table 4.12), indicating a preference for relatively hot and dry areas. Model predictions are 92.3% correct with 80.6% sensitivity and 95.6% specificity and the minimal adequate model explains 68.6% of the variation in the observed data. The kappa value of 0.58 indicates that this model had the second best agreement between observed and predicted distributions. The optimum minimum and maximum temperature and precipitation for this mosquito are 14.9° C, 23.7° C and 165 mm, respectively. The land cover types mostly associated with this mosquito were marsh wetlands, irrigated croplands and grasslands (Table 4.13) which correlates with its distribution in eastern Europe and Turkey where there are vast grasslands.

Results of the model validations are given in Table 4.14. These demonstrate that, using the observed data geographically limited to the western and eastern edges of Europe, the sensitivity and specificity of the predictions of mosquito presence/absence in the central region ranged from 71-89% and from 73-100% , respectively. Kappa ranges from 0.25-0.55 which, as expected, is somewhat lower than the values shown in Table 4.12.

Table 4.12. Contents and fit of minimum adequate models.

Species	Explanatory variables	% Correct	Specificity (%)	Sensitivity (%)	Variance explained (%)	Kappa
An. atroparvus	TMIN, TAVE, PTOT (+), CCMAX (+), TRMIN (-), TRAVE, WDFAVE (+), LANDCOVER	74.1	73.4	74.6	39.7	0.39
An. labranchiae	TMIN, TMAX (+), TAVE (+), CCMIN (-), CCAVE, TRAVE, LANDCOVER	96.3	98.1	84.5	74.8	0.68
An. messeae	TMIN, TAVE (-), PTOT (+), CCAVE, TRMIN (-), TRAVE, WDFAVE, LANDCOVER	79.4	73.7	85.7	47.8	0.41
An. sacharovi	TMIN, PTOT (+), CCAVE (-), TRAVE, WDFMIN (+), WDFMAX (-), WDFAVE (-), LANDCOVER	92.3	97.8	74	44.9	0.35
An. superpictus	TMIN, TMAX, TAVE (+), PTOT, TRAVE (-), WDFMAX (-), WDFAVE (-), LANDCOVER	92.3	95.6	80.6	68.6	0.58

(-) and (+) indicate negative or positive association between outcome and explanatory variable throughout the observed range. Underlined parameters have a non-linear relationship, with defined optima (described in text)

Table 4.13. The effect of land cover on mosquito distributions

Species	X^2 significance (df)	Most significant land cover classes
An. atroparvus	P > 0.05 (31)	N/A
An. labranchiae	P < 0.001 (22)	Mediterranean shrub (+) Marsh wetland (+) Semi desert shrub (+) Irrigated cropland (+) Cool conifer forest (-)
An. messeae	P >0.05 (31)	N/A
An. sacharovi	P <0.001 (23)	Mediterranean shrub (+) Marsh wetland (+) Irrigated cropland (+) Deciduous forest (-) Mixed forest (-)
An. superpictus	P <0.001 (28)	Marsh wetland (+) Irrigated cropland (+) Grassland (+) Deciduous forest (-) Mixed forest (-)

(+) or (-) indicates whether land cover class is positively or negatively associated with mosquito presence

Table 4.14. Results of separate model validations on a subset of the original dataset

Species	% Correct	Sensitivity (%)	Specificity (%)	Kappa
An. atroparvus	72.8	72.9	72.7	0.28
An. labranchiae	98.8	70.6	99.6	0.55
An. messeae	86.2	86.5	86.1	0.49
An. sacharovi	90.8	71.4	95.4	0.25
An. superpictus	94.3	88.5	96.5	0.42

Predicted mosquito distributions

An. atroparvus was observed to be present in northern and western Europe, Spain, Portugal and northern Italy (Fig. 4.4a) and its predicted distribution ranged from most of North-west Europe through to the Spanish peninsula and Portugal, but not in the Balkans, North Scandinavia, the Alpine regions and North Africa (Fig. 4.4 b). The model falsely predicts absence in the Balkans.

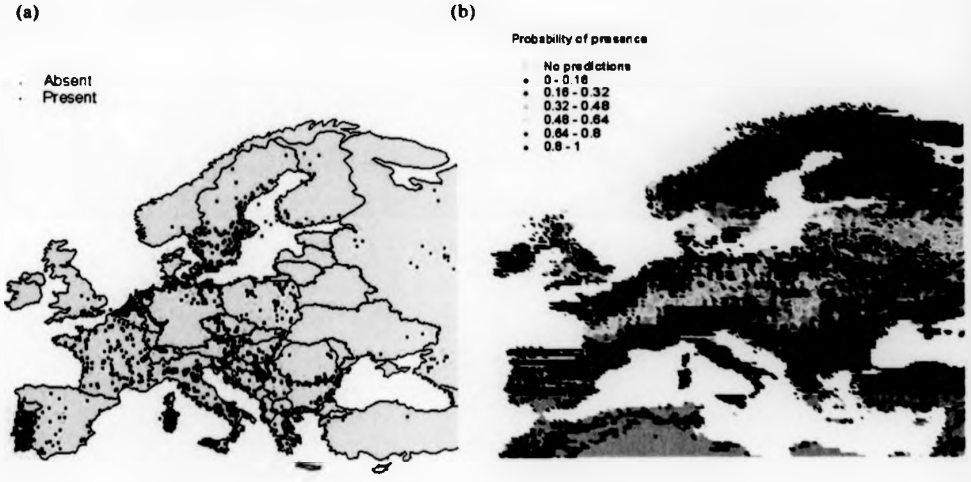

Figure 4.4. Observed (a) and predicted (b) distribution of *An. atroparvus* in Europe.

The observed distribution of *An. messeae* extends along the coastlines of England and the Netherlands, northern Germany, in large areas of Scandinavia and parts of Russia (Fig 4.5a). *An. messeae* was predicted present in Scandinavia and north-west Europe, including the Baltic states and Russia (Fig. 4.5b). The model falsely predicts absence in the Balkans and south-eastern France.

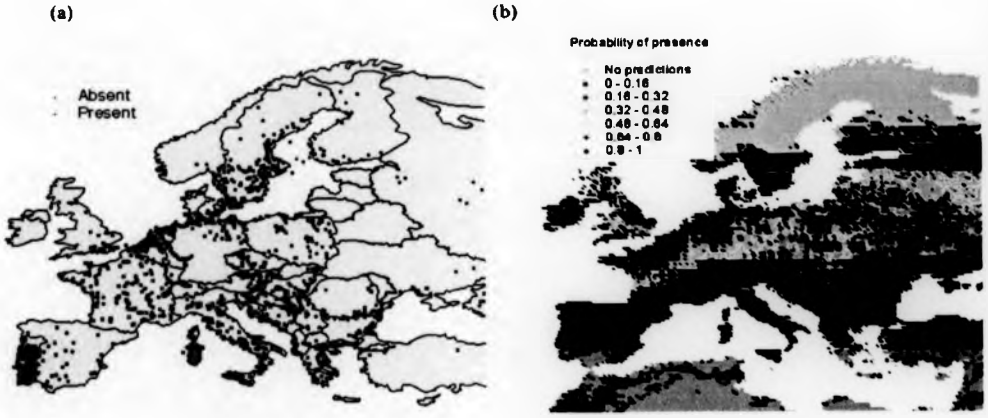

Figure 4.5. Observed (a) and predicted (b) distribution of *An. messeae* in Europe.

The Mediterranean vector *An. labranchiae* was eradicated from parts of Italy following DDT spraying in the 1940s and 1950s but has now reinvaded Sardinia, Sicily and the mainland (Fig. 4.6a). It is present in North Africa but has reportedly disappeared from Spain where it was formerly present (C. Ramsdale, personal communication). The predicted range of *An. labranchiae* extends across Italy, coastal parts of the Balkans, eastern Spain and North Africa (Fig. 4.6b). The model falsely predicts a small focus of presence in the south-west of France and in eastern Spain.

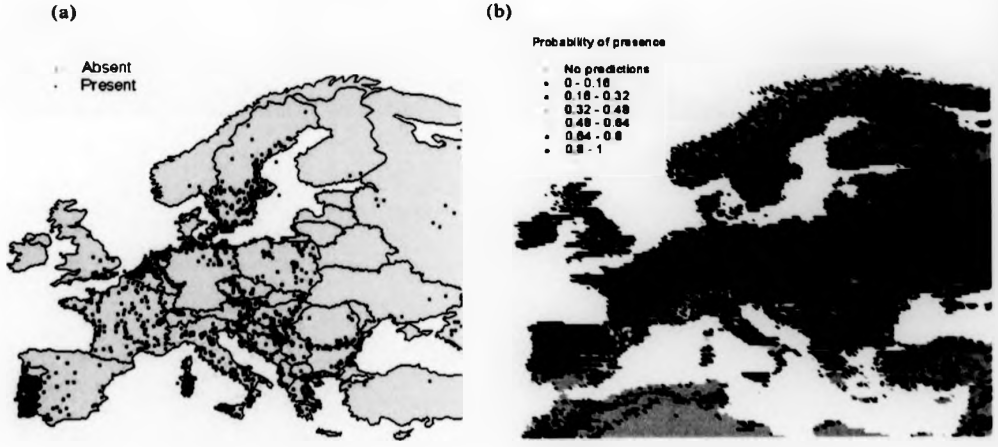

Figure 4.6. Observed (a) and predicted (b) distribution of *An. labranchiae* in Europe.

The current distribution of *An. sacharovi* is restricted to the eastern coast of Italy, Russia, the Balkans, and across Turkey to the Middle East (Fig. 4.7a). It is predicted to be present mainly in south-east Europe, from eastern Spain along the Alps to the Balkans, Turkey, and the Black Sea (Fig. 4.7b). The model wrongly predicts presence along the Alps, through to France and Spain and seems to underestimate presence in Greece.

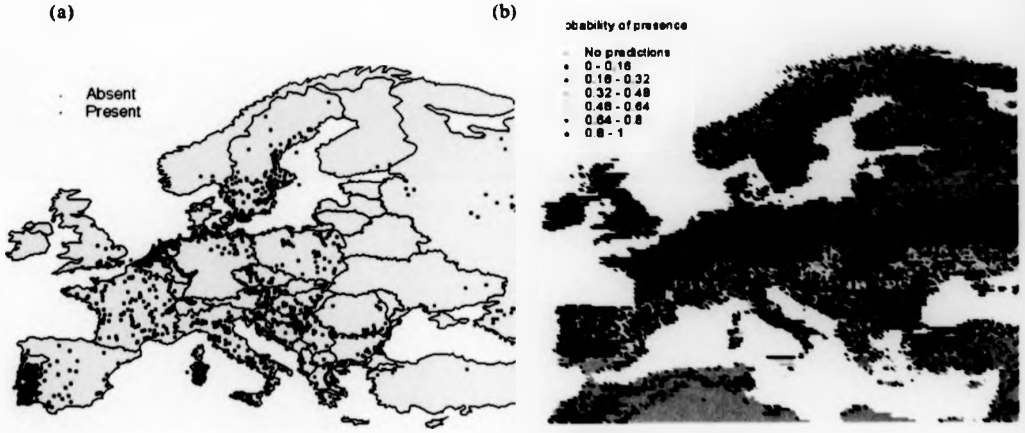

Figure 4.7. Observed (a) and predicted (b) distribution of *An. sacharovi* in Europe.

The observed present distribution of *An. superpictus* (the only mosquito which is not a member of the *An. maculipennis* complex) includes the Balkans, Turkey and Italy (Fig. 4.8a). Its predicted distribution is similar to, but less extensive than *An. sacharovi*, ranging from the Alps, through to the Balkan states, into Turkey and northern Africa (Fig. 4.8b). There are false negative predictions throughout Italy, in southern France, the East of Spain, and North Africa.

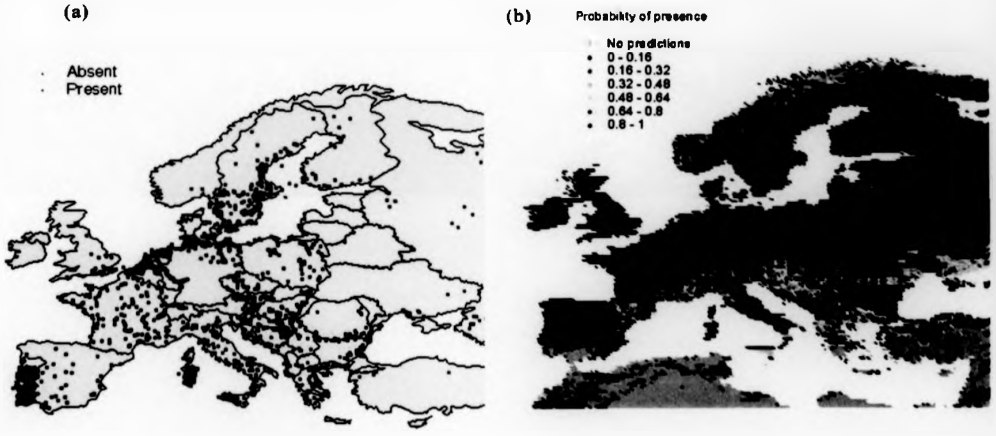

Figure 4.8. Observed (a) and predicted (b) distribution of *An. superpictus* in Europe.

Relative Vectorial capacity

Measures of relative vectorial capacity were calculated for each of the five species in all 0.25 degree grid cells in the European map (see Figure 4.9-4.4.13 and note that the map scales differ). For all five species, this measure ranged between 0 and 0.647, the most 'efficient' vector in Europe being *An. labranchiae* (Table 4.15).

Table 4.15. Relative vectorial capacity of European malaria vectors

Species	Relative vectorial capacity range
An. atroparvus	0 - 0.175
An. labranchiae	0 – 0.647
An. messeae	0 – 0.005
An. sacharovi	0 – 0.053
An. superpictus	0 – 0.191

In the current scenario, *An. messeae* is not predicted to be an efficient vector anywhere in Europe (Fig 4.9). It is most abundant in northern Europe, including Scandinavia and Russia, where temperatures will be too low to support transmission of *P. vivax*. Furthermore, in comparison to the other mosquitoes, the survival rate of *An. messeae* is apparently relatively low (Table 4.7).

Figure 4.9. Relative vectorial capacity of *An. messeae* in Europe.

For *An. sacharovi* there is also little evidence of any vectorial efficacy in Europe with only small areas of North Africa showing an RVC of 0.015-0.05 (Fig 4.10). This is surprising as this mosquito was considered to be one of the most efficient vectors in Europe, based on anecdotal evidence of high anthropophily in endemic areas (e.g. Hackett and Missiroli 1935, Hackett 1937). *An. sacharovi* is also the suspected vector of malaria in Turkey but the models generated models do not pick up on this. As discussed previously, the HBI measures used for the RVC models do not correlate with these historical observations (Table 4.7), which explains the low predictions of RVC. Additionally, *An. sacharovi* also has a relatively low survival rate which may explain why it seems to be one of the least efficient vectors in Europe (*p* appears twice in the formula for vectorial capacity and will thus have an important effect on the outcome).

Figure 4.10. Relative vectorial capacity of *An. sacharovi* in Europe.

The current relative vectorial capacity of *Anopheles atroparvus* is predicted to be highest in southern Spain and Portugal with RVC values of 0.04-0.2 (Fig 4.11). This corresponds with the fact that these areas are the hottest zones where *An. atroparvus*, according to the models presented, has a high probability of presence (i.e. high abundance).

Figure 4.11. Relative vectorial capacity of *An. atroparvus* in Europe.

An. superpictus is predicted to be an effective vector in North Africa, Turkey and a small isolated area in Spain (Fig 4.12), all corresponding to locations of high abundance. This mosquito is currently a suspected vector of *P. vivax* in Turkey and thus the accuracy of these predictions is supported by present epidemiological observations. .

Figure 4.12. Relative vectorial capacity of *An. superpictus* in Europe.

For *An. labranchiae*, RVC is highest (0.15-0.75) across northern Africa and in isolated areas in south-east Spain, Sicily and Sardinia (Fig 4.11). Again, it is observed from the predictive maps that these areas are among some of the hottest where *An. labranchiae* is currently abundant. This mosquito was predicted to be the most efficient vector in Europe which is consistent with the observations of several previous authors who commented on the consistently high levels of malaria in *An. labranchiae* areas (e.g. Hackett 1937, Bruce-Chwatt and de Zulueta 1980).

Figure 4.11. Relative vectorial capacity of *An. labranchiae* in Europe.

Disease risk, R_0

At the country level, the average risk of malaria (R_0) calculated for 43 countries in Europe ranged between 0 – 1.09. According to this model, endemic malaria conditions (i.e. where R_0>1) currently only exist in Moldova (Table 4.16). There were 16 countries with an R_0 indicating unsuitable conditions for malaria transmission (Andorra, Austria, Belgium, Denmark, Faeroe Islands, Finland, France, Germany, Iceland, Ireland, Luxembourg, Netherlands, Norway, Sweden, Switzerland and United Kingdom). The predicted R_0 for all 43 countries is shown in Appendix 4.2

Table 4.16. Predicted average malaria risk in 10 European countries

Country	R_0
Moldova	1.09
Romania	0.89
Hungary	0.61
Ukraine	0.41
Bosnia-Herzegovina	0.39
Turkey	0.35
Croatia	0.31
Albania	0.29
Russia	0.28
Poland	0.25

Values shown are in ascending order (i.e. predictions of average R_0)

At the 0.25° resolution, the predicted disease risk varied from 13.5 in an isolated area in Romania (near Brasov) where the principal vector present in *An. superpictus* to 0 in most of central and western Europe (Fig 4.14). The model predictions indicate that R_0 is presently above 1 in areas of Eastern Europe, indicating that these are areas in which endemic malaria transmission could currently be sustained. There is no indication that R_0 is high in the European part of Turkey although malaria transmission does currently occur just across the Bosporus strait. This is most likely due to the fact that *An. superpictus* is not predicted to be an efficient vector in the European part of Turkey whereas in the Asian part (for which no R_0 predictions have been made) it is predicted to have a higher vectorial capacity. Additionally, predictions indicate that malaria transmission is not feasible in Greece, the last country to eradicate the disease. This is

due to the low RVC predictions for *An. sacharovi* throughout the country. Thus, in light of socio-economic, entomological and climatic conditions, it can be concluded that the most vulnerable areas for malaria today are all situated in Eastern Europe. The sensitivity of these predictions is demonstrated in Figure 4.15 which shows the malaria risk calculated using low and high values of daily survival rate (p). It is evident that even relatively small fluctuations in this parameter can have a great influence on the final R_0 predictions. For instance, the malaria risk in Ukraine is approximately 0.25 when calculated using the low survival rate but 5 if the high survival rate is used for the calculations.

Figure 4.14. Predicted malaria risk (R_0) throughout present day Europe.

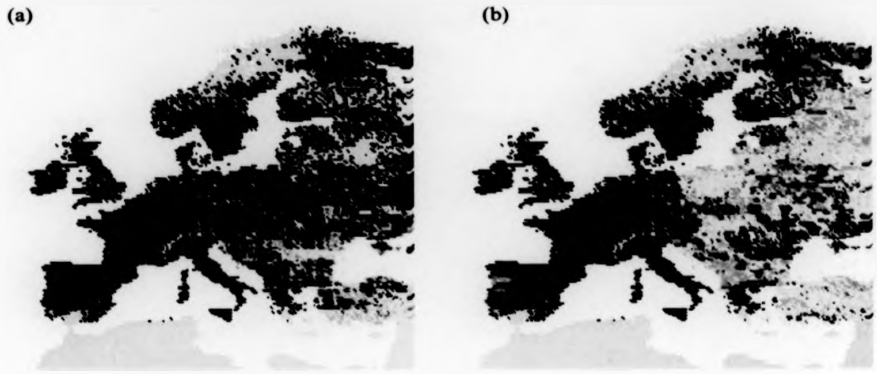

Malaria risk (R0)

- No predictions
- 0 - 0.125
- 0.125 - 0.25
- 0.25 - 0.375
- 0.375 - 0.5
- 0.5 - 0.625
- 0.625 - 0.75
- 0.75 - 0.875
- 0.875 - 1
- 1 - 2
- 2 - 4
- 4 - 10
- 10 - 25

Figure 4.15. Error maps of malaria risk in present day Europe calculated using low (a) and high (b) values of mosquito daily survival rate.

Discussion

This study shows that statistical models, based on low resolution climate and land cover data, can accurately predict the presence or absence of particular mosquito species in precise locations, throughout a continent. The reliability of the predictions was measured using geographically independent datasets. Half of the observed data (clustered in the West and East) was used to predict *Anopheles* distributions in the excluded central region. The level of accuracy obtained (sensitivity: 71–89%; specificity: 73 - 100%) is comparable to the many published studies which use high resolution environmental data to predict mosquito presence/absence within relatively small geographic regions (Beck *et al.* 2001). The kappa measure of agreement ranged between 0.45-0.85, demonstrating that the observed associations did not arise purely by chance. For all five European vectors, the relationship between mosquito presence and the significant environmental variables from minimal adequate models correlate well with the climatic features of where the mosquitoes are present in the observed dataset. Similarly, the modelled associations between land cover features and the presence of each mosquito give an accurate account of real-life observations on the ecology of these mosquitoes. The environmental datasets used here have global coverage and are freely available without charge. Similar analyses could therefore be carried out relatively easily in other regions with large historical mosquito datasets, such as the United States, Africa and Asia.

Although some studies have used low resolution remotely sensed data to investigate temporal patterns in mosquito abundance (Linthicum *et al.* 1987, Thomson *et al.* 1996, Gleiser *et al.* 1997), there have been few attempts to develop large scale geographic risk maps of mosquito presence/absence. Interpolated meteorological spatial data have been used to predict the distribution of *An. farauti* (Laveran) s.s in northern Australia (Bryan *et al.* 1996), *Anopheles gambiae* (Giles) s.s. and *An. arabiensis* (Patton) s.s. (Lindsay *et al.* 1998) and *Anopheles gambiae* s.l. (Rogers 1996) in Africa. The analytical methods used were definition of a "climate index" of suitability according to the results of previous laboratory and field studies (Bryan *et al.* 1996), definition of minima and maxima of climate variables in all 1° pixels within the recorded distribution (Lindsay *et al.*. 1998), and discriminant analysis based on the climate properties of 1° pixels inside and outside of the reported distribution (Rogers 1996). These models were then fitted to climate surfaces. The resulting predictive maps were relatively accurate,

either by visual comparison with the observed mosquito distribution (Bryan *et al.* 1996; Lindsay *et al.* 1998), or statistical tests - up to 95% correct predictions of presence/absence for individual pixels (Rogers 1996). As the authors acknowledge, such predictions need to be treated with some caution. In each case the "observed" data were derived from low resolution interpolated distributions, i.e., boundaries drawn on paper maps, based on a combination of field observations and expert opinion. In any defined area (i.e., 1° pixel), mosquitoes were assumed to be either wholly present or wholly absent. Hence the observed distributions exclude any of the real patchiness due to local environmental variation (often independent of climate) that is revealed by analysing individual captures. While this approach may identify the climate limits of a geographic range, it has little power to investigate variation in abundance (and R_0) within a range.

In contrast, the two published studies using low resolution environmental databases to explain spatial variation in mosquito species or genotype ratios (rather than abundance) provide more convincing evidence of accurate predictions for specific points. Using published data on mosquito collection, Thomson *et al.* 1997 showed that the proportion of the 2Rbc inversion amongst the Mopti form of *An. gambiae* s.s in Africa is negatively correlated with NDVI (resolution 5 km) at each collecting site. Lindsay *et al.* 1998 generated risk maps of the species ratio of *An. gambiae* to *An. arabiensis,* from statistical associations between interpolated climate data and the relative abundance of each species (scanned from paper maps). The results were validated by the detection of a highly significant positive correlation with published species ratios from 14 field sites in Tanzania.

Using relatively few, simple explanatory variables, the European *Anopheles* models uniquely identify and quantify the differences between the habitats of the five species. The distribution of European malaria vectors has frequently been linked with irrigated cropland (such as rice fields) and marshes (Jetten and Takken 1994) which is supported by the results presented here. Furthermore, they confirm the familiar separation of the *An. maculipennis* complex into species adapted to either high or low latitudes, with two or more species only occasionally occupying the same site, possibly indicating some level of inter-specific competition as well as different abiotic requirements for the five species (Mosna 1937, Artemiev 1980, Jetten and Takken 1994). In particular, the two high latitude species, *An. atroparvus* and *An. messeae,* preferred lower temperatures, with peak abundance at minimum temperatures of 8.5°C

and 6.2°C, respectively, compared with a range of 14.3°C to 15.2°C for the other three species.

Areas of discrepancy between observed and predicted distributions are concentrated in the East of Europe and parts of the Mediterranean. When focusing on the particular predictions for each species, it is observed that *An. messeae* and *An. atroparvus* are falsely predicted to be absent in the Balkans. This is mainly due to a lack of observed data (e.g. the Balkans are among the most infrequently represented areas) but also because of the particular climatic requirements of these species. According to the models, both species prefer areas with comparatively low temperatures, low diurnal temperature ranges and high amounts of rainfall. By examining the climate data for the Balkans, it was observed that these requirements are not met, thus producing false negative predictions. The false positive predictions of *An. sacharovi* in the Alpine region are most likely due to a combination of high rainfall, comparatively high temperatures and the presence of marsh wetlands which, according to the models, makes these areas suitable for this mosquito. *An. sacharovi* is predicted to be absent in most of Greece although it is one of the most abundant mosquitoes here (Hadijnicolaou and Betzios 1973). In this case, the absence of shrubs, marshes and irrigated cropland from Greece may explain this. According to the land cover data used, most of Greece is covered by crops (Appendix 4.3) while this land cover type is not significantly related to the distribution of *An. sacharovi*. Similarly, the wrongly predicted absence of *An. superpictus* in Italy is caused by the extensive presence of Mediterranean and semi desert shrubs which, according to these models, are not associated with the European-wide presence of this mosquito.

Another general reason for the false predictions in eastern Europe is that this area represents the edge of the distribution for *An. atroparvus* and *An. messeae* and the western Mediterranean represents the edges for *An. sacharovi* and *An. superpictus* i.e. where mosquito populations may be less static than elsewhere and retreat or reappear with fluctuations in climate. Sampling of mosquitoes in such locations can therefore provide potentially unreliable results. Furthermore, the time discrepancies between the land-use and mosquito data as well as the inability of the land-use data to pick up land cover patchiness at a very local scale may have caused inaccurate predictions. Finally, due to factors described earlier, misidentification of field caught *Anopheles maculipennis* s.l. is possible, and should ideally be checked against more recent field collections from similar localities where identification of *An. maculipennis* species has

been made using more refined methods such as PCR and gas chromatography (Phillips *et al* 1990, Proft *et al* 1999).

The calculations of relative vectorial capacity for all five mosquitoes provide a valuable estimation of malaria transmission potential in Europe. However, because knowledge of some of the important factors is relatively limited, the results should be interpreted with caution. For instance, the daily survival rate used for all mosquitoes is based on measurements from laboratory settings. There are no measures of European *An. maculipennis* complex survivorship in nature, the only available data being from McHugh (1989) who estimated the daily survival of *An. freeborni* (a North American member of the *An. maculipennis* complex) to be 0.74. The validity of using experiments from an artificial setting to determine the longevity in nature is questionable and other measures should ideally be obtained. Additionally, this work assumes that daily survival is unrelated to temperature which is not the case (Bradley 1993). As discussed, previous authors have used a non-verified relationship between survival rate and temperature (Lindsay and Birley 1996), but because there is no apparent empirical evidence for this relationship, it has not been used in this study. Another variable of concern in the calculation of relative vectorial capacity is the human blood index (HBI) which has been shown to vary greatly for all five species (Table 4.6). This variation is clearly geographically dependent – i.e. the HBI will be higher in urban locations but lower in rural settings where more livestock are present. The HBI used in this study was calculated as the average of all reported observations but this may have caused an underestimation of relative vectorial capacity and hence R_0 as the majority of published studies have focused on rural areas where the HBI will be comparatively low.

In spite of the caveats, it can tentatively be concluded that *An. atroparvus*, *An. labranchiae* and *An. superpictus* are the most efficient vectors of *P. vivax*. Romi *et al.* (2001) reported that the vectorial capacity of *An. labranchiae* in natural breeding sites in Italy ranges between 0.96-3.3 and deduced that *An. labranchiae* is a potentially efficient *P. vivax* vector. They based this conclusion on reports that the critical vectorial capacity for Africa is 0.02 , i.e. a vectorial capacity above this threshold means that the mosquito is an efficient vector (Molineaux and Gramiccia 1980). Overall, the calculations of relative vectorial capacity presented here correlate with what has been commented on by previous authors; namely that *An. atroparvus* was the major vector across Europe because of its widespread distribution and that *An. labranchiae* most likely was responsible for maintaining the high levels of malaria observed in the Mediterranean

(Hackett 1937, Bruce-Chwatt and de Zulueta 1980). Additionally, *An. superpictus* is predicted to be an efficient vector in Turkey where it is indeed today responsible for transmission of *P.vivax* (Ramsdale and Haas 1978).

The predictions of malaria risk, R_0, throughout Europe show that the currently most vulnerable areas are in eastern Europe and small areas of European Turkey. This correlates well with observed data. As mentioned, there is currently malaria transmission in Turkey and the majority of indigenous cases since 1990 have been reported from countries in this region, along the shores of the Black Sea where the vector *An. sacharovi* is predicted to be present. Considering the socio-economy of the different regions in Europe, these are also the areas which have been subject to the largest declines in health service quality and civil unrest which makes them more susceptible to transmission of malaria. The predicted risk of malaria in Greece is surprisingly low considering that the last indigenous cases were reported from Greek Macedonia. It would be logical to assume that the last country to see local malaria cases should also have the highest current risk of transmission, however this is not the case here. This is most likely due to the fact that Greece is now an EU member state with a relatively high GDP ($6340) compared to the other Balkan countries (e.g. $1840 in Albania). Greece became a member of the EU in 1981 which will have significantly improved its economy for the past twenty years and thus, according to the models developed in this study, decreased the chances of local malaria transmission re-emerging.

The sensitivity of malaria risk predictions to variations in the parameters of RVC is high, as demonstrated by the simulations in this chapter. For instance, in Ukraine we observe a 20-fold increase in R_0 simply by using the high instead of the low value of daily survival rate. Clearly, when using predictions based on biological parameters it is firstly necessary to be relatively confident that the values of these variables have been appropriately measured but also be aware that any predictions are necessarily subject to large errors as our knowledge about the biology of European mosquitoes is somewhat limited.

In order to improve the limitations of the *Anopheles* database and utilise it as a resource for further investigations which may be useful for policy making, a number of future studies would be highly useful. Firstly, the geographic discrepancies between predicted and observed data should be reduced by searching for additional mosquito data from regions of discrepancy and from regions currently under-represented in the mosquito sampling database. A way of expanding the database could be to search

zoological records of local or national museums that were not included in this study due to cost and time restrictions. Another possibility is to further strengthen the links to other European entomologists who may be actively involved in local *Anopheles* sampling. Secondly, it is necessary to test the hypothesis that there is a correlation between the probability of mosquito presence versus mosquito abundance, preferably by identifying a series of standardised mosquito samples carried out within the region. For instance, entomologists in Ekaterinburg, Russia, have monitored the abundance of local *An. messeae* for more than twenty years and stronger collaboration links with these scientists are highly desirable. Finally, the models developed in this study provide the first quantitative link to investigating the effect of environmental changes (such as global warming) on the distribution of European malaria vectors and, ultimately, the risk of malaria re-emergence in Europe.

Thirdly, the relative measure of RVC could be improved by collecting new data on key parameters of vectorial capacity. Human blood index could be allowed to vary in relation to specific local features (e.g. number of live stock) and the link between socio-economy and RVC and R_0 needs to be examined in greater depth, preferably using data from currently endemic areas in Europe.

In spite of the improvements which should be made, the current model outputs still give us the best available handle to investigate the potential impact of climatic changes on malaria risk (R_0) in Europe; and in Chapter 5 these models will be used to simulate R_0 across Europe as a result of the climate changes predicted for the 2020s, 2050s and 2080s.

The effect of climate changes on the risk of malaria re-emergence in Europe.

Abstract

During the past 5-10 years, there has been much public interest about the possible effects of projected global climate changes on the re-emergence of malaria transmission in Europe. Predictive modelling of future malaria patterns in the region has been inconclusive not in the least because the environmental factors determining the past and present distribution of disease and mosquito vectors were not fully considered. This study combines the results presented in Chapters 2,3 and 4 on the effect of climate on the past and present risk of malaria in Europe in order to predict the effect of climate changes on future disease patterns

Using the model developed for English and Welsh counties during the 19th and 20th centuries, temperature increases of 1 and 2.5°C were predicted to increase the incidence of ague deaths in any county by 8.2 and 14.5 %, respectively, while a temperature decrease of 1°C would have caused a 6.5% decrease in ague deaths. Considering the fact that R_0 in the UK is currently minuscule, the projected proportional increases in risk following global warming are unlikely to lead to the re-establishment of endemicity.

In an analogous virtual experiment, the effects of temperature increases and decreases on indigenous malaria case rates were also simulated for 17 European countries during 1900 to 1975. With a warming of 1.5°, 2° and 5°C, the number of malaria cases in any year was predicted to increase by 6.2, 10.7 and 24.2% respectively. An across-the-board 1.5°C decrease in temperature caused a predicted decrease of 8.1% in malaria cases. In-depth simulations for four different countries (Finland, Italy, Spain and Sweden) showed that temperature increases had the greatest effect in northern countries while decreases in temperature were equally important in northern and southern areas.

The spatial distribution of five former European malaria vectors was predicted for the 2020s, 2050s and 2080s using the most recent HADCM3 SRES scenarios. With these projected climate changes, the two northern-most vectors *An. atroparvus* and *An. messeae* were predicted to increase in both geographical range and probability of presence (assumed to be linearly related to abundance). Three southern mosquitoes *An. labranchiae*, *An. sacharovi* and *An. superpictus* were predicted to increase in abundance throughout their distributional range which did not change significantly. Predictions of relative vectorial capacity for the same species showed a potential increase in the roles of *An. atroparvus*, *An. labranchiae* and *An. superpictus* as malaria vectors in the future while the two other species did no appear to develop any significant vectorial efficiency.

Finally, predictions of future R_0 (malaria risk) showed that the greatest changes may occur in eastern Europe where, by the 2050s and 2080s increasingly large areas could become suitable for malaria transmission (i.e. $R_0 > 1$). The risk of disease in the rest of Europe was predicted to remain low ($R_0 << 1$) even towards the end of the 21st century. Although some of these predictions have been generated from rather crude assumptions, they still demonstrate the feasibility with which basic statistical and more sophisticated biological approaches can be combined to predict the effect of climate changes on future patterns of malaria across a previously endemic continent. This approach shows great potential and the reliability of predictions could be improved relatively easily, as more data and parameter values are added to the database in the future.

Introduction

In response to the increased concern about the effect of man-made climate changes on human health, numerous recent publications have focused on the potential impact on vector-borne diseases across the world. As has been shown in the previous chapters, malaria was once an important disease in Europe and this fact has led to many speculations about the prospects of the disease re-emerging here as a result of global changes. In this chapter, two independent approaches are taken to investigate future malaria risk. Firstly, the coefficients previously derived from the impact of climate on the inter-annual variability in malaria risk are used to estimate the average proportional change in the risk that would be expected to ensue from the predicted changes in climate (e.g. across-the-board temperature increases of 1-5°C). This analytical approach is first carried out using the model for malaria mortality rates across the UK in the 19th and 20th century (from Chapter 2) and then repeated using the model for inter-annual variability in malaria case rates in Europe in the 20th century (from Chapter 3).

The second approach is to investigate the current risk of malaria in Europe on the basis of the current distribution of *Anopheles* vectors (from Chapter 4). This is done by applying not only the statistical associations detected between climate and mosquito distributions but also the experimentally determined associations between temperature and other key determinants of vectorial capacity. Finally, these measurements of relative vectorial capacity (cumulative for all sympatric *Anopheles* vector species) are converted to an absolute measure of malaria risk (R_0) by taking into account how national socio-economic indicators appear to affect the relationship between national measurements of relative vectorial capacity and the reported ratio of secondary cases: imported malaria cases (i.e. R_0). With this climate-driven model of spatial heterogeneity in current risk across Europe, the impact of various climate change scenarios is then simulated. Of course, these predictions only measure the impact of climate change due to effects on parasite and vector biology. The predictions do not take into account other potential changes in Europe which could impact on malaria risk, such as demography, human, migration, socio-economics, land use, malaria chemotherapy, and so on.

Climate changes: detection and attribution

Climate observations have been undertaken for centuries in many parts of the world and these show strong indications that our climate is really changing:

- Since the 1950s, global average temperatures in the lowest 8 km of the atmosphere have increased by 0.1°C per decade (IPCC 2001).
- During the 20th century, the average temperature in Europe has increased by 0.8°C. Specifically, temperature increases in the Alps have exceeded 1°C when compared to the long term mean (Kovats *et al.* 1999).
- Global average sea levels rose between 0.1 and 0.2 metres during the 20th century (IPCC 2001).
- It is very likely that precipitation has increased by 0.5 to 1% per decade in mid- and high latitudes and 0.2 to 0.3% per decade over the tropical land areas. The frequency of heavy precipitation events is likely to have increased by 2-4% in the late 20th century at mid- and high latitudes (IPCC 2001).

Following the first public debates about climatic change more than twenty years ago, the United Nations formed the Intergovernmental Panel on Climate Change (IPCC) in 1988 to assess available scientific and socio-economic information on climate change and its impacts. This panel represents the World Meteorological Organisation (WMO) and the United Nations Environment Programme (UNEP) and its conclusions are endorsed by major scientific organisations such as the Royal Society and the National Research Council. According to the IPCC the main driving factor behind the climate change problem is the continued increase of the atmospheric concentration of greenhouse gases the effects of which have now been summarised in three extensive reports.

In their most recent report, the IPCC (2001) stated that 'there is new and stronger evidence that most of the warming observed over the past 50 years is due to human activities'. This has been mainly based on comparisons of long-term observed temperatures and precipitation patterns to model projections (including anthropogenic and natural effects) which have found that real climate has behaved in a very similar way to what was predicted by these models (e.g. Hansen *et al.* 1998, IPCC 2001). However, it is vital not to overlook the fact that climate has forever undergone natural cycles of variability. A well-known example of natural climatic variability is the El Niño Southern Oscillation (ENSO), a periodic warming of the East Pacific which occurs

every 2-7 years and is known to cause extreme weather events (floods and droughts) in parts of South America, Africa and Asia (Patz and Lindsay 1999). Another explanation for the observed warming – particularly at the local scale – may be changes in other environmental factors such as deforestation which are thought to increase temperatures, further complicating the role of human activities in the observed global warming.

Naturally, these facts have caused some debate among climatologists about whether the observed increase in average temperatures really is human induced or just due to natural variations in climate (e.g. Michaels 1993). It has been argued that most predictions are based on rather unspecific and unsupported assumptions about the relationship between the burning of fossil fuels and climatic changes and that in some places, e.g. the Arctic, temperatures have actually dropped during the past 50 years (Gardner, 1998).

Climate changes: the predictions

In 2000, the SRES series of plausible scenarios of population growth, economic development as well as greenhouse gas and sulphur emissions were defined (IPCC 2000). Each scenario follows one of four story lines (A1, A2, B1 and B2) which describe four different demographic, politico-economic, societal and technological futures (Fig 5.1).

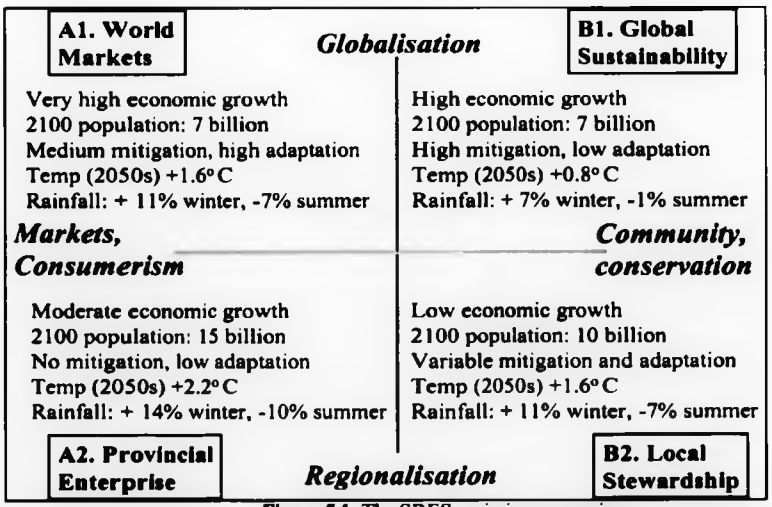

Figure 5.1. The SRES emissions scenarios

(reproduced with kind permission from Tony McMichael).

Without exception, these models predict rises in global average temperatures and sea levels. The projected rate of warming is much larger than any observed changes during the 20th century and is very likely to be without precedent during at least the last 10,000 years. Specific projections reported by the IPCC (2001) state that:

- Global average temperatures are projected to increase by 1.4 to 5.8°C over the period 1990-2100. The highest increases will be observed at northern high latitudes in the cold season (e.g. northern areas of North America and Central Asia).
- Global average precipitation is projected to increase, particularly at high and mid latitudes during the winter.
- Global mean sea level is projected to rise by 0.09 - 0.88 m. between 1990 and 2100.

Such changes are expected to affect the ecosystem in a variety of ways. For instance, they can alter the frequency of extreme weather events such as cyclones, floods, droughts and heat waves. The number of extremely cold days is predicted to decrease while hotter and wetter days are thought to become more common. These predictions are clearly uncertain mainly because future anthropogenic and natural influences are difficult to establish but also due to the poor quantification of the change in greenhouse-gas concentration as well as ocean heat uptake (Stott and Kettleborough 2002).

Climate changes: the models

To date, a total of 19 models to predict changes in future climate have been developed all of which are variations of the general circulation models (GCMs) which assume that climate is a product of inter-related factors (i.e. the atmosphere, biosphere, cryosphere, geosphere and the oceans). All current models are based on emission of greenhouse gases (particularly carbon dioxide $C0_2$ and methane CH_4) but vary in their geographical and biological focus as well as in the emission scenario used, i.e which demographic and geographic factors are chosen as the driving forces for greenhouse-gas emissions. The scientific basis of climate change models has been well-established; we know that global average temperatures are related to the amount of atmospheric $C0_2$ and CH_4 (Fig. 5.2) and thus changes in the concentration of these gases may well result in an increase in temperatures.

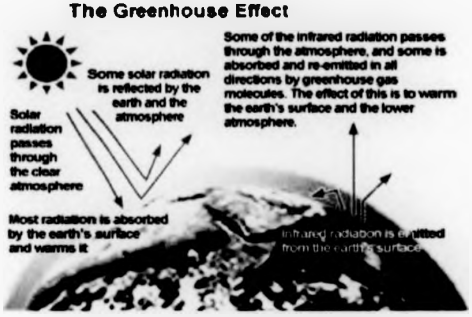

Figure 5.2. The role of greenhouse gases.
From the United States Environment Protection Agency, EPA, (2002).

The most complete models for predicting changes in future climate are coupled atmosphere-ocean general circulation models (AOGCMs) which consist of an atmosphere general circulation model (AGCM) coupled to an ocean general circulation model (OGCM).

The HADCM3, which was developed in 1998 at the Hadley Centre (UK Meteorological Office), is the newest example of an AOGCM (Hadley Centre 2002a). The atmospheric component of the HADCM3 has 19 levels with a resolution of 2.5° by 3.75° of longitude, producing a global grid of 96 x 73 grid cells. This is equivalent to a resolution of approximately 417 km x 278 km at the Equator and 295 km x 278 km at 45° of latitude (through southern France and northern Italy). The oceanic component has 20 levels with a resolution of 1.25 x 1.25°.

The HADCM3 SRES climate change scenarios were chosen for this modelling exercise as they are the most recent developed by the Hadley Centre and have already commonly been used for predictions of climate change effects on infectious diseases, soil erosion and water resources (Hadley Centre 2002a).

Evidence of climate change in non-health related systems

Results of long-term studies indicate that the observed climate changes during the past decades may already have affected some biological systems. Observations of shrinkage of glaciers, thawing of permafrost as well as later freezing and earlier break-up of ice on

rivers and lakes are thought to have been due to increased temperatures (IPCC 2001). Additionally, a northwards shift in some birds and butterflies has been reported (e.g. Parmesan 1996, Thomas and Lennon 1999). Other similar observations include a lengthening of the plant growing season in the UK by at least 11 days during the past 40 years as well as a trend of earlier egg laying in various English bird species (Crick and Sparks 1999, Menzel and Fabian 1999). Although these are of relative interest to scientists, the real demand for information on early effects of climate changes lies in the subject of human health. As Kovats *et al.* (2001) conclude "Further, confirmed effects on humans are likely to have a larger impact on the international policy debate...than effects on butterflies".

Climate changes and human health: the background

Although scientists readily recognise the potential threat of human-induced changes, we have only recently begun to clarify and model any risks to human health and particularly those due to global climate change and ozone depletion.

These potential effects of global climate changes on human health can broadly be divided into direct and indirect effects, depending on whether they occur through the impacts of climate variables on human biology or are mediated by climate-induced changes in other biological or ecological systems (Fig. 5.3).

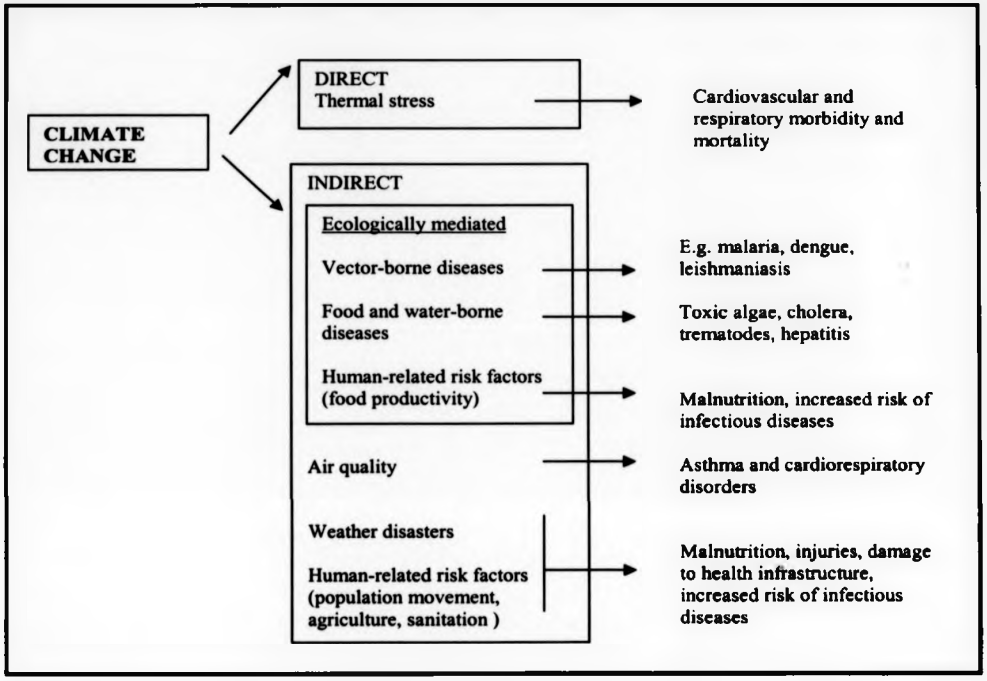

Figure 5.3. Health impacts attributable to climatic changes.
Derived from Martens 1998.

Climate changes and human health: direct effects

A major direct effect of global warming is heat stress which, due to effects on the circulatory system, can result in increases in morbidity and mortality due to heat exhaustion or heat stroke. It has been well documented that heatwaves are associated with a short term increase in overall mortality, particularly in large cities where temperature increases are exacerbated by the urban heat-island effect (Rooney *et al.* 1998). The 1995 and 1987 heatwaves in London and Athens resulted in 137 and 2000 excess deaths, respectively (Katsouyanni *et al.* 1988, Rooney *et al.* 1998). By 2050 it has been predicted that increases in the frequency of summer heatwaves in the US will increase summer mortality by as much as 70% even if the population acclimatises to the increased heat (Kalkstein and Greene 1997). Decreases in winter mortality due to milder

winters may, however, compensate for the higher number of summer deaths and, in countries with a high level of excess winter mortality (e.g. the UK), the beneficial impact may outweigh the detrimental (Paul Wilkinson, personal communication).

Climate changes and human health: indirect effects

The incidence of respiratory diseases is highly related to seasonal changes, partly because trophospheric ozone concentrations increase with increasing temperatures. For instance in Barcelona, periods of higher than average summer temperatures increase daily respiratory mortality by 21.6% (Saez *et al.* 1995). Additionally, climate changes are expected to increase ambient concentrations of ozone and the frequency of ozone pollution episodes, leading to more asthma problems. The observed increase in asthma prevalence since the 1970s is possibly related to elevated temperature and pollution levels but the exact cause still remains unknown (Haines and Parry 1993).

Human-related factors such as changes in agricultural practices due to rising sea levels and changes in precipitation patterns, resulting in decreases in crop yield are thought to be a second major indirect effect of climate changes. Parry *et al.* (1999) predicted increases in crop yields at mid and high latitudes and significant decreases at lower latitudes. By the 2080s, an additional 70 million people were predicted to be at risk of hunger in Africa alone.

Temperature increases and the predicted increased amounts of precipitation may cause flooding, droughts and associated disruptions in agriculture and water supplies and the resulting poor personal hygiene and sanitation can favour transmission of organisms such as *Escherichia coli*, *Vibrio cholerae*, *Salmonella* spp., hepatitis A and E, *Ascaris lumbricoides* and *Trichuris trichiura*. In addition to increased transmission due to sub-standard sanitation, trematode infections may increase due to a direct effect of temperature on the development of the infective soil stages (Colwell and Patz 1998). The 1991 cholera outbreak in Peru coincided with an ENSO related warm event in the tropical Pacific (Colwell 1996) which is thought to have favoured the outbreak due to an indirect effect on the abundance of zooplankton (the 'reservoirs' of *V. cholerae*). By combining the use of climate data and remote sensing to observe phytoplankton (which determines the production of zooplankton), it is feasible to model the relationship between sea temperatures and cholera epidemics and thus predict future outbreaks (Colwell 1996).

Climate changes and vector-borne diseases: detection of early effects?

Insect vectors and the pathogens they transmit are highly sensitive to temperature and usually also precipitation. Most parasites and viruses do not replicate below a certain temperature threshold, but above this threshold, any temperature increases are likely to directly increase speed of development and therefore also the extrinsic incubation cycle, leading to an increased probability of completing parasite development during the life span of the mosquito (Bradley 1993). The indirect effects of increases in temperature and precipitation may be mediated by the ecology and behaviour of the vector. Such effects can take three major forms: (1) expansion of the favourable habitats, (2) changes from seasonal to perennial transmission and (3) the migration of vectors into previously disease-free areas (e.g. higher altitudes).

Thus, there are good biological reasons why climate changes should affect vector borne diseases, however the very complicated cycles as well as the existence of other confounding variables (e.g. drug resistance and man-made environmental modifications) makes it hard to assess the real effects of climate changes. As discussed below, this causes potential problems when looking at spatial trends in vector and parasite patterns and therefore the alternative approach of determining how climate affects the inter-annual variability in diseases may be preferable.

In spite of this, spatial changes in disease patterns have formed the most frequently quoted claims that global warming has already had an impact on some vector-borne disease foci. These claims have mainly concentrated on malaria, with particular focus on the African highlands. For instance, Tulu (1996) attributed the sharp increase in malaria incidence, hospitalisations and deaths during 1968-1993 in Debre Zeit, Ethiopia, to increased temperatures but did acknowledge the potential role of non-climatic factors. In the same location, the amount of residual DDT sprayed decreased by more than 95% from 1972-85 and evidence of from in vitro studies indicated that chloroquine resistance may have contributed to the increased hospitalisations.

Similarly, Loevinsohn (1994) found a correlation between increased malaria cases in Rwanda in 1987 and 1988 and temperatures. This claim has since been criticised mainly by the fact that the analysis does not extend to 1990 when an increase in temperatures did not cause the expected increase in malaria (Reiter 2001). Furthermore, it has emerged that the WHO organised an improvement of disease surveillance at the time of the observed increase in the 1980s which significantly confounds Loevinsohn's results (Reiter 2001). A third claim related to malaria in Africa states that the introduction of

malaria and increase in cases at highland areas in Burundi since 1999 may be related to observed increases in temperatures (Bonora *et al.* 2001). This claim was not substantiated by quantitative analyses and there was no attempt to examine trends in other factors such as population migration, drug resistance etc.

To further demonstrate the debatable role of climate in malaria patterns, Hay *et al.* (2002) recently analysed long term trends in climate at four highland sites in East Africa. They found no significant changes in climate variables and the number of months suitable for *P. falciparum* transmission, concluding that climate changes were not responsible for the observed increases in malaria in these areas.

Outside Africa, an increase in *P. falciparum* infections in Pakistan during 1981-1993 was positively correlated with temperature (Bouma *et al.* 1996). Mean monthly temperatures and precipitation during September-December explained 82% of the observed variation in malaria over the study period. Importantly, the study was undertaken during years when insecticide spraying did not change, data on refugees were not included and increases in chloroquine resistance were examined and found to correlate with only a few peaks in *P. falciparum* infections. This is a thorough study which highlights the importance of examining inter-annual variability and also includes information on potentially confounding factors. The main counter-claim of this work is the likely impact of the El-Niño-related climate anomalies which were not accounted for (Kovats *et al.* 2001).

Aside from malaria, the apparent discovery of *Aedes aegypti* and dengue cases at high altitudes in parts of South America and India has also been attributed to increased temperatures (Jackson 1995). However, it has emerged that both vectors and disease were present here during the 1980s (Paul Reiter, personal communication).

In temperate regions, there have been recent claims that the distribution of *Ixodes* ticks and tick-borne diseases has shifted north-wards and the incidence of tick-borne encephalitis (TBE) and abundance of ticks increased since the 1980s as a result of increasing temperatures (Talleklint and Jaenson 1998, Lindgren *et al.* 2000). Their data on tick abundance were based on questionnaire surveys which are subject to large bias and the increase in TBE cases may have been due to increased awareness of the disease (Kovats *et al.* 2001). Additionally, it has since been shown that years with very high TBE incidence before the study period (omitted from the analysis) were actually associated with less than average warm spring days (Hay 2001). Randolph (2001) analysed temporal TBE patterns in central Europe and the Baltics using statistical and

biological models and concluded that changes in human behaviour (i.e. increased contact with infected ticks), rather than climate variations, were more likely to have caused the observed increases in disease.

These studies have made important advances in understanding how climate may impact on spatial patterns of disease but have also highlighted some important caveats which are likely to cloud the observed associations (e.g. taking into account non-climatic factors, using time-series of sufficient duration and the lack of standardisation of many vector monitoring projects, Kovats *et al.* 2001).

Climate changes and vector borne diseases: predicted impacts

Climate change impacts on vector-borne diseases have previously been predicted using different biological and statistical models (see below) which usually suggest a significant increase in the areas suitable for transmission of various diseases (Table 5.1). The use of models to predict changes in vector-borne diseases in the tropics has been extensively reviewed in Chapter 1. Thus, the following section will focus on particular predictions for diseases (other than malaria) in Europe as this is the main geographic areas of interest for this thesis.

The average annual temperature in Europe increased by 0.8°C during the 20th century (Kovats *et al.* 1999) and the climate change models developed by the Hadley Centre predict average increases of 2-5°C by the end of this century (Hulme and Jenkins 1998). Although there are still considerable uncertainties in forecasting climate changes at the regional level (Kovats *et al.* 1999), there have been numerous speculations about the possible consequences to human health - with particular attention to vector-borne diseases. There are currently three endemic vector-borne diseases in Europe; leishmaniasis, Lyme disease and tick-borne encephalitis (TBE) all of which are highly focal in their distribution.

Visceral and cutaneous leishmaniasis, transmitted by phlebotomine sandflies, is distributed along the Mediterranean where it is of both veterinary and human health importance. In Italy, the proportional abundance of the two main vectors, *Phlebotomus perfiliewi* and *P. perniciosus*, and the prevalence of VL are positively associated with winter temperatures (Kuhn 1999) and global warming simulations indicated a possible expansion of the geographical range of *P. perniciosus* (Kuhn 1997). The combination of this expansion and the importation of canine leishmaniasis into currently non-endemic areas (Gothe *et al.* 1997) may introduce disease transmission at higher latitudes.

However, the limited distribution of European leishmaniasis in the arid and semi-arid environments of the Mediterranean also suggests a strong link with land cover which may be more important than that of climate (Kuhn 1997). It is therefore likely that the potential effect of climate changes on this disease in Europe may be insignificant if there are no concurrent changes in land cover.

Lyme disease and TBE are present in southern Scandinavia as well as central and eastern Europe. Using statistical and biological approaches, Randolph (2001) predicted that climate changes may cause the enzootic cycles of TBE to retreat from the southern edges of its distribution (i.e. Croatia, Hungary and Slovenia) while new foci are predicted to emerge in Scandinavia.

Another disease which has been considered in relation to climate changes in Europe is the dengue virus, transmitted by culicine mosquitoes. Serologically confirmed dengue epidemics (transmitted by *Aedes aegypti*) were observed in Greece during the 1920s (Halstead and Papaevangelou 1980) but the disease and vectors were eradicated after the Second World War, most likely because of the anti malarial DDT campaigns. In the past twenty years *Ae. albopictus*, the second most important world-wide dengue vector, has been found in Albania and Italy (Romi 1995, Romi *et al.* 1997b, Adhami and Reiter 1998), most likely imported in used car tyres from Asia (Knudsen *et al.* 1996). There has been growing concern that this mosquito could spread to the rest of Europe and that *Ae. aegypti* may also again return to the region in a similar way (Reiter 2001). The predicted temperature increases may result in higher mosquito abundances and decreased virus development rates which could cause the re-establishment of dengue transmission.

However, the use of such models and the validity of the real life examples quoted above has been fiercely debated (Haines 1998, Haines *et al.* 1998, Reiter 1998 a,b) and at present no firm link between climate changes and vector-borne disease transmission has been established. From this it is evident that new approaches to monitoring vectors and disease (especially frequent and long-term time series) are needed to properly assess the potential impact of climate changes on vector-borne diseases (Kovats *et al.* 2001). As highlighted in previous chapters, the best way to predict the future is to understand the past – i.e. a comprehensive review of historical disease and vector data such as that presented in this thesis is the strongest possible basis for future predictions.

Table 5.1 Global status of the most important vector-borne diseases.

Disease	Vector	DALYs (thousands)	Present distribution	Likely change of distribution with climate changes
Malaria	mosquito	40,213	(sub) tropics	+ + +
Filariasis	mosquito	5,549	(sub) tropics	+
Leishmaniasis	sandfly	1,810	Asia, S. Europe, Africa, S. America	++
Schistosomiasis	water snail (intermediate host)	1,713	(sub) tropics	+ +
African Trypanosomiasis	tsetse fly	1,585	Tropical Africa	+
Onchocerciasis	black fly	951	Africa, S.America	+
Dengue	mosquito	433	tropics	+ +

+ = likely, + + = very likely, + + + = highly likely

* DALY (Disability Adjusted Life Year) is defined as the number of years of life lost to the disease, weighted by the quality of life experienced by the person and the social value of that year of life (WHO 2002b)

Climate Changes and malaria: biological models

All biological models developed for malaria have been based on the basic case reproduction number R_0 (or variations thereof) or the selection of arbitrary stressors to define temperature and precipitation thresholds for transmission and geographic distribution of malaria. To date, six such models have been developed (Table 5.2).

Table 5.2. Biological models used to predict the impact of climate changes on malaria.

Model number	Model type	Outcome	Location	Reference
1	CLIMEX (suitability index)	Locations with temperature and rainfall suitable for vector presence.	Australia.	Bryan *et al.* (1996).
2	MOZ (suitability index)	Locations with temperature and rainfall suitable for parasite and vector presence.	World-wide	Martin and Lefebvre (1995).
3	R_0	The effect of temperature increases on extrinsic incubation cycle of *P. vivax* and *P. falciparum*.	No predictive map	Bradley (1993).
4	R_0	The increase in female mosquitoes, vectorial capacity and R_0 with increased temperatures.	No predictive map	Massad and Forattini (1998).
5	Vectorial capacity	Malaria epidemic potential (number of mosquitoes per person).	World-wide	Martens *et al.* (1995).
6	R_0	Malaria risk (R_0).	UK	Lindsay and Thomas (2001).

Model number 1 (Table 5.2) is based on the CLIMEX approach described in Chapter 1 and was used to predict the distribution of *An. farauti s.s*, the most important former malaria vector in Australia. The authors used field and laboratory data to define the temperature and precipitation thresholds of the vector. These thresholds were then incorporated in CLIMEX to derive climate suitability indices for locations (number not indicated) in northern Australia. Predicted current distributions corresponded well with observed ranges in northern Australia. Climate changes for 2030 were simulated by 1.5°C temperature increases and 10% summer rainfall increases. These changes were predicted to extend the range of *An. farauti s.s.* 800 km into Queensland. The paper does not provide specific information on the climate threshold selected or details on how these were selected, making it difficult to assess the validity of the approach. . However, the approach is limited in terms of its conservative estimations of the determinants of mosquito distributions (e.g. there was no attempt to correlate *An. farauti s.s.* presence with land cover, potentially the most important explanatory variable). Also, the climate

change simulations are relatively crude with no information given on the resolution of predictions.

Model 2, the MOZ (malaria potential occurrence zone) model (Martin and Lefebvre 1995) estimates potential malaria transmission (i.e. locations where climatic conditions are suitable for malaria transmission). It is based on the often used minimum and maximum temperature thresholds for the development of parasites (minimum thresholds are 19°C for *P. falciparum*, 15°C for all other malaria parasites and maximum threshold is 32°C for all parasites), originally obtained in laboratory conditions (MacDonald 1957). The presence of mosquitoes is determined by a moisture index (the ratio of rainfall: potential evapotranspiration) the lower threshold of which is set to 0.6 based on the observation that savannahs (the driest mosquito habitats) have a moisture index of 0.6-0.8. Thus, any location with a moisture index below 0.6 is considered unsuitable for mosquitoes. Reference climate data were obtained by extrapolation from about 7500 global meteorological station records and climate change scenarios generated by different GCMs. Model predictions operate at grid squares of 0.5° latitude and 0.5° longitude (approximately 62,483 points). The outcome of the model is the climatic suitability of each location each month for parasite and vector presence. For the current climate scenarios, MOZ incorrectly predicts no malaria transmission in the region between Turkey and India and transmission in former malarious areas such as Europe. The five climate change simulations predict that potentially malarious areas may increase by 274% which includes geographical spread to temperate countries of the Northern Hemisphere and to Australia. This increase is predicted to be reflected in an expansion of seasonal (1-7 months a year) transmission while the number of areas with perennial (8-12 months) transmission will decrease. MOZ is a biological model based on relatively limited data relating to parasite and vector distributions. There are several problems with this model; for instance, there is no consideration of temperature effects on vector development and survival and determining the potential distribution of anophelines by a moisture index is a too generalised approach. Additionally, the maximum tolerable temperature of 32°C for malaria parasites has not been properly documented and it is highly questionable whether this threshold is actually so low in many tropical areas. MOZ also lacks information on the local or regional variations in vector and/or parasite characteristics; indeed the paper concludes that inaccurate predictions by MOZ is due to "peculiar vector biogeography" in some areas. These

peculiarities should be taken into account to make the model more applicable and trustworthy.

The majority of malaria-climate predictions have been made using derivatives of the equation for vectorial capacity (or R_0). Model 3 demonstrates the utility of this in an approach to estimate the general effects of temperature increases on malaria transmission (*P. vivax* and *P. falciparum*). This model is based on the relationship between temperature and the extrinsic incubation cycle already described in Chapter 4 (page 165-166). No other temperature effects were included (i.e. there was no attempt to calculate separate effects on survival rate and gonotrophic cycle). The model showed that at low temperatures a 2°C increase can have a great effect on R_0, assuming that other variables in the equation (and other factors in the mosquito) are unaffected. While there are no specific predictions, this approach shows how simple calculations can be useful for the initial understanding of factors such as temperature limits to transmission, parasite development at different temperatures and the relationship between temperature and vector habits all of which are essential knowledge for developing full models of malaria transmission in relation to climate changes.

Model 4 describes the increase in malaria risk (R_0) with increasing temperatures. The model consists of two parts; firstly estimates of vector biting rate, adult female fertility, rate of development and parasite extrinsic incubation period as functions of temperatures. These were then used to calculate adult female mosquito density, R_0, force of infection (number of infective bites per person per unit time) and, lastly, the proportion of infected individuals at varying temperatures. The number of adult females and R_0 steadily rise with temperature increases whereas the proportion of malaria-infected individuals is predicted to increase steeply until it reaches a maximum value and saturates. This model is a full biological approach, however, the approach requires detailed knowledge of vector and pathogen biology some of which was not available for the model. The main limitation with this model is the inclusion of arbitrary density-dependence to limit the size of mosquito populations which is not clearly presented in the paper. Another caveat is the use of temperature-dependent biological parameters from different mosquito species in the same model (e.g. HBI derived from *An. quadrimaculatus* and adult mortality rate from *An. culicifacies*). The adult mosquito mortality rate is chosen as an indicator of the metabolic rate based on findings in *Drosophila* flies but there is no justification that this is correct for anophelines. The final model predicts R_0 as a function of mosquito abundance and vectorial capacity but this is

not a particularly useful prediction as the outcome is completely arbitrary and cannot be used for any sensible spatial predictions. It seems that this model is based on an unnecessarily complicated approach considering that the final predictions are the same as those calculated more simply in model **3**.

Model number **5** consists of several systems; the climate system, the malaria system (divided into a human subsystem and a mosquito subsystem) and the impact system. The climate system simulates temperature changes (but not concurrent changes in precipitation) at a resolution of 5° latitude by 7.5° longitude using the UK Met office GCM (a coupled ocean-atmosphere model as described above). The mosquito subsystem is based on the critical mosquito density (number of mosquitoes per person) which is essentially a re-write of the vectorial capacity equation. The revision of vectorial capacity to critical density involves the removal of unquantified parameters (such as mosquito abundance!). Ultimate 'risk' of malaria is calculated as the reciprocal of the critical density and termed the epidemic potential (EP). Predictions of future malaria risk are assessed by the ratio of future to present EP, with a high ratio indicating high malaria risk (there are no indications to what separates a high ratio from a low ratio). By the year 2100, the final model predicts a large expansion in malarious areas including parts of North America, Europe and Asia. A doubling of the malaria epidemic potential in the tropics is projected whereas in temperate regions the model predicts more than a 100-fold increase.

There are a large number of problems with this model. Firstly, the use of the simplified vectorial capacity equation creates an important caveat; namely that the outcome is a relative measure only which cannot realistically be used to estimate real risk of transmission. Critically, the calculations also do not include measures of mosquito abundance. Another important limitation of this model is the fact that differences in mosquito distributions and biology across the areas of prediction are not taken into account, hence it incorrectly predicts current transmission in North America, Europe and Japan. The climate change scenarios do not include predictions of precipitation changes which is of considerable importance because of the strong relationship between malaria vectors and rainfall. Additionally, predictions of *P. falciparum* transmission are made for Europe where this parasite can probably not be transmitted due to vector refractoriness (see Chapters 3 and 4). Finally, and most importantly, the relative degree of future malaria risk in all areas was calculated as the ratio of future EP to present EP which is inappropriate because a high ratio does not necessarily correlate with an R_0 above 1

(Rogers and Randolph 2000). Thus, the predictive map of potential malaria risk is not particularly useful.

The same model has been applied at the level of the African continent, examining the potential effect of climate changes on highland malaria (Lindsay and Martens, 1998). Here, it was concluded that the greatest potential changes can occur at high altitudes where malaria transmission currently does not take place. Because this study is more localised, the potential accuracy of the model has improved (although it has never been properly validated) however the basic approach still neglects all of the factors mentioned above. Recently, though, the model was improved by including the current distribution and biological characteristics of at least 18 malaria vectors across the world (Martens *et al.* 1999). In this version, EP was renamed 'transmission potential'. Using climate change predictions from the HADCM3 scenario, the model predicted an expansion of malaria areas to central Asia, North America and northern Europe and an additional 300 and 150 million people at risk of *P. falciparum* and *P. vivax* transmission, respectively, by the 2080s. Although an important step, the improvements for Europe are inaccurate; the model assumes that the major European vectors were *An. atroparvus* and *An. messeae* the latter of which probably never played an important role in malaria transmission. Significantly, one of the most efficient vectors *An. labranchiae* is not included in the model. Furthermore, the inclusion of a negative association between temperature and mosquito adult daily survival rate which is highlighted as an important step may be inaccurate as the relationship used has never been biologically confirmed; temperature associations are likely to be non-linear (Chapter 4).

Model 6 represents the only attempt to predict the effect of climate changes on temperate malaria using R_0. This approach has been described in detail in Chapter 4. Using temperature-dependent variables for mosquito and parasite (*P. vivax*) development, the areas of Great Britain at risk of malaria for present and future scenarios were predicted at a 10 km resolution. Climate changes were projected using the low, medium-low and medium-high UK CIP scenario, based on results from the HADCM2 models (Hulme and Jenkins 1998). The model output is the number of months of the year when $R_0 \geq 1$ (i.e. potential disease spread). For the medium-high scenario (the most likely future scenario) in the 2020s, malaria risk was predicted to be highest in the south of England and by the 2080s, most southern and central parts of the country had 4+ months with climatic conditions suitable for malaria transmission. Unlike the approach presented in this thesis, Lindsay and Thomas include the duration of

infectiousness and thus calculate an absolute measure of R_0. However, as with the other approaches discussed above, this study was mainly limited by the lack of knowledge about local *An. atroparvus* populations (e.g. the proportion of human blood meals is given as an average for all indoor-resting mosquitoes while in reality this is highly species-specific for European mosquitoes). Predictions are also somewhat held back by not including the abundance of mosquitoes (a crucial component of the calculations) which, in turn, is determined by factors such as land cover. By using the mosquito models developed previously (see Chapter 4) as a baseline for predictions of vectorial capacity and R_0 we have overcome some of the main limitations of Lindsay and Thomas' study.

Climate Changes and malaria: statistical models

As discussed in Chapter 1, statistical models require extensive datasets but, once the data have been collected, are the most simple to develop and probably also provide us with the most accurate predictions. A large number of statistical models have been developed to quantify the association between malaria or mosquitoes and environmental variables (see Chapter 1) but only two of these have been used to predict changes in malaria transmission or mosquito density as a result of climate changes.

Rogers (1996) used discriminant analysis to construct predictive distribution maps of *An. gambiae* in southern Africa. Observed mosquito distribution data (presence or absence) were obtained from a historical (1968) map which was digitised to a 1° grid resolution map. Monthly climate variables were downloaded for each 1° pixel and a discriminant analysis performed to identify which variables best predicted the distributional range of *An. gambiae*. The resulting predictive maps for current climate scenarios were relatively accurate: between 79 to 95% correct predictions. Simulated climate changes predicted from the HADCM2 predicted an extension in the geographical range of *An. gambiae* towards Namibia and northern South Africa by the 2050s. As the authors acknowledge, such predictions need to be treated with some caution. The "observed" data were derived from low resolution interpolated distributions and in any defined area, mosquitoes were assumed to be either wholly present or wholly absent. Thus, the observed – and predicted – distributions exclude local patchiness which could have been revealed by analysing individual captures as has been done in this thesis. While this approach may identify the climate limits of a geographic range, it has little power to investigate variation in abundance (and R_0) within a range.

In an attempt to provide an alternative to the biological disease models discussed above, Rogers and Randolph (2000) used the statistical approach to (1) identify the climate constraints currently operating on world-wide malaria and (2) to predict future distributions using GCM scenarios. Stepwise discriminant analysis was applied to a set of 1500 points inside and 1500 outside the global limits of *P. falciparum* distribution (scanned from a WHO map) to identify the most important climatic variables (derived from the CRU 1960-1990 mean monthly climate surfaces at 0.5° resolution) which distinguished between malaria presence and absence. These variables were then used in a maximum likelihood model to generate predictions in terms of probability of presence (0.5 was taken as the cut-off between presence and absence). Climate change scenarios were simulated using the HADCM2 model outputs. Predictions were made of the current distribution of *P. falciparum* with 78% accuracy (assessed against the original observed dataset) with false positive areas in South America, Iran, southern United States and Australia. The climate changes projected by the HADCM2 were predicted to have only a small effect on the distribution of malaria by the 2050s; currently unsuitable areas in the southern United States, Turkey, Turkmenistan, Uzbekistan, Brazil and China could become suitable for *P. falciparum* transmission. On the other hand, malaria was predicted to diminish in western India and Africa. The main limitation of this approach is the use of the coarse distribution data (most likely based on less reliable reports of transmission). Predictions are of presence or absence only (i.e. the range of malaria) rather than disease risk – unlike the approach adopted in this thesis. The validation procedure is also questionable. Clearly, the accuracy of validations depend on the size of grid cells chosen and for this purpose, 0.5° is relatively large, making the predictions apparently highly accurate. Thus, although this model may be an improvement in relation to its biological counteracts (e.g. Martens *et al.* 1995), there are still some important caveats which limits its use in making reliable predictions of future malaria transmission.

Climate changes and malaria transmission in Europe; can disease re-emerge here?

The increased concern about man-made climate changes have led to numerous media speculations about the possibility of malaria re-emergence in the UK and Europe as a whole (Box 5.1).

Box 5.1. 2001 and 2002 headlines from English national newspapers

From a scientific perspective, there are several factors which could potentially favour the re-establishment of malaria transmission in Europe with climate change. Firstly, since the early 1970s there has been an 800% increase in the number of imported malaria cases in Europe (Sabatinelli *et al.* 1999). The recent cases of imported *P. vivax* and *P. falciparum* transmitted by local vectors in central, southern and eastern Europe (e.g. Baldari *et al.* 1998, Kruger *et al.* 2001) demonstrate that malaria transmission is still feasible. In 2000, there were 15,527 imported cases of *P. vivax* and 11,807 of *P. falciparum* in Europe (WHO 2002a). We know that European mosquitoes readily transmit tropical strains of *P. vivax* (see Chapter 3) and that there is a possibility that tropical *P. falciparum* may also be able to develop in *An. plumbeus* (Marchant *et al.* 1998, Kruger *et al.* 2000). The increased temperatures predicted by climate models will speed up *Anopheles* development rates and hence also increase overall seasonal abundance. Additionally, the parasite development cycle will be reduced, increasing the probability that malaria parasites can develop successfully within the mosquito during its life span (Bradley 1993). In combination with the steady increase in the number of imported parasites, this is a scenario which could potentially cause the re-emergence of endemic malaria transmission.

On the other hand, the factors acting against the potential future transmission of malaria in Europe are more considerable. Firstly, the chance of a mosquito encountering an infected blood meal in most western European countries is exceedingly low due to the rapid detection and treatment of cases. Because of a high personal health consciousness, people in these areas will seek medical advice relatively fast when feeling ill and will therefore not act as infectious reservoirs for long. When the patient is then treated with chloroquine (the usual drug of choice) gametocytes are effectively cleared from the blood within a week (David Warhurst, personal communication). In addition to socio-economy, we know that land cover and agricultural factors are also strongly linked to the local transmission of European malaria (Chapter 2, 3 and 4). The changes in these elements during the 19th century played important roles in the natural disappearance of malaria from most of the European continent. Particularly for western Europe, the absence of any real endemic malaria transmission in spite of the increase in imported cases as well as the increases in temperature during the last 100 years indicate the significance of non-climatic factors in preventing the return of the disease to this area. However, considering the link between socio-economy and malaria, the situation may be different in the more unstable areas such as eastern Europe. Already, the re-establishment of transmission in the former Soviet Union has been linked to a reduction in medical resources and general decay of social structures (Bismil'din *et al.* 2000). Following the recent unrest in eastern Europe, health resources are scarce and thus imported infections are less likely to be treated quickly, creating a potentially larger natural reservoir of malaria parasites. In such instances, the effect of climate changes may be considerably more important. The importance of considering other factors in relation to future disease transmission can therefore not be underestimated and these factors, in turn, can only be identified by examining historical patterns in disease.

It has recently been stated (Rogers *et al.* 2002) that 'attempts to relate past trends in malaria prevalence to climate records are the critical tests of the real role of climate in the recent history of malaria and therefore its likely impact in the future'. Instead of focusing on trends, we believe that the most valuable analysis is to examine the inter-annual variability in malaria patterns. Using statistical models, the studies presented in this thesis have created a good understanding of how environmental factors affected the historical inter-annual variability of malaria as well as the current distribution of mosquito vectors in Europe. The knowledge gained from these models will be used in this chapter to predict how a variety of climate change scenarios may impact on the risk

of malaria transmission in Europe. By doing this, it is possible to assess to what extent the many speculations about the risk of malaria re-emergence in Europe are supported by the evidence.

Aims and Objectives

The principal aim of this study is to predict the effect of climate changes on the risk of malaria re-emergence in Europe.

The specific objectives are:

1. To estimate the proportional impact on malaria risk in the UK as the result of the climate changes expected during the next 80 years (according to the HADCM3 SRES models), on the basis of the statistically proven climatic effects on inter-annual variability in malaria death rates across the UK during the 19th and 20th century (see Chapter 2).
2. To estimate the proportional impact on malaria risk in Europe as the result of the climate changes expected during the next 80 years, on the basis of the statistically proven climate effects on inter-annual variability in malaria case rates across Europe during the 20th century (see Chapter 3).
3. To estimate the impact on vector distributions, relative vectorial capacity and the absolute risk of malaria (R_0) across Europe as the result of the climate changes expected during the next 80 years, on the basis of:
    - the statistically proven climatic effects on the current spatial distributions of vectors (see Chapter 4).
    - the average daily survival rate and the human blood index for each malaria vector species in Europe (derived from reported field observations).
    - the reported experimentally determined associations between temperature and other key determinants of vectorial capacity (the extrinsic incubation period and the gonotrophic cycle for each vector species.
    - the observed way that national socio-economic indicators in Europe appear to affect the relationship between these derived national measurements of relative vectorial capacity and the reported ratio of secondary malaria cases : imported malaria cases (i.e. R_0).

Methods

Climate change scenarios

The HADCM3 SRES A2 and B2 climate change scenarios were supplied in a grid with a resolution of 2.5° by 3.75°. Data consisted of daily and monthly measures of minimum, maximum and average temperature and precipitation. Climate variables were downloaded for 2010-2039, 2040-2069 and 2070-2099 for both scenarios. From these, daily and monthly data for the 2020s (the average climate during 2010-2039), the 2050s (average of 2040-2069) and the 2080s (average of 2070-2099) were calculated. Next, from daily measures of precipitation, the monthly minimum, maximum and average wet day frequency was calculated (a wet day was defined as any day with a rainfall of above 0 mm, Matthew Livermore personal communication). From daily measures of minimum and maximum temperatures, the monthly minimum, maximum and average diurnal temperature range was calculated (diurnal temperature range was defined as the difference between daily maximum and minimum temperatures). All monthly temperature measures were converted to annual averages and precipitation to annual total in the selected years as described in Chapter 2 (i.e. the annual minimum temperature represents the average of the coldest month of that year). Thus, for each year there were 10 climate variables of interest (Table 5.3). The climate predictions from the A2 and B2 scenarios for the study area were compared and were found to be only slightly different. However, because A2 showed marginally greater changes (i.e. the worst case scenario), this scenario was selected for the predictions. The A2 climate projections predict an average temperature increase of 2-5°C and a change in average annual precipitation of –0.2 to 0.5 mm per day throughout Europe by the 2080s (Hadley Centre 2002b, Appendix 5.1)

Predictions of cloud cover were not available and therefore this variable remained constant in the predictions of mosquito distributions. Land cover types at 1 km resolution also remained constant for the prediction scenarios.

Using the same approach as described in Chapter 4, the climate variables were extracted to a grid with a resolution of 0.25°. These were used as the initial conditions for predictions of mosquito distributions, vectorial capacity and disease risk.

Table 5.3. Climate variables obtained from the HADCM3 A2 SRES model (ranges throughout the study area, i.e. including North Africa).

Variable	Range 2020	Range 2050	Range 2080
Minimum average temperature (° C)	-19.7 - 25.5	-18.3 – 28	-17.7 – 28.1
Maximum average temperature (° C)	5.5 – 47.6	6.8 – 50	7.5 – 50
Mean average temperature (° C)	-6.1 – 33.6	-4.5 – 36.3	-3.9 – 37.4
Total precipitation (mm)	1 – 3385	3 – 3528	3 – 3753
Minimum wet day frequency	0 – 27	0 – 27	0 – 28
Maximum wet day frequency	0 – 31	0 – 31	0 – 31
Average wet day frequency	0 – 28	0 – 28	0 – 29
Minimum diurnal temperature range (° C)	3.7 – 22	4.1 – 19.3	3.1 – 19.1
Maximum diurnal temperature range (° C)	9 – 24.2	9.2 – 22.3	9.3 – 21.8
Average diurnal temperature range (° C)	4.2 – 23	4.4 – 20.8	5.8 – 17.2

Measures of cloud cover were not included in the predictions and therefore had the same range as described in Chapter 4.

Malaria in the UK

Average temperatures in the UK during 1840 to 1910 varied annually across a 2°C range. Using the inter-annual variability model developed for ague deaths in the UK (Chapter 2), the number of deaths was predicted during 1840-1910 for 1°C temperature increases and decreases to illustrate the general temperature sensitivity of malaria during this period. The same approach was used to estimate the proportional impact of the 2.5°C increase predicted to occur by the 2050s. This was simply done simulating the effect of an increase and decrease in average temperature (the only significant temperature variable in the final model) in each county in each year by 1°C on the total number of malaria deaths per year per county using Equation 2.1 (page 47). From this the predicted national total of ague deaths in the UK was calculated and the predicted temporal trend plotted for comparison with the observed trend.

Note that as in Chapter 2 simulations do not take into account the cumulative effect which would have resulted in steadily increasing rates due to the absence in the model of density-dependent variables such as herd immunity.

Malaria in Europe

The average temperature in Europe varied across a range of 3°C from 1900 to 1975. The sensitivity of malaria to this range was predicted using the inter-annual malaria

variability model developed in Chapter 3. To correspond with the projected climate change scenarios for Europe in the 2080s, predictions were also made for 2°C and 5°C temperature increases. Again this was done by simulating the effect of increases and decreases in temperatures in each country in each year on the number of malaria cases per country per year using Equation 3.1 (page 106). In order to show the sensitivity of these predictions, the value of the temporal trend (i.e. year) was increased and decreased by 5%. This was simply done by increasing/decreasing the year constant (see Box 3,1) by 5%. The interaction between year and ddt used original (i.e. unchanged) values of year. Because of the unavailability of data points in many European countries, the analysis of the effects of climate changes focused on four specific countries: Finland, Italy, Spain and Sweden. These countries were selected because of the large number of data points available compared to the average number for other localities and because they represent two countries with a natural decline of malaria (Finland and Sweden) as well as two countries where malaria was eradicated using DDT (Italy and Spain).

Mosquitoes, relative vectorial capacity and disease risk (R_0)

The effect of climate changes on the distribution of five European mosquitoes (*An. atroparvus*, *An. labranchiae*, *An. messeae*, *An. sacharovi* and *An. superpictus*) was predicted using the models described in Chapter 4. For each 0.25 ° grid cell containing HADCM3 projected climate, the probability of mosquito presence was calculated using Equation 4.1 (page 161). These predictions were made for each of the five mosquito species during the 2020s, 2050s and 2080s.

The relative vectorial capacity for each of the five mosquito species in each 0.25 ° grid cell has previously been calculated in Chapter 4 (Equation 4.4 page 167). Using the probability of mosquito presence and the predicted (HADCM3) average maximum temperature for each grid cell, the relative vectorial capacity of each of the five mosquitoes was calculated for each climate change scenario.

In order to predict disease risk, a total relative vectorial capacity (RVC) was calculated for each 0.25° grid cell by adding up the RVC measure for all mosquito species present in that particular cell. This was carried out for the whole of Europe for all three climate change scenarios (2020s, 2050s and 2080s). The country of origin of each grid cell was determined by linking the 0.25° map with a world map (see Chapter 4) and a measure of disease risk was then calculated for the cell by:

R_0 = RVC * 'constant'

where 'constant' refers to the country-specific constant calculated in Chapter 4. This constant is determined by GDP and life expectancy of the particular country as well as the country-independent variables such as the relationship between probability of presence and mosquito presence and the probability that a mosquito acquires infection when biting a malaria infected human (i.e. c in the vectorial capacity).

Using the vectorial capacity generated for the 2020s, 2050s and the 2080s, R_0 was calculated for these climate change scenarios. As already described in Chapter 4, the impact of errors was simulated by varying the daily survival rate parameter (p) and predicting R_0 for the upper and lower limits of p quoted in Table 4.8. Projections of GDP and life expectancy were not included in any of the predictive maps. Although GDP projections do exist (IPCC 2000), they were not used for this study as they only extend to 2020 – far too short for the time frame addressed here.

Therefore, this method accounts for the effect of predicted temperature and precipitation changes on both parasite intrinsic incubation period and vector abundance and assumes that the magnitude of socio-economic effects on R_0 will continue to be determined by GDP and life expectancy, as defined above.

All prediction calculations were made in Excel '97 in the 0.25° by 0.25° grid of Europe used previously. This grid was converted for use in the Geographical Information System ArcView 3.1 in which all predictive maps were constructed.

Results

Inter-annual variability in malaria death rates in the UK

Simulating a 1°C temperature increase (above average) during 1840-1910 led to a proportional increase of 8.2% in the number of malaria deaths while a simulated 1°C decrease in temperatures led to a 6.5% decrease in death rates (Table 5.4, Figure 5.4). A simulated increase in temperature of 2.5°C led to a proportional increase in malaria death rate of 14.5% (Figure 5.4). Thus, the national risk of malaria in the UK appears to be marginally more sensitive to temperature increases than temperature decreases. But the statistical model suggests that even a 2.5°C increase in temperature would be responsible for only a relatively minor increase in risk at the national level.

Table 5.4. Predicted ague deaths for varying temperatures in England and Wales during 1840-1910.

Scenario	Predicted cases (95% CI)	% Difference (95% CI)
Observed	8209	-
1°C increase	8882 (8808,8964)	8.2 (7.3, 9.2)
2.5°C increase	9399 (9293,9563)	14.5 (13.2,16.5)
1°C decrease	7675 (7519,7864)	-6.5 (-8.4,-4.2)

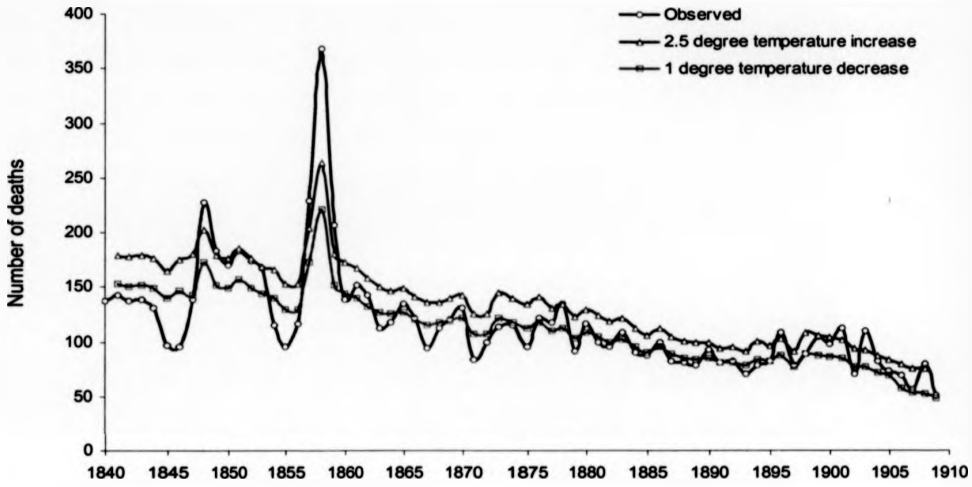

Figure 5.4. Simulated effect of temperature changes on ague deaths in England and Wales during 1840 to 1910.

Inter-annual variability in European malaria incidence

Simulating 1.5°C temperature increases (above average) during 1900 to 1975 in Europe caused a proportional increase of 6.6% in the number of malaria cases while a simulated 1.5°C decrease in temperatures led to a 8.6% decrease in death rates (Table 5.5). Simulated increases in temperatures of 2°C and 5°C led to a proportional increase in malaria death rate of 11.3 and 24.9%, respectively. These results suggest that the risk of malaria in Europe – unlike that in England – was more sensitive to temperature decreases than increases. The model indicates that even the simulated 5°C temperature increases would have caused only a small increase in malaria risk at the continental level.

Table 5.5. Predicted malaria cases for varying temperatures throughout Europe during 1900 to 1975.

Scenario	Number of cases (95% CI)	% Difference (95 % CI)
Predicted (observed conditions)	20,974,539	-
5°C increase	26,197,199 (24,833,854 – 27,791,264)	24.9 (18.4,32.5)
2°C increase	23,344,661 (22,820,298 – 23,596,356)	11.3 (8.8,12.5)
1.5°C increase	22,358,858 (21,897,419 – 22,421,782)	6.6 (4.4,6.9)
1.5°C decrease	19,170,728 (18,688,314 – 19,737,041)	-8.6 (-10.9,-5.9)

At the country level, it seems that the northern countries (Finland and Sweden) were more sensitive to global warming than the southern areas (Italy and Spain) - i.e. the confidence intervals of predictions do not overlap as seen in Appendix 5.2. Temperature increases of 1.5-5°C caused between 13.2- 29.1% increases in malaria cases in Finland and Sweden compared to 5.8-27.5% increases in Italy and Spain (Table 5.6, Figure 5.5-5.8). Thus, temperature thresholds were most likely more important in determining patterns of malaria transmission in northern than in southern regions. This may be due to the different temperature requirements of *P. vivax* and *P. falciparum* as the model does not distinguish between the two parasites.

Table 5.6. Predicted malaria deaths for varying temperatures in four European countries during 1900 to 1975.

Scenario	Finland	Italy	Spain	Sweden
Observed	7512	8,348,636	2,506,691	1545
5°C increase	9697 (29.1)	10,644,510 (27.5)	3,160,937 (26.1)	1991 (28.9)
2°C increase	9202 (22.5)	9,342,123 (11.9)	2,799,973 (11.7)	1809 (17.1)
1.5°C increase	8766 (16.7)	8,832,856 (5.8)	2,732,293 (9)	1748 (13.2)
1.5°C decrease	6392 (-14.9)	6,161,293 (-26.2)	1,957,725 (-21.9)	1359 (-12.0)

Values refer to the number of malaria cases predicted by the different scenarios and numbers in brackets show the percentage difference from the observed number of cases.

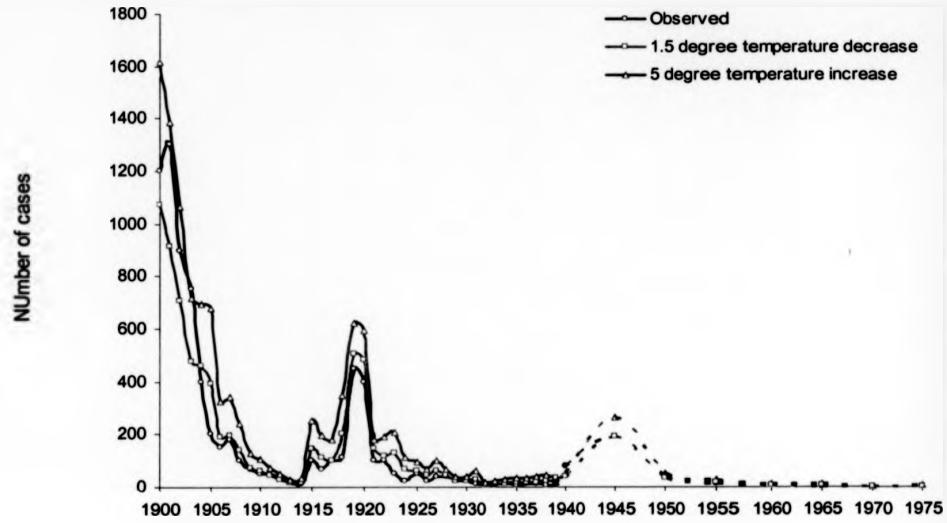

Figure 5.5. Effect of temperature changes on malaria cases in Finland during 1900 to 1975. Dotted lines indicate that annual data were only available at 5-year intervals.

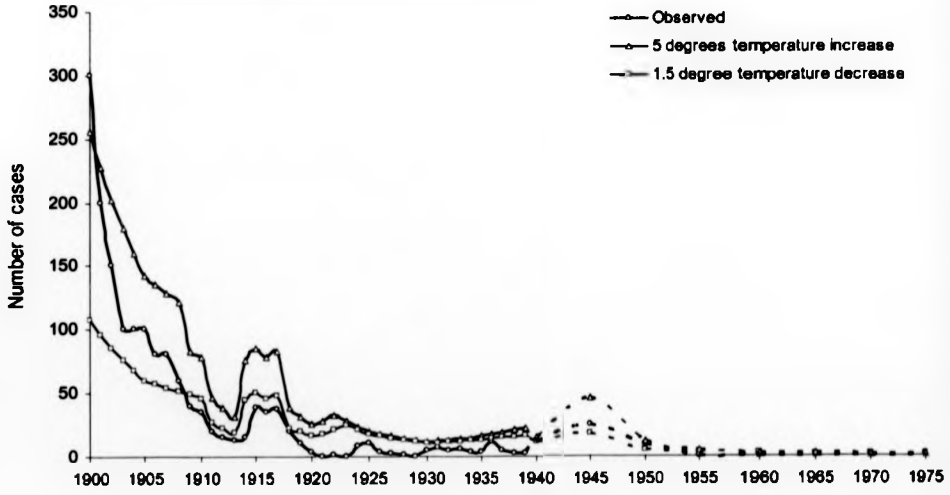

Figure 5.6. Effect of temperature changes on malaria cases in Sweden during 1900 to 1975. Dotted lines indicate that annual data were only available at 5-year intervals.

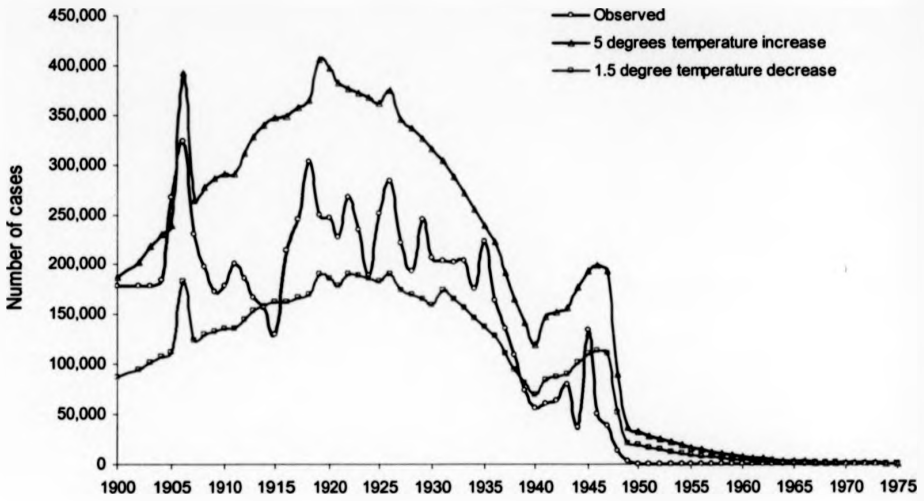

Figure 5.7. Effect of temperature changes on malaria cases in Italy during 1900 to 1975.

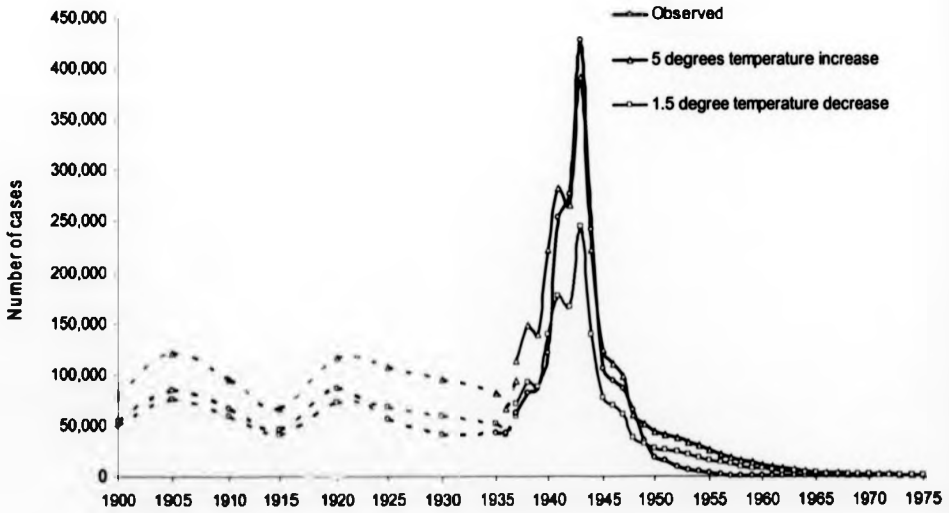

Figure 5.8. Effect of temperature changes on malaria cases in Spain during 1900 to 1975. Dotted lines indicate that annual data were only available at 5-year intervals.

Sensitivity of predictions in Europe

The sensitivity of predictions of the effect of climate changes on malaria in Italy and Sweden was assessed by increasing and decreasing the temporal trend by 5%. The results are shown in Table 5.7 and Figures 5.9 and 5.10. These indicate that a relatively small fluctuation of 5% in the temporal trend (i.e. a signficant variable in the predictor equation) can cause changes (or errors) of between –7.1% and 7.9% in the predictions of malaria cases. Errors of such magnitude are particularly significant in areas with low malaria prevalence, such as most of northern Europe.

Table 5.7. Predicted ague deaths for varying temperatures in four European countries during 1900 to 1975.

Scenario	Italy Predicted	Italy sensitivity range *	Sweden predicted	Sweden sensitivity range *
5°C increase	10,644,510	10,048,417 – 11,272,536 (-5.6 – 5.9)	1991	1909 – 2110 (-4.1 – 6)
2°C increase	9,342,113	8,846,981 – 9,874,613 (-5.3 – 5.7)	1809	1736 – 1932 (-4.0 – 6.8)
1.5°C increase	8,832,856	8,205,723 – 9,530,652 (-7.1 – 7.9)	1748	1646 – 1854 (-5.8 – 6.1)
1.5°C decrease	6,161,293	5,779,293 – 6,598,745 (-6.2 – 7.1)	1359	1269 – 1460 (-6.6 – 7.4)

The number of malaria cases predicted using a 5% decrease (lower limit) and 5% increase (upper limit) in the temporal trend. Values in brackets are the percentage difference from the number predicted using the original temporal trend.

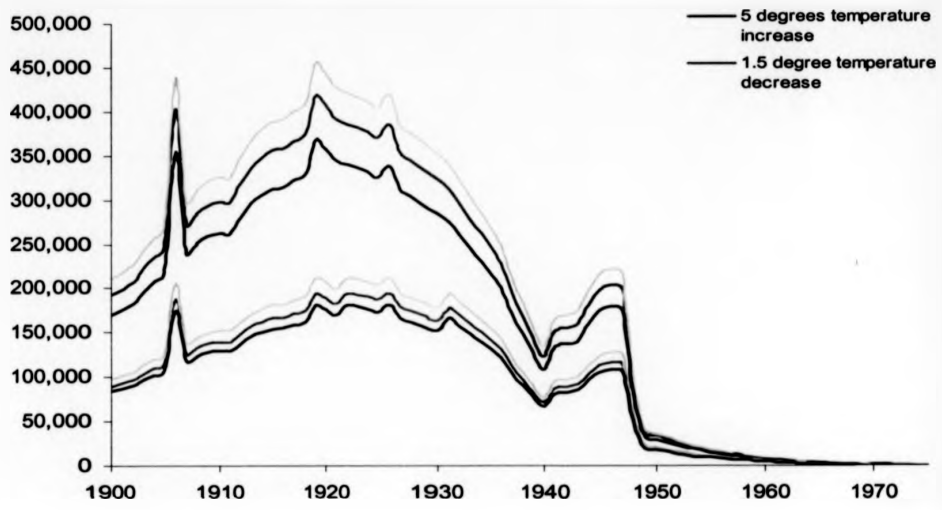

Figure 5.9. Sensitivity of predicted effects of temperature changes on malaria in Italy during 1900 to 1975. Upper limit indicates predictions for an increase of 5% in the temporal trend while lower limits are predictions using a 5% decrease in the temporal trend.

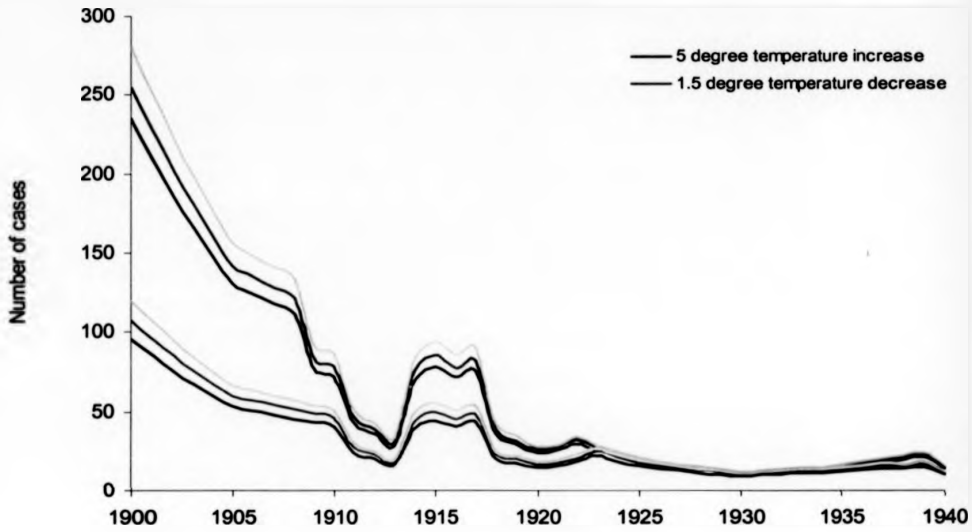

Figure 5.10. Sensitivity of predicted effects of temperature changes on malaria in Sweden during 1900 to 1975. Upper limit indicates predictions for an increase of 5% in the temporal trend while lower limits are predictions using a 5% decrease in the temporal trend. Predictions have not been made for the time interval without annual data.

Mosquito distributions in Europe

The predicted distribution of *An. atroparvus* for the three climate change scenarios (2020s, 2050s and 2080s) in comparison to the current predicted distribution is shown in Figure 5.11. In the 2020s, this mosquito is predicted to retreat from areas in Spain and Portugal as temperatures become too hot (the optimum average temperature for *An. atroparvus* is 17.9°C). Its distribution is predicted to spread further into Russia and the overall probability of presence in the UK, Germany, France and Denmark increases from between 0.48-0.8 to 0.64-1. During the 2050s, *An. atroparvus* is predicted to increase in probability of presence (and therefore presumably abundance) throughout its current distribution band in the UK, Germany, France, Denmark, the Baltic states and southern Sweden so that by the 2080s it is common (probability of presence 0.8-1) in most of these areas.

An. messeae is currently predicted to be present in Scandinavia and north-west Europe, including the Baltic states and Russia (Fig 5.12a). By the 2020s, its distributional range is not predicted to change much although the probability of presence in the mentioned areas has increased (Fig 5.12b). This pattern is repeated during the 2050s and 2080s with increases in abundance throughout large areas of Scandinavia and west Europe, resulting in a probability of presence between 0.64 and 1 in most of these places. The southern limit of *An. messeae* does not seem to be affected by climate changes and only a limited spread towards Russia is observed.

The predicted current distribution of *An. labranchiae* is restricted to Italy, North Africa and isolated areas in Spain and the Balkans (Fig 5.13a). With the projected climate changes over the next 80 years, this distribution is not predicted to expand. However, the probability of presence (i.e. abundance) increases so that by the end of the century, there is an almost 100% chance of this mosquito being present in most of Italy and some areas of Spain and the Balkans (Fig. 5.13).

The predicted distribution of *An. sacharovi* currently extends to south-east Europe, from eastern Spain along the Alps to the Balkans, Turkey, and the Black Sea (Fig. 5.14a). With the projected climate changes for the 2020s, its range is predicted to extend slightly northwards, covering larger areas of Eastern and central Europe (Fig 5.14b). This distribution is further expanded until, by the 2080s, *An. sacharovi* is predicted to be present in high abundances throughout Turkey, most of the Balkans, Italy, Austria, Switzerland, eastern France and Spain as well as North Africa (Figs. 5.14c and d).

A similar scenario is observed for *An. superpictus*, currently predicted to be present around the Alps, through to the Balkan states, into Turkey and northern Africa (Fig 5.15a). The range of this mosquito is predicted to expand with climate changes, creating a larger band of presence across the Alps and in the Balkan states (Fig. 5.15). By the 2050s, *An. superpictus* is predicted to be abundant in most of the Balkans and northern Turkey as well as in isolated areas of Spain. In the 2080s the pattern of distribution is further expanded and the probability of presence in all areas is now 0.64-1 compared to relatively lower values in the current scenario.

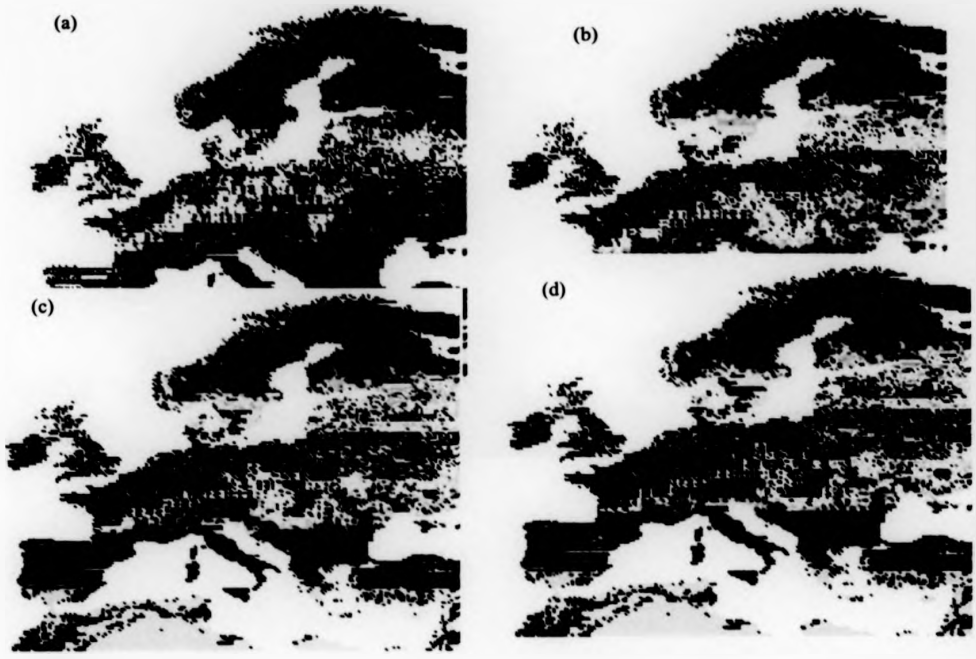

Figure 5.11. Predicted distribution of *An. atroparvus* in (a) present day Europe, (b) 2020s, (c) 2050s and (d) 2080s.

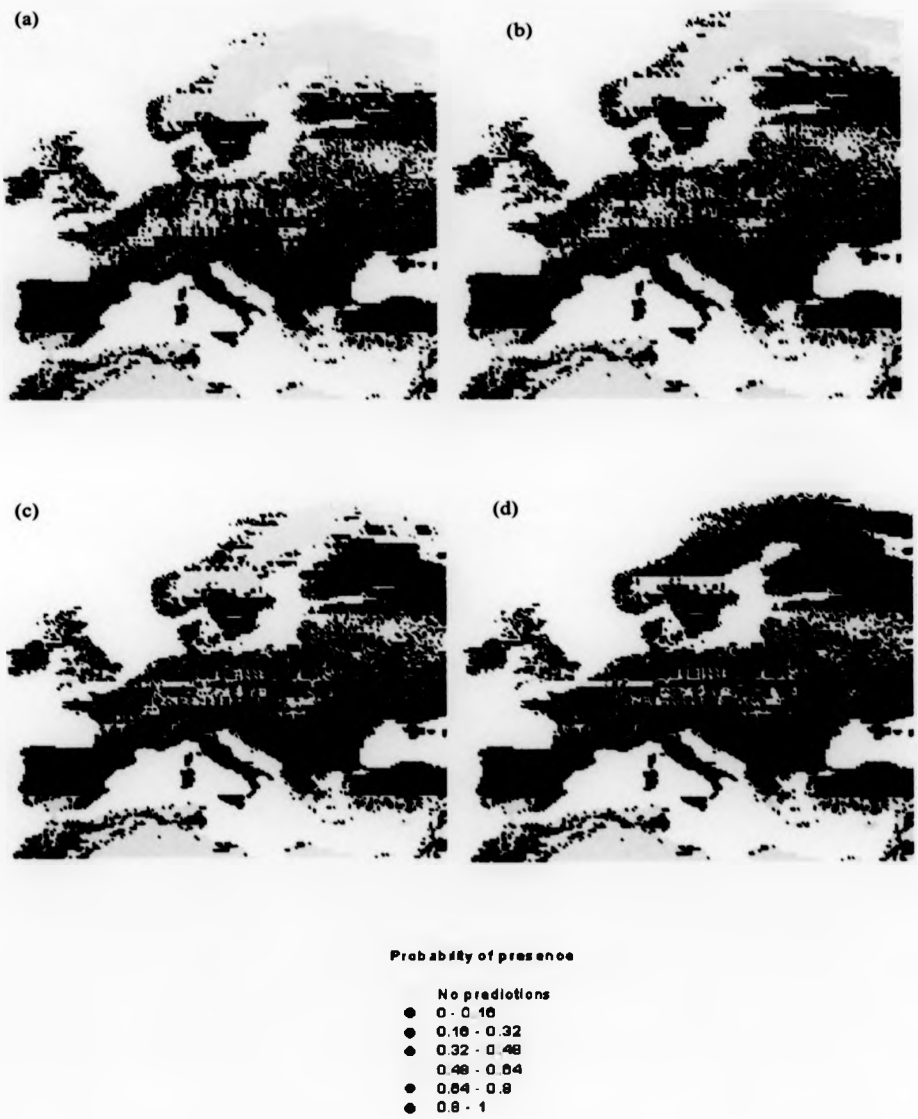

Figure 5.12. Predicted distribution of *An. messeae* in (a) present day Europe, (b) 2020s, (c) 2050s and (d) 2080s.

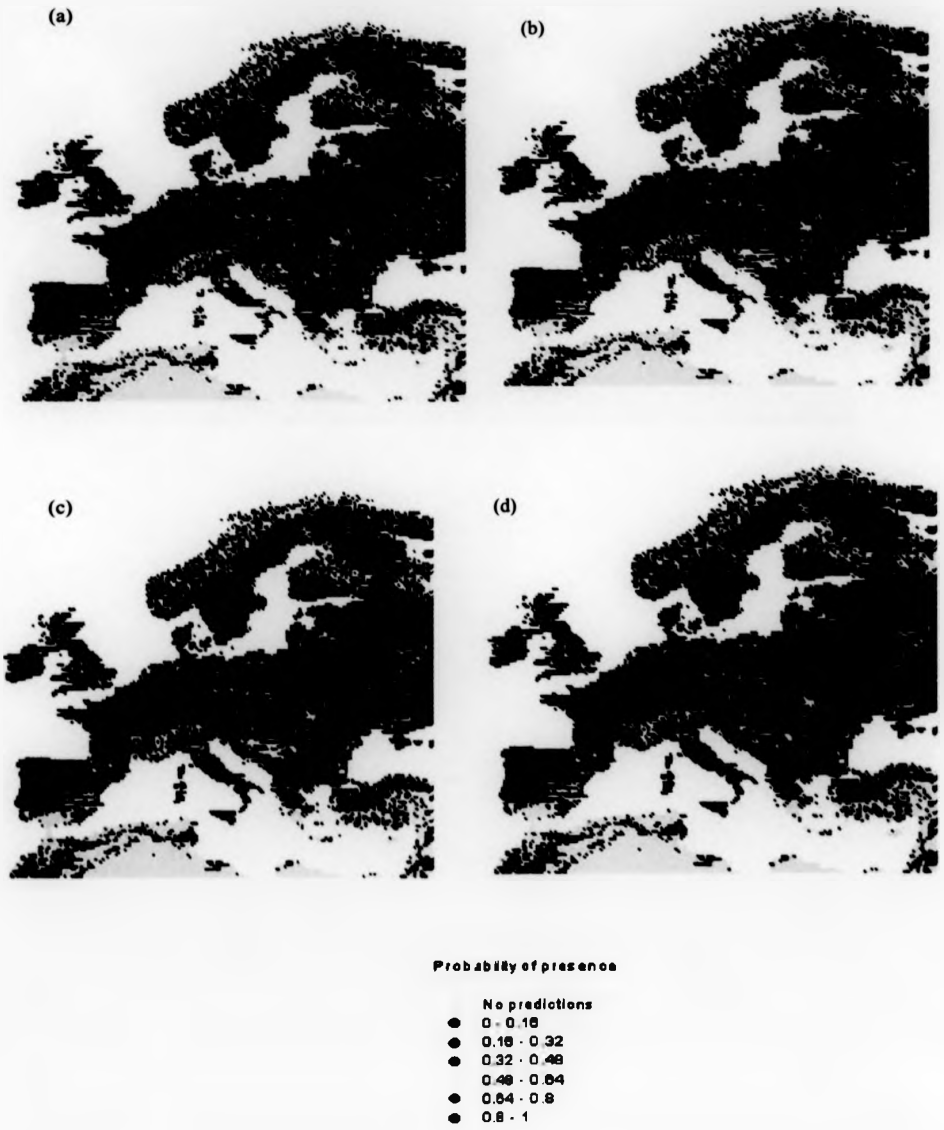

Figure 5.13. Predicted distribution of *An. labranchiae* in (a) present day Europe, (b) 2020s, (c) 2050s and (d) 2080s.

Figure 5.14. Predicted distribution of *An. sacharovi* in (a) present day Europe, (b) 2020s, (c) 2050s and (d) 2080s.

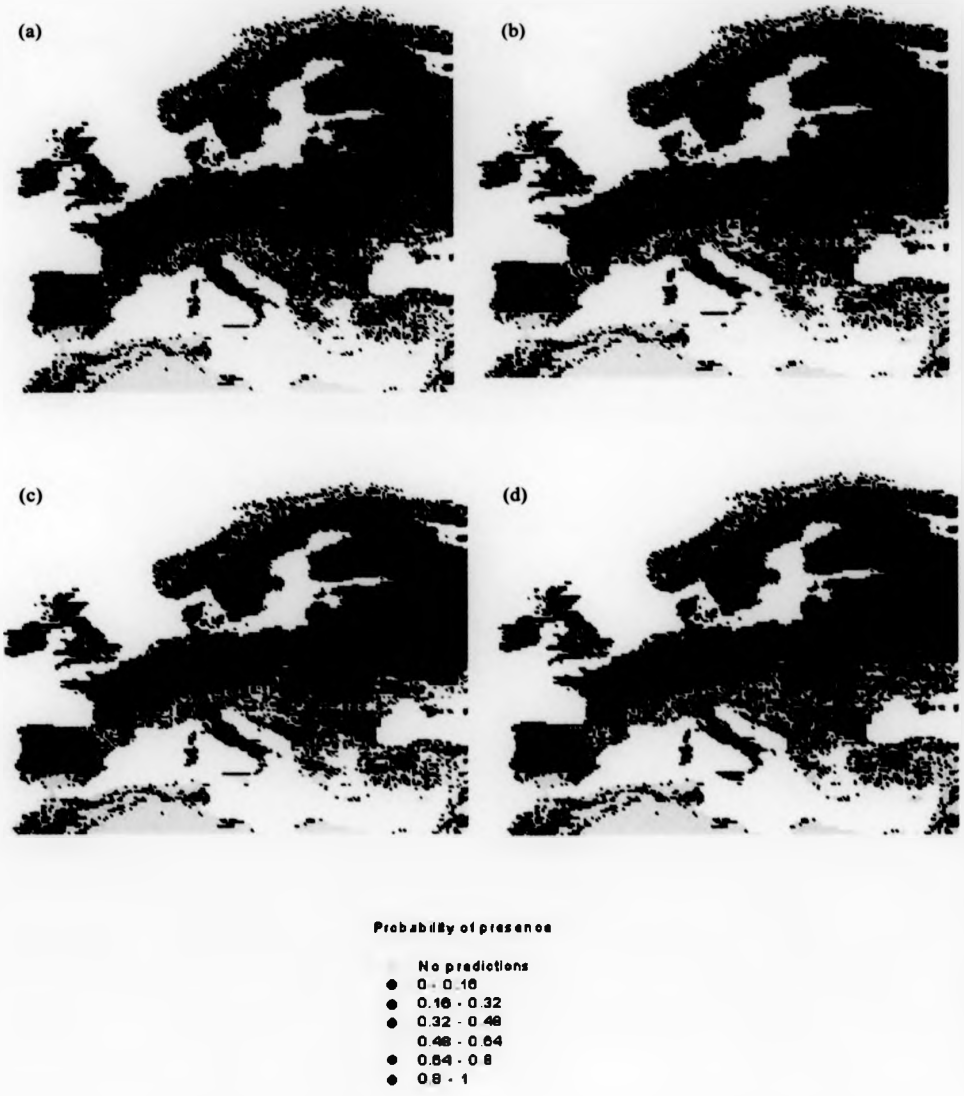

Figure 5.15. Predicted distribution of *An. superpictus* in (a) present day Europe, (b) 2020s, (c) 2050s and (d) 2080s.

Relative vectorial capacity of European mosquitoes

The relative vectorial capacity calculated in Chapter 4 for the five mosquitoes at the present climate scenario ranged from 0 to 0.647. The highest relative vectorial capacity was calculated for *An. labranchiae* and the lowest for *An. messeae*. Of course these measurements do not take into account the difference in vector competence (i.e. variations in the 'b' and 'c' parameters in the vectorial capacity equation) as reliable measurements were not available.

By applying the climate-driven measurements of relative vectorial capacity to the predicted climate change scenarios, it is predicted that vectorial capacity increases significantly for some mosquitoes (Table 5.8). The spatial predictions of relative vectorial capacity for each species is shown in Figures 5.16 – 5.20. Note that the scales are very different in the five figures.

Table 5.8. Predicted relative vectorial capacity of five malaria vectors throughout Europe in the future.

Species	Relative vectorial capacity range present day	Relative vectorial capacity range 2020s	Relative vectorial capacity range 2050s	Relative vectorial capacity range 2080s
An. atroparvus	0 – 0.175	0 – 0.112	0 – 0.142	0 – 0.161
An. messeae	0 – 0.005	0 – 0.006	0 – 0.006	0 – 0.007
An. labranchiae	0 – 0.647	0 – 0.735	0 – 0.887	0 – 0.920
An. sacharovi	0 – 0.053	0 – 0.064	0 – 0.078	0 – 0.086
An. superpictus	0 – 0.191	0 – 0.220	0 – 0.271	0 – 0.282

At present and for the next 20-40 years, *An. messeae* is not predicted to be an efficient vector of European malaria. By the 2050s, it is predicted to have a relative vectorial capacity of around 0.001 in small areas of Russia and France (Fig 5.16c). The extent of these areas with a relative vectorial capacity of > 0 increases by the 2080s when the average relative vectorial capacity has also increased to between 0.001 and 0.003 (Fig 5.16d). Overall, this mosquito is probably never likely to have a large impact on malaria transmission in Europe.

The effects of climate changes on the relative vectorial capacity of *An. sacharovi* are significant only in north-eastern Turkey and North Africa. Even by the 2080s, its role as a potential malaria vector in the main parts of Europe is limited (Fig. 5.17). This is surprising as historically it was suspected to have been one of the most important

vectors, however the model predictions are, as already discussed in Chapter 4, driven by the low human blood index and survival rate.

An. atroparvus is currently predicted to be most efficient as a vector in southern Spain and Portugal (Fig. 5.18a). The efficiency of this mosquito as a malaria vector is expected to decrease by the 2020s where areas of southern Europe become less suitable for *An. atroparvus* due to the hot temperatures in the Iberian peninsula. However, by the 2050s, its relative vectorial capacity has increased to between 0.04-0.12 in areas of western and central Europe. By the 2080s, *An. atroparvus* has a relative vectorial capacity of above 0.04 and even 0.08 in large areas of England and Ireland, France, Poland and Russia (Fig 5.18). It seems that *An. atroparvus* may have a future role of malaria transmission in western Europe, however we must note that it is currently predicted to be a potentially efficient vector in Spain and Portugal where there are no reported cases of indigenous malaria.

By comparison, *An. superpictus* could become a marginally more wide-spread vector. In the 2050s the relative vectorial capacity of this mosquito is predicted to be 0.06-0.24 in southern Spain, Italy and Greece and large areas of northern Turkey and North Africa (Fig 5.19c). In addition to these areas, by the 2080s, there are also locations in the Balkans where conditions may allow for malaria transmission by *An. superpictus* (Fig 5.19d).

The predictions for *An. labranchiae* show a slightly worrying pattern. By the 2020s, this mosquito is predicted to be an efficient vector in southern Spain, central and southern Italy, a small area in the Balkans as well as North Africa with a relative vectorial capacity ranging from 0.15 to 0.45 in most areas (Fig 5.20). By the 2080s, the relative vectorial capacity of *An. labranchiae* in most of southern Italy reaches 0.6-0.75 and there are larger areas in the Balkans where this mosquito could potentially be a vector (Fig 5.20d). Hence, this species could potentially become the most dangerous of malaria vectors in Europe.

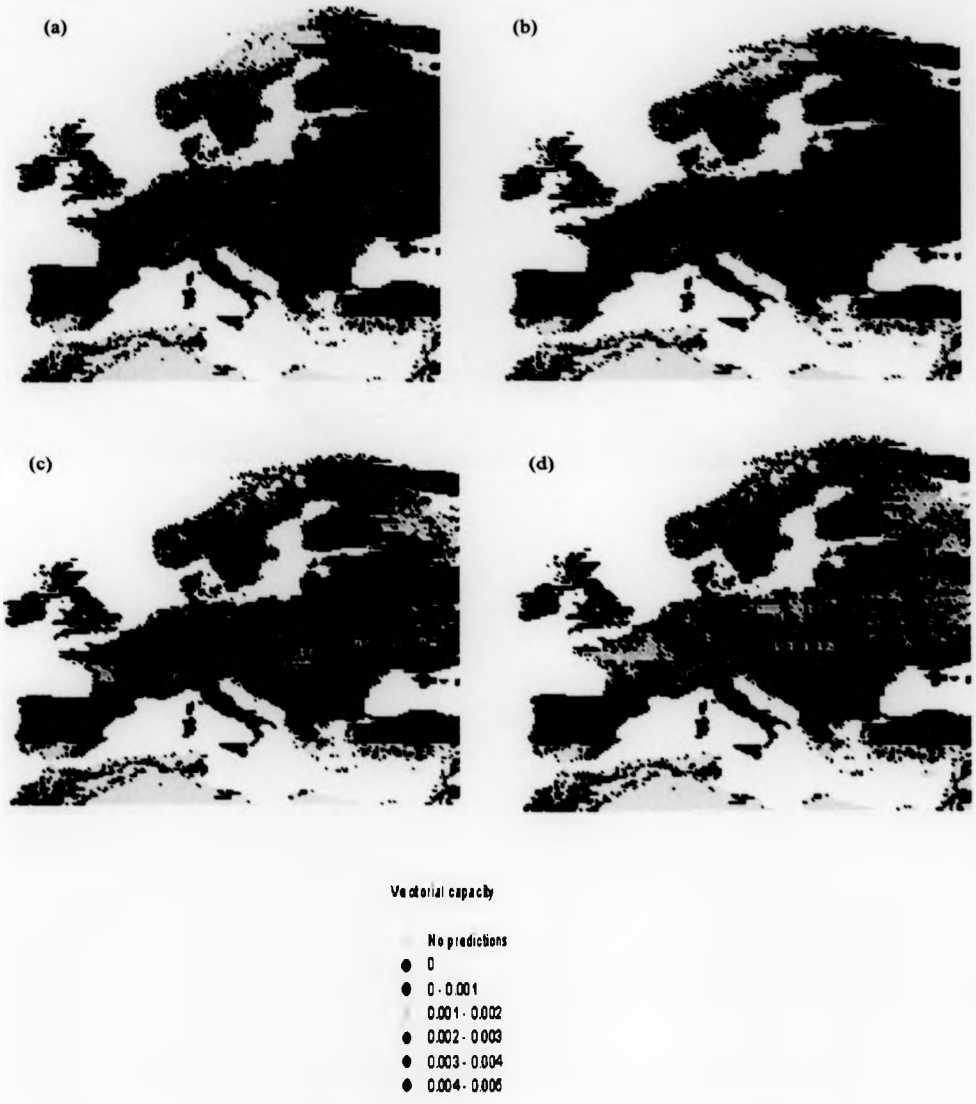

Figure 5.16. Predicted relative vectorial capacity of *An. messeae* in (a) present day Europe, (b) 2020s, (c) 2050s and (d) 2080s.

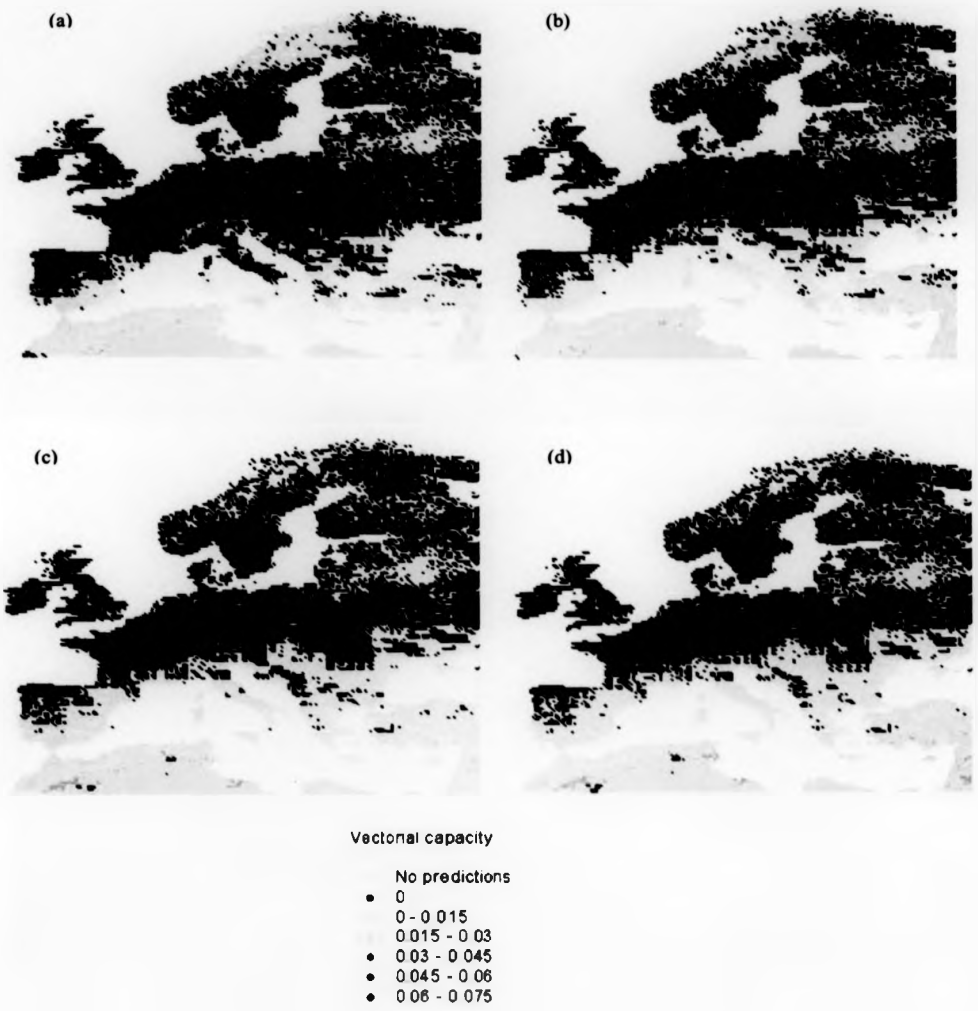

Figure 5.17. Predicted relative vectorial capacity of *An. sacharovi* in (a) present day Europe, (b) 2020s, (c) 2050s and (d) 2080s.

Figure 5.18. Predicted relative vectorial capacity of *An. atroparvus* in (a) present day Europe, (b) 2020s, (c) 2050s and (d) 2080s.

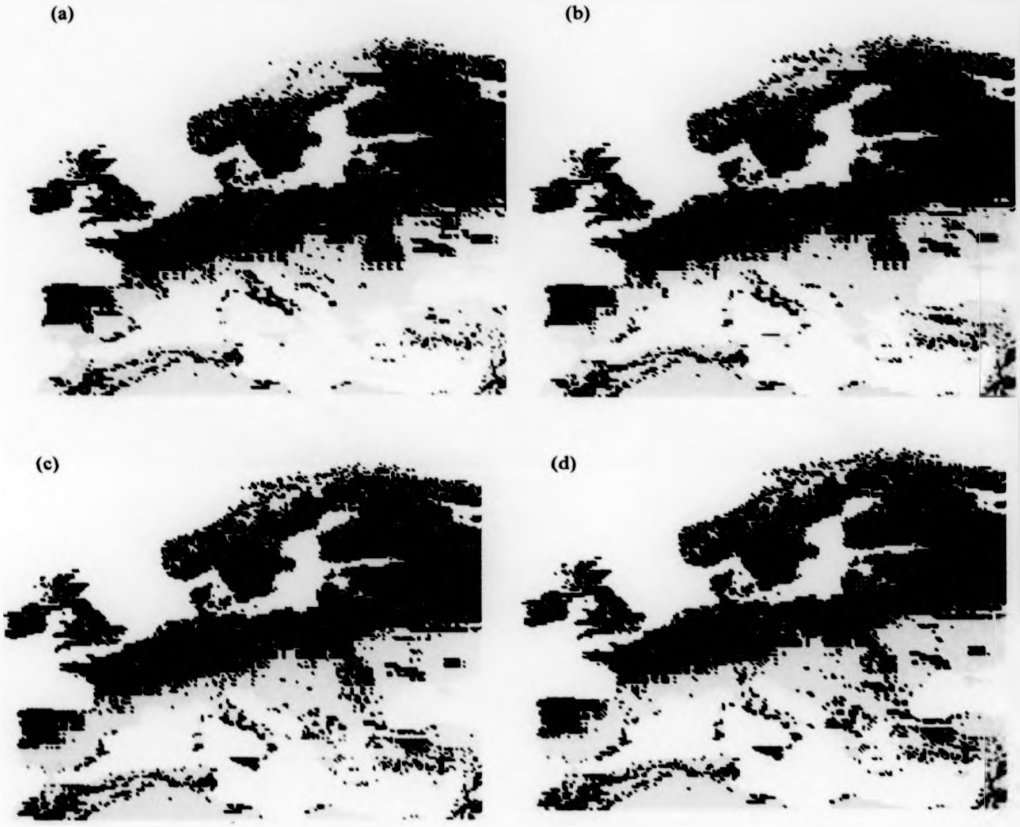

Figure 5.19. Predicted relative vectorial capacity of *An. superpictus* in (a) present day Europe, (b) 2020s, (c) 2050s and (d) 2080s

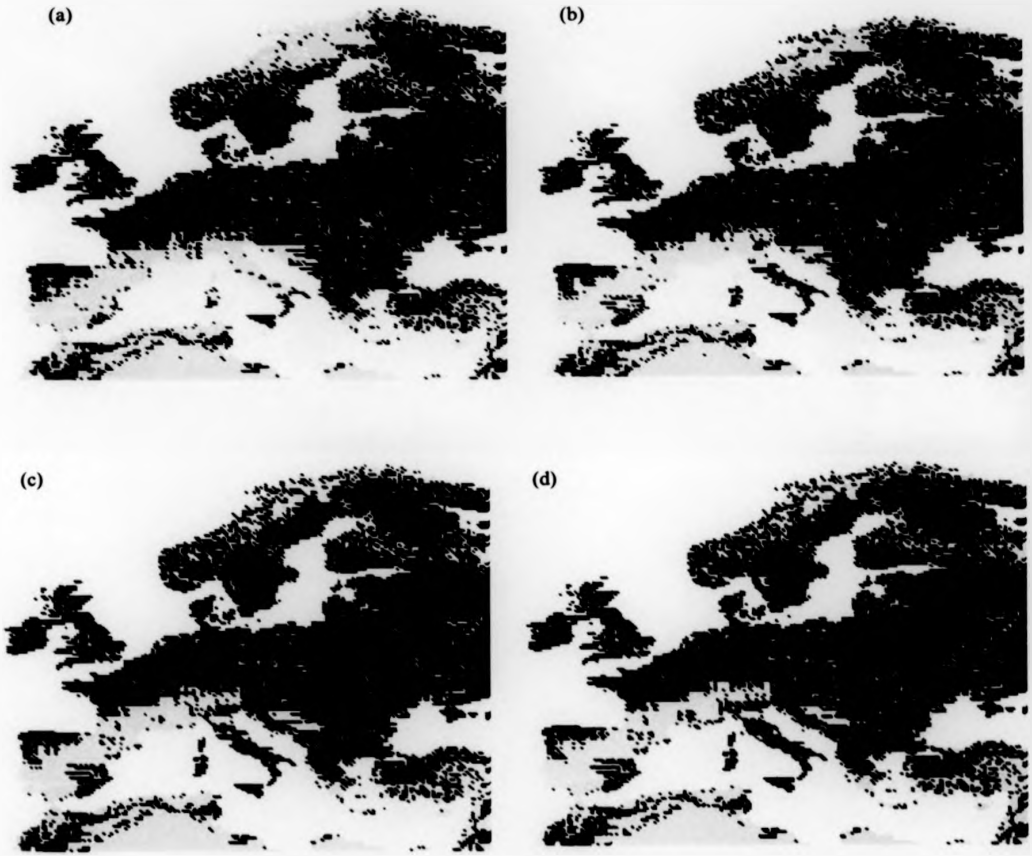

Figure 5.20. Predicted relative vectorial capacity of *An. labranchiae* in (a) present day Europe, (b) 2020s, (c) 2050s and (d) 2080s.

Absolute measures of malaria risk; R_0

The predictions of malaria risk in Europe for the current climate scenario show an R_0 above 1 in areas of Eastern Europe and the Balkans (Fig 5.21a). The changes in climate projected to occur by the 2020s are predicted to increase the risk of malaria in Eastern Europe, with larger areas now showing an $R_0 > 1$ (Fig. 5.21b). By the 2050s, extensive areas of Romania and isolated locations in Croatia and Bosnia have a disease risk of between 4 and 10 and areas with an $R_0 > 1$ have now spread further into eastern Europe, including Poland, Hungary, Belarus and Ukraine (Fig. 5.21c). In the 2080s, the risk of malaria transmission in Romania has increased further and now reaches up to 25 in some areas. Similarly, in Croatia and Bosnia, the areas with an R_0 above 4 have expanded. In most of eastern Europe, disease risks are predicted to be well above 1, indicating that – according to these models - transmission of malaria is possible. For all three climate change scenarios, there are no indications of malaria being a threat in western, central and southern Europe as well as Scandinavia. Although the relative vectorial capacity risk is predicted to be greatest in Italy for both current and future scenarios, this does not seem to have had an impact on the risk of disease. This is due to the very important role of socio-economic factors which, it seems, far outweigh the impacts of relative vectorial capacity on malaria risk. From this exercise it can therefore be concluded that at present there are conditions suitable for malaria transmission in some areas of eastern Europe. With the projected climate changes, and in the absence of an improvement in socio-economic status, the risk of malaria in these areas is predicted to increase substantially so that by the end of the century (i.e. the 2080s) there exists a predicted risk of malaria re-emerging in most countries east of the 14° longitude line (i.e. Poland).

Figures 5.22 and 5.23 show the 'sensitivity simulations' – i.e. the predictions of malaria risk calcuated with varying parameters of relative vectorial capacity (in this case daily survival rate, p). As described in Chapter 4, R_0 was calculated using the lower and upper ranges of daily survival rate which have been obtained from previously published literature. It is evident that these variations have caused significant changes in the predictions of malaria risk. This is primarily because RVC is particularly sensitive to changes in p as this appears twice in Equation 4.3. (see page 164).

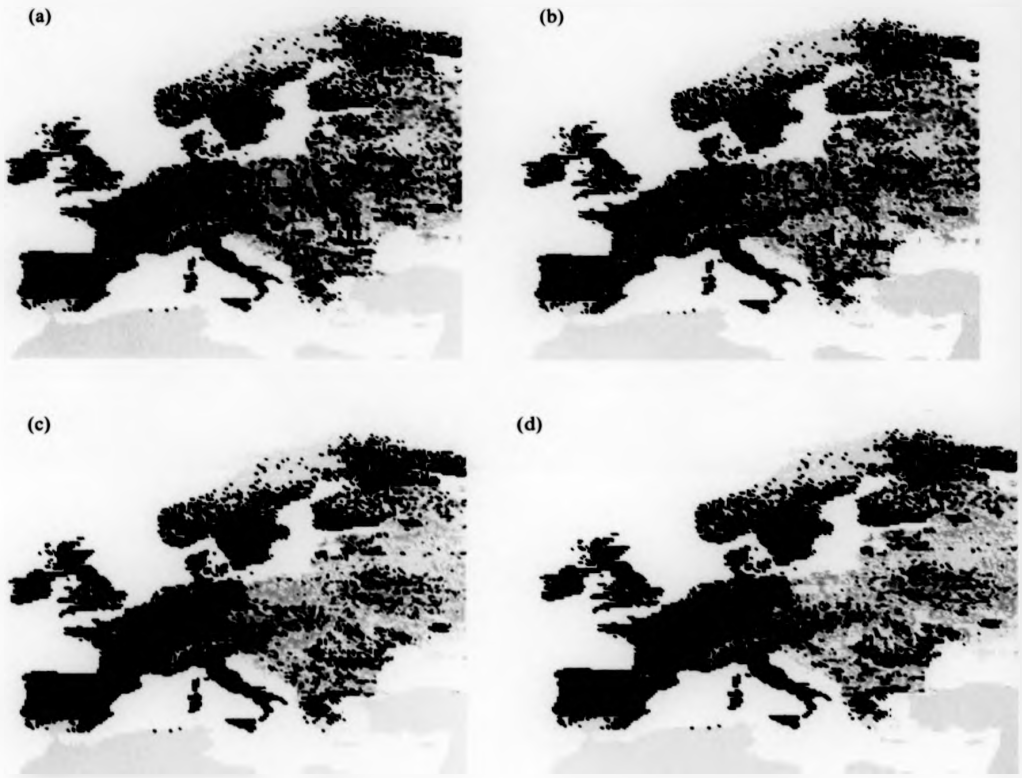

Figure 5.21. Malaria risk (R_0) in Europe during (a) the present day, (b) 2020s, (c) 2050s and (d) 2080s.
(North Africa and Turkey have been excluded due to factors described in the text).

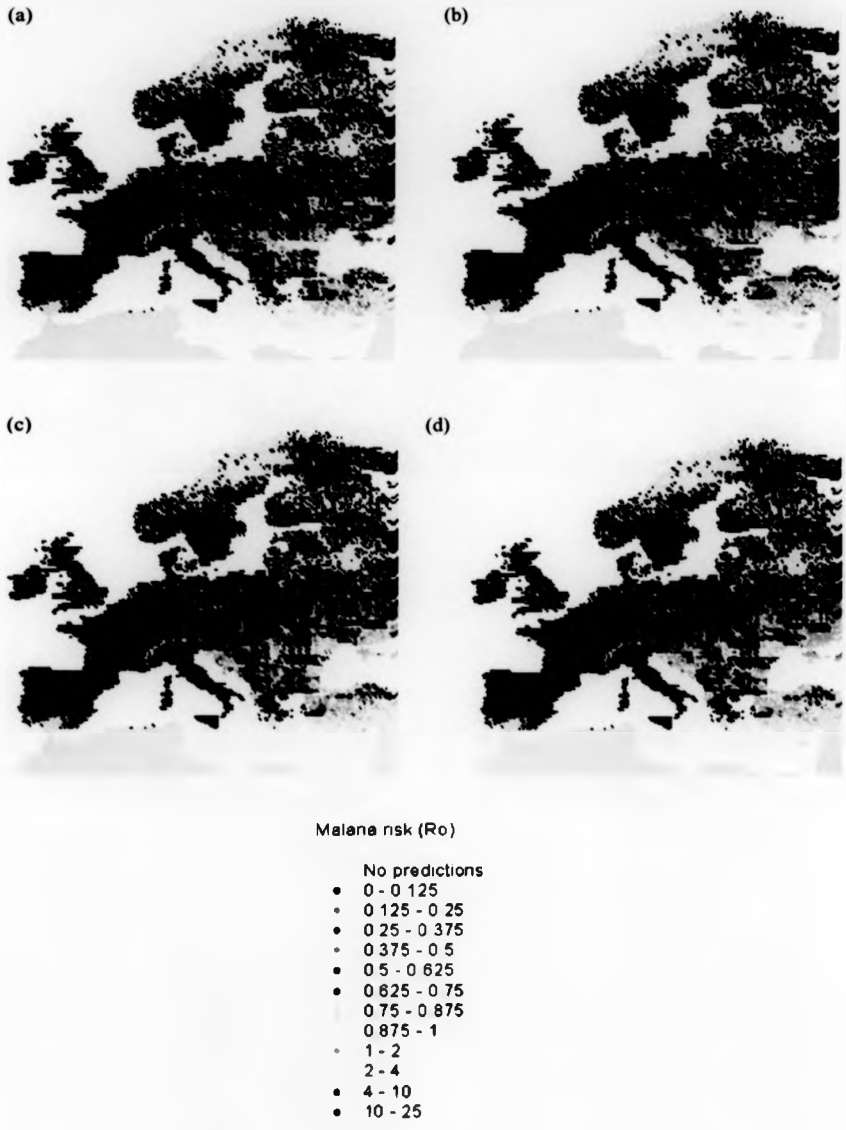

Figure 5.22. Malaria risk (R_0) in Europe during (a) the present day, (b) 2020s, (c) 2050s and (d) 2080s predicted using the lower range of daily survival rate. (North Africa and Turkey have been excluded due to factors described in the text).

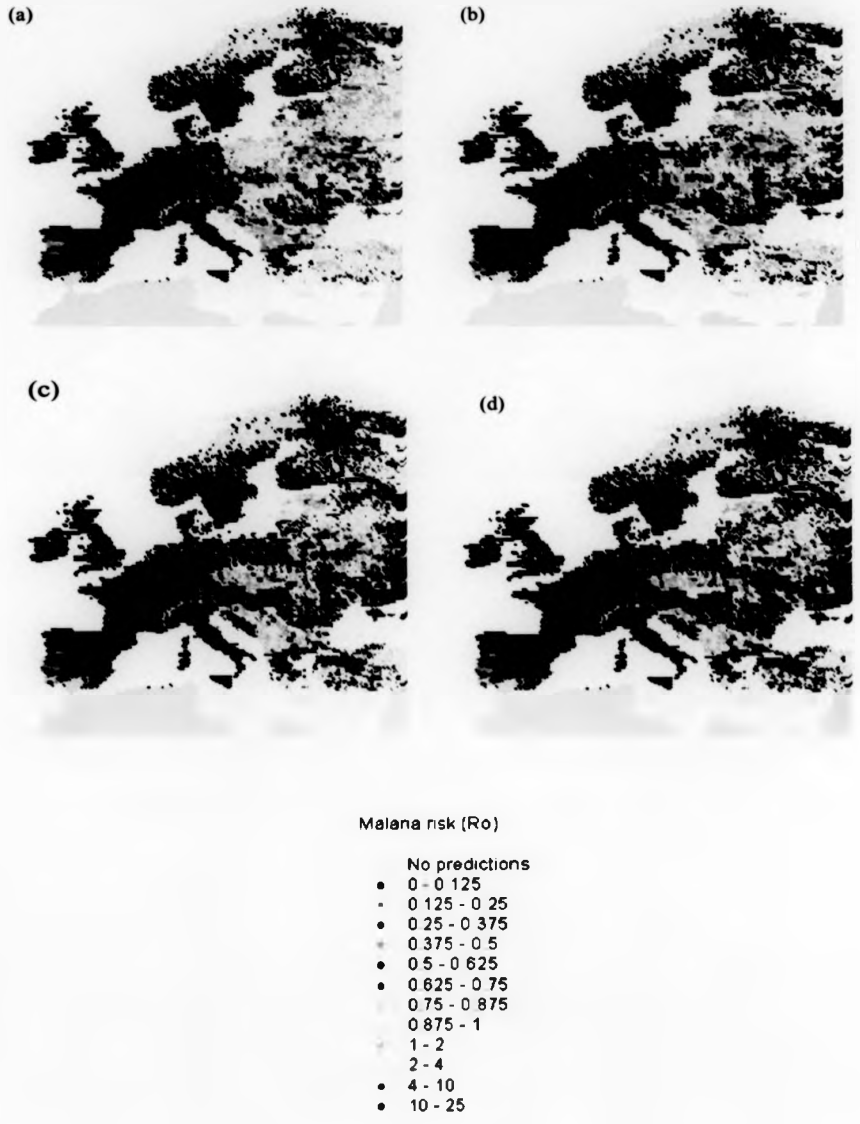

Figure 5.23. Malaria risk (R_0) in Europe during (a) the present day, (b) 2020s, (c) 2050s and (d) 2080s predicted using the upper range of daily survival rate. (North Africa and Turkey have been excluded due to factors described in the text).

Discussion

Using relatively simple multivariate model simulations, predictions of the impact of climate on the risk of malaria in England and Europe as well as the likely impact of climate change on malaria vector distributions, vectorial capacity and malaria risk (R_0) in the next 80 years have been generated.

This is the first time that disease and climate data have been used in combination to quantify the potential link between climate and English malaria (or ague). On the basis of average annual temperatures calculated from a smoothed dataset, Reiter (2000) argued that a drastic drop in temperatures during the 16th to the 18th century (the Little Ice Age) did not have a marked effect on ague. Because mentions of ague did not disappear during this period, he concluded that the disease was still very prevalent – hence suggesting that climate did generally not influence trends in malaria. In contrast, using the Central England Temperature Series, a monthly composite of station data, Lindsay and Joyce (2001) observed a period of successive cold summers which started in 1860. This decrease in temperatures coincide with the decline of ague after the last epidemic in 1857-59 and the authors conclude that this cold period, in combination with social and agricultural factors, may have played a role in pushing the disease towards extinction. The interpretation presented here, based on analysis of concurrent climate, agricultural and malaria data, differs from both of the above. A significant effect of both temperature and precipitation is demonstrated, explaining the malaria epidemics observed both in this country and throughout Europe (Hirsch 1883) in the "unusually hot summers" of 1848 and 1859 (Whitley 1863, MacDonald 1920, Smith 1956). However, outside these brief epidemics the long-term trend during the nineteenth century was surprisingly consistent, with no noticeable increase in the rate of decline in the 1860s, and was probably driven by non-climatic factors. This consistency was also observed by Nicholls (2000) in a socio-historical study of Fenland ague.

There has been much speculation about the role of climate changes in the possible re-emergence of malaria in England (e.g. Reiter 2001). In his 2002 report 'Getting ahead of the curve', the Chief Medical Officer stated that 'by 2050 the climate of the UK may be such that indigenous malaria could become re-established' and that 'local outbreaks of malaria caused by *Plasmodium vivax* may occur in the UK...' (Department of Health 2002). Indeed, global warming is predicted to increase UK temperatures by as much as 2.5°C by the 2050s (UKCIP 2002, Hulme and Jenkins 1998)

thereby increasing the chances of *P. vivax* completing its developmental cycle at optimum temperature in *An. atroparvus*, *An. messeae* or *An. plumbeus*. While sporadic transmission of malaria in Britain is certainly feasible today (and even more so in a warmer climate), it is unlikely that endemic transmission will ever reappear. For a 2.5°C increase in average temperatures during 1840-1910 it is predicted that malaria deaths could have increased by 14.5%. Considering the low number of deaths observed during the late 19th and early 20th centuries, the predicted proportional increases in malaria mortality are insignificant and clearly indicate the low possibility of climate changes causing malaria re-emergence in this country. This study has confirmed that malaria disappeared from England mainly due to changes in agriculture and land cover which are unlikely to be reversed in the future. Between 1940 and 1981, 20,000 km^2 of wet ground was drained in Britain and in East Anglia alone, 90% of fens have been lost since 1934 (Matt Millett, Wetlands Advisory Service, personal communication). Combined with the vast socio-economic change and improvements in the detection and treatment of imported cases, these factors have created a country in which the basic case reproduction number, R_0, is currently minuscule, as demonstrated by the absence of any secondary malaria cases in this country since 1953 (Crockett and Simpson, 1953), despite a cumulative reported total of 52,907 imported cases. A 14.5% rise in risk may have been important in the 19th century but is now highly unlikely to lead to the re-emergence of local malaria transmission in the UK.

The use of long-term concurrent historical malaria and climate data for Europe in this study demonstrates how simple mathematical models can be used to quantify and predict the effects of changing climate on national disease patterns. As with the UK, the role of predicted climate changes in the possible re-emergence of malaria in Europe has been widely discussed. Using a semi-biological approach to predict the effects of global warming, Martens *et al.* (1995) predicted that large areas of Europe could become malarious by the year 2100 while Rogers and Randolph (2000) developed a statistical model which showed that malaria transmission in Europe is unlikely even by the 2050s. With simulated temperature increases of 1.5-5°C, the model for European malaria predicted 6.6-24.9% increases in malaria cases during 1900 to 1975. Because R_0 is so low today (i.e. there have only been 26 reported indigenous cases in the 17 countries since 1990, WHO 2002a), even the 24.9% predicted increase in malaria cases is unlikely to lead to any large scale endemic transmission. As demonstrated in Chapter 3, changes in agriculture as well as the spraying of DDT in the highly endemic countries played the

thereby increasing the chances of *P. vivax* completing its developmental cycle at optimum temperature in *An. atroparvus*, *An. messeae* or *An. plumbeus*. While sporadic transmission of malaria in Britain is certainly feasible today (and even more so in a warmer climate), it is unlikely that endemic transmission will ever reappear. For a 2.5°C increase in average temperatures during 1840-1910 it is predicted that malaria deaths could have increased by 14.5%. Considering the low number of deaths observed during the late 19th and early 20th centuries, the predicted proportional increases in malaria mortality are insignificant and clearly indicate the low possibility of climate changes causing malaria re-emergence in this country. This study has confirmed that malaria disappeared from England mainly due to changes in agriculture and land cover which are unlikely to be reversed in the future. Between 1940 and 1981, 20,000 km^2 of wet ground was drained in Britain and in East Anglia alone, 90% of fens have been lost since 1934 (Matt Millett, Wetlands Advisory Service, personal communication). Combined with the vast socio-economic change and improvements in the detection and treatment of imported cases, these factors have created a country in which the basic case reproduction number, R_0, is currently minuscule, as demonstrated by the absence of any secondary malaria cases in this country since 1953 (Crockett and Simpson, 1953), despite a cumulative reported total of 52,907 imported cases. A 14.5% rise in risk may have been important in the 19th century but is now highly unlikely to lead to the re-emergence of local malaria transmission in the UK.

The use of long-term concurrent historical malaria and climate data for Europe in this study demonstrates how simple mathematical models can be used to quantify and predict the effects of changing climate on national disease patterns. As with the UK, the role of predicted climate changes in the possible re-emergence of malaria in Europe has been widely discussed. Using a semi-biological approach to predict the effects of global warming, Martens *et al.* (1995) predicted that large areas of Europe could become malarious by the year 2100 while Rogers and Randolph (2000) developed a statistical model which showed that malaria transmission in Europe is unlikely even by the 2050s. With simulated temperature increases of 1.5-5°C, the model for European malaria predicted 6.6-24.9% increases in malaria cases during 1900 to 1975. Because R_0 is so low today (i.e. there have only been 26 reported indigenous cases in the 17 countries since 1990, WHO 2002a), even the 24.9% predicted increase in malaria cases is unlikely to lead to any large scale endemic transmission. As demonstrated in Chapter 3, changes in agriculture as well as the spraying of DDT in the highly endemic countries played the

most important roles in the decline of European malaria and its re-emergence can therefore not be assessed using only climatic predictions.

To make assumptions about future malaria transmission in Europe without taking into account the distribution and efficiency of anopheline vectors is biologically questionable. The results presented here demonstrate a significant effect of projected climate changes on the probability of presence (i.e. abundance) throughout Europe of all five *Anopheles* species investigated. Of particular interest are the effects on the mosquitoes *An. atroparvus*, *An. labranchiae*, *An. sacharovi* and *An. superpictus* all of which are predicted to increase in abundance throughout western and central Europe, the Mediterranean and eastern Europe, respectively. The distribution of *An. atroparvus* could expand further into North and central Europe while that of *An. sacharovi* is predicted to extend further into central and eastern areas. These are among the first risk maps which predict the effects of modelled climate changes on mosquito distributions across a large scale. The predictions by Bryan *et al.* (1996) were based on 'ecoclimatic indices' derived from observed temperature and precipitation thresholds of *An. farauti s.s* development and showed an expansion of favourable habitats towards the central parts of Australia with increased temperature and precipitation. Rogers (1996) showed that the distribution of *An. gambiae* in Southern Africa could extend southwards and westwards into areas of Namibia and northern South Africa, increasing the area of suitable habitats available for this mosquito. Neither of these predictions are based on models containing data from individual mosquito captures, thus ignoring most of the patchiness in mosquito distributions which arises due to geographical differences in land cover and climate. The advantages of the approach presented here have been discussed in detail in Chapter 4. The limitation of using these models for predicting future scenarios is mainly that no predictions are available for how land cover changes with time. This variable is clearly related to the distribution of European mosquitoes and any accurate risk maps should ideally take projections of future agricultural changes into account when these become available. Another smaller caveat is caused by the lack of predictions for changes in cloud cover. However, as this is closely correlated with rainfall which is simulated in the HADCM3 model, the errors caused are most likely negligible.

The calculations of relative vectorial capacity included human biting rate and gonotrophic cycle duration as a temperature-dependent variable. Predictions of vectorial capacity for the five *Anopheles* species in Europe during the next 100 years show

significant effects of climate changes on the major vector *An. labranchiae* in southern and eastern Europe, *An. atroparvus* in central and western areas and *An. superpictus* in the south-easternmost regions. On the other hand, the effects of climate changes on *An. sacharovi*, another important vector, and *An. messeae* are small with the only significant changes in small areas of Turkey, North Africa and Russia. Although the longevity of mosquitoes (p) is also sensitive to changes in temperature (e.g. Bradley 1993), the value of this parameter was not permitted to change with temperature because of lack of data for the *An. maculipennis* members. This is likely to have underestimated the impact of temperature in some areas (i.e. p increases with temperature). As discussed in Chapter 4, the vectorial capacity of *An. messeae* and *An. sacharovi* is predicted to be low because of the low reported daily survival rate of these mosquitoes. Considering the status of *An. sacharovi* as one of the most important former vectors, the comparatively low vectorial capacity and insignificant effect of climate changes is surprising. *An. labranchiae* and *An. atroparvus* are both predicted to be efficient vectors in present and future scenarios which correlates with previous observations by European malariologists. The dissimilarities between predicted and 'observed' efficiency of *An. sacharovi* may be due to the use of inappropriate survival rate data rather than errors in the actual model structure.

Measures of disease risk (or basic case reproduction, R_0) were predicted for the three climate change scenarios using outputs from the vectorial capacity calculations. Current potential for malaria transmission (i.e. $R_0 > 1$) is observed in some areas of eastern Europe which, by the end of the 21st century increases significantly to include most countries to the east of the German-Polish border. The statistical model developed by Rogers and Randolph (2000) to predict global malaria risk by the 2050s defines areas suitable for malaria transmission by climatic constraints – i.e. most of Europe is considered to be more or less equally suitable for malaria. In real life we know that this is not the case. As described previously, Lindsay and Thomas (2001) predict that large areas of southern England could climatically support local malaria transmission by the 2050s and 2080s. As acknowledged by the authors, these predictions do not take into account other more important factors such as changes in precipitation, wetlands and socio-economy and therefore their reliability is probably limited. Previous analyses presented in Chapter 2 have shown that historical malaria in Europe was highly associated with changes in agriculture which, in turn, are driven by socio-economic factors. By including socio-economy (i.e. GDP and life expectancy) as well as

information on mosquito presence or absence in these predictions of malaria transmission in Europe, it is ensured that each specific location is assessed according to the most important risk factors related to malaria. With respect to malaria, countries in eastern Europe have repeatedly been considered as being most at risk of re-introduction (e.g. Kovats *et al.* 1999, Reiter 2001) mainly due to less efficient health systems caused by the recent civil unrest.

As already shown in Chapter 4, the sensitivity of these predictions to fluctuations in biological parameters is high. For instance, using the high values of mosquito daily survival rate, the models in this thesis predict that there will be a strong risk of malaria transmission in most of eastern Europe while predictions with low values of p show very limited risk anywhere in Europe. Clearly, even small variations in an important variable such as survival rate can have a tremendous impact on predictions of disease risk. Thus, the realiability of the climate change predictions is strongly limited unless we can be certain that the biological parameters used are accurate. As discussed previously, this is certainly not the case for European mosquitoes. Therefore, the inclusion of error maps (i.e. risk predicted with varying parameters) is important, particularly if the predictions are to be presented to policy makers who decide on future malaria control targeting.

The models presented in this work wrongly assumed that GDP and life expectancy will not change during the next 100 years. As mentioned, future GDP has been projected but only up to the year 2020 (IPCC 2001) which is too short a time interval for this analysis. Assuming that GDP increases in eastern Europe (e.g. an 83% increase has been predicted for Romania from 2000 to 2020) this has resulted in an overestimation of R_0 in these areas. Another limitation of these predictions, which has previously been discussed, is the assumption that mosquito abundance equals probability of presence. Thus, considering all caveats and limitations, the models presented here indicate a strong possibility that changes in climate, due to effects on the local vector populations, may create favourable conditions for malaria transmission in large areas of eastern Europe. On the other hand – and contrary to what has previously been predicted or assumed (e.g. Department of Health 2002, Martens *et al.* 1995) – the re-emergence of malaria in the more prosperous areas of Europe is highly unlikely due to the persistence of the factors which cause the disease to disappear almost a hundred years ago.

Final Discussion

Final Discussion

Three general model types have previously been used to determine the effect of climatic changes on the future distribution and transmission of malaria; statistical, biological and climate suitability models. This thesis presents a new approach by firstly defining how inter-annual variability in malaria is affected by temperatures and then making spatial predictions of disease risk (R_0) using real data. In an improvement on previous statistical models, the analyses presented here examine the inter-annual variability rather than merely spatial or temporal trends. The methods used here also show an improvement of published biological malaria models as they do not ignore the effect of climate changes on vector abundance and because they take into account future predictions of both temperature and rainfall Additionally, this analysis presents the first attempt to combine socio-economic and biological variables to predict disease risk which is measured in absolute terms instead of ranges of presence and absence or non-sensible variables derived from biological equations.

Studying historical malaria in Europe

As well as improving the existing predictions of future disease transmission, the study of historical malaria in Europe will also enable us to fully understand what caused the disease to disappear from particularly northern and western areas where the natural decline was most pronounced.

Although the English and Welsh malaria data used may have been less than accurate due to problems with misdiagnoses and reporting criteria, this dataset has nevertheless provided us with a unique opportunity to closely examine historical malaria patterns in a high-latitude area. The possibility of extending this study to a higher resolution is of major interest. As shown in Chapter 2, ague deaths were also reported at parish and statistical district levels, however, due to difficulties in obtaining relevant explanatory variables the temporal and spatial patterns of malaria could unfortunately not be examined at this higher resolution. Such an analysis would clearly be of interest both in order to compare the relationship between environmental variables and malaria at county and parish level but also because it would potentially allow for the identification of high resolution areas which may be particularly at risk of future local malaria transmission. By repeating the study at this higher resolution, the spatial inconsistencies between climate and disease data may also be improved. In the current study, climate averages were calculated for whole counties, thereby ignoring any local scale patchiness in temperature and precipitation which may have caused

fluctuations in malaria. Another problem with the climate data used is the fact that temperatures and precipitation were averaged for the whole year. Published literature have tended to use climatic data for the mosquito or malaria season (i.e. averages for a few months). The use of annual averages in this study may have underestimated the real effect of climate on temporal patterns in ague deaths. Thus, if seasonal temperatures and precipitation had been used, it is likely that climate could have had a stronger effect on the temporal variation in ague deaths in comparison to that of wetlands and cattle (i.e. the effect of agricultural factors may in reality not be as strong as observed here).

This study has shown that malaria was of considerable importance throughout Europe. Since finishing the current work, it has become evident that historical datasets similar to the one used for the UK also exist in other countries. In Holland, long-time series of malaria cases as well as mosquito densities are available at the village level for which explanatory variables (such as marsh coverage and agricultural factors) can also be obtained. (Willem Takken, personal communication). Similarly, the great extent to which the disease was studied especially in Italy (Mario Coluzzi, personal communication) and Greece indicates that extensive datasets may also be available for these areas. Localised analyses of malaria patterns in southern Europe would provide a valuable comparison to the results obtained from northern parts as the data presented in this thesis suggest that the long-term temporal patterns were significantly different between the two regions. By doing such studies we can obtain results which will ultimately provide more reliable predictions of future malaria transmission in both north and south Europe.

The study of malaria patterns in previously endemic areas has proven to be a useful tool for assessing the potential re-emergence of the disease in such regions. Apart from Europe, malaria was also widely distributed in both North America and Australia until the early 20th century (Fig. 6.1). The last officially reported case of indigenous malaria in North America occurred in 1951 while the last Australian case was reported in 1981. In these two continents, the disappearance of the disease was also attributed to a combination of socio-economic and agricultural changes as well as intensive control efforts. Like in Europe, it has been argued that future environmental changes may cause the re-emergence of malaria in North American and Australia (Bryan *et al.* 1996, Humphreys 2001) but so far there have not been any published attempts to determine the historical role of climate in the distribution and disappearance of malaria in order to properly substantiate these claims. A study similar to the historical analysis presented here is currently being undertaken at the London School of Hygiene and Tropical Medicine (Annemarie ter Veen, personal communication) to determine

the quantitative effect of a number of agricultural, socio-economic and climatic variables on the temporal and spatial patterns of malaria in North America during the early 20th century.

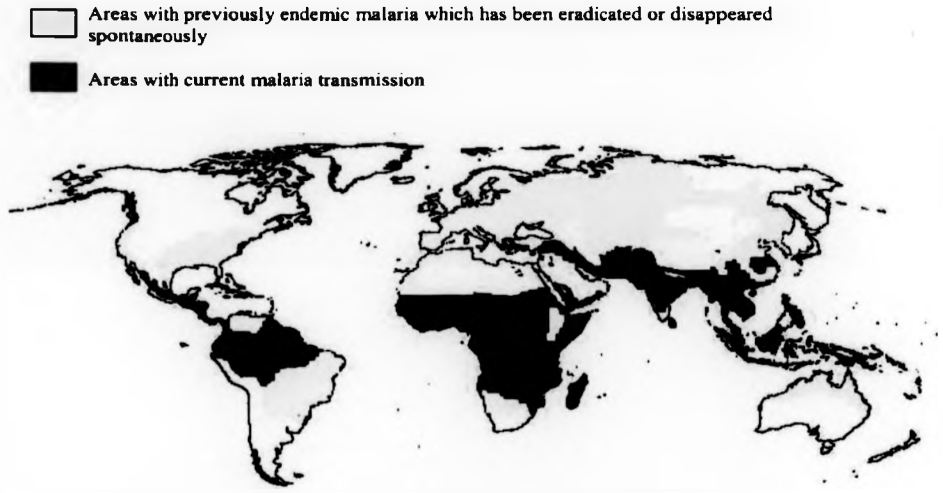

Figure 6.1. World-wide historical and present distribution of malaria (based on Bruce-Chwatt and de Zulueta 1980, Molineaux 1988 and WHO 2001).

The current and future risk of malaria in Europe

As has already been discussed, the mosquito database and corresponding environmental variables used in this study were limited mainly by the lack of data from many regions but also because of temporal and spatial discrepancies between mosquito, climate and land cover data.

Firstly, there were only limited data available on the presence and absence of malaria vectors in Europe and no reliable information which allowed modelling of mosquito abundances. Although some sources did provide abundance measures of mosquitoes in specific areas, it was not possible to standardise these values due to differences in trapping methods and duration. More data on both geographical distribution as well as mosquito density would

undoubtedly become available by extending searches to local collections in museums, universities and other scientific institutions as well as private files. Such sources may additionally provide more recent data (e.g. from within the last 5 years) which is more compatible with the recent remotely sensed land use and climate data currently available at high resolution.

The calculation of relative vectorial capacity for the five former European malaria vectors indicate that the current vector efficiency of the mosquitoes is relatively low. The main limitation of these calculations is the use of mosquito probability of presence as a proxy measure of abundance. By doing this, it is assumed that the two variables are linearly related (i.e. mosquito abundance equals probability of presence multiplied by an undefined constant). This is clearly not the case – at low probabilities of presence, there may be a linear relationship but at the other scale (i.e. where probability of presence asymptotes towards 1), it is not apparent how the two are related. Thus it would be of considerable interest to examine how the predicted probability of presence from this study relates to an absolute measure of abundance. This could simply be done by surveying mosquito populations in locations for which predictions have been made. Another limitation of the calculations is the anthropophily data (i.e. human blood index) used. A conservative average estimate of HBI was calculated from published data, most likely underestimating the real values (e.g. the HBI of *An. sacharovi* is surprisingly low considering that this was one of the most anthropophilic vectors). The human blood index is clearly geographically dependent (i.e. high versus low human population density areas) but because of lack of data this was kept constant for all locations in Europe. Additionally, the survival rate of the five mosquitoes was fixed across the study area although it is undoubtedly dependent on both temperature and humidity. Thus, predictions of current and particularly future relative vectorial capacity have not accounted for geographic and climatic effects on two important variables.

All the vectorial capacity and R_0-based models discussed previously (including the work in this thesis) are based on the often used temperature thresholds of malaria parasite development derived under laboratory settings (McDonald 1957). There is no information available on how many observations form the basis of these thresholds and thus we have no means of assessing their reliability. It is likely that these experiments need revising, particularly under more natural conditions in varying geographic locations. Finally, another limitation common to all climate-based models of mosquito distributions and vectorial capacity is the assumption that there is a simple relationship between macro (i.e. satellite- or station-derived) and micro-climate (i.e. temperature and humidity in the mosquito resting

and/or breeding site). We do not know that this is true and, ideally, the assumption should be tested and any relationship quantified. In theory, it should be feasible to make comparisons of station or satellite climate data with measurements undertaken at the micro-habitat level.

Predictions of malaria risk (i.e. R_0) throughout Europe for current and future climate scenarios showed that the highest risk of disease transmission is and will be restricted to eastern Europe. The risk of malaria re-emerging in western areas – even with the climate projected for the 2080s – is predicted to be non-existent. The low R_0 predicted for Greece and Italy is surprising considering that these two countries were among the most malarious in Europe as well as the last to eradicate indigenous transmission (as summarised in Chapter 3). This caveat can be explained by the lack of sufficient mosquito data for these areas but also by the comparatively good socio-economy of the two countries. Because risk is assessed using GDP and life expectancy, these countries are not considered to be in the high risk zone (i.e. low GDP and life expectancy), thus making R_0 less than expected. Italy is one of the few countries in the EU which has reported officially confirmed cases of indigenous transmission since eradication and this suggests that conditions (both climatic and socio-economic) suitable for transmission currently exist in some areas of the country. These are unfortunately not identified in our models due to the problems discussed above. In this context, it will be worth investigating how relative vectorial capacity and R_0 vary with GDP and life expectancy at local levels in areas which have reported indigenous transmission (i.e. do low GDP villages or regions within a country have higher ratio of R_0 to relative vectorial capacity than more prosperous areas?). An additional project which may be undertaken in the future is to overlay the predictive R_0 maps on population density maps in order to estimate the population at risk of malaria in Europe.

The risk of malaria re-emergence was also assessed using data on current indigenous transmission in European countries. These measures were obtained from the WHO and represent only those cases which have been officially reported and confirmed. According to non-published accounts of larger numbers of cases in parts of eastern Europe and Russia (Natalia Nikolaeva, personal communication), the WHO reports may be underestimating the true situation of indigenous malaria in Europe. However, in spite of efforts to (a) ascertain the extent of indigenous malaria not reported by the WHO and (2) obtain case numbers in these areas, no such information was found and thus could not be analysed.

Predictions of future changes in mosquito distributions, relative vectorial capacity and malaria risk were based on the latest climate change scenarios developed by the Hadley Centre (i.e. the HADCM3 SRES models). Although a variety of changes are included in these

projections, they do not account for alterations in one of the most important factors – namely land cover. At present there are no predictions of how land cover types may change over the coming decades. However, considering past trends in agriculture across Europe (e.g. the loss of wetlands and the vast increase in croplands) it is very likely that we will also see considerable changes within the next hundred years which will have a marked impact on the distribution and abundance of European mosquitoes and potential malaria risk.

In this study, the risk of malaria is also to a large extent dependent on socio-economic factors (i.e. GDP and life expectancy). Predictions of R_0 assume that the difference between these variables in European countries remains the same in the future (i.e. that low GDP and life expectancy countries remain low and vice versa). With the planned expansion of the European Economic and Monetary Union (EEU), this is probably not an accurate assumption and thus should be considered as a serious caveat because projections of future GDP were insufficient and therefore not used in this study.

Conclusions

To summarise, there are few main limitations with the studies presented in this thesis most of which can be eliminated or significantly improved by undertaking relatively simple research:

1. The reliability of the original UK ague data (i.e. do they really represent malaria deaths?).
2. The relatively crude linking of country-level malaria and agricultural and socio-economic data with comparatively high resolution climate data in European countries.
3. The false negative and positive predictions of some mosquito vectors in Europe caused mainly by lack of observed data points as well as temporal discrepancies between mosquito, climate and land cover data.
4. Assuming that mosquito abundance is linearly correlated with probability of presence throughout Europe.
5. The assumption that the human blood index (i.e. anthropophily) of mosquitoes is geographically independent when calculating relative vectorial capacity across Europe.
6. Not taking into account the effects of temperature and humidity on mosquito survival rates as well as inter-specific differences in vector competence.
7. The lack of reliable data on the supposedly large number of indigenous malaria cases in the potentially vulnerable regions in eastern Europe.
8. Low predictions of current malaria risk in Greece (the last country to eradicate malaria), possibly caused by a lack of mosquito data and the comparatively good socio-economic status of the country (compared to Eastern European countries).

9. Finally, the inability to include projected changes in land cover, GDP and life expectancy in the predictions of future malaria risk in Europe.

In spite of these caveats, the results from this study are encouraging. The potential re-emergence of malaria in Europe, particularly as a result of climate changes, is clearly a popular and important area of interest. The analyses presented in this thesis strongly indicate that the prospect of malaria transmission returning to western Europe is minuscule but significant in parts of eastern Europe. As discussed, some of the original data and calculations used are relatively crude, yet, the large database constructed for this study is far from static. There is a possibility of including improved data when they become available during the next few years which should hopefully allow for the making of more accurate predictions of the real risk of future malaria transmission in Europe.

Bibliography

Abdel-Rahman MS, El-Bahy MM, El-Bahy NM and Malone JB (1997). Development and validation of a satellite based geographic information system (GIS) model for epidemiologiy of *Schistosoma* risk assessment on snail level in Kafr El-Sheikh governate. *J Egypt Soc Parasitol*, **21**: 299-316.

Abdikarimov ST (2001). [Current malaria situation in Kyrzyzstan 1995-1999] Med *Parazitol Mosk*, **1**: 33-34.

Adhami J and Reiter P (1998). Introduction and establishment of *Aedes* (Stegomyia) *albopictus* skuse (Diptera: Culicidae) in Albania. *J Am Mosq Control Assoc*, **14**: 340-343.

Aitchison RS (1893). A medical handbook for the use of practitioners and students. *C. Griffin & Co., London.*

Aitken W (1866). The science and practice of medicine. C.Griffin & Co, London.

Aliev S and Saparova N (2001). [Current malaria situation and its control in Tadjikistan]. *Med Parazitol Mosk*, **1**: 35-7

Armitage P, Berry G and Matthews JNS (2001). Statistical methods in medical research. *Blackwell science, Oxford.*

Artemiev MM (1980). Anopheles mosquito – main malaria vectors in the USSR. In: *International scientific project on ecologically safe methods for control of malaria and its vectors; Collected Lectures, 2: 45-71. The USSR committee for science and technology (GKNT)/United Nations Environment Programme (UNEP), Russia.*

Astolfi P, Lisa A, Degioanni A, Tagarelli A and Zei G (1999). Past malaria, thalassemia and woman fertility in southern Italy. *Ann Hum Biol*, **26**: 163-73.

Baldari MA, Tamburro A, Sabatinelli G, Romi R, Severini C, Cuccagna C, Fiorilli G, Allegri MP, Buriani C and Toti M (1998). Malaria in Maremma, Italy. *Lancet*, **351**: 1246-1247.

Balfour MC (1935). Malria studies in Greece. *Am J Trop Med Hyg*, **3**: 301-303.

Balfour MC (1936). Some features of malaria in Greece and experience with its control. *Riv Mal*, **1**: 114-131.

Barber MA (1936). A survey of malaria in Cyprus. *Am J Trop Med*,**16**: 431.

Barber MA and Rice JB (1935). Malaria studies in Greece: the malaria infection rate in nature and in the laboratory of certain species of *Anopheles* of east Macedonia. *Ann Trop Med*, **29**: 329-348.

Barlow GH (1861). A manual of the practice of medicine. *J. Churchill, London.*

Barr AR (1988). The *Anopheles maculipennis* complex (Diptera: Culicidae) in western North America. In *(M. W Service ed.) Systematics Association Special Volume No. 37. Clarendon Press, Oxford.*

Bashwari LA, Mandil AM, Bahnassy AA, Al-Shamsi MA, Bukhari HA (2001). Epidemiological profile of malaria in a university hospital in the eastern region of Saudi Arabia. *Saudi Med J*, **22**:133-138

Bates M (1939). The use of salt solutions for the demonstration of physiological differences between the lavae of certain European anopheline mosquitoes. *Am J Trop Med*, **19**: 357-384.

Bates M (1940). The nomenclature and taxonomic status of the mosquitoes of the *Anopheles maculipennis* compex. *Ann Ent Soc Am*, **33**: 343-356.

Bates M, Beklemishev WN and La Face L (1949). Anophelines of the Palaearctic region. In *(M Boyd ed.) Malariology. Saunders, Philadelphia.*

Baylis, M., Bouayoune H, Touti J and El Hasnaovi H (1998). Use of climatic data and satellite imagery to model the abundance of *Culicoides imicola*, the vector of African horse sickness virus, in Morocco. *Med Ved Ent.*, **12**: 255-266.

Beck LR, Rodriguez MH, Dister SW, Rodriguez AD, Washino RK and Spanner MA (1997). Assessment of a remote sensing-based model for predicting malaria transmission risk in villages of Chiapas, Mexico. *Am J Trop Med Hyg*, **56**: 99-106

Beck LR, Bradley M, Lobitz M and Wood BL (2001). Remote sensing and human health: new sensors and new opportunities. *Emerg Inf Dis*, **6**: 217-226.

Becker N and Ludwig HW (1983). Mosquito control in West Germany. *Bull Soc Vector Ecol*, **8**: 85-93.

Becker N and Ludwig HW (1989). Mikrobiologische Stechmückenbekämpfung. *Biologie in unserer Zeit*, **19**: 105-111.

Becker N and Ludwig HW (1993). Investigations on possible resistance in *Aedes vexans* field populations after a 10-year application of *Bacillus thuringiensis israelensis*. *J Am Mosq Control Assoc*, **9**: 221-224.

Becker N and Rettich F (1994). Protocol for the introduction of new *Bacillus thuringiensis israelensis* products into the routine mosquito control program in Germany. *J Am Mosq Control Assoc*, **10**: 527-533.

Bismil'din FB, Shapieva ZZ and Anpilova EN (2001). [Current malaria situation in the Republic of Kazakhstan] *Med Parazitol Mosk*, **1**: 24-33.

Blacklock B (1921). Notes on a case of indigenous infection with *P. falciparum*. *Ann Trop Med Parasit*, **15**: 59-72.

Blacklock B and Carter HF (1920). The experimental infection in England of *Anopheles plumbeus* , Stephens, and *Anopheles bifurcatus*, L., with *Plasmodium vivax*. *Ann Trop Med Parasit*, **13**: 413-420.

Boelaert M, Arbyn M and Van der Stuyft P (1998). Geographical Information Systems (GIS), gimmick or tool for health district management. *Trop Med Int Health*, **3**: 163-165.

Bonora S, De Rosa FG, Boffito M and Di Perri G (2001). Rising temperature and the malaria epidemic in Burundi. *Trends Parasitol*, **17**: 572-573.

Bouma M and Rowland M (1995). Failure of passive zooprophylaxis: cattle ownership in Pakistan is associated with a higher prevalence of malaria. *Trans R Soc Trop Med Hyg*, **89**: 351-353.

Bouma MJ and van der Kaay HJ (1996). The El Nino Southern Oscillation and the historic malaria epidemics on the Indian subcontinent and Sri Lanka: an early warning system for future epidemics? *Trop Med Int Health*, **1**: 86-96

Bouma MJ and Dye C (1997). Cycles of malaria associated with El Nino in Venezuela. *JAMA*, **278**: 1772-1774.

Bouma M, Sorndorp H and Van der Kaay HJ (1994). Health and climate change. *Lancet*, **343**:302.

Bouma MJ, Dye C and Van der Kaay HJ (1996). Falciparum malaria and climate change in the North West Frontier Province of Pakistan. *Am J Trop Med Hyg*, **55**: 131-137.

Bouma, M.J., Poveda, G., Rojas, W., Chavasse, D., Quiñones, M., Cox, J. & Patz, J. (1997). Predicting high risk years for malaria in Colombia using parameters of El Niño Southern Oscillation. *Trop Med Int Health*, **2**: 1122-1127.

Bradley DJ (1989). Current trends in malaria in Britain. *J R Soc Med*, **82**: S8-S13.

Bradley D J (1993). Human tropical diseases in a changing environment. In *Environmental change and human health. Wiley, Chichester (Ciba Foundation Symposium).*

Brightwell R, Dransfield RD and Williams BG (1992). Factors affecting seasonal dispersal of the tsetse flies *Glossina pallidipes* and *G. longipennis* (Diptera: Glossinidae) at Nguruman, south-west Kenya. *Bull Ent Res*, **82**: 167-182.

Bristowe JS (1880). A treatise on the theory and practice of medicine. *Smith Elder & Co., London.*

British Museum (1938). Catalogue of political and personal satires, volume IV. *London.*

Brooker S (2002). Schistosomes, snails and satellites. *Acta Trop*, 82: 207-214.

Bruce-Chwatt L.J and de Zulueta J (1980). The rise and fall of malaria in Europe. A historico-epidemiological study. *Oxford University Press, Oxford.*

Bruce-Chwatt LJ (1976). Ague as malaria (an essay on the history of two medical terms). *J Trop Med Hyg*, **79**: 168-176.

Bruce- Chwatt LJ (1977). Malaria eradication in Portugal. *Trans R Soc Trop Med Hyg*, **71**: 232-240.

Bruce-Chwatt LJ (1985). Essential malariology. *John Wiley and Sons, New York.*

Bruce-Chwatt LJ and De Zulueta J (1980). The rise and fall of malaria in Europe. A historico-epidemiological study. *Oxford University Press, London.*

Brumback BA, Ryan LM, Schwarts JD, Neas LM, Stech PC and Burge HA (2000). Transitional regression models, with application to environmental time series. *J M Statits Ass*, **95**: 16-27.

Buck A de (1936). Some results of six years mosquito infection work. *Am J Hyg*, **24**: 1-18.

Bryan JH, Foley DH and Sutherst RW (1996). Malaria transmission and climate change in Australia. *Med J Aust*, **164**: 345-347.

Buonomini G and Mariani M (1953). World Anophelines belonging to the subgenus *Maculipenna* Buonomine e Mariani, 1946. *Riv Malariologia*, **32**: 173-188.

Castelli F, Cabona MG, Brunori A and Carosi G (1994). Short report: imported mosquito: an uninvited guest. *Am J Trop Med Hyg*, **50**: 548-549.

Cefalu M, Oddo F and Sacca G (1961). Vita extra-domestica di *Anopheles labranchiae* in Sicilia. Osservazioni in un'area di sospensione dei trattamenti con DDT. *Parassitologia*, **3**: 23-51.

Checkley W, Epstein LD, Gilman RH, Figueroa D, Cama RI, Patz JA and Black RE (2000). Effect of El Nino and ambient temperature on hospital admissions for diarrhoeal diseases in Peruvian children. *Lancet*, **355**: 442-50

Cheng S, Kalkstein LS, Focks DA and Nnaji A (1998). New procedures to estimate water temperatures and water depths for application in climate-dengue modeling. *J Med Entomol*,**35**: 646-52

CIESIN (2002). http://www.ciesin.org/datasets/gpw/globldem.doc.html)

Clarke KC, Osleeb JR, Shery JM, Meert Jp and Larsson RW (1991). The use of remote sensing and geographic information systems in UNICEF's dracunculiasis (Guinea worm) eradication effort. *Prev Vet Med*, **11**: 229-235.

Coetzee M, Craig M and le Sueur D (2000). Distribution of African malaria mosquitoes belonging to the *Anopheles gambiae* complex. *Parasitol Today*, **16**: 74-77.

Coluzzi M (1994). Malaria and the Afrotropical ecosystems: impact of man-made environmental changes. *Parassitologia*, **36**: 223-227.

Colwell RR (1996). Global climate and infectious disease: the cholera paradigm. *Science*, **274**: 2025-2031.

Colwell, RR and Patz JA (1998). Climate, infectious disease and health. *American Academy of Microbiology, Washington.*

Craig MH, Snow RW and le Sueur D (1999). A climate-based distribution model of malaria transmission in sub-Saharan Africa. *Parasitol Today*, **15**: 105-111.

Creighton C (1891). A history of epidemics in Britain. *Frank Cass & Co. London*

Crick HQP and Sparks TH (1999). Climate change related to egg laying trends. *Nature*, **399**: 423-424.

Crockett GS and Simpson K (1953). Malaria in neighbouring Londoners. *BMJ*, **1**: 1141.

Croner CM, Sperling J and Broome FR (1996). Geographic information systems (GIS): new perspectives inunderstanding human health and environmental relationships. *Stats Med*, **15**: 1961-1977.

Cross ER and Hyams KC (1996). The potential effect of global warming on the geographic and seasonal distribution of *Phlebotomus papatasi* in Southwest Asia. *Env Health Perspec*, **104**: 724-727.

Cross ER, Newcomb WW and Tucker CJ (1996). Use of weather data and remote sensing to predict the geographic and seasonal distribution of *Phlebotomus papatasi* in Southwest Asia. *Am J Trop Med Hyg*, **54**: 530-536.

CRU (2002). http://www.cru.uea.ac.uk/~markn/cru05/cru05_intro.html

Curtis CF and Davies CR (2001). Present use of pesticides for vector and allergen control and future requirements. *Med Vet Entomol*, **15**: 231-235.

Dansgaard W and Tauber H 91969). Glacier oxygen-18 ocntent and Pleistocene oceant emperatures. *Science*, **166**: 499-502.

Davidson A (1892). Geographical pathology : an inquiry into the geographical distribution of infective and climatic diseases. *Y.J. Pentland, Edinburgh and London.*

Daskova NG and Rascinyn SP (1982). Review of data on susceptibility of mosquitos in the USSR to imported strains of malaria parasites. *Bull WHO*, **60**: 893-897.

Department of Health (2002). Getting Ahead of the Curve: a Strategy for Combating Infecious Diseases (including other aspects of health protection). A report by the Chief Medical Officer. *Department of Health, UK.*

Detinova TS, Beklemishev WN and Bertram DS (1963). Methodes a appliquer pour classer par goupes d'age les dipteres presentant une importance medicale. *WHO monograph series 47. WHO, Geneva.*

Dister SW, Fish D, Bros SM, Frank D H and Wood BL (1997). Landscape characterization of peridomestic risk for Lyme disease using satellite imagery. *Am J Trop Med Hyg*, **57**: 687-692.

Dobson MJ (1980). Marsh fever – the geography of malaria in England. *J Hist Geo*, **6**: 357-389.

Dobson MJ (1997). Contours of death and disease in early modern England. *Cambridge University Press, Cambridge.*

Duncan K (1993). The possible influence of climate on historical outbreaks of malaria in Scotland. *Proc R Coll Physicians Edinb*, **23**:55-62.

Dye C (1992). The analysis of parasite transmission by bloodsucking insects. *Ann Rev Entomol*, **37**: 1-19.

Ekblom T (1945). Studien über die Malaria und Anopheles in Schweden und Finland. *Acta Pathologica et Microbiologica Scandinavica*, **59**: S1-S89.

Elliott TS, Payne GM and Lewis MJ (1983). Campylobacter entiritis in Nottingham. *Ecol Dis*, **2**:291-294.

Elnaeim DA, Connor SJ, Thomson MC, Mukhtar M, Hassan MK, Aboud MA and Ashford RW (1998). Environmental determinants of the distribution of *Phlebotomus orientalis* in Sudan. *Ann Trop Med Parasit*, **92**: 869-876.

EPA (2002) http://www.epa.gov/globalwarming/climate/

Estrada-Peña A (1998). Geostatistics and remote sensing as predictive tools of tick distribution: a cokriging system to estimate *Ixodes scapularis* (Acari: Ixodidae) habitat suitability in the United States and Canada from advanced very high resolution radiometer satellite imagery. *J Med Ent*, **35**: 989-995.

Eurostat (2002). http://europa.eu.int/comm/eurostat/

Eurosurveillance (1998). Surveillance of malaria in European Union countries. *European communicable disease bulletin*, **3**: 45-52.

Ewart WM (1897). On the decrease of ague and aguish affections in London. *Journal of Balneology and Climatology*, **1**: 24-48.

Focks DA, Haile DG, Daniels E and Mount GA (1993a). Dynamic life table model for *Aedes aegypti* (Diptera: Culicidae): Analysis of the literature and model development. *J Med Ent*, **30**: 1003-1017.

Focks DA, Haile DG, Daniels E and Mount GA (1993b). Dynamic life table model for *Aedes aegypti* (Diptera: Culicidae): Simulation results and validation. *J Med Ent*, **30**: 1018-1028.

Focks DA, Daniels E, Haile DG and Keesling JE (1995). A simulation model of the epidemiology of urban dengue fever: literature analysis, model development, preliminary validation and samples of simulation results. *Am J Trop Med Hyg*, **53**: 489-506.

Gardner G (1998). Many climate change scientists do not agree that global warming is happening. ***BMJ*, 316**: 1164.

Garrett-Jones C, Boreham PFL and Pant CP (1980). Feeding habits of anophelines (Diptera: Culicidae) in 1971-78 with reference to the human blood index. *Bull Ent Res*, **70**:165-185.

Giacomini T, Axler O, Mouchet J, Lebrin P, Carlioz R, Paugam B, Brassier D, Donetti L, Giacomini F, andVachon F (1997). Pitfalls in the diagnosis of airport malaria. Seven cases observed in the Paris area in 1994. *Scand J Infect Dis*, **29**: 433-5

Gill CA (1920-21). Malaria in England with special reference to the role of temperature and humidity. *J Hyg*, **19-20**: 320-332.

Gill CA (1921). The role of meteorology in malaria. *Ind J Med Res*, **8**: 633-693.

Gleiser RM, Gorla DE and Ludueña Almeida FF (1997). Monitoring the abundance of *Aedes (Ochlerotatus) albifasciatus* (Macquart 1838) (Diptera: Culicidae) to the south of Mar Chiquita Lake, central Argentina with the aid of remote sensing. *Ann Trop Med Parasit*, **91**: 917-926.

Gockchinar T and Kalipsi S (2001).[Current malaria situation in Turkey]. *Med Parazitol Mosk*, **1**: 44-45.

Gothe R, Nolte I and Kraft W (1997). Leishmaniose des Hundes in Deutschland: epidemiologische Fallanalyse und Alternative zur bisheringen kausalen Therapie. *Tierärztl Prax*, **25**: 68-73.

Greenwood B and Mutabingwaa T (2002). Malaria in 2002. *Nature*, **415**: 670-672.

Guillet P, Germain MC, Giacomini T, Chandre F, Akobeto M, Faye O, Kone A, Manga L and Mouchet J (1998). Origin and prevention of airport malaria in France. *Trop Med Int Health*, **3**: 700-705.

Hackett LW (1934). The present status of our knowledge of the subspecies of *Anopheles maculipennis*. *Trans R Soc Trop Med Hyg*, **28**: 109-128.

Hackett LW (1937). Malaria in Europe: an ecological study. *Oxford University Press, Oxford.*

Hackett LW (1949). Conspectus of malaria incidence in northern Europe, the Mediterranean region and the near east. In *(ed. MF Boyd.) Malariology; a comprehensive survey of all aspects of this group of diseases from a global standpoint. Saunders Company, London.*

Hackett LW and Missiroli A (1931). The natural disappearance of malaria in certain regions of Europe. *Am J Hyg*, **13**: 57-78.

Hackett LW and Missiroli A (1935). The varieties of *An. maculipennis* and their relation to the distribution of malaria in Europe. *Riv Mal*, **14**: 45-109.

Haines A (1998). Global warming and vector-borne disease. *Lancet*, **351**: 1737-1738.

Haines A and Parry M (1993). Climate change and human health. *J Roy Soc Med*, **86**: 707-711.

Haines A, McMichael AJ, Kovats RS and Saunders M (1998). Majority view of climate scientists is that global warming is indeed happening. *BMJ*, **316**: 1530.

Hadjinicolaou J and Betzios B (1972). Biological studies of *Anopheles sacharovi* Favr in Greece. *WHO.*

Hadley Centre (2002a). (http://www.met-office.gov.uk/research/hadleycentre/models/HadCM3.html.)

Hadley Centre (2002b) http://www.met-office.gov.uk/research/hadleycentre/models/modeldata.html).

Halstead SB and Papaevangelou G (1980). Transmission of dengue 1 and 2 viruses in Greece in 1928. *Am J Trop Med Hyg*, **29**: 637-637.

Hansen J, Sato M, Glascoe J and Ruedy R (1998). A common-sense climate index: is climate changing noticeably? *Proc Natl Acad Sci*, **95**: 4113-4120.

Hartshorne H (1881). Essentials of the principles and practice of medicine. A handbook for students and practitioners. *Smith, Elder & Co., London.*

Hassan AN, Dister SW and Beck LR (1998a). Spatial analysis of lymphatic filariasis distribution in the Nile Delta in relation to some environmental variables using geographical information system technology. *J Egypt Soc Parasitol*, **28**: 119-131.

Hassan AN, Beck LR and Dister SW (1998b) . Prediction of villages at risk for filariasis transmission in the Nile Delta using remote sensing and geographic information technologies. *J Egypt Soc Parasitol*, **28**: 75-87.

Hay SI (2001). The world of smoke, mirrors and climate change. *Trends Parasitol*, **17**: 466.

Hay SI, Tucker CJ, Rogers DJ and Packer MJ (1996). Remotely sensed surrogates of meteorological data for the study of the distribution and abundance of arthropod vectors of disease. *Ann Trop Med Parasitol*, **90**:1-19

Hay SI, Snow RW and Rogers DJ. (1998). Predicting malaria seasons in Kenya using multitemporal meteorological satellite sensor data. *Trans R Soc Trop Med Hyg*, **92**: 12-20.

Hay SI and Lennon JJ (1999). Deriving meteorological variables across Africa for the study and control of vector-borne disease: a comparison of remote sensing and spatial interpolation of climate. *Trop Med Int Health*, **4**: 58-71.

Hay SI, Omumbu JA, Craig MH and Snow RW (2000a). Earth observation, geographic information systems and *Plasmodium falciparum* malaria in Sub-Saharan Africa. *Adv Parasitol*, **47**: 174-216.

Hay SI, Myers MF, Burke DS, Vaughn DW, Endy T, Ananda N, Shanks GD, Snow RW and Rogers DJ (2000b). Etiology of interepidemic periods of mosquito-borne disease. *Proc Natl Acad Sci USA*,.**97**: 9335-9.

Hay SI, Rogers DJ, Toomer JF and Snow RW (2000c). Annual *Plasmodium falciparum* entomological inoculation rates (EIR) across Africa. I. Literature survey, internet access and review. *Trans R Soc Trop Med Hyg*, **94**: 113-127.

Hay SI, Cox J, Rogers DJ, Randolph SE, Stern DI, Shanks GD, Myers MF and Snow RW (2002). Climate change and the resurgence of malaria in the East African highlands. *Nature*, **415**: 905-909.

Hendrickx G, Napala A, Dao B, Batawui D, De Deken R, Vermeilen A and Slingenbergh JHW (1999). A systematic approach to area-wide tsetse distribution and abundance maps. *Bull Ent Res*, **89**: 231-244.

Hewitt S, Kamal M, Muhammad N and Rowland M (1994). An entomological investigation of the likely impact of cattle ownership on malaria in an Afghan refugee camp in the North West Frontier Province of Pakistan. *Med Vet Entomol*, **8**:160-164.

Hightower AW, Ombrok M, Otieno R, Odhiambo R, Oloo AJ, Lal AA, Nahlen BI and Hawley WA (1998). A geographic information system applied to a malaria field study in Western Kenya. *Am J Trop Med Hyg*, **58**: 266-272.

Hirsch A (1883). Handbook of geographical and historical pathology. Volume I: Acute infective diseases. *The New Sydenham Society, London.*

Holvoet G, Michielsen P and Vandepitte J (1983). Autochtonous falciparum malaria in Belgium. *Ann Soc Belge Med Trop*, 63: 111-117.

Hulme M and Jenkins GJ (1998). Climate Change scenarios for the United Kingdom: Summary Report. UKCIP Technical Report. *Climatic Research Unit, Norwich.*

Humphreys M (2001). Malaria. Poverty race and public health in the United States. *The Johns Hopkins University Press, Baltimore and London.*

Ijumba JN and Lindsay SW (2001). Impact of irrigation on malaria in Africa: paddies paradox. *Med Vet Entomol*, **15**:1-11.

IPCC (2000). Emissions Scenarios. Special Report of the Intergovernmental Panel on Climate Change. Nebojsa Nakicenovic and Rob Swart (Eds.). Cambridge University Press, Cambridge, UK.

IPCC (2001) Climate Change 2001: Impacts, Adaptation and Vulnerability". James J. McCarthy, Osvaldo F. Canziani, Neil A. Leary, David J. Dokken and Kasey S. White (Eds.) Cambridge University Press, Cambridge, UK.

Jackson EK (1995). Climate change and global infectious disease threats. *Med J Australia*, **163**: 570-574.

Jaenson TGT, Lokki J and Saura A (1986). *Anopheles* (Diptera: Culicidae) and malaria in northern Europe, with special reference to Sweden. *J Med Entomol*, **23**: 68-75.

James SP (1920). Malaria at home and abroad. *John Bale, Sons and Danielssson, London.*

James SP (1929). The disapperance of malaria from England. *Proc R Soc Med*, **23**: 71-85.

James SP (1931). Some general results of a study of induced malaria in England. *Trans R Soc Trop Med Hyg*, **24**: 477-538.

James SP, Nicol WD and Shute PG (1932). A study of indicted malignant tertian malaria. *Proc R Soc Med*, **25**:1153-1181.

Jetten TH and Takken W (1994). Anophelism without malaria in Europe: A review of the ecology and distribution of the genus *Anopheles* in Europe. *Wageningen agricultural university, The Netherlands.*

Jetten TH and Focks DA (1997). Potential changes in the distribution of dengue transmission under climate warming. *Am J Trop Med Hyg*, **57**: 285-297.

Jetten TH, Martens WJM and Takken W (1996). Model simulations to estimate malaria risk under climate change. *J Med Entomol*, **33**: 361-371.

Jones WHS (1907). Malaria: a neglected factor in the history of Greece and Rome. *MacMillan and Bowes, Cambridge.*

Kalkstein LS and Greene JS (1997). An evaluation of climate/mortality relationships in large US cities and the possible impacts of a climate change. *Env Health Perspec*, **105**: 84-93.

Kampen H, Maltezos E, Pagonaki M, Hunfeld KP, Maier WA and Seitz HM (2002). Individual cases of autochtonous malaria in Evros Province, northern Greece: serological aspects. *Parasitol Res*, **88**: 261-266.

Karch S, Monteny N , Jullien JL, Sinegre G and Coz J (1990). Control of *Culex pipiens* by *Bacillus sphaericus* and role of nontarget arthropods in its recycling. *J Am Mosq Control Assoc*, 6; 47-54.

Kasap H (1987). Development of *Plasmodium vivax* in *Anopheles superpictus* under experimental conditions. *Am J Trop Med Hyg*, **37**: 241-245.

Kasap H (1990). Comparison of experimental infectivity and development of *Plasmodium vivax* in *Anophles sacharovi* and *An. superpictus* in Turkey. *Am J Trop Med Hyg*, **42**: 111-117.

Katsouyanni K, Trichopoulos D, Zavitsanos X and Touloumi G. (1988). The 1987 Athens heatwave. *Lancet*, **2**: 573.

Kitron U and Kazmierczak JJ (1997). Spatial analysis of the distribution of Lyme disease in Wisconsin. *Am J Epid*, **145**: 558-566.

Kitron U, Pener H, Costin C, Orshan L, Greenberg Z and Shalom U (1994). Geographic Information Systems in malaria surveillance: mosquito breeding and imported cases in Israel, 1992. *Am J Trop Med Hyg*, **50**:550-556.

Kitron U, Michael J, Swanson J and Haramis L (1997). Spatial analysis of the distribution of LaCrosse encephalitis in Illinois, using a GIS and local and global spatial statistics. *Am J Trop Med Hyg*, **57**: 469-475.

Kleinschmidt I, Bagayoko M, Clarke GPY, Craig M and le Sueur D (2000). A spatial statistical approach to malaria mapping. *Int J Epid*, **29**: 355-361.

Kleinschmidt I, Omumbo J, Briet O, van de Giesen, Sogoba N, Kumasenu Mensah N, Windmeijer P, Moussa M and Teuscher T (2001a). An empirical malaria distribution map for West Africa. *Trop Med Int Health*, **6**: 779-786.

Kleinschmidt I, Sharp BL, Clarke GP, Curtis B and Fraser C (2001b). Use of generalized linear mixed models in the spatial analysis of small-area malaria incidence rates in Kwazulu Natal, South Africa. *Am J Epidemiol,* **153**: 1213-21

Kligler IJ and Mer G (1937). Studies on the effect of various factors on the infection rate of *Anopheles elutus* with different spcies of *Plasmodium*. *Ann Trop Med*, **31**: 71-83.

Knudsen AB, Romi R and Majori G (1996). Occurrence and spread in Italy of *Aedes albopictus*, with implications for its introduction into other parts of Europe. *J Am Mosq Control Assoc*, **12**: 177-83

Kovats RS, Haines A, Stanwell-Smith R, Martens P, Menne B and Bertollini R (1999). Climate change and human health in Europe. *BMJ*, **318**: 1682-1685.

Kovats RS, Campbell-Lendrum DH, McMichael AJ, Woodward A and Cox J St H (2001). Early effects of climate change: do they include changes in vector-borne diseases? *Phil Trans R Soc Lond B*, **356**: 1057-1068.

Kruger A, Rech A, Su XZ and Tannich E (2001). Two cases of autochthonous *Plasmodium falciparum* malaria in Germany with evidence for local transmission by indigenous *Anopheles plumbeus*.*Trop Med Int Health*, **6**: 983-5.

Kuhn KG (1997). Climatic predictors of the abundance of sandfly vectors and the incidence of leishmaniasis in Italy. *MSc thesis, University of London.*

Kuhn KG (1999). Global warming and leishmaniasis in Italy. *Bull Trop Med Int Health*, **2**: 1-2.

Leeson HS (1939). Longevity of *Anopheles maculipennis* race *atroparvus*, van Thiel, at controlled temperature and humidity after one blood meal. *Bull Ent Res*, **30**: 295-301.

Lindblade KA, Walker ED, Onapa AW, Katungu J and Wilson ML (2000). Land use change alters malaria transmission parameters by modifying temperature in a highland area of Uganda. *Trop Med Int Health*, **5**: 263-74

Lindgren E, Tälleklint L and Polfeldt T (2000). Impact of climatic change on the northern latitude limit and population density of the disease-transmitting European tick *Ixodes ricinus*. *Env Health Perspect*, **108**:119-123

Lindsay SW and Birley MH (1996). Climate change and malaria transmission. *Ann Trop Med Parasit*, **90**: 573-588.

Lindsay SW and Martens P (1998). Malaria in the African highlands: past, present and future. *Bull WHO*, **76**: 33-45.

Lindsay SW, Parson L and Thomas CJ (1998). Mapping the ranges and relative abundance of the two principal African malaria vectors, *Anopheles gambiae* sensu stricto and *An. arabiensis*, using climate data. *Proc. R. Soc. London. B.*, **265**: 847-854.

Lindsay SW and Joyce A (2000). Climate change and the disappearance of malaria from England. *Global Change & Human Health*, **1**: 184-187.

Lindsay SW and Thomas CJ (2000). Mapping and estimating the population at risk from lymphatic filariasis in Africa. *Trans R Soc Trop Med Hyg*, **94**: 37-44.

Lindsay SW and Thomas CJ (2001). Global warming and risk of vivax malaria in Great Britain. *Global Change & Human Health*, **2**: 80-84.

Linthicum KJ, Bailey CL, Davies FG and Tucker CJ (1987). Detection of rift valley fever viral activity in Kenya by satellite remote sensing imagery. *Science*, **235**: 1656-1659.

Linthicum KJ, Bailey CL, Tucker CJ, Mitchell KD, Logan TM, Davies FG, Kamau CW, Thande PC and Wagateh JN (1990). Application of polar-orbiting,

meteorological satellite data to detect flooding of Rift Valley Fever virus vector mosquito habitats in Kenya. *Med Vet Entomol*, 4: 433-8

Loevinsohn M (1994). Climatic warming and increased malaria incidence in Rwanda. *Lancet*, **343**: 714-718.

Lörincz F (1937). Malaria in Hungary. *Riv Malariologia*, **16**: 465-479.

Lwambo NJ, Siza JE, Brooker S, Bundy DA and Guyatt H (1999). Patterns of concurrent hookworm infection and schistosomiasis in schoolchildren in Tanzania. *Trans R Soc Trop Med Hyg*, **93**: 497-502.

MacArthur W (1951). A brief story of English malaria. *Brit med Bull*, **8**: 76-79.

MacDonald A (1920). On the relation of temperature to malaria in England. *J R Army Med Corps*, **35**: 99-119.

Malone JB, Huh OK, Fehler DP, Wilson PA, Wilensky DE Holmes RA and Elmagdoub AI (1994). Temperature data from satellite imagery and the distribution of schistosomiasis in Egypt. *Am J Trop Med Hyg*, **50**: 714-722.

Manson P (1987). Manson's tropical diseases.*Bailliere Tindall, London.*

MARA/ARMA (1998). Towards an atlas of malaria risk in Africa: first technical report of the MARA/ARMA collaboration. *MARA/ARMA. Durban, South Africa.*

Marchant P, Eling W, van Gemert GJ, Leake CJ and Curtis CF (1998). Could British mosquitoes transmit falciparum malaria. *Parasitol Today*, **14**:344-345.

Marchi A and Munstermann LE (1987). The mosquitoes of Sardinia: species records 35 years after the malaria eradication campaign. *Med Vet Ent*, **1**: 89-96.

Martens P (1998). Health impacts of climate change and ozone depletion: An ecoepidemiologic modelling approach. *Env Health Perspect*, **106**: 241-251 (S).

Martens P, Niessen LW, Rotmans J, Jetten TH and McMichael AJ (1995). Potential impact of global climate change on malaria risk. *Env Health Perspect*, **103**:458-464.

Martens P, Kovats RS, Nijhof S, de Vries P, Livermore MTJ, Bradley DJ, Cox J and McMichael AJ (1999). Climate change and future populaitons at risk of malaria. Global Env Change,9: S89-S107

Martin PH and Lefebvre MG (1995). Malaria and climate: sensitivity of malaria potential transmission to climate. *Ambio*, **24**: 200-207.

Martini E, Mayer F and Weyer F (1932). Über die durchwinterung unserer *Anopheles maculipennis. Riv Mal*, **11**; 753-784.

Massad E and Forattini OP (1998). Modelling the temperature sensitivity of some physiological parameters of epidemiologic significance. *Ecosystem Health*, **4**: 119-129.

McDonald G (1957). The epidemiology and control of malaria. *Oxford University Press, Oxford.*

McHugh CP (1989). Ecology of a semi-isolated poulation of *Anopheles freeborni*: Abundance, trophic status, parity, survivorship, gonotrophic cycle length and host selection. *Am J Trop Med Hyg*, **41**: 169-176.

Meller H (1962). Vergleichende beobachtungen uber die biologie von *Anopheles atroparvus* und *Anopheles stephensi* unter laboratoriumsbedingungen. *Z Trop Med Par*, **13**: 80-102.

Mellor PS and Leake CJ (2000). Climatic and geographic influences on arboviral infections and vectors. *Rev sci tech off int epiz*, **19**: 41-54.

Mendis K, Sina BJ, Marchesini P and Carter R (2001). The neglected burden of *Plasmodium vivax* malaria. *Am J Trop Med Hyg*, **64**: 97-106.

Menzel A and Fabian P (1999). Growing season extended in Europe. *Nature*, **397**: 659.

Michaels P (1993). Conspiracy, consensus or correlation? What scientists think about the 'popular vision' of global warming. *World Clim Rev*, **1**:11.

Milligan PJM and Baker RD (1988). A model of tse-tse transmitted animal trypanosomiasis. *Parasitology*, **96**: 211-239.

Mingaleva GN and Artem'ev MM (1993). [The seasonal course in the population count of *Anopheles* in northern Tajikistan] *Med Parazitol Mosk*, **4**: 38-40.

Molineux L (1988). The epidemiology of human malaria as an explanation of its distribution, including some implications for its control. In *Malaria; Principles and practice of malariology. Eds. Wernsdorfer WH and McGregor I. Churchill Livingstone, Edinburgh.*

Molineaxu L and Gramiccia G (1980). Le projet Garki. World Health Organisation, Geneva.

Molyneux DH (1997). Patterns of change in vector-borne diseases. *Ann Trop Med Parasit*, **91**:827-839.

Monteiro C, Rueff J, Falcao AB, Portugal S, Weatherall DJ and Kulozik AE (1989). The frequency and origin of the sickle cell mutation in the district of Coruche/Portugal. *Hum Genet*, **82**: 255-8

Morrison AC, Getis A, Santiago M, Rigau-Perez JG and Reiter P (1998). Exploratory space-time analysis of reported dengue cases during an outbreak in Florida, Puerto Rico, 1991-1992. *Am J Trop Med Hyg*, **58**: 287-298.

Mosna E (1937). Sulle caratteristiche termiche dei focolai di *Anopheles maculipennis*. *Riv Parassit*, **1**:139-153.

Mott KE, Nuttall I, Desjeux P and Cattand P (1995). New geographical approaches to control of some parasitic zoonoses. *Bull WHO*, **73**: 247-257.

Mouchet J, Manguin S, Sircoulon J, Laventure S, Faye O, Onapa AW, Carnevale P, Julvez J and Fontenille D (1998). Evolution of malaria in Africa for the past 40 years: impact of climatic and human factors. *J Am Mosq Control Assoc*, **14**:121-30

New M, Hulme M and Jones P (2000). Representing twentieth century space-time climate variability. II: Development of 1901-1996 monthly grids of terrestrial surface climate. *J Climate*, **13**: 2217-2238.

Nicholls A (1997). Fenland ague in the nineteenth century. BSc dissertation.

Nicholls A (2000). Fenland ague in the nineteenth century. *Med Hist*, **44**: 513-530.

Nicholson MC and Mather TN (1996). Methods for evaluating Lyme disease risks using geographic information systems and geospatial analysis. *J Med Ent*, **33**: 711-720.

Nicolaiciuc D, Popa MI and Popa L (1999). Malaria in the whole world and Romania. *Roum Arch Microbiol Immunol*, **58**:289-96.

Nikolaeva N (1996). Resurgence of malaria in the former Soviet Union (FSU). *Unpublished.*

Nuttall GH, Cobbett L and Strangeways-pigg T (1901). Studies in relation to malaria. The geographical distribution of *Anopheles* in relation to the former distribution of ague in England. *J Hyg*, **1**: 4-44.

Olivaria J and Hill RB (1935). Algunos datos sobre las preferencias hematicos de las *A. maculipennis*. *Med de los Paises Calidos*, **8**: 169.

Omumbo J, Ouma J, Rapouda B, Craig MH, le Sueur D and Snow RW (1998). Mapping malaria transmission intensity using geographical information systems GIS), an example from Kenya. *Ann Trop Med Parasit*, **92**: 7-21.

Parmesan C (1996). Climate and species range. *Nature*, **382**: 765-766.

Parry M, Rosenzweig C, Iglesias A, Fischer G and Livermore M (1999). Climate change and world food security: a new assessment. *Global Env Change*, **9**: S51-S67.

Patz JA and Lindsay SW (1999). New challenges, new tools: the impact of climate change on infectious diseases. *Curr Opin Microbiol*, **2**: 445-451.

Patz JA, Martens WJM, Focks DA and Jetten TH (1998). Dengue fever epidemic potential as projected by general circulation models of global climate change. *Env Health Perspec*, **106**: 147-153.

Perry BD, Lessard P, Norval RAI, Kundert K and Kruska R (1990). Climate, vegetation and the distribution of *Rhipicephalus appendiculatus* in Africa. *Parasitol Today*, **6**: 100-104.

Phillips A, Sabatini A, Milligan PJM, Boccolini D, Broomfield G and Molyneux DH (1990). The *Anopheles maculipennis* complex (Diptera: Culicidae): comparison of the cuticular hydrocarbon profiles determined in adults of five Palaearctic species. *Bull Ent Res*, **80**: 459-464.

Pires CA, Ribeiro H, Capela RA and Ramos HDC (1982). Research on the mosquitoes of Portugal (Diptera, Culicidae) VI – The mosquitoes of Alentejo. *An Inst Hig Med Trop*, **8**: 79-102.

Postiglione M, Tabanli S and Ramsdale CD (1973). The *Anopheles* of Turkey. *Riv Parassit*, *34*: 127-159.

Poveda G, Rojas W, Quinones ML, Velez ID, Mantilla RI, Ruiz D, Zuluaga JS and Rua GL (2001). Coupling between annual and ENSO timescales in the malaria-

climate association in Colombia. *Environ Health Perspect*,**109**: 489-493.

Proft J, Maier WA and Kampen H (1999). Identification of six sibling species of the *Anopheles maculipennis* complex (Diptera: Culicidae) by a polymerase chain reaction assay. *Parasitol Res*, 85: 837-843.

Ramsdale CD and Couzzi M (1975). Studies on the infectivity of tropical African strains of *Plasmodium falciparum* to some southern European vectors of malaria. *Parassitologia* **17**: 39-44.

Ramsdale CD and Haas E (1978),. Some aspects of the epidemiology of resurgent malaria in Turkey. *Trans R Soc Trop Med Hyg*, **72**: 570-580.

Ramsdale CD and Wilkes TJ (1985). Some aspects of overwintering in southern England of the mosquitoes *Anopheles atroparvus* and *Culiseta annulata* (Diptera: Culicidae). *Ecol Ent*, **10**: 449-454.

Ramsdale CD and Snow KR (1995). Mosquito control in Britain. *University of East London, Dagenham, Essex.*

Randolph SE (1993). Climate, satellite imagery and the seasonal abundance of the tick *Rhipicephalus appendiculatus* in southern Africa: a new perspective. *Med Vet Ent*, **7**: 243-258.

Randolph SE (1994). Population dynamics and density-dependent seasonal mortality indices of the tick *Rhipicephalus appendiculatus* in eastern and southern Africa. *Med Vet Ent*, **8**: 351-368.

Randolph SE (1997). Abiotic and biotic determinants of the seasonal dynamics of the tick *Rhipicephalus appendiculatus* in South Africa. *Med Vet Ent*, **11**: 25-37.

Randolph SE (2001). The shifting landscape of tick-borne zoonoses: tick-borne encephalitis and Lyme borreliosis in Europe. *Phil Trans R Soc Lond B*, **356**: 1045-1056.

Randolph SE and Craine NG (1995). General framework for comparative quantitative studies on transmission of tick-borne diseases using Lyme borreliosis in Europe as an example. *J Med Entomol*, **32**: 765-777.

Randolph SE and Rogers DJ (1997). A generic population model for the African tick *Rhipicephalus appendiculatus*. *Parasitology*, **113**: 265-279.

Razakov SA and Shakhgunova GS (2001). [Current malaria situation in the Republic of Uzbekistan] *Med Parazitol Mosk*, **1**: 39-41.

Reiter P (1998 a). Global warming and vector-borne disease in temperate regions and at high altitude. *Lancet*, **351**: 839-840.

Reiter P (1998 b). Global warming and vector-borne disease. *Lancet*, **351**: 1738.

Reiter P (2000). From Shakespeare to Defoe: Malaria in England in the Little Ice Age. *Emerg Inf Dis*, **6**: 1-11.

Reiter P (2001). Climate change and mosquito-borne disease. *Environ Health Perspect*, **109**: S141-S161.

Rejmankova E, Roberts DR, Pawley A, Mauguin S and Polanco J (1995). Predictions of adult *Anopheles albimanus* densities in villages based on distances to remotely sensed larval habitats. *Am J Trop Med Hyg*, **53**: 482-488.

Richards FO Jr (1993). Use of Geographic Information Systems in control programs for Onchocerciasis in Guatemala. *Bull PAHO*, **27**: 52-55.

Riera Palmero J (1994). Work, rice and malaria in Valencia in the XVIIIth century. *Physis Riv Int Stor Sci*; **31**:771-85.

Roberts DR, Paris JF, Mauguin S, Harbach RE, Woodruff R, Rejmankova E, Polanco J, Wullschleger B and Legters LJ (1996). Predictions of malaria vector

distribution in Belize based on multispectral satellite data. *Am J Trop Med Hyg*, **54**: 304-308.

Robinson TP (1997). Practical applications of geographic information systems in tsetse and trypanosomiasis control. *International Symposium on diagnosis and control of livestock diseases using nuclear and related techniques. "Towards disease control in the 21st century".* **IAEA-SM-348.**

Robinson TP (1998). Geographic information systems and the selection of priority areas for control of tsetse-transmitted trypanosomiasis in Africa. *Parasitol Today*, **14**: 457-461.

Robinson T, Rogers DJ and Williams B (1997). Mapping tsetse habitat suitability in the common fly belt of Southern Africa using multivariate analysis of climate and remotely sensed vegetation data. *Med Vet Ent*, **11**: 235-245

Rodgriguez AD, Rodriguez MH, Hernandez JE, Dister SW, Beck LR, Rejmankova E and Roberts DR (1996). Landscape surrounding human settlements and malaria mosquito abundance in southern Chiapas, Mexico. J Med Entomol, 33:39-48.

Rogers DJ (1988). A general model for the African trypanosomiases. *Parasitology*, **97**: 193-212.

Rogers DJ (1996). Regional impacts of climate change; changes in disease vector distributions. In *M. Hulme (ed.) Climate change and Southern Africa: an exploration of some potential impacts and implications in the SADC region.* University of East Anglia, Norwich.

Rogers DJ (2000). Satellites, space, time and African trypanosomiasis. *Adv Parasitol*, **47**: 129-171.

Rogers DJ and Randolph SE (1993). Distribution of tsetse and ticks in Africa: Past, present and future. *Parasitol Today*, **9**: 266-271

Rogers DJ and Williams B (1994). Tsetse distribution in Africa: seeing the wood and the trees. In *Large-scale ecology and conservation biology (eds. PJ Edwards, R May and NR Webb) The 35th Symposium of the British Ecological Society with the Society for Conservation Biology University of Southampton. Blackwell Scientific Publications, London.*

Rogers DJ and Randolph SE (2000). The global spread of malaria in a future, warmer world. *Science*, **289**:1763-1766.

Rogers DJ, Hay SI and Packer MJ (1996). Predicting the distribution of tsetse flies in West Africa using temporal Fourier processed meteorological satellite data. Ann Trop Med Parasitol, 90: 225-241.

Rogers DJ, Randolph SE, Snow RW and Hay SI (2002). Satellite imagery in the study and forecast of malaria. *Nature*, **415**: 710-715.

Roll Back Malaria (2002). http://www.rbm.who.int/newdesign2/

Romi R (1995). History and updating on the spread of *Aedes albopictus* in Italy. *Parassitologia*, **37**: 99-103

Romi R, Di Luca M and Majori G (1999). Current status of Aedes albopictus and Aedes atropalpus in Italy. *J Am Mosq Control Assoc*, **15**: 425-427.

Romi R, Sabatinelli G and Majori G (2001). Could malaria reappear in Italy? *Emerg Inf Dis*, **7**: 915-919.

Romi R, Pierdominici G, Severini C, Tamburro A, Cocchi M, Menichetti D, Pili E and Marchi A (1997a). Status of malaria vectors in Italy. *J.Med Entomol*, **34**:263-271.

Romi R, Sabatinelli G, Savelli LG, Raris M, Zago M and Malatesta R. (1997b). Identification of a North American mosquito species, *Aedes atropalpus* (Diptera: Culicidae), in Italy. *J Am Mosq Control Assoc*,**13**:245-6

Rooney C, McMichael AJ, Kovats RS and Coleman M. (1998). Excess mortality in England and Wales, and in Greater London, during the 1995 heatwave. *J Epidemiol Community Health*, **52**: 482 –492.

Rosa A (1936). Sulla durata di vita della varieta di *Anopheles maculipennis*. *Riv Mal*, **15**: 399-403.

Ross R (1921). Malignant malaria contracted in Britain. *BMJ*, **1**: 871.

Sabatinelli G, Ejov M and Jørgensen P (2000). Malaria in the WHO European Region (1971-1999). *Euro Surveill*, **6**: 61-5

Saez M, Sunyer J, Castellsague J, Murillo C and Anto JM (1995). Relationship between weather temperature and mortality: a time series analysis approach in Barcelona. *Int J Epidemiol*, **24**: 576-582.

Schaefer M, Sotrch V, Kaiser A, Beck M and Becker N (1997). Dispersal behavior of adult snow melt mosquitoes in the Upper Rhine Valley, Germany. *J Vector Ecol*, **22**: 1-5.

Schellenberg JA, Newell JN, Snow RW, Mungala V, Marsh K, Smith PG and Hayes RJ (1998). An analysis of the geographical distribution of severe malaria in children in Kilifi District, Kenya. *Int J Epid*, **27**: 323-329.

Sellers RF (1980). Weather, host and vector; their interplay in the spread of insect-borne animal virus diseases. *J Hyg*, **85**: 65-102.

Service MW (1968). Observations on the ecology of some British mosquitoes. *Bull Ent Res*, **59**: 161-194.

Service MW (1993). The *Anopheles* vector. In *Bruce-Chwatt's essential malariology (eds. Gilles HM and Warrell DA). Arnold, London.*

Shanks GD, Biomndo K, Hay SI and Snow RW (2000). Changing patterns of clinical malaria since 1965 among a tea estate population located in the Kenyan highlands. *Trans R Soc Trop Med Hyg*, **94**: 253-5

Sharma VP, Dhiman RC, Ansari MA, Nagpal BN, Srivastava A, Manavalan P, Adiga S, Radhakrishnan K and Chandrasekhar MG (1996). Study on the feasibility of delineating mosquitogenic conditions in and around Delhi using Indian remote sensing satellite data. *Ind J Malariol*, **33**: 107-125.

Shlenova MF (1938). La vitesse de la digestion sanguine chez *A. maculipennis* messeae a des temperatures reellement stables. *Med Parazitol Mosk*, **7**: 716-735.

Shute PG (1940). Failure to infect English specimens of *Anophels maculipennis* var. *atroparvus* with certain strains of *Plasmodium falciparum* of tropical origin. *J Trop Med Hyg*, **43**:175.

Shute PG and Ungureanu E (1939). Preliminary report of the longevity of the races of *Anopheles maculipennis*. *WHO.*

Shute PG and Maryon M (1974). Malaria in England, past, present and future. *J R Soc Health*, **94**: 23-49.

Singh RB, Hales S, de Wet N, Raj R, Hearnden M and Weinstein P (2001). The influence of climate variation and change on diarrheal disease in the Pacific Islands. *Env Health Perspect*, **109**:155-159.

Smith WDL (1956). Malaria and the Thames. *Lancet*, **1**: 433-436.

Smith T, Charlwood JD, Takken W, Tanner M, Spiegelhalter DJ (1995). Mapping the densities of malaria vectors within a single village. *Acta Trop*, **59**:1-18

Snow RW, Gouws E, Omumbo J, Rapouda B, Craig MH, Tanser FC, le Sueur D and Ouma J (1998). Models to predict the intensity of Plasmodium falciparum

transmission: applications to the burden of disease in Kenya. *Trans R Soc Trop Med Hyg*, **92**: 601-606.

Snow RW, Craig MH, Deichmann U and le Sueur D (1999). A preliminar continental risk map for malaria mortality among African children. *Parasitol Today*, **15**: 99-104.

Stott PA and Kettleborough JA (2002). Origins and estimates of uncertainty in predictions of twenty-first century temperature rise. *Nature*, **416**: 723-726.

Sutherst RW (1998). Implications of global change and climate variability for vector-borne diseases: generic approaches to impact assessments. *Int J Parasit*, **28**: 935-945.

Sutherst RW, Maywald GF and Skarrat DB (1995). Predicting insect distributions in a changed climate. In *Insects in a Changing Environment..(eds Harrington, R. & Stork, N.E). 17th Symposium of the Royal Entomological Society, 7-10th September 1993 at Rothamsted Experimental Staion, Harpenden. Academic Press, London.*

Swellengrebel NH and de Buck A (1938). Malaria in the Netherlands. *Scheltema and Holkema, Amsterdam.*

Takken W, Geene R, Adam W, Jetten TH and van der Velden J (2002). Distribution and dynamics of larval populations of *Anopheles messeae* and *A. atroparvus* in the delta of the rivers Rhine and Meuse, the Netherlands. *Ambio*, **31**: 212-218.

Talbor RS (1672). Pyretologia : a rational account of the cause & cure of agues, with their signes, diagnostick & prognostick. *R.R Robinson, London.*

Talleklint L and Jaenson TGT (1998). Increasing geographical distribution and density of *Ixodes ricinus* (Acari: Ixodidae) in central and southern Sweden. *J Med Entomol*, **35**: 521-526.

Tanner TH (1854). A manual of the practice of medicine. *Henry Renshaw, London.*

Tanner TH (1865). A manual of the practice of medicine. *Henry Renshaw, London.*

Taylor F (1891). A manual of the practice of medicine. *J & A. Churchill, London.*

Taylor F (1893). A manual of the practice of medicine. *J & A. Churchill, London.*

Taylor F (1894). A manual of the practice of medicine. *J & A. Churchill, London.*

Thomas CD and Lennon JJ (1999). Birds extend their ranges northwards. *Nature, 399*: 213.

Thomas CJ and Lindsay SW (1999). Local-scale variation in malaria infection amongst rural Gambian children estimated by satellite remot sensing. *Trans R Soc Trop Med Hyg*, **94**: 159-163.

Thomson MC and Connor SJ (2000). Environmental information systems for the control of arthropod vectors of disease.*Med Vet Ent*, **14**: 227-244.

Thomson MC, Connor SJ and Flasse SP (1996). The ecology of malaria - as seen from Earth-observation satellites. *Ann Trop Med Parasit*, **90**: 243-264.

Thomson MC, Connor, SJ and Flasse SP (1997). Mapping malaria risk in Africa: what can satellite data contribute? *Parasitol Today*, **13**: 313-318.

Thomson MC, Elnaiem DA, Ashford RW and Connor SJ (1999a). Towards a kala azar risk map for Sudan: mapping the potential distribution of *Phlebotomus orientalis* using digital data of environmental variables. *Trop Med Int Health*,**4**:105-13

Thomson MC, Connor SJ, D'Alessandro U, Rowlingson B, Diggle P, Cresswell M and Greenwood B (1999b). Predicting malaria infection in Gambian children from satellite data and bed net use surveys: the importance of spatial correlation in the interpretation of results. *Am J Trop Med Hyg*, **61**: 2-8.

Thomson MC, Obsomer V, Dunne M, Connor SJ and Molyneux DH (2000). Satellite mapping of Loa loa prevalence in relation to ivermectin use in west and central Africa. *Lancet*, **356**: 1077-1078.

Tishkoff SA, Varkonyi R, Cahinhinan N, Abbes S, Argyropoulos G, Destro-Bisol G, Drousiotou A, Dangerfield B, Lefranc G, Loiselet J, Piro A, Stoneking M, Tagarelli A, Tagarelli G, Touma EH, Williams SM and Clark AG (2001). Hpalotype diversity and linkage disequilibrium at human G6PD: recent origin of alleles that confer malarial resistance. *Science*, **293**: 455-462.

Tulu AN (1996). Determinants of malaria transmission in the highlands of Ethiopia: the impact of global warming on morbidity and mortality ascribed to malaria. *PhD thesis, University of London.*

UKCIP (2002). Climate Change scenarios for the United Kingdom. The UKCIP02 briefing report. Hulme M, Turnpenny J and Jenkins G (eds.). *Tyndall Centre for Climate Change Research, School of Environmental Sciences, University of East Anglia, Norwich.*

USGS (2002). http://edcdaac.usgs.gov/glcc/euras_int.html

Van Thiel PH (1927). Sur l'origine des variations de taille de l'*Anopheles* maculipennis dans les Pays-Bas. *Bull Soc Path Exot*, **20**: 366-390.

Verhave JP (1987). The dutch school of malaria research. *Parassitologia*, **29**: 263-274.

Vine MF, Degnan D and Hanchette C (1997). Geographic information systems: their use in environmental epidemiologic research. *Env Health Perspect*, **105**: 598-605.

Vutchev D (2001). Tertial malaria outbreak three decades after its eradication. *Jpn J Infect Dis*, **54**: 79-80.

Wesenberg-Lund C (1921). Contributions to the biology of the Danish Culicidae. *Kongelige Danske Videnskabs Selskabs Skrifter*, **7**: 1-8.

White GB (1978). Systematic appraisal of the *Anopheles maculipennis* complex. *Mosq Syst*, **10**: 13-44.

Whitley G (1863). Report by Dr. George Whitley as to the quantity of ague and other malarious diseases now prevailing in the principal marsh districts of England. *Sixth report of the medical officer of the privy council. Department of Health.*

Willis T (1685). The london practice of physick. *Thomas Basset and William Crooke, London.*

WHO (1997). World malaria situation in 1994. *Weekly Epidemiological Records, World Health Organisation, Geneva*; **72**: 285-292.

WHO (2001). http://www.who.int/ith/chapter07_01.html

WHO (2002a) http://csid.who.dk/mal

WHO (2002b). http://www.who.int/whosis/

Worboys M (1994). From miasmas to germs: malaria 1850-1879. *Parassitologia*, **36**: 61-68.

World Bank (1993). World Development Report 1993. Investing in health; world development indicators. *Oxford University Press, Oxford.*

Worldwide Directory of Cities and Towns (2002).
http://www.calle.com/world/index.html

Yousif F, El-Emam M, Abdel-Kader A, Sharaf El-Din A, El-Hommossany K and Shiff C (1998). Schistosomiasis in newly reclaimed areas of Eygpt 1 – distribution

and population seasonal fluctuation of intermediate host snails. *J Egypt Soc Parasitol*, **28**: 915-928.

Zamburlini R and Cargnus E (1998). [Observations on subgenus *Aedes* (genus Aedes, Diptera, Culicidae) in northeast Italy and first report of *Aedes geminus* Peus. *Parassitologia*, **40**: 297-303.

Zulueta J de (1973). Malaria and Mediterranean history. *Parassitologia*, **14**: 1-15.

Zulueta J de (1994). Malaria and ecosystems: from prehistory to posteradication. *Parassitologia*, **36**: 7-15.

Zulueta J de, Ramsdale CD and Coluzzi M (1975). Receptivity to malaria in Europe. *Bull WHO*, **52**: 109-111.

Poor print and also pale on some of the appendices pages

Extract from the Annual Report of the Registrar General 1841 to show the classification of diseases. Ague deaths are classified under 'Zymotic diseases' (red highlight).

60 FIFTH ANNUAL REPORT of the REGISTRAR-GENERAL [D.

1841.—CAUSES of DEATHS in ENGLAND and in the ELEVEN DIVISIONS.

CAUSES OF DEATH.	ENGLAND.	Metropolis.*	South Eastern.	South Midland.	Eastern.	South Western.	Western.	North Midland.	North Western.	York.	Northern.	
		MALES AND FEMALES.										
		1	2	3	4	5	6	7	8	9	10	
All Causes	343,847	45,507	28,994	24,525	20,713	32,536	41,988	23,098	53,380	33,624	18,488	21
Specified Causes	336,664	45,087	28,487	23,750	19,900	31,899	40,728	22,637	52,803	33,019	17,916	20
I. Zymotic (or Epidemic, Endemic, and Contagious) Diseases	63,148	7,874	4,627	4,514	3,692	5,321	7,402	4,556	10,975	5,936	3,399	4
Sporadic Diseases:—												
II. Of Uncertain or Variable Seat	48,053	5,456	4,350	4,361	3,527	5,368	5,837	3,005	6,470	4,250	2,791	2
III. Of the Nervous System	49,593	7,560	4,064	2,771	1,920	3,687	5,010	3,580	8,960	6,431	2,289	3
IV. Of the Respiratory Organs	82,183	14,177	7,979	6,351	5,526	8,645	11,373	5,729	15,056	8,137	4,389	4
V. Of the Organs of Circulation	4,546	993	580	292	246	453	561	304	476	349	190	
VI. Of the Digestive Organs	22,398	3,390	1,865	1,393	996	1,804	3,157	1,475	4,043	2,141	1,253	
VII. Of the Urinary Organs	1,650	234	205	118	108	150	162	142	207	162	96	
VIII. Of the Organs of Generation	3,555	510	348	223	159	274	385	250	672	389	208	
IX. Of the Organs of Locomotion	2,289	251	191	160	110	190	315	160	381	291	105	
X. Of the Integumentary System	528	55	35	42	35	55	56	39	89	68	29	
XI. Old Age	37,253	3,373	3,447	2,892	3,016	4,618	4,766	2,610	3,709	3,744	2,428	
XII. External Causes:—Poisoning, Asphyxia, Injuries	11,468	1,211	906	633	565	1,334	1,704	787	1,765	1,121	739	
I.												
1 Small Pox	6,368	1053	372	94	49	768	1261	453	971	391	393	
2 Measles	6,894	973	174	720	206	346	529	233	1691	556	441	
3 Scarlatina	14,161	663	1253	807	1116	963	1392	1607	2813	1610	763	
4 Hooping Cough	8,099	2278	466	827	476	530	837	418	927	708	404	
5 Croup	4,177	391	253	264	115	362	490	244	871	492	287	
6 Thrush	1,139	260	106	131	227	103	73	78	53	85	9	
7 Diarrhœa	3,240	465	212	178	147	264	479	211	764	298	148	
8 Dysentery	515	78	57	39	25	39	51	35	99	53	22	
9 Cholera	443	28	15	20	10	29	63	34	137	74	23	
[redacted]	1,659	220	238	149	133	270	153	111	148	110	87	
	135	15	11	7	7	2	7	14	29	18	21	
	149	16	21	15	6	10	10	13	27	6	15	
13 Typhus	14,846	1151	1033	1195	1119	1549	1910	1049	2262	1360	708	
14 Erysipelas	1,139	251	97	38	47	108	123	49	148	160	68	
15 Syphilis	177	29	19	10	9	18	21	7	35	15	10	
16 Hydrophobia	7	3	..	..	..	..	3	..	..	..	..	
II.												
17 Inflammation	3,306	238	355	317	459	229	365	210	416	196	256	
18 Hæmorrhage	1,101	165	126	72	61	140	128	67	165	91	47	
19 Dropsy	13,095	1720	1333	973	707	1755	1704	694	1673	1080	631	
20 Abscess	869	169	111	89	56	62	117	56	99	74	15	
21 Mortification	1,329	241	142	102	101	138	197	83	126	111	55	
22 Purpura	120	12	8	7	4	12	18	14	19	10	7	
23 Scrofula	1,193	105	146	129	117	122	145	72	169	76	40	
24 Carcinoma	2,746	373	329	186	225	341	327	175	279	228	125	
25 Tumor	285	100	33	22	22	20	44	14	8	11	5	
26 Gout	178	61	23	12	8	29	15	8	4	7	2	
27 Atrophy	3,335	363	252	255	354	415	364	262	639	354	155	
28 Debility	16,189	1114	1185	1471	1123	1546	1981	1068	2645	1681	1314	
29 Malformations	206	36	32	17	23	23	31	15	8	8	4	
30 Sudden Deaths	3,901	759	275	309	268	536	401	267	280	323	135	
III.												
31 Cephalitis	2,498	615	191	141	110	193	233	137	333	270	117	
32 Hydrocephalus	7,973	1739	658	414	260	605	637	395	1495	1041	381	
33 Apoplexy	5,581	866	692	414	300	669	716	300	599	539	249	
34 Paralysis	5,495	751	561	441	324	614	633	405	640	401	297	
35 Convulsions	24,563	2778	1569	1125	677	1221	2399	2143	3549	3778	930	
36 Tetanus	118	20	12	12	1	14	12	8	12	11	10	
37 Chorea	28	6	1	3	..	2	3	3	3	3	3	
38 Epilepsy	1,079	181	116	71	52	127	115	67	143	110	34	
39 Insanity	312	43	51	29	23	28	39	20	28	20	6	
40 Delirium Tremens	264	83	24	24	13	25	20	11	26	22	9	
41 Brain, &c., Disease of	1,682	478	189	94	87	189	203	91	132	136	53	

Causes of death classified in the Annual Report of the Registrar General in 1840, 1870 and 1900.

1840	1870	1900
Abscess	Abortion, miscarriage	Abortion, miscarriage
Ague	Acute nephritis	Acute nephritis
Aneurism	Addison's disease	Albuminuria
Apoplexy	Ague	Alcoholism
Arthritis	Anaemia	Aneurysm
Ascites	Aneurysm	Angina pectoris
Asthma	Angina pectoris	Anthrax (splenic fever)
Atrophy	Apoplexy	Apoplexy
Brain diseases	Arthritis	Appendicitis
Bronchitis	Ascites	Asiatic cholera
Carbuncle	Asthma	Atelectasis
Carcinoma	Atelectasis	Brain tumour
Cephalitis	Bright's disease	Bronchitis
Cerebro-spinal fever	Bronchitis	Calculus
Childbirth	Bronchocele	Cancer (non-defined)
Cholera	Calculus	Carcinoma
Chorea	Cancer	Caries
Colic	Carbuncle	Cerebral haemorrhage
Convulsions	Caries	Cerebro-spinal fever
Croup	Cerebro-spinal fever	Chicken-pox
Cystitis	Chicken-pox	Chorea
Debility	Chorea	Chronic Rheumatism
Delirium tremens	Cirrhosis of liver	Cirrhosis of liver
Diabetes	Cleft palate	Congenital defects
Diarrhoea	Convulsions	Convulsions
Dropsy	Cowpox	Cow-pox
Dysentery	Croup	Crop
Enteric fever	Cyanosis	Diabetes mellitus
Enteritis	Dentition	Diarrhoea
Epilepsy	Diabetes mellitus	Dilatation of heart
Erysipelas	Diarrhoea	Diphtheria
Fistula	Diphtheria	Diseases of Bladder and Prostate
Gastritis	Diseases of bladder	Diseases of mouth (non-specified)
Generation organ diseases	Diseases of testes, penis and scrotum	Diseases of spleen
Gout	Disorders of menstruation	Diseases of supra renal capsules
Haematemesis	Dyspepsia	Diseases of Thyroid body
Haemorrhage	Eczema	Disorders of menstruation
Heart diseases	Embolism	Dysentery
Hepatitis	Endocarditis	Eczema
Hernia	Enteric fever	Embolism, thrombosis
Hydrocephalus	Enteritis	Emphysema
Hydrophobia	Epidemic rose rash	Enteric fever
Hydrothorax	Epilepsy	Enteritis (not epidemic)
Ileus	Epistaxis	Epidemic diarrhoea (infective enteritis)
Inflammation	Erysipelas	Epilepsy
Influenza	Fistula	Epistaxis
Instnity	Gallstones	Erysipelas
Intemperance	Glanders	Fatty degeneration of heart
Intussusception	Gonorrhea	Fibroid disease of lung
Ischuria	Gout	Gastric catarrh

Jaundice	Haematemesis	Gastric ulcer
Joint diseases	Haematuria	Gastro-enteritis
Kidney diseases	Hemiplegia	General paralysis of insane
Laryngitis	Hernia	General tuberculosis
Liver diseases	Hydatid disease	German measles
Lung diseases	Hydrophobia	Glanders
Malformations	Hypertrophy of heart	Gonorrhea
Measles	Idiopathic tetanus	Gout
Mortification	Ileus	Haemophilia
Nephritis	Impertorate anus	Heart disease (non-specified)
Old age	Inflammation of brain	Hernia
Ovarian dropsy	Influenza	Hypertrophy of heart
Pancreas diseases	Insanity	Industrial poisoning (arsenic)
Paralysis	Intemperance	Industrial poisoning (lead)
Paramenia	Intussusception of intestine	Industrial poisoning (phosphorus)
Pericarditis	Laryngismus stridulus	Infective endocarditis
Peritonitis	Laryngitis	Influenza
Phlegmon	Lupus	Injury at birth
Phthisis	Lymphatic disease	Insanity (not puerperal)
Pleurisy	Measles (morbilli)	Intestinal obstruction
Pneumonia	Melaena	Laryngismus stridulus
Puerperal fever	Mumps	Laryngitis
Purpura	Old age	Leukaemia
Quinsey	Ophthalmia	Locomotor ataxy
Relapsing fever	Other accidents of childbirth	Lupus
Remittent fever	Other diseases from parasites	Malaria
Rheumatic fever	Other diseases from vegetables	Measles (morbilli)
Rheumatism	Other diseases of circulatory system	Meningitis
Scarlatina	Other diseases of liver	Mumps
Scarlet fever	Other diseases of respiratory system	Neuritis
Scrofula	Other diseases of the nervous system	Opium, morphia-habit
Simple-and ill defined fever	Other forms of Tuberculosis	Opthalmia
Skin diseases	Other miasmatic diseases	Other traumas of pregnancy and birth
Small-pox	Other skin diseases	Other diseases of blood vessels
Spleen diseases	Otitis	Other diseases of digestive system
Splenic fever	Ovarian disease	Other diseases of intestines
Starvation	Paralysis	Other diseases of liver and gall bladder
Stomach diseases	Paraplegia	Other diseases of nervous system
Stone	Peleurisy	Other diseases of ovary
Stricture	Pelvic abscess	Other diseases of respiratory system
Sudden deaths	Pemphyigus	Other diseases of skin
Syphilis	Pericarditis	Other diseases of stomach
Tabes mesenterica	Perineal abscess	Other diseases of urinary system
Teething	Peritonitis	Other diseases of uterus and vagina
Tetanus	Phagedaena	Other infective conditions
Thrush	Phlebitis	Otitis
Tumour	Phlegmasia dolens	Ovarian tumour
Typhus fever	Phlegmon	Paraplegia, diseases of cord
Ulcer	Phthisis	Parasitic diseases
Ulceration	Plancenta praevia	Pemphigus
Whooping cough	Pneumonia	Pericarditis
Worms	Premature birth	Peritonitis (not puerperal)
	Puerperal convulsions	Permature birth

	Puerperal fever	Phagedaena
	Puerperal mania	Phlebitis
	Purpura	Phlegmasia alba dolens
	Pyaemia	Phlegmon (not anthrax)
	Quinsy	Phthisis (non-defined)
	Relapsing fever	Placenta praevia
	Remittent fever	Plague
	Rheumatic fever	Pleurisy
	Rheumatism	Pneumonia (broncho)
	Rickets	Pneumonia (epidemic)
	Scarlet fever	Pneumonia (lobar)
	Scurvy	Pneumonia (non-defined)
	Senile gangrene	Ptomaine poisoning
	Simple and ill-defined fever	Puerperal convulsions
	Simple cholera	Puerperal fever (non-defined)
	Small-pox (doubtful)	Puerperal mania
	Small-pox (not vaccinated)	Puerperal pyaemia
	Small-pox (vaccinated)	Puerperal septicaemia
	Softening of brain	Pulmonary tuberculosis
	Sore throat	Purpura
	Spina Bifida	Pyaemia (not puerperal)
	Spleen diseases	Pyrexia
	Splenic fever	Rabies (hydrophobia)
	Starvation	Relapsing fever
	Stomatitis	Rheumatic arthritis, rheumatic gout
	Stricture of intestine	Rheumatic fever, acute rheumatism
	Suppression of urine	Rheumatism of heart
	Syncope	Rickets
	Syphilis	Sarcoma
	Tabes mesenterica	Scarlet fever
	Thrush	Scrofula
	Tubercular meningitis	Scurvy
	Typhus	Senile gangrene
	Ulceration of intestine	Septicaemia (not puerperal)
	Ulceration of intestine	Small-pox (doubtful)
	Uraemia	Small-pox (not vaccinated)
	Varicose veins	Small-pox (vaccinated)
	Whooping cough	Softening of brain
		Starvation
		Syphilis
		Tabes mesentera
		Teething
		Tetanus
		Tonsillitis, quinsy
		Tubercle of other organs
		Tuberculous meningitis
		Tuberculous peritonitis
		Typhus
		Ulcer, bed-sore
		Uterine tumour (non-malignant)
		Valvular disease (not infective)
		Varicose veins
		Want of breast-milk
		Whooping cough

Extract from the Annual Report of the Registrar General 1881 to show the classification of diseases. Ague deaths are classified under 'Malarial Diseases' (red highlight)

160 *Causes of Death*, 1881.

DEATHS from different Causes registered in each of the REGISTRATION COUNTIES in the Year 1881—*cont.*

CAUSES OF DEATH.	Division I. London. Middlesex (part of). Males.	Females.	Surrey (part of). Males.	Females.	Kent (part of). Males.	Females.	Division II. South Eastern Counties. Surrey (ex Met.) Males.	Females.	Kent (ex Met.) Males.	Females.	Sussex. Males.	Females.	Hampshire. Males.	Females.	Berkshire. Males.	Females.
MIASMATIC DISEASES.																
Small-pox: Vaccinated	161	128	35	36	113	93	–	4	2	–	4	2	1	1	1	–
Small-pox: Unvaccinated	221	175	75	41	210	165	1	1	1	2	3	4	–	–	1	1
Small-pox: No Statement	200	271	84	106	70	59	12	8	23	18	18	10	3	1	10	8
Chickenpox	13	16	4	4	1	4	–	–	1	1	–	1	1	1	–	–
Measles	893	867	306	298	89	96	30	36	45	40	33	21	32	30	16	7
Epidemic Rose Rash	7	6	3	1	–	–	–	1	2	2	–	–	–	–	–	1
Scarlet Fever	638	642	224	220	[illegible]	[illegible]	90	67	90	144	60	56	31	40	40	36
Typhus	27	31	12	16	3	1	1	1	1	3	–	1	–	–	1	1
Relapsing Fever	–	–	1	–	–	–	–	–	–	–	–	–	–	–	–	–
Influenza	4	2	–	2	1	–	1	–	–	2	3	–	1	3	–	–
Whooping-cough	815	779	212	268	46	52	36	43	69	65	37	54	60	113	19	15
Mumps	6	9	–	4	–	1	–	2	–	–	1	2	–	9	–	–
Diphtheria	225	226	64	70	20	26	32	28	49	79	42	35	128	117	10	15
Cerebro-spinal Fever	3	2	–	1	–	–	1	–	–	–	–	–	–	2	–	–
Simple and Ill-defined Fever	30	43	19	16	3	3	2	3	23	15	6	7	11	13	2	2
Enteric Fever	367	413	120	115	35	39	33	27	36	61	35	56	49	47	19	23
Other Miasmatic Diseases	–	–	–	–	–	–	–	–	–	–	–	–	–	–	–	–
DIARRHOEAL DISEASES.																
Simple Cholera	35	23	15	15	6	7	2	1	3	3	1	–	–	3	1	1
Diarrhoea, Dysentery	1060	1028	406	334	103	92	93	80	143	136	103	83	111	106	32	36
MALARIAL DISEASES.																
[redacted]	6	7	1	2	1	4	4	1	7	9	–	1	5	5	–	1
	5	3	2	1	1	–	–	–	4	3	1	1	3	1	1	–
ZYMOTIC DISEASES.																
Hydrophobia	4	1	–	–	–	–	–	–	–	–	1	–	–	–	–	–
Glanders	–	–	1	–	–	–	–	–	–	–	1	–	–	–	–	–
Splenic Fever	–	–	–	–	–	–	–	–	–	–	1	–	–	–	–	–
Cowpox and other Effects of Vaccination	4	6	–	2	–	–	–	2	1	–	–	–	1	2	–	1
VENEREAL DISEASES.																
Syphilis	175	186	51	64	10	12	13	13	19	7	13	13	17	11	3	4
Gonorrhoea, Stricture of Urethra	42	–	10	–	3	–	3	–	6	–	4	–	7	–	2	–
SEPTIC DISEASES.																
Phagedaena	3	4	–	2	–	–	1	–	2	–	–	1	3	–	–	–
Erysipelas	140	124	50	61	17	6	27	32	61	39	29	19	23	26	15	10
Pyaemia, Septicaemia	51	40	15	14	5	6	3	10	6	5	10	5	9	4	7	4
Puerperal Fever	–	279	–	91	–	25	–	47	–	40	–	38	–	44	–	10
PARASITIC DISEASES.																
Thrush	55	37	23	22	4	3	7	4	9	13	10	7	4	4	4	7
Other Dis. from Vegetable Parasites	–	–	–	–	–	–	–	–	–	–	–	–	–	–	–	–
Hydatid Disease	5	5	2	1	–	–	–	–	1	1	–	1	–	1	–	–
Other Dis. from Animal Parasites	2	4	–	1	–	–	1	2	2	3	2	4	5	5	1	9
DIETIC DISEASES.																
Starvation, Want of Breast-milk	58	49	14	10	3	2	10	6	9	9	2	6	6	8	3	3
Scurvy	1	1	–	–	–	–	–	–	–	–	–	–	–	–	–	2
Intemperance: Chronic Alcoholism	46	119	21	13	3	4	3	6	31	14	5	7	8	2	2	1
Intemperance: Delirium Tremens	47	9	26	6	3	1	7	–	9	1	11	1	4	–	6	1
CONSTITUTIONAL DISEASES.																
Rheumatic Fever, Rheumatism of Heart	137	156	48	61	10	20	22	24	33	28	28	25	24	24	9	9
Rheumatism	41	49	12	14	1	3	7	3	12	10	10	9	9	3	3	10
Gout	68	14	22	9	5	1	12	7	12	4	15	6	14	3	3	–
Rickets	36	29	13	7	6	2	10	8	6	6	6	4	5	4	–	9
Cancer	532	1123	174	259	45	104	96	164	117	146	97	207	114	112	41	62
Tabes Mesenterica	496	[illegible]	211	187	19	45	40	56	66	70	49	45	39	32	29	19
Tubercular Meningitis (Acute Hydrocephalus)	579	441	166	171	33	36	61	46	69	70	65	64	104	66	34	30
Phthisis	1690	2002	1097	914	141	166	442	510	481	[illegible]	661	587	701	531	222	294
Other Forms of Tuberculosis, Scrofula	510	243	95	[illegible]	22	14	34	[illegible]	36	47	38	51	35	18	15	11
Purpura, Haemorrhagic Diathesis	41	11	15	4	2	–	4	4	6	3	3	4	6	7	1	–
Anaemia, Chlorosis, Leucocythaemia	56	48	9	12	4	1	6	12	17	11	4	12	4	11	1	4
Diabetes Mellitus	74	73	38	17	6	5	12	15	21	15	12	11	20	14	10	6
Other Constitutional Diseases	31	20	15	9	1	2	3	5	5	8	7	8	3	7	1	–
DEVELOPMENTAL DISEASES.																
Premature Birth	544	495	174	130	67	57	121	91	150	124	148	115	121	99	41	41
Atelectasis	41	38	13	6	4	–	3	3	7	6	11	6	4	4	–	1
Cyanosis	56	53	20	20	9	6	16	3	10	21	13	7	4	9	5	3
Spina Bifida	15	18	9	3	2	1	2	3	3	5	6	3	3	6	–	2
Imperforate Anus	14	3	4	1	2	1	2	1	2	3	4	1	2	1	1	–
Cleft Palate, Harelip	12	9	6	5	1	–	7	3	6	1	1	3	1	–	–	–
Other Congenital Defects	21	16	6	4	3	3	3	2	7	9	8	9	1	9	1	5
Old Age	680	1056	282	[illegible]	60	129	161	190	242	[illegible]	[illegible]	261	[illegible]	240	100	116

Note.—For continuation of this Table, see page 166.

Extract from the Annual Report of the Registrar General 1901 to show the classification of diseases. Ague has been renamed malaria and is classified separately (red highlight).

CAUSES of DEATH in Registration Counties, 1901—*continued.*

CAUSES OF DEATH.	Part of Division VI. West Midland Counties.				Division VII. North Midland Counties.										Division VIII. N. W. Counties			
	Worcestershire.		Warwickshire.		Leicestershire.		Rutland-shire.		Lincoln-shire.		Notting-hamshire.		Derbyshire.		Cheshire.*		Lancashire	
	Males.	Females.	Males.	Females.	Males.	Females.	Males.	Females.	Males.	Females.	Males.	Females.	Males.	Females.	Males.	Females.	Males.	Females.
Small-pox { Vaccinated	—	—	—	—	—	—	—	—	—	—	—	—	—	—	—	—	—	—
Small-pox { Not Vaccinated	—	—	—	—	—	—	—	—	—	—	—	—	—	—	1	—	4	—
Small-pox { Doubtful	1	—	1	—	—	—	—	—	—	—	—	1	—	—	—	—	3	1
Cow-pox and other effects of Vaccination	—	1	—	—	—	—	—	—	—	—	—	—	—	—	—	—	—	—
Chicken-pox	1	1	1	2	—	—	—	—	—	1	—	1	—	1	1	1	12	9
Measles (Morbilli)	41	34	210	166	32	22	—	—	32	30	126	106	37	26	113	106	989	813
German Measles	1	—	1	1	1	—	—	—	—	—	—	1	—	—	1	2	3	2
Scarlet Fever	32	19	109	105	11	16	—	—	25	23	21	21	21	18	52	43	569	580
Typhus	—	—	—	—	—	—	—	—	1	—	—	—	—	—	—	—	16	12
Plague	—	—	—	—	—	—	—	—	—	—	—	—	—	—	—	—	2	1
Relapsing Fever	—	—	—	—	—	—	—	—	—	—	—	—	—	—	—	—	—	1
Influenza	32	28	100	73	12	14	—	3	55	51	33	30	66	45	53	72	343	351
Whooping-cough	82	84	137	167	16	18	—	1	93	81	88	100	82	82	106	145	541	675
Mumps	1	1	1	3	1	—	—	1	1	—	—	1	—	2	3	2	9	10
Diphtheria	26	42	88	95	110	102	—	—	37	52	42	43	33	45	98	74	660	716
Cerebro-spinal Fever	1	—	3	2	1	—	—	—	—	1	—	2	—	—	2	2	6	7
Pyrexia (origin uncertain)	1	—	3	—	—	—	—	—	1	—	—	1	—	—	3	2	13	10
Enteric Fever	23	29	106	75	20	21	—	1	50	44	72	60	40	27	77	58	546	351
Asiatic Cholera	—	—	—	—	—	—	—	—	—	—	—	—	—	—	—	—	—	—
Food, Ptomaine-poisoning	1	—	1	1	1	—	—	—	—	—	1	—	—	—	1	—	6	2
Epidemic Diarrhœa, Infective Enteritis	48	41	329	268	65	57	1	1	35	21	86	120	57	43	144	123	1357	1332
Diarrhœa (not otherwise defined)	92	79	300	233	101	128	2	3	140	106	232	217	144	136	240	203	2019	1767
Dysentery	2	1	1	4	2	4	—	—	4	3	1	2	—	—	6	1	23	18
[redacted]	1	—	—	—	1	—	—	—	1	—	—	—	—	—	—	—	1	2
[redacted]	—	—	2	—	1	—	—	—	1	1	2	—	—	—	1	—	11	1
Glanders	—	—	—	—	—	—	—	—	—	—	—	—	—	—	—	—	—	—
Anthrax (Splenic Fever)	—	—	—	—	—	—	—	—	—	—	—	—	—	—	—	—	1	—
Syphilis	8	6	46	23	7	5	—	—	12	11	20	16	7	15	29	15	140	124
Gonorrhœa	8	—	20	—	4	—	—	—	6	—	12	1	2	—	10	—	50	2

Note.—For continuation of this Table [illegible] page 181

Historical map of England and Wales (1843) used in ArcView 3.1 for display and manipulation of climate and malaria data.

Frequency distribution of explanatory variables used for the English malaria models.

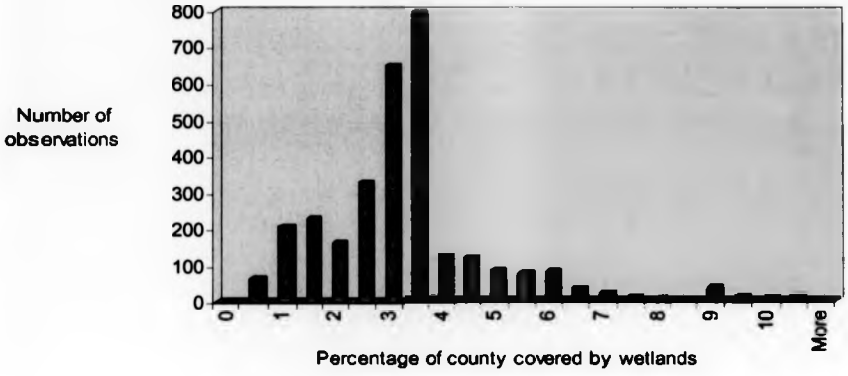

Figure 1. Frequency distribution of wetland coverage (% of county covered by wetlands).

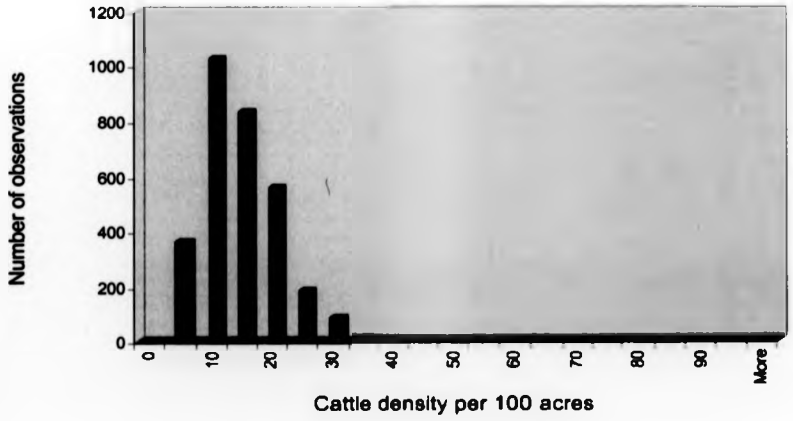

Figure 2. Frequency distribution of cattle density (number of cattle per 100 acres).

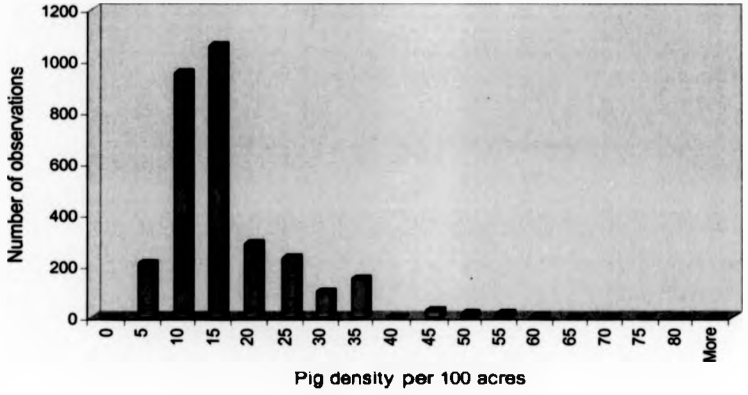

Figure 3. Frequency distribution of pig density (number of pigs per 100 acres).

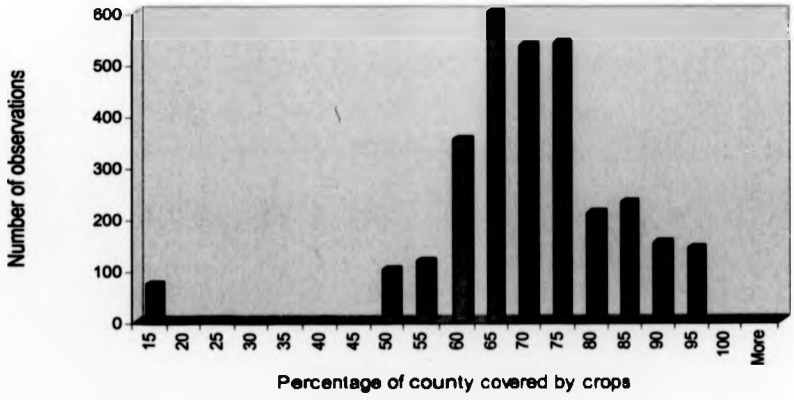

Figure 4. Frequency distribution of crop coverage (percentage of county covered by crops).

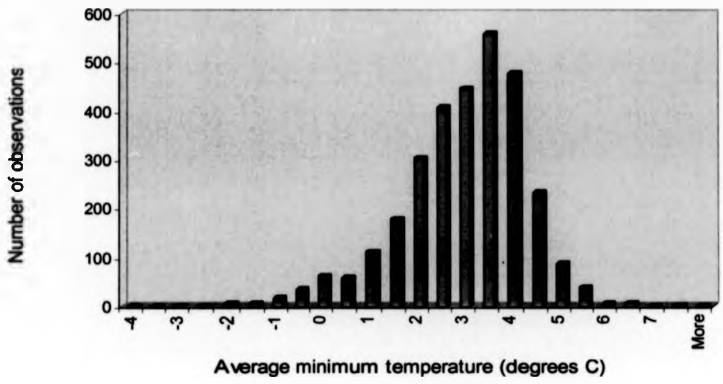

Figure 5. Frequency distribution of average minimum temperature.

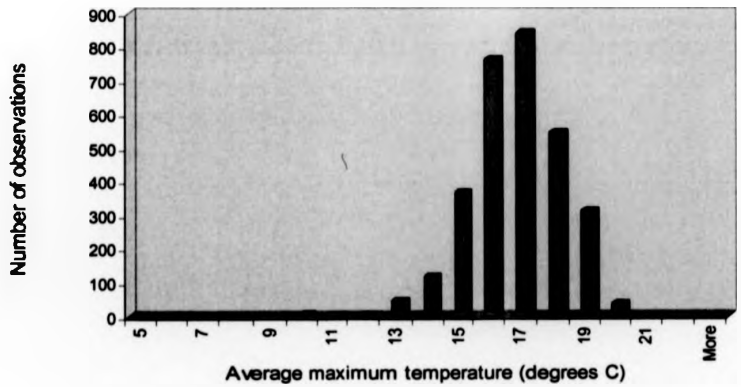

Figure 6. Frequency distribution of average maximum temperature.

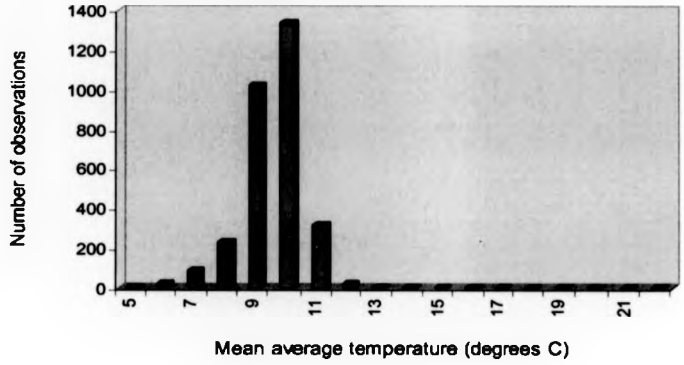

Figure 7. Frequency distribution of mean average temperature.

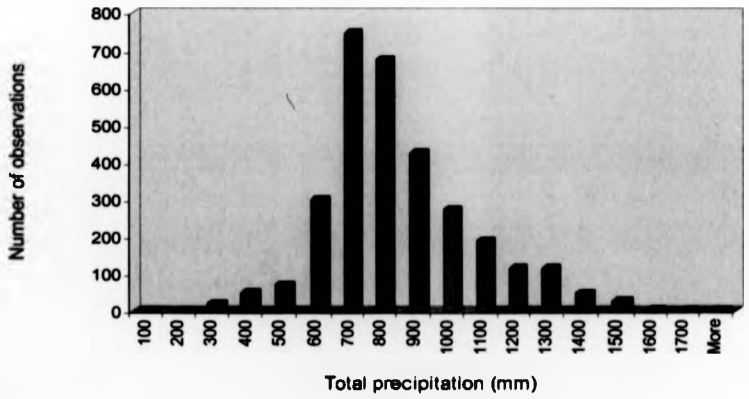

Figure 8. Frequency distribution of total precipitation.

Temporal trends in explanatory variables used for the English malaria models.

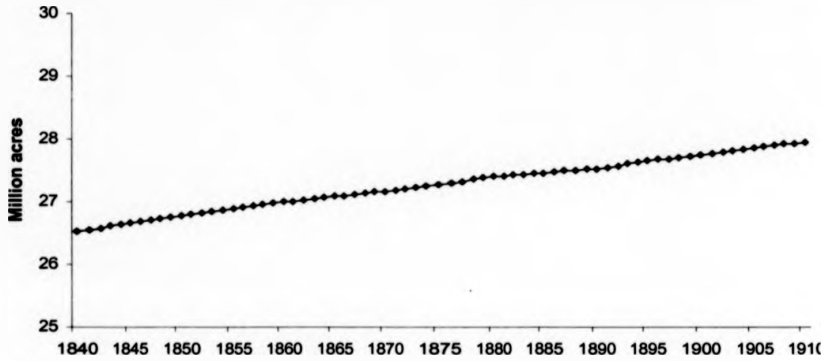

Figure 1. Total annual acres of crops, bare fallow and grasses in England and Wales during 1840-1910.

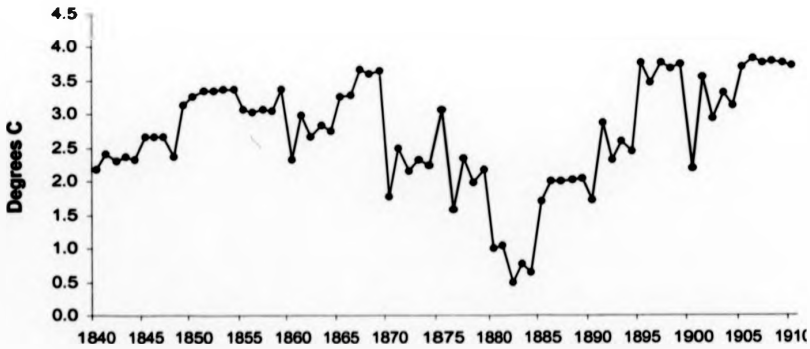

Figure 2. Annual minimum average temperatures in England and Wales during 1840-1910.

Figure 3. Annual maximum average temperatures in England and Wales during 1840-1910.

Spatial patterns in explanatory variables used for the English malaria models.

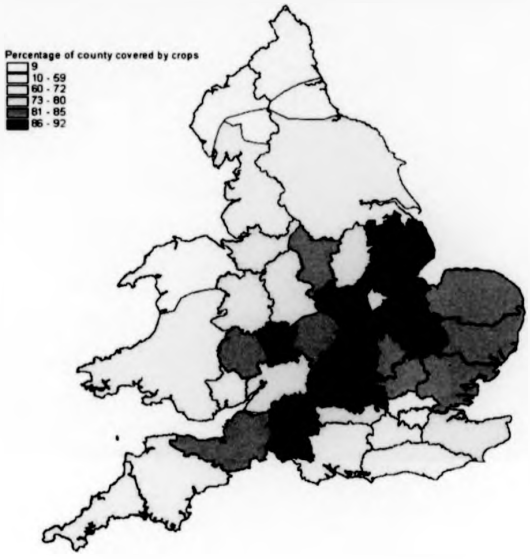

Figure 1. Average crop coverage in English and Welsh counties during 1840 to 1910.

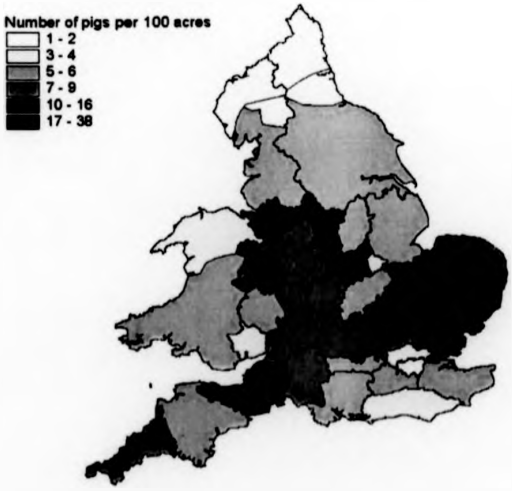

Figure 2. Average pig density in English and Welsh counties during 1840 to 1910.

Average inland water coverage, cattle and pig densities in English and Welsh counties during 1840 to 1910.

INLAND WATER		CATTLE DENSITY		PIG DENSITY	
County	% Coverage	County	Number/100 acres	County	Number/100 acres
Essex	9.32	Leicestershire	22.92	Bedfordshire	10.75
Cheshire	6.75	Derbyshire	21.65	Berkshire	6.18
Lincolnshire	5.66	Cheshire	21.45	Buckinghamshire	8.32
Lancashire	5.54	Cornwall	18.98	Cambridgeshire	9.85
London	5.06	Somersetshire	18.79	Cheshire	10.39
Kent (part of)	4.93	Staffordshire	17.94	Cornwall	8.17
Cumberland	4.28	Lancashire	17.71	Cumberland	2.47
North Wales	3.83	Northamptonshire	17.46	Derbyshire	9.97
Hampshire	3.57	Shropshire	14.79	Devonshire	5.66
Monmoutshire	3.05	Warwickshire	14.59	Dorsetshire	7.39
South Wales	2.90	Rutlandshire	14.27	Durham	1.89
Norfolk	2.67	Herefordshire	13.84	Essex	9.56
Somersetshire	2.51	Devonshire	13.83	Gloucestershire	8.37
Sussex	2.14	Buckinghamshire	13.68	Hampshire	6.04
Gloucestershire	2.10	South Wales	13.52	Herefordshire	5.10
Dorsetshire	2.07	Cumberland	12.80	Hertfordshire	7.60
Durham	2.03	Nottinghamshire	12.61	Huntingdonshire	8.35
Northumberland	2.03	Gloucestershire	12.23	Kent (part of)	6.40
Cornwall	2.01	North Wales	12.15	Lancashire	4.72
Yorkshire	1.52	Worcestershire	12.00	Leicestershire	38.49
Suffolk	1.37	Huntingdonshire	11.37	Lincolnshire	6.19
Middlesex	1.19	Westmoreland	11.17	London	2.27
Devonshire	1.02	Dorsetshire	11.04	Middlesex	10.23
Berkshire	0.77	Lincolnshire	10.92	Monmoutshire	4.47
Worcestershire	0.75	Monmoutshire	10.81	Norfolk	7.66
Staffordshire	0.74	Yorkshire	10.73	North Wales	4.31
Westmoreland	0.73	Middlesex	10.09	Northamptonshire	5.44
Nottinghamshire	0.72	Sussex	9.93	Northumberland	1.00
Surrey	0.70	Wiltshire	9.65	Nottinghamshire	4.68
Warwickshire	0.64	Bedfordshire	8.86	Oxfordshire	7.91
Derbyshire	0.61	Oxfordshire	8.77	Rutlandshire	2.74
Herefordshire	0.51	Norfolk	8.41	Shropshire	7.50
Cambridgeshire	0.48	Surrey	8.34	Somersetshire	10.59
Oxfordshire	0.46	Durham	7.46	South Wales	5.50
Hertfordshire	0.42	Northumberland	7.46	Staffordshire	7.42
Bedfordshire	0.41	Cambridgeshire	6.94	Suffolk	15.58
Buckinghamshire	0.41	Essex	6.91	Surrey	6.24
Shropshire	0.39	Kent (part of)	6.09	Sussex	4.27
Northamptonshire	0.37	Hertfordshire	5.80	Warwickshire	7.14
Leicestershire	0.36	Berkshire	5.72	Westmoreland	0.97
Huntingdonshire	0.33	Hampshire	5.61	Wiltshire	7.60
Wiltshire	0.33	Suffolk	5.38	Worcestershire	9.11
Rutlandshire	0.17	London	3.98	Yorkshire	4.91

Residuals from the inter-annual and inter-county variability ague models.

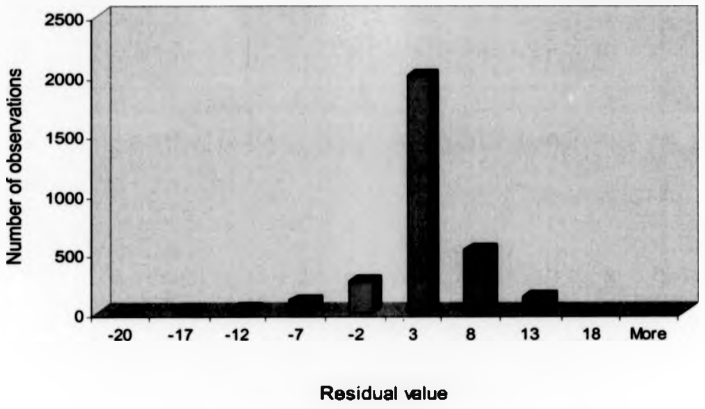

Figure 1. Temporal ague model: distribution of residuals (i.e. observed – predicted ague deaths).

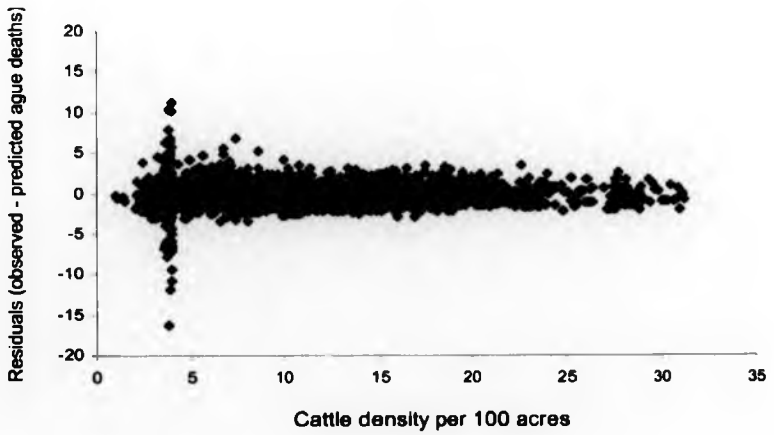

Figure 2. Temporal ague model: residuals versus cattle density

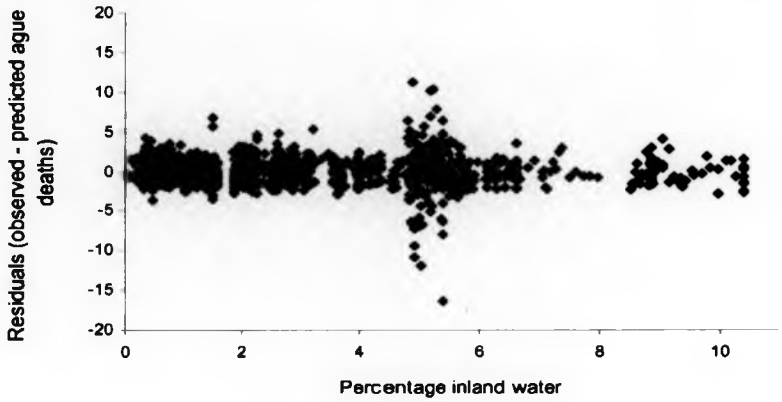

Figure 3. Temporal ague model: residuals versus wetland coverage.

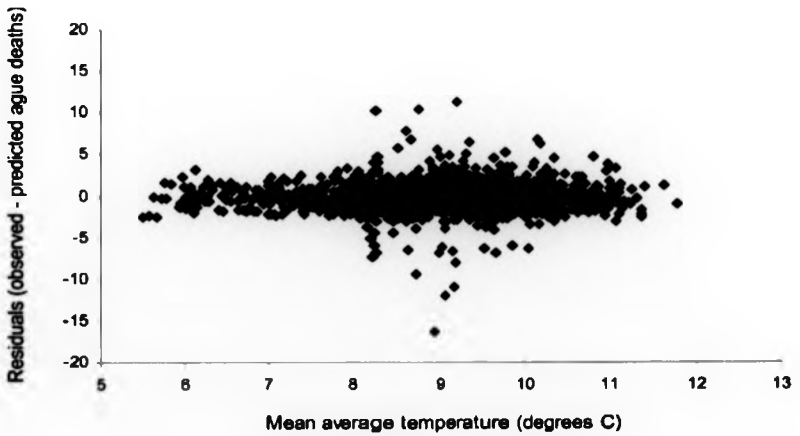

Figure 4. Temporal ague model: residuals versus mean average temperature.

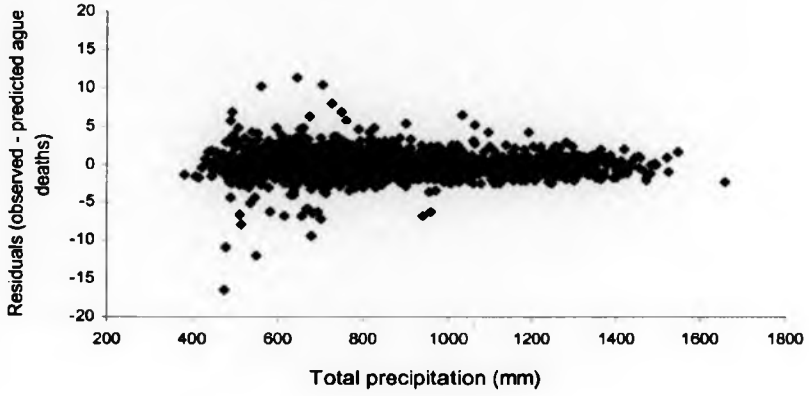

Figure 5. Temporal ague model: residuals versus total precipitation.

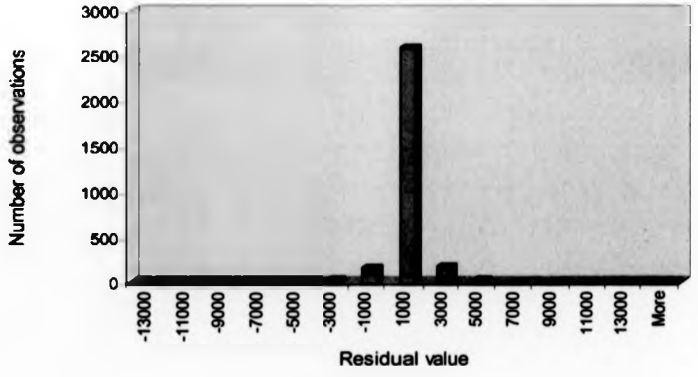

Figure 6. Temporal all-cause mortality model: distribution of residuals (i.e. observed – predicted deaths from all causes)

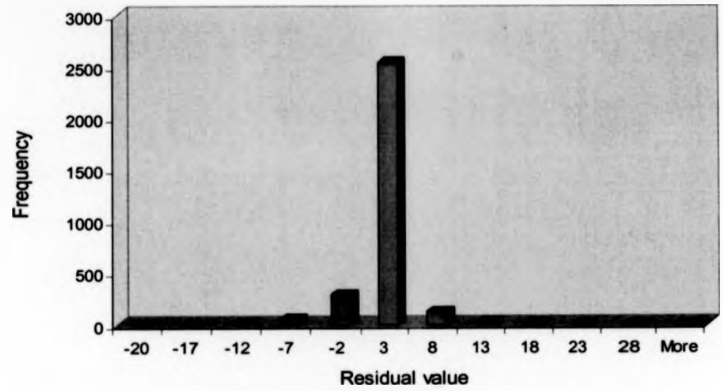

Figure 7. Spatial ague model: distribution of residuals (i.e. observed – predicted ague deaths).

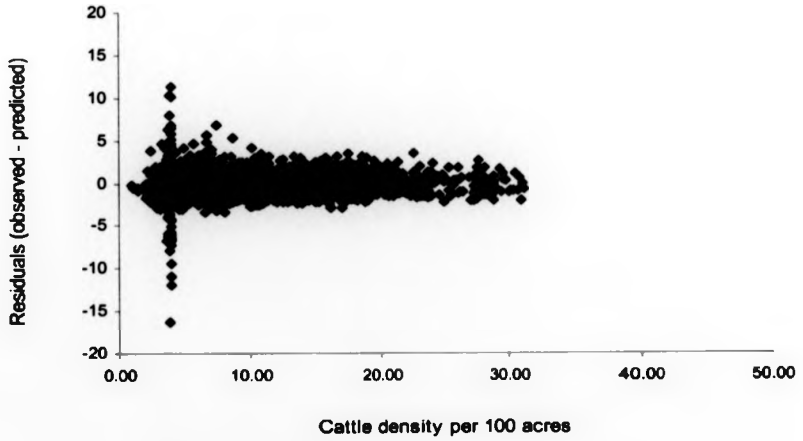

Figure 8. Spatial ague model: residuals versus cattle density.

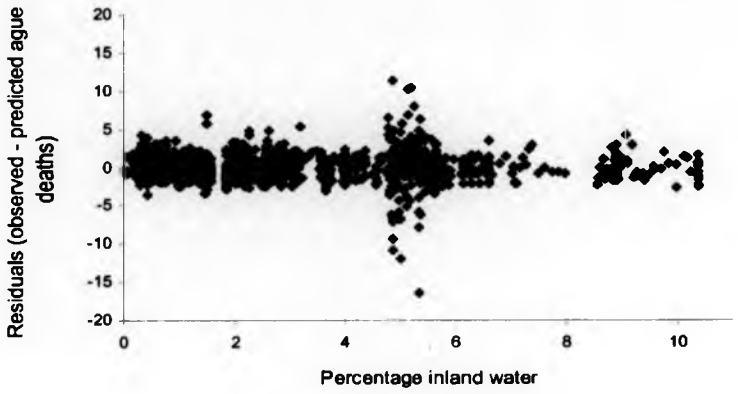

Figure 9. Spatial ague model: residuals versus wetland coverage.

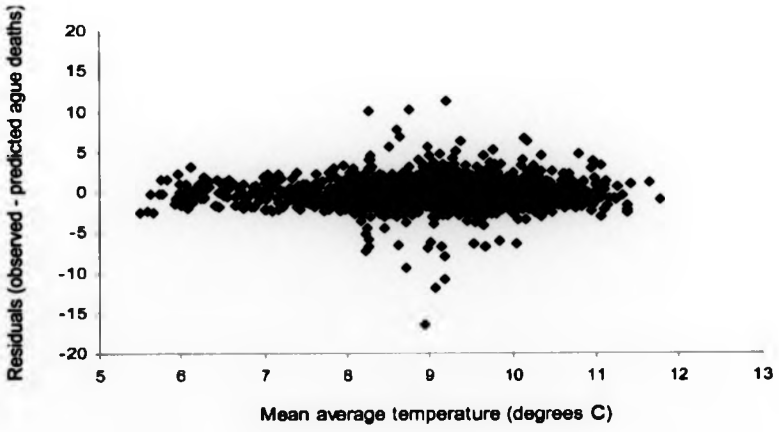

Figure 10. Spatial ague model: residuals versus mean average temperature.

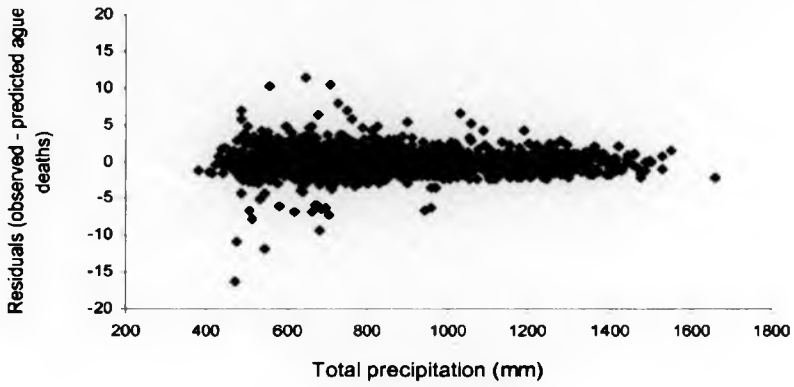

Figure 11. Spatial ague model: residuals versus total precipitation.

Repeats of inter-annual variation analysis on the most 'malarious' counties.

Box 1. Repeat of temporal analysis on counties with above 60 malaria deaths per 100,000 inhabitants during the study period. Amended STATA output.

```
STATA command
xi: glm  ague water% cattle tave ptotal year yearsq rate-1 i.county, f(b
population) scale(x2)

Statistics
Generalized linear models                       No. of obs      =        490
Optimization     : ML: Newton-Raphson           Residual df     =        476
                                                Scale param     =          1
Deviance         =  946.1671176                 (1/df) Deviance =   1.987746
Pearson          =  955.539912                  (1/df) Pearson  =   2.007437

Explanatory variables
(8 county coefficients and statistics not shown)
------------------------------------------------------------------------------
       ague |      Coef.   Std. Err.      z    P>|z|     [95% Conf. Interval]
------------+-----------------------------------------------------------------
      water% |   .4543537   .1474649     3.08   0.002     .1653795    .7413278
      cattle |  -.0203989   .0384086    -1.53   0.015    -.0825680   -.0097834
       tave  |   .057634    .0451458     1.68   0.012      .016118    .1408501
      ptotal |   .002463    .0003247     0.45   0.652    -.0007827    .0004902
       year  |  -.0088012   .0074195    -1.19   0.236     -.023343    .0057407
      yearsq |  -.0004514   .0000992    -4.55   0.000    -.0006458   -.0002571
      rate-1 |   .0302307   .0054429     5.55   0.000     .0195627    .0408986
------------------------------------------------------------------------------
(Standard errors scaled using square root of Pearson X2-based dispersion)
```

Box 2. Repeat of temporal analysis on counties with above 40 malaria deaths per 100,000 inhabitants during the study period. Amended STATA output

```
STATA command
xi: glm  ague water_ cattle tave ptotal year2 year2sq deviation_1
i.county, f(b population) scale(x2)

Statistics
Generalized linear models                       No. of obs      =        979
Optimization     : ML: Newton-Raphson           Residual df     =        958
                                                Scale param     =          1
Deviance         =  1857.433714                 (1/df) Deviance =   1.717907
Pearson          =  1905.686621                 (1/df) Pearson  =   1.750819

Explanatory variables
(15 county coefficients and statistics not shown)
------------------------------------------------------------------------------
       ague |      Coef.   Std. Err.      z    P>|z|     [95% Conf. Interval]
------------+-----------------------------------------------------------------
      water% |    .407538   .1136092     4.06   0.000     .2334237    .6880839
      cattle |  -.018554    .0184283    -1.84   0.047    -.9353638   -.0001738
       tave  |   .0261805   .0291823     1.86   0.031     .0923768    .0081057
      ptotal |    .004737   .0019564     2.42   0.015     .0009034    .0085744
       year  |  -.0181014   .0043268    -4.18   0.000    -.0265817   -.0096211
      yearsq |  -.0001834   .0000593    -3.09   0.002    -.0002997   -.0000671
      rate-1 |   .0249339   .0031311     7.96   0.000     .018797     .0310708
------------------------------------------------------------------------------
(Standard errors scaled using square root of Pearson X2-based dispersion)
```

Box 3. Repeat of temporal analysis on counties with above 30 malaria deaths per 100,000 inhabitants during the study period. Amended STATA output

```
STATA command
xi: glm  ague water_ cattle tave ptotal year2 year2sq deviation_1
i.county, f(b population) scale(x2)

Statistics
Generalized linear models                       No. of obs      =       1609
Optimization     : ML: Newton-Raphson           Residual df     =       1579
                                                Scale param     =          1
Deviance         =  2712.575308                 (1/df) Deviance =  1.717907
Pearson          =  2764.543237                 (1/df) Pearson  =  1.750819

Explanatory variables
(24 county coefficients and statistics not shown)
------------------------------------------------------------------------------
       ague |      Coef.   Std. Err.      z    P>|z|     [95% Conf. Interval]
------------+-----------------------------------------------------------------
     water% |   .4482779   .0884339     5.07   0.000     .2746051
     cattle |  -.0226258   .0107437    -2.43   0.027    -.0964311   -.0019836
      tave  |   .0267583   .0245478     1.59   0.024     .0213711    .0713544
     ptotal |   .0052914   .0016746     3.21   0.001     .0020654    .0085174
      year  |  -.0170935    .003567    -4.79   0.000    -.0240847   -.0101023
     yearsq |  -.0001994   .0000503    -3.97   0.000    -.0002979   -.0001008
     rate-1 |   .0241391   .0027558     8.76   0.000     .0187377    .0295404
------------+-----------------------------------------------------------------
(Standard errors scaled using square root of Pearson X2-based dispersion)
```

Frequency distribution of explanatory variables used for the European malaria models.

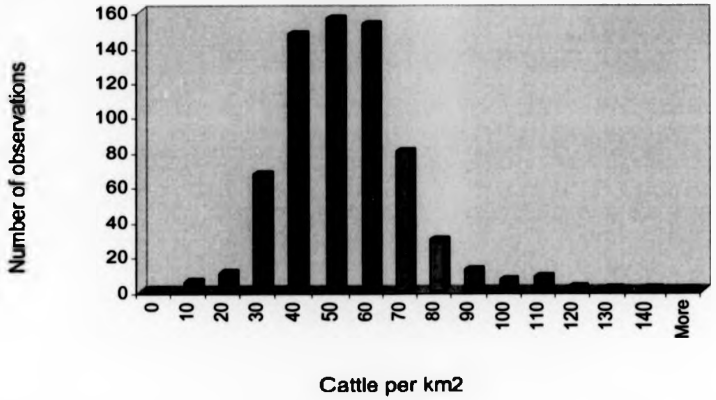

Figure 1. Frequency distribution of cattle density per km^2 in Europe during 1900-1975.

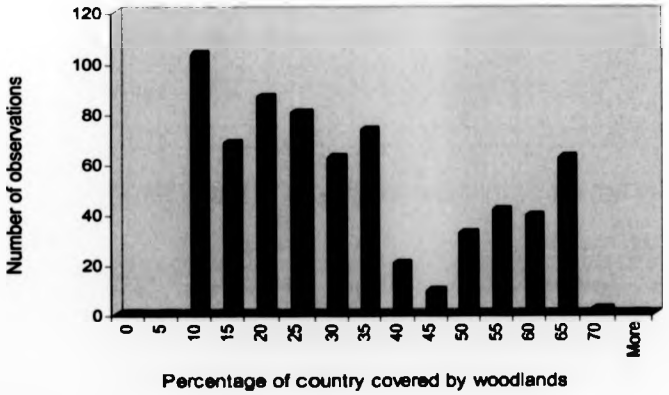

Figure 2. Frequency distribution of woodland coverage in Europe during 1900-1975.

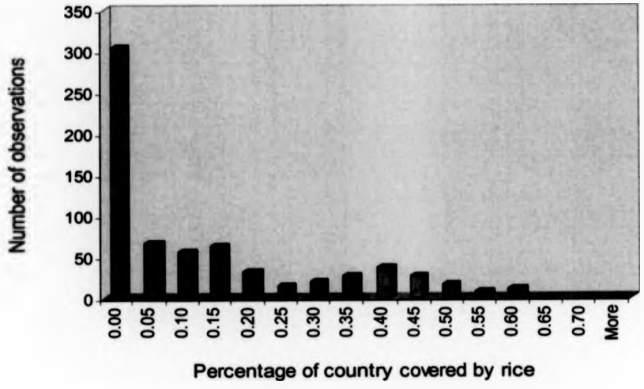

Figure 3. Frequency distribution of rice coverage in Europe during 1900-1975.

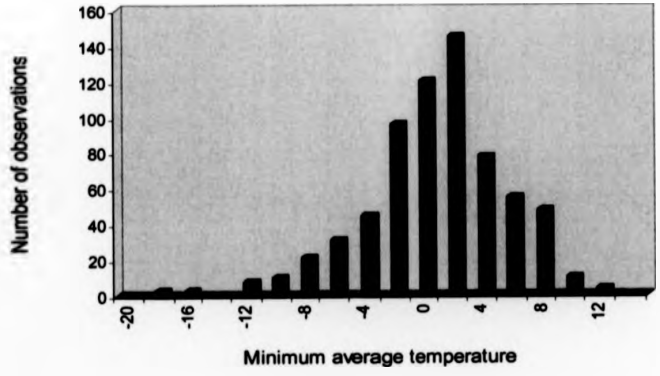

Figure 4. Frequency distribution of minimum average temperature in Europe during 1900-1975.

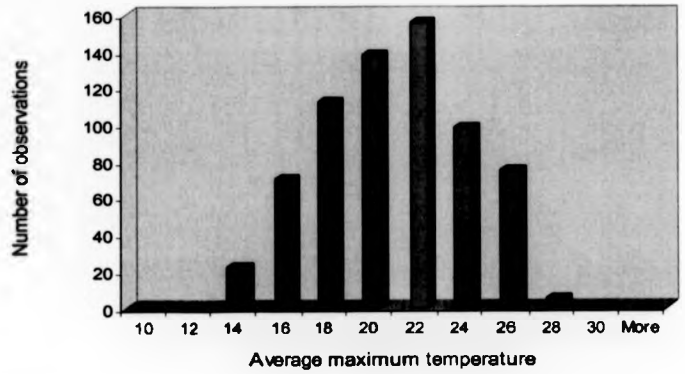

Figure 5. Frequency distribution of maximum average temperature in Europe during 1900-1975

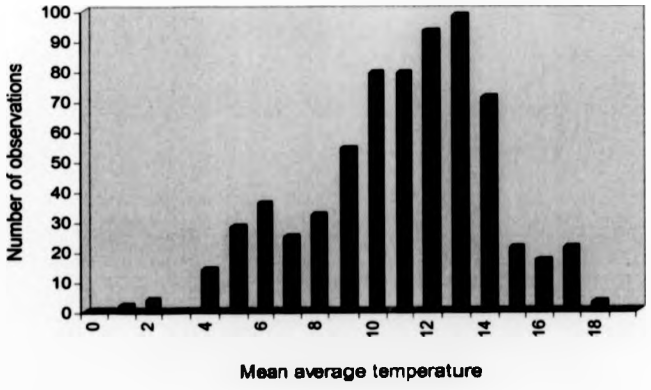

Figure 6. Frequency distribution of mean average temperature in Europe during 1900-1975.

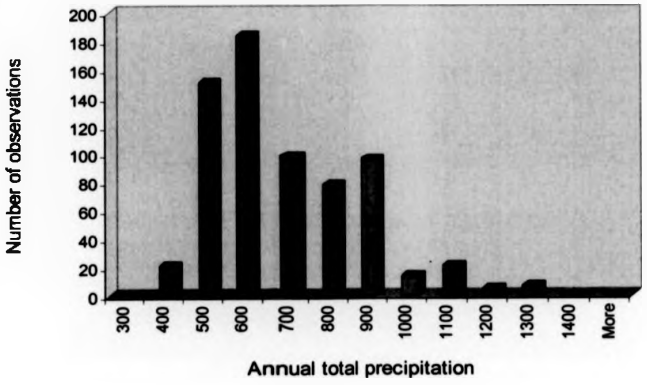

Figure 7. Frequency distribution of annual total precipitation in Europe during 1900-1975.

Residuals from the inter-annual and inter-country variability malaria models.

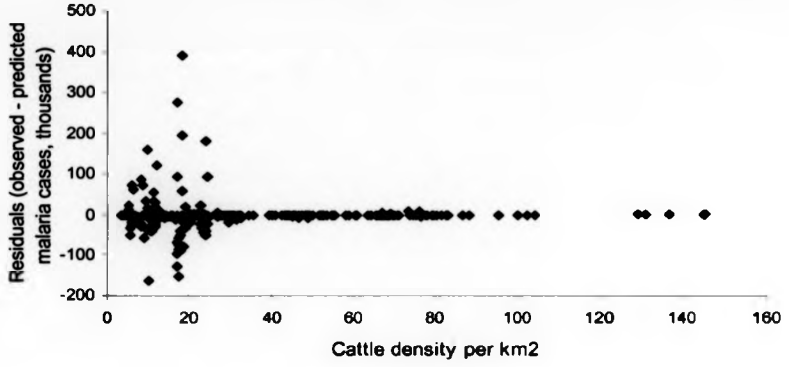

Figure 1. Temporal malaria model: residuals versus cattle density.

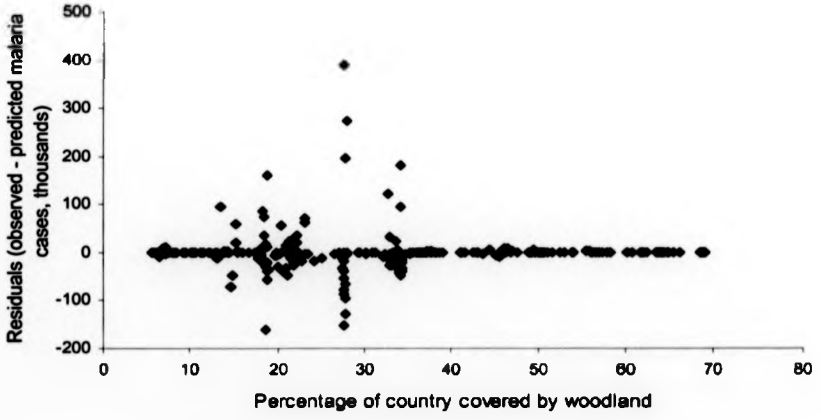

Figure 2. Temporal malaria model: residuals versus woodland coverage.

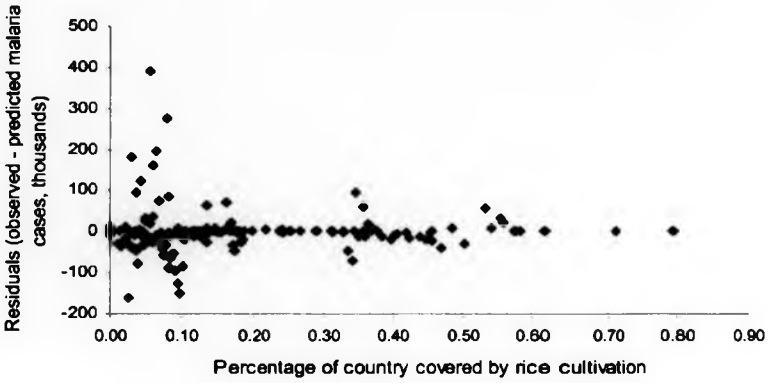

Figure 3. Temporal malaria model: residuals versus rice cultivation.

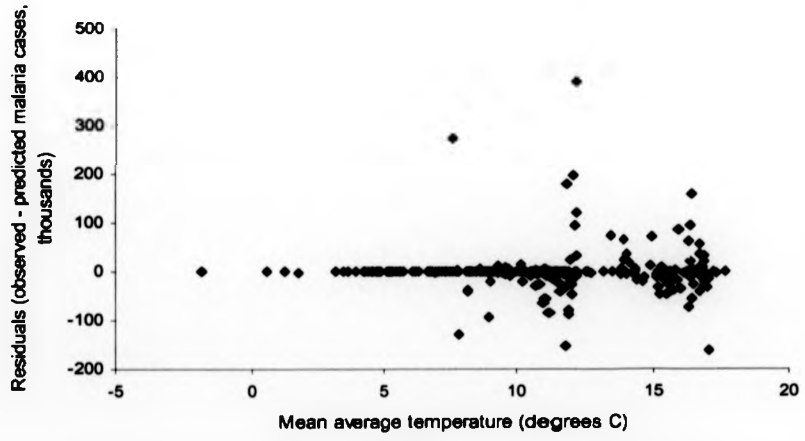

Figure 4. Temporal malaria model: residuals versus mean average temperature.

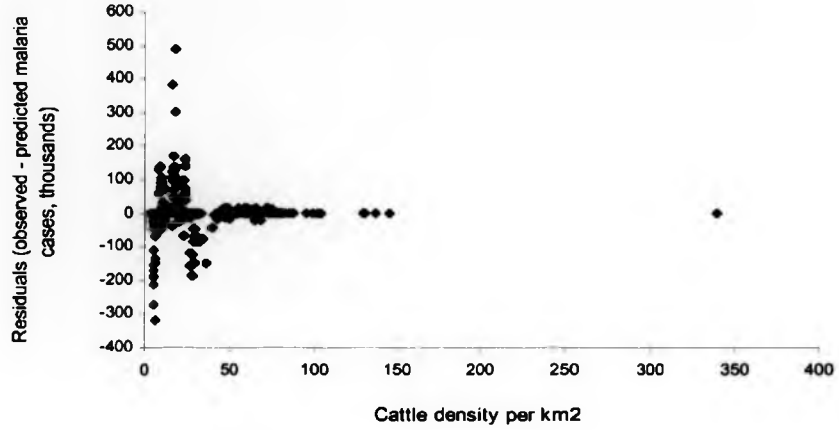

Figure 5. Spatial malaria model: residuals verus cattle density.

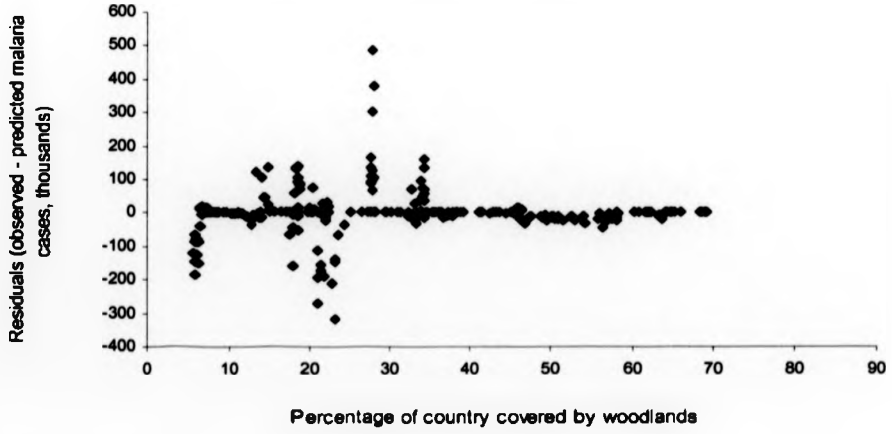

Figure 6. Spatial malaria model: residuals versus woodland coverage.

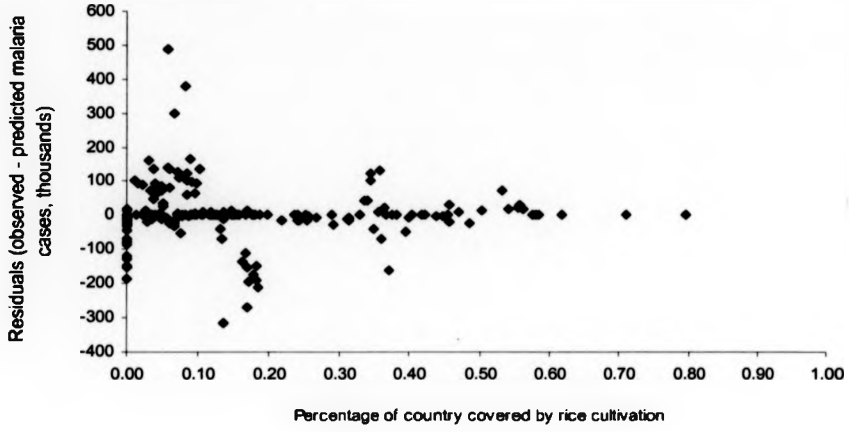

Figure 7. Spatial malaria model: residuals versus rice cultivation.

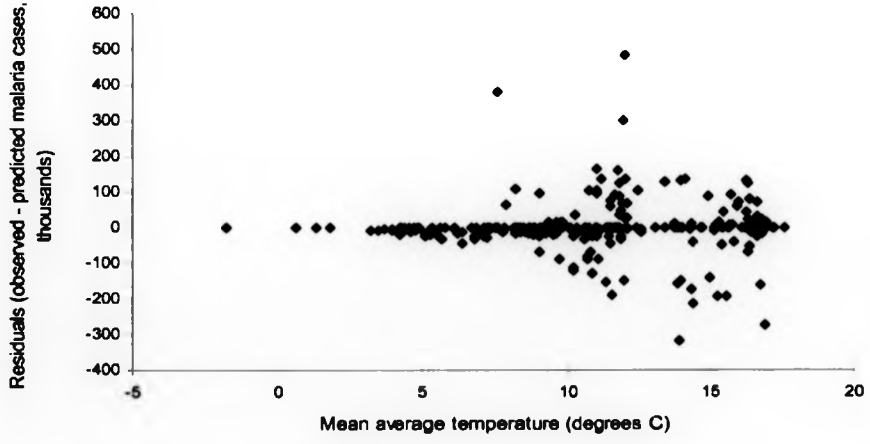

Figure 8. Spatial malaria model: residuals versus mean average temperature.

Difference and 95% confidence intervals of the difference between observed and predicted malaria cases in four European countries with no change in cattle densities, woodland coverage and rice cultivation since 1900.

Country (scenario)	Number of cases	% Difference	Lower CI limit	Upper CI limit
Finland (observed)	7512			
Finland (no change in cattle densities)	9555	27.2	24.2	32.3
Finland (no change in woodland coverage)	13980	86.1	82.6	89.8
Sweden (observed)	1545			
Swden (no change in cattle densities)	2966	92.2	88.6	100.7
Sweden (no change in woodland coverage)	2843	84.0	80.6	88.9
Italy (observed)	8348636			
Italy (no change in cattle densities)	9509096	13.9	11.4	16.8
Italy (no change in woodland coverage)	10535979	26.2	22.6	29.9
Italy (no change in rice cultivation)	7555516	-9.5	-10.9	-5.1
Spain (observed)	2506691			
Spain (no change in cattle densities)	2529251	0.9	0.1	2.7
Spain (no change in woodland coverage)	2975442	18.7	15.6	21.2
Spain (no change in rice cultivation)	7795809	211.0	197.1	214.5

Number of original data points (*Anopheles* surveys) in all European countries contained in the final database (listed in ascending order of data availability).

Country	Number of data points	Percentage of total
Norway	1	0.1
Estonia	2	0.1
Latvia	2	0.1
Lithuania	3	0.2
Slovenia	3	0.2
Ukraine	7	0.4
Macedonia	10	0.5
Slovakia	14	0.8
Croatia	16	0.9
Uzbekistan	22	1.2
Albania	24	1.3
Bosnia	28	1.5
Denmark	28	1.5
Kazakhstan	28	1.5
Czech republic	31	1.7
Finland	32	1.7
Romania	32	1.7
Spain	34	1.9
Bulgaria	35	1.9
England	36	2.0
Switzerland	37	2.0
Austria	41	2.2
Hungary	41	2.2
Greece	43	2.3
Belgium	47	2.6
Yugoslavia	55	3.0
Poland	56	3.1
Russia	98	5.3
Germany	108	5.9
Netherlands	119	6.5
France	126	6.9
Sweden	170	9.3
Italy	206	11.2
Portugal	298	16.3

Measures of life expectancy, GDP, predicted population-weighted relative vectorial capacty, equation constant and R_0 for 41 European countries in the present day. (Note that the table is sorted by life expectancy in ascending order).

Country	Life expectancy	GDP	Population -weighted vectorial capacity	"Constant"	R_0
Moldova	69	2170	0.0144	73.65	1.09
Russia	69	3220	0.0068	37.21	0.28
Latvia	69	3410	0.0037	33.70	0.14
Romania	70	1390	0.0111	92.77	0.89
Ukraine	70	2340	0.0115	37.68	0.41
Hungary	70	2720	0.0216	29.04	0.61
Estonia	70	3830	0.0012	16.07	0.02
Poland	71	1790	0.0085	35.45	0.25
Lithuania	71	2710	0.0052	17.30	0.08
Belarus	71	3110	0.0064	13.63	0.08
Turkey	72	1840	0.0223	20.30	0.35
Bulgaria	72	1840	0.0065	20.30	0.10
Czech Republic	72	2470	0.0041	12.19	0.04
Albania	73	1840	0.0330	12.36	0.29
Bosnia Herzegovina	73	1840	0.0445	12.36	0.39
Macedonia	73	1840	0.0212	12.36	0.19
Montenegro	73	1840	0.0199	12.36	0.18
Serbia	73	1840	0.0121	12.36	0.11
Slovakia	73	1840	0.0103	12.36	0.09
Slovenia	73	1840	0.0085	12.36	0.07
Croatia	73	2470	0.0556	7.43	0.31
Portugal	74	5930	0.0460	1.01	0.04
Ireland	75	11120	0.0000	0.21	0.00
United Kingdom	75	16550	0.0003	0.11	0.00
Denmark	75	23700	0.0018	0.06	0.00
Iceland	75	23700	0.0000	0.06	0.00
Belgium	76	18950	0.0055	0.05	0.00
Austria	76	20140	0.0021	0.05	0.00
Germany	76	23650	0.0053	0.04	0.00
Faeroe Islands	76	23700	0.0000	0.04	0.00
Finland	76	23980	0.0014	0.04	0.00
Greece	77	6340	0.0238	0.23	0.00
Andorra	77	12450	0.0014	0.07	0.00
Spain	77	12450	0.0423	0.07	0.00
Italy	77	18520	0.1167	0.04	0.00
Netherlands	77	18780	0.0048	0.03	0.00
France	77	20380	0.0112	0.03	0.00
Luxembourg	77	20380	0.0048	0.03	0.00
Norway	77	24220	0.0001	0.02	0.00
Sweden	78	25110	0.0003	0.01	0.00

The distribution of land cover types in Europe (from the 1 by 1 km resolution 1992 Eurasia Land Cover Characteristics Data Base, distributed by USGS EROS (USGS 2002).

Minimal adequate models for *An. labranchiae*, *An. messeae*, *An. sacharovi* and *An. superpictus*.

Box 1. Minimal adequate model for *An. labranchiae*.

```
STATA command
xi: glm  labranchiae tmin tminsq tmax tave ccmin ccave ccavesq trave travesq
i.ecosyst_land, l(1)

Statistics
Generalised linear models                         No. of obs      =       1833
Optimization     : ML: Newton-Raphson             Residual df     =       1784
                                                  Scale param     =   .0293926
Deviance         =  52.43644939                   (1/df) Deviance =   .0293926
Pearson          =  52.43644939                   (1/df) Pearson  =   .0293926

Explanatory variables
(40 land cover variables not included)
------------------------------------------------------------------------------
labranchiae| Coef.    Std. Err.      z    P>|z|     [95% Conf. Interval]
-------------------------------------------------------------------------------
     tmin  | 7.886901   .8396137    9.39   0.000     6.241289    9.532514
    tminsq | -.1234548  .0127084   -9.71   0.000    -.1483629   -.0985467
     tmax  | 5.680366   2.813668    6.60   0.030     3.834322    7.195054
     tave  | 8.58025    3.82107     2.25   0.025     1.09109    16.06941
     ccmin | -.4586843  .117589    -3.90   0.000    -.6891544   -.2282141
     ccave | 6.144954   2.031853    3.02   0.002     2.162595    10.12731
   ccavesq | -.0796476   .02401    -3.32   0.001    -.1267179   -.0325774
     trave |13.90983    10.23658    3.52   0.001     9.623559    18.52659
   travesq | -.9795935  .0522484  -18.75   0.000    -1.081998   -.8771886
------------------------------------------------------------------------------
```

Box 2. Minimal adequate model for *An. messeae*.

```
STATA command
xi: glm  messeae tmin tminsq tave ptotal ccave ccavesq  trmin trave travesq
wdfave wdfavesq i.ecosyst_land, l(1)

Statistics
Generalized linear models                         No. of obs      =       1833
Optimization     : ML: Newton-Raphson             Residual df     =       1785
                                                  Scale param     =   .1333125
Deviance         =  237.9627576                   (1/df) Deviance =   .1333125
Pearson          =  237.9627576                   (1/df) Pearson  =   .1333125

Explanatory variables
(37 land cover variables not included)
------------------------------------------------------------------------------
 messeae |      Coef.   Std. Err.      z    P>|z|     [95% Conf. Interval]
-------------------------------------------------------------------------------
    tmin |   .3494162   .0751755     4.65   0.000     .2020749    .4967575
  tminsq |  -.0077266   .0013314    -5.80   0.000    -.0103361    -.005117
   tave  |  -.2333245   .0496783    -4.70   0.000    -.3306921   -.1359569
  ptotal |   .0000973   .0000168     5.78   0.000     .0000513    .0001643
   ccave |   1.568617   .1862165     8.42   0.000     1.203639    1.933595
 ccavesq |  -.0138041   .0017264    -8.00   0.000    -.0171877   -.0104205
   trmin |  -.1794104   .0854901    -2.10   0.036    -.3469679   -.0118529
   trave |   .4459867   .2407706     1.85   0.024     .1559151    .9178885
 travesq |  -.0280519   .0145574    -1.93   0.018    -.0565838   -.0014801
  wdfave |  6.2062792   .4529273     4.55   0.000    2.2950513   8.1175071
wdfavesq |  -.1895685   .0215683    -2.48   0.000    -.2485987   -.0215854
------------------------------------------------------------------------------
```

Box 1. Minimal adequate model for *An. sacharovi.*

```
STATA command
xi: glm sacharovi  tmin tminsq ptotal ccave trave travesq wdfmin wdfmax wdfave
i.ecosyst_land, l(1)

Statistics
Generalized linear models                         No. of obs      =       1833
Optimization     : ML: Newton-Raphson             Residual df     =       1788
                                                  Scale param     =  .0550554
Deviance         =  98.43911539                   (1/df) Deviance =  .0550554
Pearson          =  98.43911539                   (1/df) Pearson  =  .0550554

Explanatory variables
(36 land cover variables not included)
------------------------------------------------------------------------------
sacharovi |      Coef.   Std. Err.      z    P>|z|     [95% Conf. Interval]
------------------------------------------------------------------------------
     tmin |  5.2152658   .6598566    10.25   0.000     1.1821634   9.1384016
   tminsq |  -.1602825   .0111639   -14.36   0.000     -.1986548   -.0985658
   ptotal |   .0413162   .0029436    14.04   0.000      .0355468    .0470856
    ccave |  -.0252997   .0123751    -2.04   0.041     -.0495544    -.001045
    trave |   .7676835   .3881516     1.98   0.048      .0069204    1.528447
  travesq |  -.0220125   .0198137    -1.11   0.037     -.0608467   -.0168218
   wdfmin |   .0468125   .0163928     2.86   0.004      .0146831    .0789419
   wdfmax |   -.050554   .0145336    -3.48   0.001     -.0790393   -.0220687
   wdfave |  -.8573804   .0498265   -17.21   0.000     -.9550386   -.7597222
------------------------------------------------------------------------------
```

Box 2. Minimal adequate model for *An. superpictus*

```
STATA command
xi: glm  superpictus  tmin tminsq tmax tmaxsq tave ptotal ptotalsq trave
wdfmax wdfave i.ecosyst_land, l(1)

Statistics
Generalized linear models                         No. of obs      =       1833
Optimization     : ML: Newton-Raphson             Residual df     =       1785
                                                  Scale param     =  .0564825
Deviance         =  100.8211886                   (1/df) Deviance =  .0564825
Pearson          =  100.8211886                   (1/df) Pearson  =  .0564825

Explanatory variables
(38 land cover variables not included)
------------------------------------------------------------------------------
superpictus |      Coef.   Std. Err.      z    P>|z|     [95% Conf. Interval]
------------------------------------------------------------------------------
       tmin |   7.252912   1.270199     5.71   0.000     4.763368    9.742457
     tminsq |  -.1451558   .0244664    -5.93   0.000     -.1931091   -.0972026
       tmax |   2.804171   .8537651     3.28   0.001      1.130822    4.477519
     tmaxsq |  -.0800117   .0203862    -3.92   0.000     -.1199678   -.0400556
       tave |   .2695871   .0427242     6.31   0.000      .1858492    .3533249
     ptotal |   .2534205   .0356447     7.11   0.000      .1835583    .3232828
   ptotalsq |  -.0005968      .0001    -5.97   0.000     -.0007927   -.0004008
      trave |   -.285424   .0972833    -2.93   0.003     -.4760957   -.0947523
     wdfmax |  -.0541862   .0216036    -2.51   0.012     -.0965286   -.0118439
     wdfave |  -3.270198   .5163334    -6.33   0.000     -4.282193   -2.258203
------------------------------------------------------------------------------
```

Malaria risk (R_0) in 41 European countries at present day and for three climate change scenarios (2020s, 2050s and 2080s).

Country	R_0 present	R_0 2020	R_0 2050	R_0 2080
Moldova	1.09	1.30	1.90	2.44
Romania	0.89	1.07	1.83	2.26
Hungary	0.61	0.73	1.08	1.41
Ukraine	0.41	0.49	0.76	1.02
Bosnia Herzegovina	0.39	0.55	1.14	1.38
Turkey	0.35	0.42	0.63	0.70
Croatia	0.31	0.43	0.76	0.90
Albania	0.29	0.41	0.65	0.76
Russia	0.28	0.33	1.61	2.17
Poland	0.25	0.30	0.80	1.13
Macedonia	0.19	0.26	0.44	0.49
Montenegro	0.18	0.24	0.31	0.33
Latvia	0.14	0.16	0.69	1.00
Serbia	0.11	0.15	0.40	0.52
Bulgaria	0.10	0.14	0.19	0.23
Slovakia	0.09	0.13	0.23	0.33
Lithuania	0.08	0.10	0.37	0.53
Belarus	0.08	0.11	0.24	0.33
Slovenia	0.07	0.10	0.16	0.17
Czech Republic	0.04	0.06	0.17	0.26
Portugal	0.04	0.06	0.02	0.02
Estonia	0.02	0.02	0.25	0.39
Greece	0.00	0.00	0.01	0.01
Italy	0.00	0.00	0.01	0.01
Spain	0.00	0.00	0.00	0.00
France	0.00	0.00	0.00	0.00
Belgium	0.00	0.00	0.00	0.00
Germany	0.00	0.00	0.00	0.00
Netherlands	0.00	0.00	0.00	0.00
Luxembourg	0.00	0.00	0.00	0.00
Denmark	0.00	0.00	0.00	0.00
Austria	0.00	0.00	0.00	0.00
Andorra	0.00	0.00	0.00	0.00
Finland	0.00	0.00	0.00	0.00
United Kingdom	0.00	0.00	0.00	0.00
Switzerland	0.00	0.00	0.00	0.00
Sweden	0.00	0.00	0.00	0.00
Norway	0.00	0.00	0.00	0.00
Faeroe Islands	0.00	0.00	0.00	0.00
Iceland	0.00	0.00	0.00	0.00
Ireland	0.00	0.00	0.00	0.00

Difference and 95% confidence intervals of the difference between observed and predicted malaria cases in four European countries with changing temperatures.

Country (scenario)	Number of cases	% Difference	Lower CI limit	Upper CI limit
Finland (observed)	7512			
Finland (1.5 degree decrease)	6392	-14.9	-16.4	-10.4
Finland (1.5 degree increase)	8766	16.7	14.1	19.9
Finland (2 degree increase)	9202	22.5	19.8	25.9
Finland (5 degree increase)	9697	29.1	26.4	34.7
Sweden (observed)	1545			
Sweden (1.5 degree decrease)	1359	-12.0	-15.1	-8.9
Sweden (1.5 degree increase)	1748	13.2	10.1	16.4
Sweden (2 degree increase)	1809	17.1	14.5	19.8
Sweden (5 degree increase)	1991	28.9	24.9	34.8
Italy (observed)	8348636			
Italy (1.5 degree decrease)	6161293	-26.7	-29.5	-20.2
Italy (1.5 degree increase)	8832856	5.6	3.7	8.6
Italy (2 degree increase)	9342123	11.9	9.8	14
Italy (5 degree increase)	10644510	27.5	24.8	31.9
Spain (observed)	2506691			
Spain (1.5 degree decrease)	1957725	-21.9	-25.9	-17.9
Spain (1.5 degree increase)	2732293	9.0	6.1	13.0
Spain(2 degree increase)	2799973	11.7	8.9	14.8
Spain (5 degree increase)	3160937	26.1	22.0	29.9

Projected changes in (a) mean annual surface temperature and (b) mean annual precipitation predicted by the HADCM3 models. Note that predictions are not from the HADCM3 SRES scenarios which were unavailable but from the HADCM3 IS92a, the emission scenarios which were used previous to the SRES scenarios.

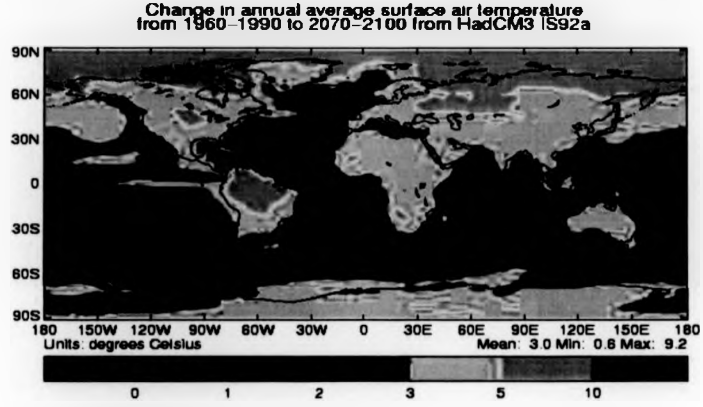

Hadley Centre for Climate Prediction and Research, The Met. Office

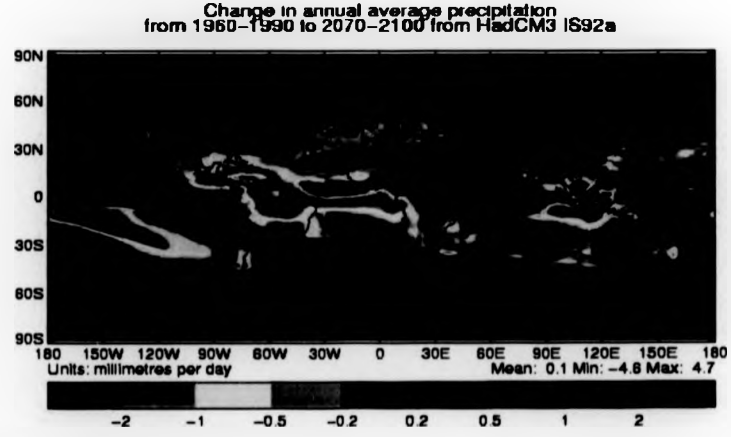

Hadley Centre for Climate Prediction and Research, The Met. Office